Studies in Marine Diterpene Chemistry

A thesis submitted in fulfilment of the

requirements for the degree of

Doctor of Philosophy

of

Rhodes University

by

Albert Wynand Wincke van Wyk

October 2007

Abstract

This thesis comprises both a natural product investigation and a synthetic component. The natural product investigations are presented in Chapters Two and Three. In Chapter Two the isolation and spectroscopic identification of the new isocopalane diterpene 12*S*,13*R*,14*S*-isocopalan-13-ol-12,14-diacetate (**2.1**) and two known 3-(14*S*)-isocopal-12-ene-15-oyl-1-acetyl-*sn*-glycerol **(2.2)** and 3-(14*S*)-isocopal-12-ene-15-oyl-2-acetyl-*sn*-glycerol (**2.3**) from a single, large, unidentified sub-Antarctic nudibranch, collected near Marion Island, approximately 2000 km south of Cape Town are described. Chapter Three discusses the isolation, spectroscopic structure elucidation and anti-oesophageal cancer activity (**3.1**-**3.4** only) of two known labdane diterpenes 6β,7α-diacetoxylabda-8,13*E*-dien-15-ol (**3.1**) and 2α,6β,7α-triacetoxylabda-8,13*E*-dien-15-ol (**3.2**) and one new 6β,7α,15-triacetoxylabda-8,13*E*-diene (**3.3**), as well as new 3α,11-dihydroxy-9,11-seco-cholest-4,7-dien-6,9-dione (**3.4**) and cholest-7-en-3,5,7-triol (**3.5**) from the endemic pulmonate mollusc, *Trimusculus costatus*. The absolute configuration of **3.2**, and hence **3.1** and **3.3** (from biogenetic arguments) was determined through X-ray diffraction of a single crystal of the camphanate ester of **3.2**. The absolute configuration of the secondary hydroxyl at C-3 of **3.4** was established using the Modified Mosher's method.

The synthetic component of the thesis commences in Chapter Four with the semi-synthesis of labdane diterpene nitriles 9α-cyano-15,16-epoxy-7β-hydroxylabda-13(16),14-dien-6-one (**4.1**), 9α-cyano-15,16-epoxy-7-hydroxylabda-7,13(16),14-trien-6-one (**4.2**) and 9α-cyano-15,16-epoxy-6β,7β-dihydroxylabda-13(16),14-diene (**4.3**) from the terrestrial labdane diterpene, hispanolone (**4.4**). This work is an extension of previous synthetic studies directed towards the synthesis of *T. costatus* metabolites. Diterpenes **4.1**-**4.3** exhibited *in planta* activity against the economically important crop pathogens, *Magnaporthea grisea* and *Puccinia recondita*. Chapter Five describes the successful semi-synthesis of two isomeric marine molluscan labdane diterpene aldehyde metabolites, labd-13*E*-ene-8β-ol-15-al (**5.1**) and labd-13*Z*-ene-8β-ol-15-al (**5.2**) from the commercially available, terrestrial plant derived, labdane diterpene manool (**5.3**). Diterpenes **5.1** and **5.2**, originally isolated from the Mediterranean nudibranch,

Pleurobranchaea meckelii and selected diterpenes arising from this synthesis were evaluated for their activity against an oesophageal cancer cell line (WHCO1). Chapter Six further develops the research discussed in Chapter Five, where ethyl 17-norabiet-13(15)-*E*-en-8β-ol-16-oate (**5.49**) and ethyl 17-norabiet-13(15)-*Z*-en-8β-ol-16-oate (**5.50**) were first semi-synthesized serendipitously. Based on their structural relationship to naturally occurring tricyclic diterpenes with anti-plasmodial activity, tricyclic diterpenes, 17-norpimaran-13α-ethoxy-8,16-olactone **(6.6)**, 17-norisopimar-15-ene-8β,13β-diol (**6.7**), 17-norisopimarane-8β,16-diol (**6.8**) and 17-norabiet-13(15)-ene-8β,16-diol (**6.9**) were semi-synthesized from the terrestrial labdane diterpene, **5.3**, and critically evaluated for their antimalarial potential from parasite inhibition and haemolytic studies.

Table of contents

List of Figures

List of Schemes

List of Tables **Page**

List of Abbreviations

$[\alpha]_D$	specific rotation
1D	one dimensional
2D	two dimensional
Ac_2O	acetic anhydride
AcOH	acetic acid
aq.	aqueous
amu	atomic mass units
br	broad
c	concentration (quoted in g/100mL)
calcd	calculated
cat.	catalytic quantity
CD	circular dichroism
conc.	concentrated
CQ	chloroquine
d	doublet
DCC	1,3-dicyclohexylcarbodiimide
DEPT	distortionless enhancement by polarisation transfer
DFHR	dihydrofolate reductase
DIBAH	diisobutylaluminium hydride
DMAP	4-dimethylaminopyridine
DMEM	Dulbecco/Vogt modified eagle's minimal essential medium
DMF	*N*,*N*-dimethylformamide
DMP	Dess-Martin periodinane
DMSO	dimethylsulfoxide
dt	double triplet
EIMS	electron impact mass spectroscopy
ELISA	enzyme-linked immunosorbent assay
eq	molar equivalent
Et_2O	diethyl ether
Et_3N	triethylamine
EtOAc	ethyl acetate
EtOH	ethanol
eV	electron-volt
FT	Fourier transform
gCOSY	gradient ^1H-^1H homonuclear correlation spectroscopy
gHMBC	gradient heteronuclear multiple bond correlation
gHSQC	gradient heteronuclear single quantum coherence

h	hour(s)
HEPES	4-(2-hydroxyethyl)-1-piperazine ethanesulfonic acid
HPLC	high performance liquid chromatography
HPV	Human Papilloma Virus
HREIMS	high resolution electron impact mass spectrometry
HRFAB	high resolution fast atom bombardment
HRFABS	high resolution fast atom bombardment mass spectrometry
HWE	Horner-Wadsworth-Emmons
IC_{50}	median inhibitory concentration
int.	integration
IR	infrared
LAH	lithium aluminium hydride
LDA	lithium diisopropylamide
lit.	literature
m	multiplet
m-CPBA	*meta*-chloroperbenzoic acid
MeOH	methanol
min	minute(s)
mmHg	millimetres of mercury
mmol	millimoles
mol	moles
mp	melting point
MS	mass spectrometry
MTPA	α-methoxy-α-trifluoromethylphenylacetic acid
MTT	3-(4,5-dimethylthiazol-2-yl)-2,5-diphenyltetrazolium bromide
mult.	multiplicity
NBS	*N*-bromosuccinimide
ND	not determined
NMR	nuclear magnetic resonance
NOE	nuclear Overhauser enhancement
NOESY	nuclear Overhauser enhancement spectroscopy
OAc	acetyl functionality
PCC	pyridinium chlorochromate
PKC	protein kinase C
PPh_3	triphenylphosphine
ppm	parts per million
PTEACl	phenyltriethylammonium chloride
p-TsOH	*para*-toluenesulfonic acid
q	quartet
R	alkyl group

rel. int.	relative intensity
ROESY	rotational nuclear Overhauser spectroscopy
RT	room temperature
s	singlet
SAR	structure-activity relationship
sat.	saturated
sp.	species
t	triplet
TBAF	tetra-*n*-butylammonium fluoride
TBDMS	tertiary-butyldimethylsilyl
TBDMSCl	tertiary-butyldimethylslyl chloride
TEPA	triethylphosphonoacetate
tert	tertiary
TESCl	triethylsilyl
TESCl	triethylsilyl chloride
THF	tetrahydrofuran
TLC	thin layer chromatography

Acknowledgments

Many thanks to the following people for their assistance with this project:

Professor Mike Davies-Coleman, my supervisor, for always being there, always having a plan and always being supportive. Thank you for being a friend.

Dr Chris Gray and Dr Rob Keyzers for sharing their knowledge and experience with me, and an extra thank you to Rob for his aid in proof-reading this thesis. Many thanks also to Mr Kevin Lobb, Dr Rosa Klein and Dr Edith Antunes for the many hours spent giving advice in their fields of expertise.

Mr Andy Soper for constant assistance with the NMR and for graciously allowing me to share his office. I am also indebted to Mr Aubrey Sonemann for his amazing ability to repair virtually anything and to Ms. Benita Tarr for all the help over the years.

Dr Denver Hendricks, Dr Catherine Whibley, Dr Omolaja Osoniyi, Dr Heinrich Hoppe, Dr Bassam Nader and Dr Todd Werk for their assistance with bioactivity tests and Dr Kirk Gustafson and Ms Laura Cartner for obtaining CD spectra for me.

All the friends that have kept me going over the past few months: Andrea, Ben, Brent, Brook, Chris, Eloïse, Greg, James, Louise A., Louise L., Liz, Paula, Sunny, Tanya and Tina as well as the students, past and present, of the Marine Natural Products Research Group and the entire tea-time crowd. A special thank you to Sunny for proof-reading and to Louise for keeping things in perspective.

The funding agencies who have supported my during my PhD- the National Research Foundation, DAAD, the Department of Environmental Affairs and Rhodes University. A further thank you to Professor Brian Robinson for the generous donation of manool.

And, finally, thank you to my parents, Albert and Dee, for all their support and always believing in me. I couldn't have made it to this point without you.

Chapter One

General Introduction

1.1 Marine gastropod molluscs as a source of biomolecular diversity

1.1.1 The classification of opisthobranch and pulmonate molluscs

Class Gastropoda is the second most species diverse class of animals after class Insecta and includes over half of all molluscan species.[1;2] Traditionally, gastropods have been classified into the three sub-classes Prosobranchia, Opisthobranchia and Pulmonata, and although the higher classification of gastropods is still a matter of dispute amongst taxonomists,[2;3] this classification is generally maintained in the marine natural products literature,[2] and will accordingly be used in this chapter. This thesis deals primarily with diterpene compounds isolated from marine opisthobranch and pulmonate molluscs and thus an overview of the diterpene secondary metabolites from these two sub-classes will be the subject of this introductory chapter.

Opisthobranchs are marine gastropod molluscs and have recently been divided into nine Orders (Figure 1.1).[4] The shell in opisthobranch molluscs, *e.g.* nudibranchs (sea slugs), is either reduced or completely absent,[2-5] rendering them vulnerable to predation. Faulkner and Ghiselin (1983) first recognized that an evolutionary trend in opisthobranch molluscs towards the loss of the shell could possibly be linked to a parallel evolutionary trend towards the adoption of a natural product based chemical defence mechanism to deter predation.[6;7] The evolutionary advantage of a chemically mediated defensive strategy is centred around the minimal energy costs of acquiring defensive chemicals from the diet when compared to the energy costs of transporting a shell as a form of physical defence. A major disadvantage of the former defensive strategy, however, is the limitation it poses on dietary selection by a mollusc species, which becomes dependent on selected invertebrate species for its chemical defence. If the dietary source of the chemical defence metabolites is removed from the ecosystem, the shell-less mollusc is again vulnerable to predation. To overcome the restrictive dietary dependence on defence metabolites, a less common defence strategy, and one that predominates in some cold water nudibranchs, is *de novo* biosynthesis.[8;9] The need for *de novo* biosynthesis in cold waters is presumably driven by the reduced biodiversity in

these regions, which in turn possibly reduces the potential for chemical defence metabolites being ingested and sequestered by these nudibranchs. Defence metabolites, whether of dietary or *de novo* biosynthetic origin, are stored in specialized glands in the nudibranch's skin for release as feeding deterrents in the presence of a predator. The diverse array of sequestered secondary metabolites isolated from opisthobranch molluscs includes polyketides, alkaloids, peptides and terpenes.[4] Diterpenes comprise the greater part of all metabolites isolated from the opisthobranchs and an excellent review of the diterpene metabolites of opisthobranch molluscs by Gavagnin and Fontana covers the literature up until 1999.[4]

PHYLUM:		Mollusca	
CLASS:		Gastropoda	
SUBCLASS:		Opisthobranchia	
ORDERS:	Cephalaspidea	Acochlidea	Rhodopemorpha
	Sacoglossa	**Anaspidea**	**Notaspidea**
	Gymnosomata	Thecosomata	**Nudibranchia**

Figure 1.1 Opisthobranch classification,[4] with Orders from which diterpenes have been isolated printed in bold.

Unlike the opisthobranch gastropods, the majority of pulmonate gastropods (classification shown in Figure 1.2) are terrestrial or freshwater species and as a result rely on a pulmonary cavity, which serves as a lung, rather than gills for respiration.[1-3] The relatively few marine species of pulmonate gastropods are found in the intertidal zone of rocky shores.[1;2] As a result of the harsh environment in which they live, being battered by waves and debris at high tide while facing desiccation at low tide, they have retained their shell to survive these environmental constraints, but employ a chemical defence mechanism while foraging to deter predation.[1;2;6;7;10;11] Although various secondary metabolites have been isolated from pulmonates belonging to the families Siphonariidae, Onchidiidae and Trimusculidae, diterpenes are confined to the family Trimusculidae (Order Eupulmonata).[1] A detailed review of the metabolites isolated from *Trimusculus* species is provided in Chapter Three.

PHYLUM:		Mollusca	
CLASS:		Gastropoda	
SUBCLASS:		Pulmonata	
ORDERS:	Systellommatophora	Basommatophora	Eupulmonata

Figure 1.2 Pulmonate classification.[1]

1.1.2 Structural diversity of diterpenes from marine opisthobranch gastropods

In Gavagnin and Fontana's recent review of diterpenes from marine opisthobranch molluscs,[4] 35 different structural classes of diterpene were recognized. While rearranged skeletons were included in these 35 classes, diterpenes in which oxygen insertion had occurred into any of the rings were omitted. Selected examples of all non-rearranged diterpene frameworks presented in Gavagnin and Fontana's review are presented in Tables 1.1-1.5. In instances where two different enantiomeric series exist they have been counted together, while the total number of diterpenes with rearranged skeletons has been provided for comparative purposes. The plethora of rearranged skeletons precludes a detailed discussion of their diversity in this brief synopsis of Gavagnin and Fontana's seminal review.

Table 1.1 Acyclic diterpenes.

Diterpene class	No. of examples	Example	Example isolated from
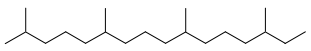 Phytane	7	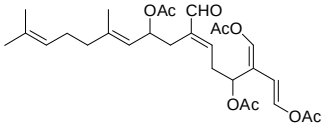	*Elysia halimedae*[12]

Table 1.2 Monocyclic diterpenes.

Diterpene class	No. of examples	Example	Example isolated from
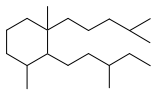 Dactylomelol†	1	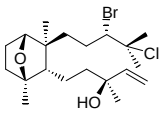 **1.3**	*Aplysia dactylomela*[13]
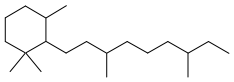 Cyclophytane	1	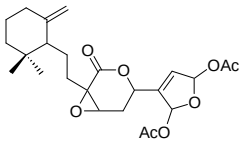	*Thuridilla hopei*[14]
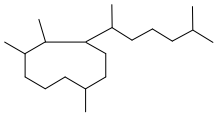 Dictyolactone†	1	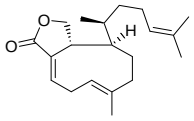	*Aplysia depilans*[15]
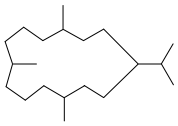 Cembrane	8	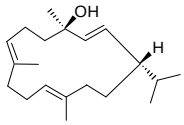	*Phyllodesmium longicirra*[16]
Rearranged (*e.g.* *d*egraded *ent*-labdane)	2	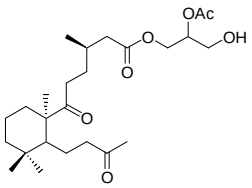	*Austrodoris kerguelenensis*[17]

† No class name exists.

Table 1.3 Bicyclic diterpenes.

Diterpene class	No. of examples	Example	Example isolated from
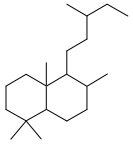 Labdane	13	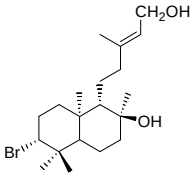	*Aplysia kurodai*[18]
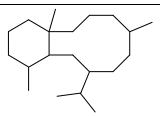 Briarane	9	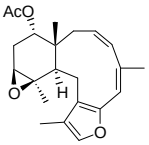	*Armina maculata*[19]
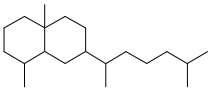 Eudesmane	2	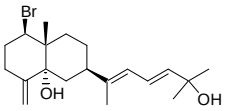	*Aplysia kurodai*[20]
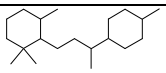 Obtustane	1	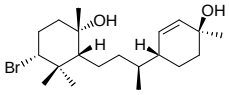	*Aplysia dactylomela*[21]
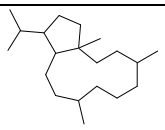 Dolabellane	16	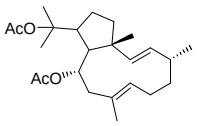	*Dolabella californica*[22]
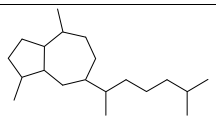 Guaiane	5	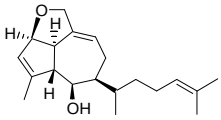	*Aplysia kurodai*[23]
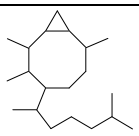 Crenulide†	4	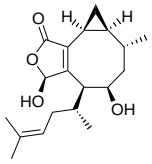	*Aplysia vaccaria*[24]
Rearranged (*e.g.* 4,5-*seco*-spongians)	29	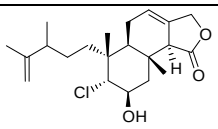	*Chromodoris hamiltoni*[25]

Table 1.4 Tricyclic diterpenes.

Diterpene class	No. of examples	Example	Example isolated from
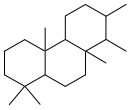 Spongian/isocopalane	Spongian: 43 Isocopalane: 17	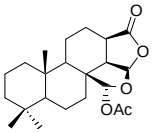	*Cadlina luteomarginata*[26]
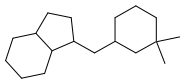 Irieol	2	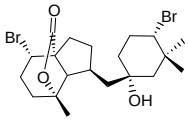	*Aplysia angasi*[27]
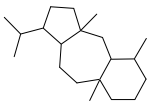 Dolastane	3	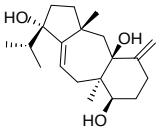	*Aplysia dactylomela*[28]
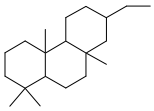 Marginatane	2	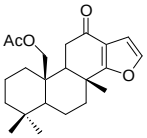	*Cadlina luteomarginata*[26]
Rearranged	14	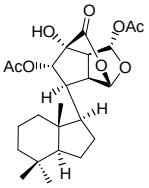	*Chromodoris cavae*[29]

Table 1.5 Tetracyclic diterpenes.

Diterpene class	No. of examples	Example	Example isolated from
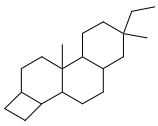 Isoparguerane (modified pimarane)	2	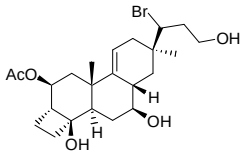 **1.10**	*Aplysia dactylomela*[30]
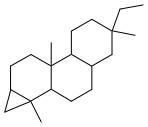 Parguerane (modified pimarane)	3	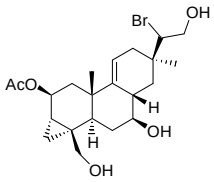 **1.9**	*Aplysia dactylomela*[30]

From the data in Tables 1.1-1.5 (summarized in Figure 1.3), it is clear that the majority of diterpenes reported from opisthobranch gastropods prior to 1999 were either bicyclic or tricyclic. Further analysis of the bicyclic diterpenes (Figure 1.4) revealed that the dolabellane (20%), labdane (16%) and briarane diterpenes (11%) predominated. The tricyclic diterpenes isolated from molluscs are strongly dominated (54%) by spongian diterpenes (Figure 1.5). The structures of 154 spongian diterpenes from marine sponges of the Orders Dictyoceratida and Dendroceratida have recently been reviewed by Keyzers *et al*.[31] This review, however, discussed only the spongian diterpenes isolated from marine sponges, while spongian diterpenes, isolated from the plethora of nudibranchs that prey on these sponges, were omitted. Interestingly, dictyoceratid and dendroceratid sponges are characterized by the absence of a spicule skeleton and are composed almost entirely of spongin fibres.[31] The absence of the physical defence associated with a spicule skeleton would make this group of sponges a particularly attractive component in a nudibranch's diet and may explain why spongian diterpenes dominate the tricyclic diterpenes isolated from marine molluscs. The

rare, and uniquely marine,[32] isocopalane diterpenes (and their *ent*-isocopalane counterparts) are reviewed in Chapter Two. Although the two tetracyclic diterpene classes illustrated in Table 1.5 are, strictly speaking, rearranged pimarane diterpenes, they are the only tetracyclic diterpenes to have been isolated from opisthobranchs and were thus included.[4]

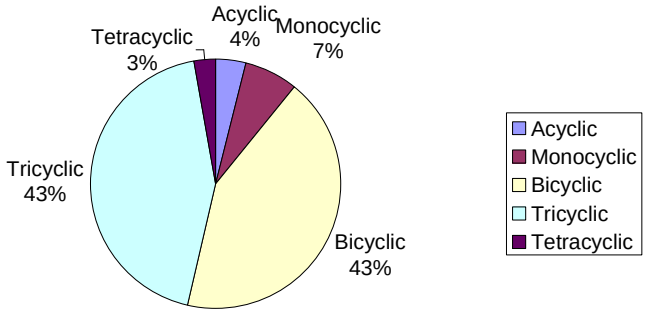

Figure 1.3 Graphical representation of the relative proportion of acyclic, monocyclic, bicyclic, tricyclic and tetracyclic diterpenes isolated from marine opisthobranch molluscs up until 1999.[4]

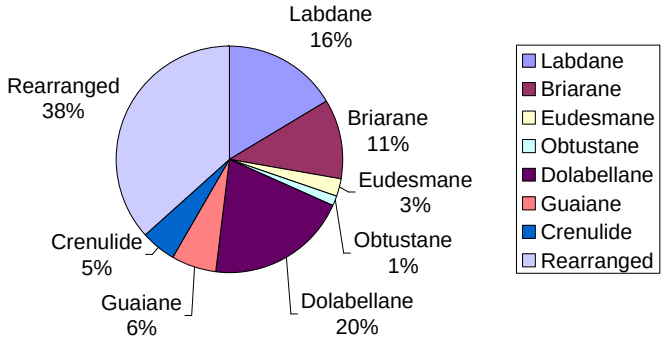

Figure 1.4 Graphical representation of the relative proportions of seven (plus rearranged) bicyclic diterpene classes isolated from opisthobranch molluscs up until 1999.[4]

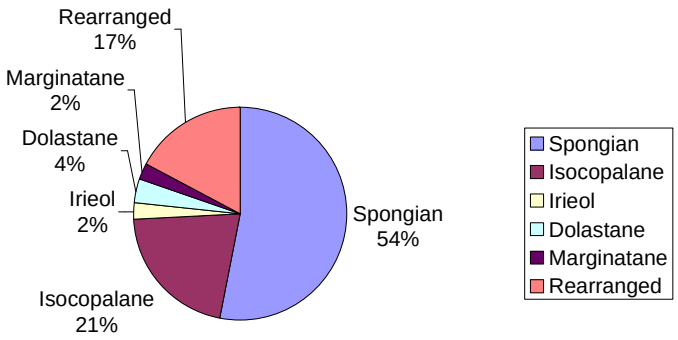

Figure 1.5 Graphical representation of the relative proportions of five (plus rearranged) tricyclic diterpene classes isolated from opisthobranch molluscs up until 1999.[4]

1.1.3 Diterpenes isolated from marine opisthobranch molluscs since 2000

In order to update Gavagnin and Fontana's review, the isolation and identification of diterpenes from marine opisthobranchs reported in the marine natural product literature 2000-2007 is described here.

1.1.3.1 Order Anaspidea

Molluscs of the Order Anaspidea are most commonly referred to as sea hares. They are known for their herbivorous diet and have been documented to feed exclusively on either red or brown algae.[4;7] Two papers describing the isolation of diterpenes from sea hares have been published since Gavagnin and Fontana's review. The first was by Wessels *et al.*[33] who reported the isolation of two new diterpenes (**1.1** and **1.2**), as well as the known metabolite (**1.3**, Table 1.2),[13] in addition to a host of known algal metabolites from *Aplysia dactylomela*, collected from Tenerife. The structures and relative configuration of **1.1** and **1.2** were determined spectroscopically, while that of **1.3** was determined through comparison of NMR data acquired with those previously published. Compounds **1.1** and **1.2** were structurally related to compounds previously isolated from the red alga *Laurencia* sp. and dactylomelol has also subsequently been isolated from a *Laurencia* sp.,[34] suggesting that **1.1**-**1.3** are of

algal origin. Analysis of the metabolites of three distinct samples of *A. dactylomela* in this study also revealed that the secondary metabolite content was dependent on site of location, again suggesting a dietary source for the secondary metabolites isolated from sea hares.

In 2002, Findlay and Li reported the isolation of four new diterpenes from *Aplysia punctata* (**1.4**-**1.7**), the structures of which were determined spectroscopically.[35] Two known diterpenes isoconcinndiol (**1.8**) and parguerol (**1.9**, Table 1.5) were also reisolated in this study and identified by comparison of spectroscopic and specific rotation data with previously published data. Three new sequiterpenes and fourteen other known non-diterpene compounds were also isolated. Many of the terpenes isolated from this sea hare were similar to those previously isolated from the *Laurencia* algal species, providing confirmation of the dietary source of these metabolites.

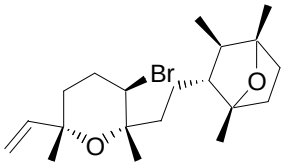

1.1

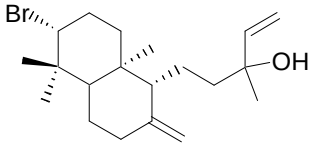

1.2

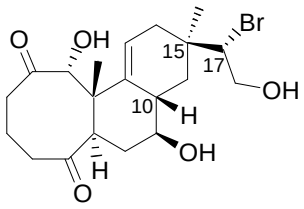

1.4

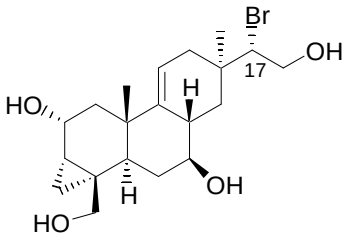

1.5

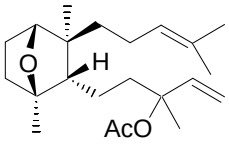

1.6

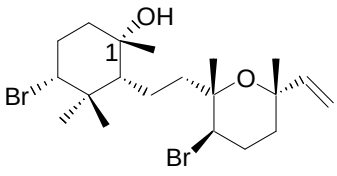

1.7

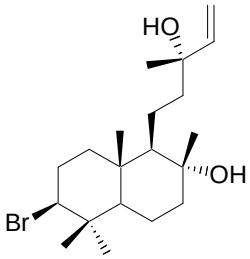

1.8

The relative configuration of **1.4** was deduced by NOE experiments and supported by comparison of the interatomic distances of the most stable conformation (obtained by computer modelling) with those determined from NOE data. A possible biogenetic pathway (Scheme 1.1) for the formation of **1.4** from isoparguerol (**1.10**) provided the authors with the name neoparguerane for compound **1.10**.

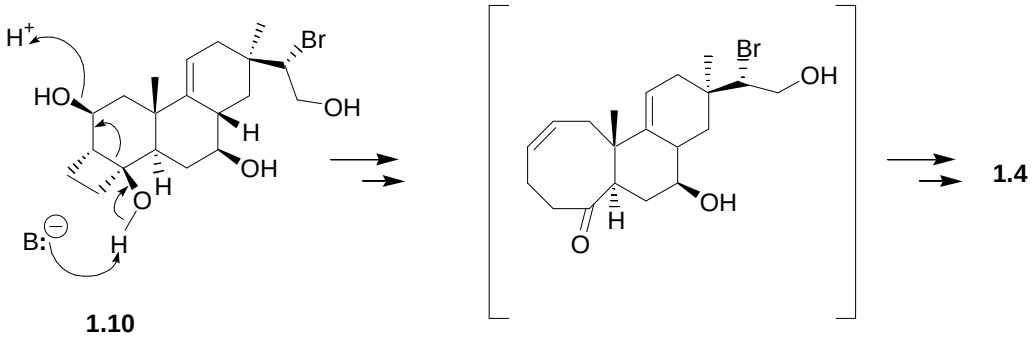

1.10

Scheme 1.1 Possible biogenetic pathway for the formation of **1.4** from **1.10**.[35]

Although compound **1.5** had previously been reported as a hydrolysis product of **1.9**, it had never been isolated from a natural source. The relative configuration of the bromine group at C-17 was assigned by determining the orientation of H-17 using NOESY data. The instability of both **1.1** and **1.5**, particularly in deuterated chloroform, prevented the acquisition of HREIMS data for these compounds. Punctatene acetate, **1.6**, was the second dacylomelol diterpene to be isolated from a sea hare and shared the same relative configuration in its bicyclic system as dactylomelol, **1.3**, isolated from *Aplysia dactylomela*,[13] the absolute stereochemistry of which was determined by single crystal X-ray diffraction. Punctatol (**1.7**) was found to have the same skeleton as laurencianol, also an algal diterpene, whose stereochemistry had also been determined by X-ray diffraction.[36]

1.1.3.2 Order Notaspidea

Fu *et al.*[37] reported the isolation of lissoclimide-type diterpenes **1.11**-**1.18** from *Pleurobranchus albiguttatus* and compounds **1.11**-**1.16** from *P. forskalii*, both collected in the

Philippines. Although related chlorinated compounds had previously been isolated from an ascidian, *Lissoclinum* sp., this was the first report of *Lissoclinum* metabolites from an opisthobranch predator.[37] Compounds **1.11**-**1.12** had previously been isolated from *Lissoclinum voeltzkowi*,[38-40] while **1.11**-**1.13** had been isolated from an unidentified *Lissoclinum* sp.[41-43] The relative configurations of **1.11**-**1.18** were determined from analysis of proton coupling constants and from NOE data.[37]

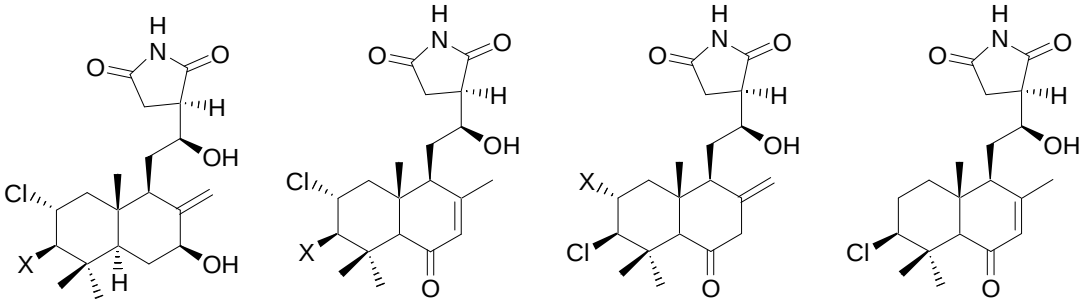

1.11 X = H
1.12 X = Cl
1.18 X = OH

1.13 X = Cl
1.14 X = H

1.15 X = Cl
1.17 X = H

1.16

1.1.3.2 Order Nudibranchia

Molluscs of the Order Nudibranchia continue to be the source of many of the new compounds isolated from marine molluscs. This is not surprising as nudibranchs are the most diverse and widespread of the opisthobranchs molluscs.[4] They are slow moving invertebrates without any visible means of physical protection against predation *e.g.* a shell or sharp spines, creating the need for a chemical defence mechanism.[44] Nudibranchs are carnivorous and their diet can encompass almost all marine animal phyla, from which many nudibranchs sequester their chemical defence allomones.[4] The bright colours that many nudibranchs display are aposomatic and provide a visual warning to potential predators. Since Gavagnin and Fontana's review,[4] four papers have been published outlining the isolation of new diterpene compounds from nudibranchs. The first of these was an anatomically guided study of the compounds found in *Glossodoris atromarginata*, collected along with a sample of the sponge being preyed upon at Gneerings Reef, South-East Queensland.[45] Seven furano-spongian diterpenes (**1.19-1.28**) were isolated, of which **1.19** and **1.20** were first time isolates from a

natural source (previously synthesized)[46] and **1.21** had never before been isolated from *G. atromarginata*. Five of the nudibranchs were dissected to establish the distribution of the metabolites in the various internal organs (**1.19**-**1.22**), mantle tissue (**1.19**, **1.23** and **1.24**) and mantle glands (**1.25**). Compounds of the C-3 α-epimeric series were found in the digestive tissue and mantle dermal formations while those of the C-3 β-epimeric series were noted exclusively in the mantle tissue. Somerville *et al*.[45] commented that these differences might be due to the compounds in the digestive tract being those of the host prey, while those in the mantle were either sequestered by the nudibranch or modified by selective enzyme transformations. They also cautioned that the axial orientation of the hydroxyl species at C-3 might result from keto-enol tautomerism leading to the more stable equatorial position being assumed during storage in the mantle.[45]

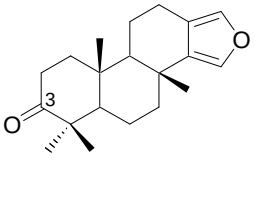

1.19

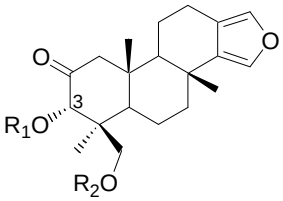

1.20 R_1 = Ac; R_2 = H
1.21 R_1 = H; R_2 = Ac
1.22 R_1 = H; R_2`= H
1.25 R_1 = Ac; R_2 = Ac

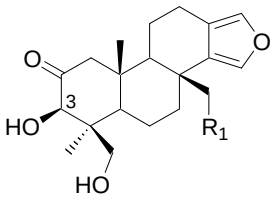

1.23 R_1 = H
1.24 R_1 = OH

A chemical study on *Austrodoris kerguelenensis*, collected in Terra Nova Bay, Antarctica, led to a revision of the structure of the 1'-acylglycerols (**1.26** and **1.27**) to their respective 2'-acylglycerols (**1.28** and **1.29**).[47] This structural revision was made after careful structural analyses of correlations in the HMBC NMR spectra of **1.28** and **1.29**. Two new acylgylcerol diterpenes (**1.30** and **1.31**) were also isolated. Comparison of the ^{1}H and ^{13}C NMR spectra of compounds **1.31** and **1.29** revealed them to be closely related, except that **1.31** lacked an acetyl group, allowing them to conclude that **1.31** was the deactyl derivative of **1.29**. Analysis of the 2D NMR data of **1.30** quickly allowed the authors to determine the structure as being very similar to known diterpene (**1.32**)[48] and limited the differences between **1.30** and **1.32** to the substitution pattern of the glyceryl moiety, where an acetyl functionality was linked instead of the tiglic acyl residue in **1.32**.

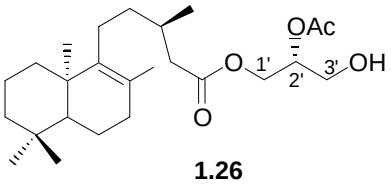

1.26

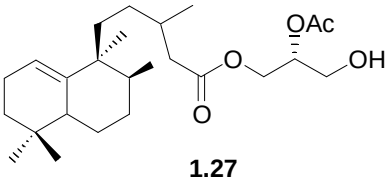

1.27

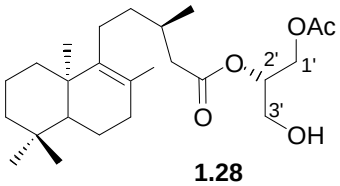

1.28

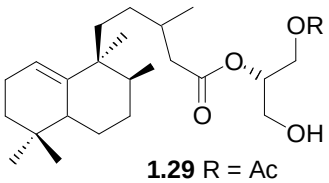

1.29 R = Ac
1.31 R = H

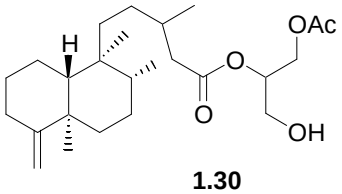

1.30

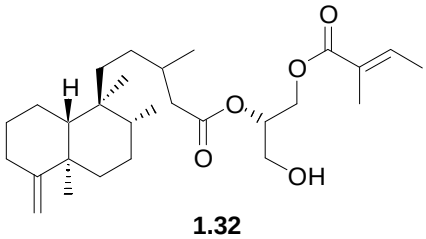

1.32

A Chinese collection of the nudibranch *Phyllidiella pustulosa* afforded four known nitrile-containing diterpenes (**1.33**-**1.36**).[49] All four compounds had previously been isolated from sponges,[50-57] suggesting that they were derived from the nudibranch's prey. Structural elucidations were made by comparison of acquired NMR data with those in the chemical literature.

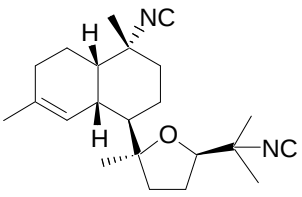

1.33

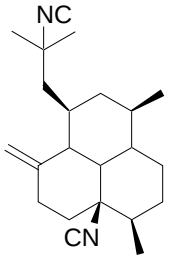

1.34

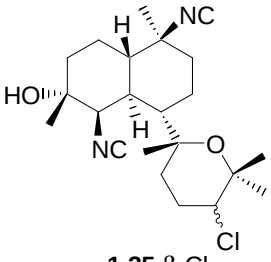

1.35 β-Cl
1.36 α-Cl

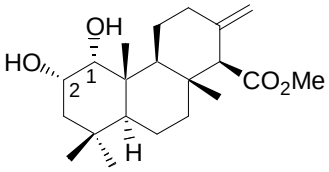

1.37

The final diterpene metabolite to have been isolated since Gavagnin's review is the *ent*-isocopalane diterpene (**1.37**), isolated from the Spanish dancer nudibranch, *Hexabranchus sanguineus*, collected in the Red Sea.[58] The large variety of structural features in the secondary metabolites isolated from this nudibranch was seen to support recent phylogenetic studies suggesting a close phylogenetic relationship between the Spanish dancer nudibranch and dorid nudibranchs.[58] Since **1.37** is included in the review in Chapter Two, no further discussion will be entered into here, apart from mentioning that this compound had previously been isolated from an Indonesian collection of the sponge, *Coelocarteria* cfr. *singaporensis*.[59]

This concludes the review of diterpenes isolated from opisthobranch molluscs since Gavagnin and Fontana's recent review.[4] Chapter Two provides details of the isolation of one new and two known isocopalane diterpenes from a sub-Antarctic nudibranch. Labdane diterpene chemistry is a common thread that runs through the remainder of this thesis from the isolation of a new labdane diterpene from the pulmonate mollusc, *Trimusculus costatus* (Chapter Three) to the synthesis of the labdane metabolites from the opisthobranchs mollusc, *Pleurobranchaea meckelii* (Chapter Five). Modifications of the labdane skeleton to explore the agrochemical and biomedicinal potential of semi-synthetic diterpene analogues are described in Chapters Four and Six.

Chapter Two

Isocopalane Diterpenes from a sub-Antarctic Nudibranch

2.1 Introduction

This Chapter describes the isolation and identification of new 12*S*,13*R*,14*S*-isocopalan-13-ol-12,14-diacetate (**2.1**) and the known 3-(14*S*)-isocopal-12-ene-15-oyl-1-acetyl-*sn*-glycerol (**2.2**) and 3-(14*S*)-isocopal-12-ene-15-oyl-2-acetyl-*sn*-glycerol (**2.3**) isocopalane diterpenes from a single, large, unidentified sub-Antarctic nudibranch. The nudibranch was collected at a depth of 115 m near Marion Island (approximately 2000 km south of Cape Town) and the research described in this Chapter represents the first natural products investigation of a marine organism from this region of the Southern Ocean. A review of the structures and the selected syntheses of isocopalane and *ent*-isocopalane diterpenes isolated from marine organisms provides the necessary background to this chapter.

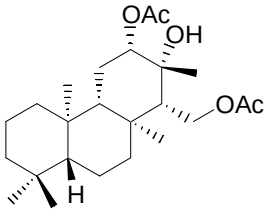

2.1

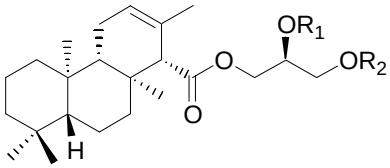

2.2 R_1 = H; R_2 = Ac
2.3 R_1 = Ac; R_2 = H

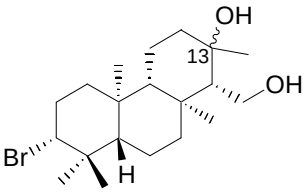

2.4

Isocopalane diterpenes (*vide infra*) and their enantiomeric series (the *ent*-isocopalane diterpenes) appear to be unique to the marine environment.[32] Isocopalane diterpenes are rare compared to the more common spongian diterpenes, (15,16-epoxy-*ent*-isocopalanes).[31] The name isocopalane was first proposed by de Miranda *et al*.[60] with an absolute configuration for this series defined by an earlier synthesis of (**2.4**) although the configuration at C-13 had not yet been determined.[61]

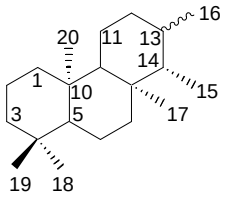

isocopalane

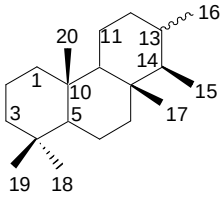

ent-isocopalane

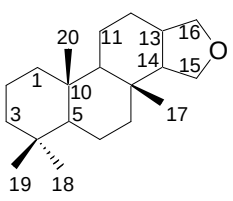

spongian

Examples of both the enantiomeric series of isocopalane diterpenes have been isolated from nudibranchs, while only one example from sponges has been an isocopalane diterpene. One example of a bromine containing isocopalane diterpene has been recorded from a sea hare. The most extensively studied examples of isocopalane and *ent*-isocopalane diterpenes have been those containing a glyceride substituent at C-15. Two numbering systems for the carbon atoms of the glycerol moiety are evident in the literature, either C-1'- C-3', or C-21- C-24. For reasons of simplicity the former glycerol numbering sequence will be used in this Chapter.

2.2 Chemical studies of isocopalanes and *ent*-isocopalanes

2.2.1 Isocopalane and ent-isocopalane diterpenes from marine molluscs

The first isocopalane diterpene isolated from a marine mollusc was isoaplysin-20, **2.4**.[62] The source of **2.4** was the sea hare *Aplysia kurodai*, collected off the coast of Japan. The structure and relative configuration of **2.4** (with the exception of the configuration at C-13) were proposed through comparison of ^{1}H and ^{13}C NMR data with those of co-occurring aplysin-20 (**2.5**).

The relative configuration at C-13 of **2.4** was later established synthetically by Imamura and Rúveda[61] through a synthesis of the debrominated analogue of **2.4** from methyl isocopalate (**2.6**). Methyl isocopalate was treated with formic acid to yield the tricyclic ester (**2.7**). The C-13 epimers (**2.8** and **2.9**) were synthesized *via* expoxidation and subsequent opening of the epoxide of the Δ^{12} olefin of **2.7**. The hydroxyl group at C-13 in **2.4** was consequently reported to have the relative configuration as shown in **2.9**. However, when Nishizawa *et al.*[63;64] introduced a β-equatorial bromine at C-3 of **2.9**, they found that the ^{1}H NMR spectra for the supposed synthetic and naturally occurring isoaplysin-20 were different.[63;64] The ^{1}H NMR spectrum of a minor product of the synthesis, once brominated at C-3 to yield (**2.10**), proved identical to that of naturally occurring isoplysin-20[63] when the ^{1}H NMR spectra of the two compounds were compared. Subsequent X-ray diffraction experiments on a single crystal of

the C-15 acetate of **2.10** established the relative configuration of isoaplysin-20 to be as indicated in **2.10**, rather than as in **2.4.**

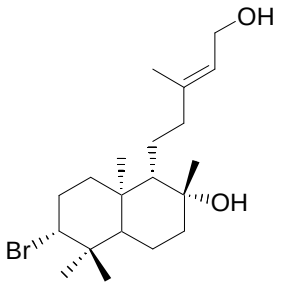

2.5

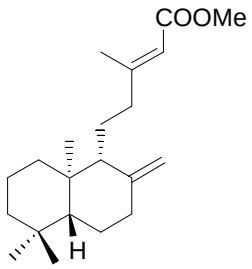

2.6

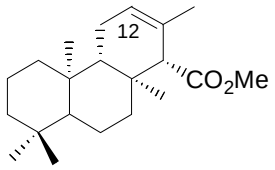

2.7

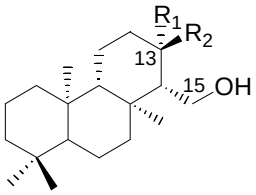

2.8 R_1 = OH, R_2 = Me
2.9 R_1 = Me, R_2 = OH

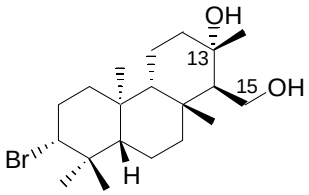

2.10

Gustafson *et al*.[65;66] isolated the first *ent*-isocopalane metabolites from the dorid nudibranch *Archidoris montereyensis* collected both in British Columbia and California. In their initial investigation,[65] they isolated (**2.11**) and established the relative configuration by X-ray analysis and the absolute configuration through hydrolysis of **2.11** to yield the known synthetic carboxylic acid (**2.12**).[67] Gustafson *et al*.[66] later reported the isolation of the related monoacetates, (**2.13** and **2.14**). Compound **2.11** has also been isolated from *A. odhneri,*[66] while **2.11**, **2.13** and **2.14** have been isolated from *A. tuberculata*.[68]

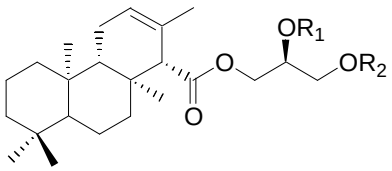

2.2 R_1 = H; R_2 = Ac
2.3 = Ac; R_2 = H

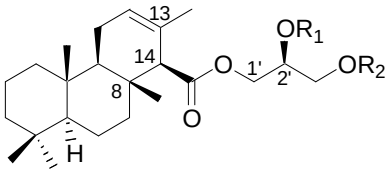

2.11 R_1 = R_2 = H
2.13 R_1 = H; R_2 = Ac
2.14 R1= Ac; R_2 = H

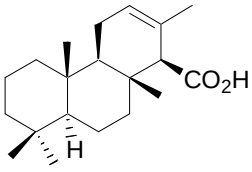

2.12

Interestingly, **2.2** and **2.3**, the diastereomers of **2.13** and **2.14,** have also been isolated from the nudibranchs *Anisodoris fontaini* (initially incorrectly identified as *Archidoris carvi*)[68;69] and *Doris verrucosa*.[70] *A. fontaini* was also the source of a further five isocopalane diterpenes (**2.15**-**2.19**).[70] The absolute configuration of these compounds, known as anisodorins 1-5, was established through the synthesis of the enantiomer of **2.15** (**2.20**) from optically active sclareol (**2.21**).[69] Synthetic **2.20** had an opposite CD curve (details not provided) and specific rotation to **2.15**, confirming that anisodorins 1-5 had an isocopalane skeleton. The absolute configuration of **2.19** was later conclusively provided by the synthesis of its enantiomer from **2.21**.[71]

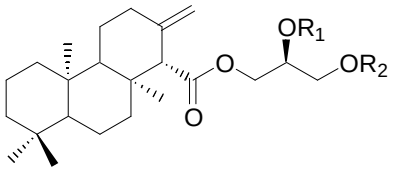

2.15 R_1 = H; R_2 = Ac
2.16 = Ac; R_2 = H

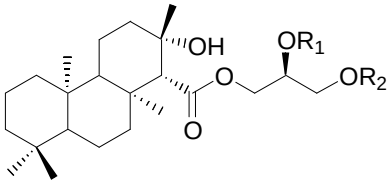

2.17 R_1 = H; R_2 = Ac
2.18 = Ac; R_2 = H

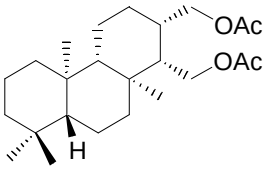

2.19

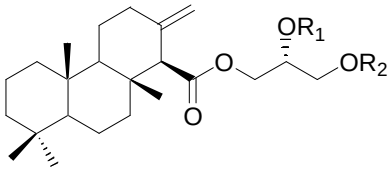

2.20 R_1 = H; R_2 = Ac

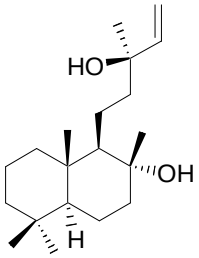

2.21

In addition to **2.2** and **2.3**, the Mediterranean nudibranch, *Doris verrucosa*,[70] also afforded verrucosin A (**2.22**) and verrucosin B (**2.23**).[72] Cimino *et al.*[72] had erroneously assigned verrucosins A and B to the (rearranged) *ent*-isocopalane series. This error was subsequently corrected by the same research group once the configuration at C-2' was unambiguously determined to be *S* by chemical methods.[70] The method (Scheme 2.1) involved the initial formation of an acetonide (**2.24**) from the acylglycerol (**2.25**), reduction and urethane formation (**2.26**). The configuration of **2.26** was determined from HPLC where the retention time of **2.26** was compared with the retention times of standard compounds with known absolute configuration.[70]

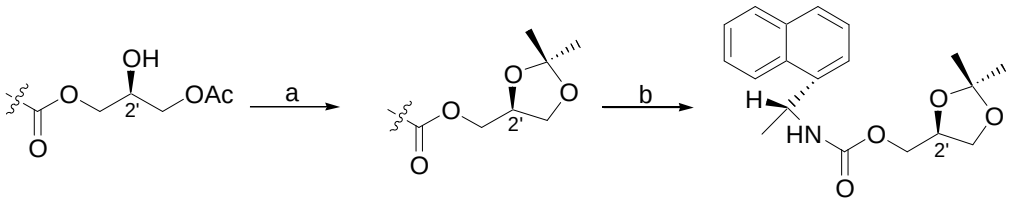

Scheme 2.1 The method used to prepare compound **2.26**.[70] *Reagents and conditions*: (a) 2,2-dimethoxypropane, *p*-TsOH, RT, 18 h; (b) (i) LAH, THF, Δ, 3.5 h, (ii) *in situ* treatment with (*R*)-(-)-1-(1-napthyl)ethyl isocyanate.

Verrucosins A and B are unusual in that the C-20 methyl moiety has migrated from C-10 to C-9 and they have a Δ^5 olefin previously not encountered in this diterpene series. Additional isocopalane diterpenes isolated from *D. verrucosa* included (**2.27-2.30**)[70] and the rearranged isocopalane diterpenes (**2.31**)[70] and (**2.32** and **2.33**)[72] Compounds **2.29** and **2.30** are the only chlorinated isocopalane diterpenes reported in the chemical literature. Diterpene **2.31** is unusual in that it is the product of two methyl migrations (C-20 from C-10 to C-9 and C-18 from C-4 to C-5) and is also the only rearranged isocopalane possessing a Δ^4 olefin.

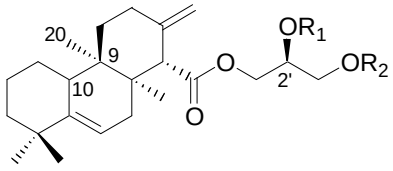

2.22 R_1 = H; R_2 = Ac
2.23 = Ac; R_2 = H

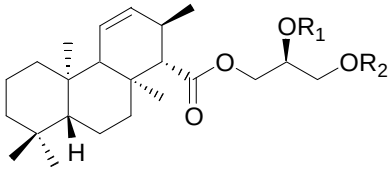

2.27 R_1 = H; R_2 = Ac
2.28 = Ac; R_2 = H

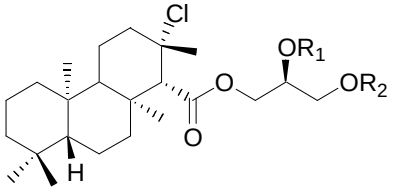

2.29 R_1 = H; R_2 = Ac
2.30 = Ac; R_2 = H

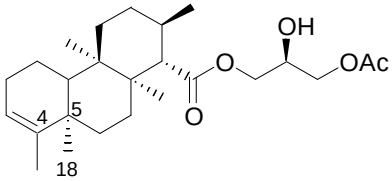

2.31

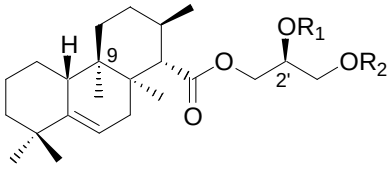

2.32 R_1 = H; R_2 = Ac
2.33 = Ac; R_2 = H

Of the non-isocopalane metabolites isolated from *D. verrucosa*, (**2.34**) is the most significant, as it appears to be the biosynthetic precursor to all the verrucosins. The absolute configuration at C-2' of **2.34** was proven synthetically[70] and consequently allowed the researchers to make use of biogenetic considerations when proposing the absolute configuration of the verrucosins.[70]

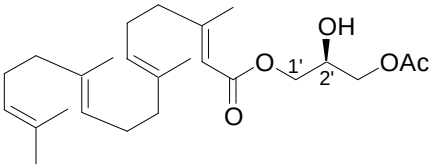

2.34

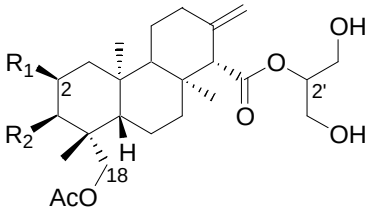

2.35 R_1 = OAc, R_2 = H
2.36 R_1 = H, R_2 = OAc

Although all the acylglyceride isocopalane and *ent*-isocopalane diterpenes discussed thus far have been linked to their glycerol substituents through esterification at C-1', austrodorins A and B (**2.35** and **2.36**), isolated from *Austrodoris kerguelenensis*, collected near the Shetland Islands, Antarctica, are exceptions to this rule and are 2'-monoglyceryl esters.[73] Austrodorins A and B have additional oxidation at C-18 and at either C-2 or C-3 respectively and were assigned to the isocopalane diterpene series by comparison of CD data with those of related isocopalane diterpenes.

2.2.2 Isocopalanes and ent-isocopalanes from marine sponges

Cimino *et al*.[74] isolated three new *ent*-isocopalanes (**2.37**-**2.39**) from *Spongia officianalis.* These metabolites were assigned to the *ent*-isocopalane series after reduction of **2.37** yielded (**2.40**) with known absolute configuration.[67] Further confirmation of the absolute configuration of **2.37** and **2.38** was provided by the semi-synthesis of these compounds from copalic acid.[75] The X-ray structure of **2.37** has also subsequently been published.[76]

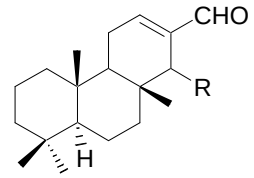

2.37 R = β-CHO
2.38 R = α-CHO
2.39 R = β-CH_2OAc
2.41 R = β-CH_2OH

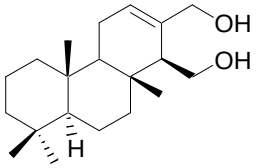

2.40

Six *ent*-isocopalane diterpenoids, the new saponified analogue of **2.39**, (**2.41**) and new metabolites (**2.42** and **2.43**) plus three known diterpenes, **2.37**-**2.39**, were isolated from the Mediterranean sponge, *S. zimocca.*[77] Comparison of the CD spectra of **2.38**, **2.39** and **2.42** with that of polygodial (**2.44**) confirmed the absolute stereochemistry of **2.37**-**2.39**, **2.41** and **2.42**. Surprisingly, the relative stereochemistry proposed for **2.43** was based solely on **2.43** having a similar C-7 ^{13}C NMR chemical shift to **2.39**. No explanation as to the significance of this particular single shift to the assignment of the relative stereochemistry of **2.43** was provided.

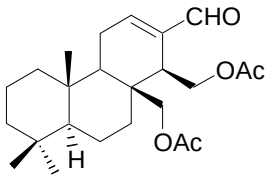

2.42

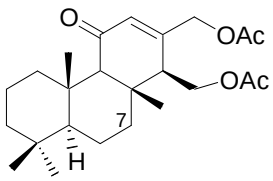

2.43

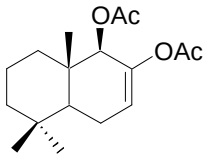

2.44

Mycgranol (**2.45**) isolated from the Kenyan sponge *Mycale* aff. *graveleyi* by Rudi *et al*.[32] is the only example of an isocopalane diterpene isolated from a marine sponge. The relative configuration of this compound was determined from ROESY data, while the absolute configuration was established from the Cotton effect observed in the CD spectrum of **2.45**, in which an *S* configuration at C-1 was implied from application of the octant rule to this compound.[78]

The most recent *ent*-isocopalane diterpenes to have been isolated from sponges are coelodiol (**1.37**) and coeloic acid (**2.46**) from the Indonesian sponge *Coelocarteria* cfr. s*ingaporensis*.[59] Coelodiol shows the same oxygenation pattern at C-1 and C-2 as previously noted in **2.45** but with the opposite configuration at C-1. Of further interest is that **2.46** is the first reported diterpene with a seco-norisocopalane type skeleton, in which oxidative cleavage of the C-1-C-2 bond in the *ent*-isocopalane skeleton has occurred. In order to determine the absolute configuration of **1.37**, the 1,2-dibenzoate derivative of the compound was prepared and the non-empirical exciton chirality CD method applied.[79] The negative sign of the Cotton effect at 236 nm was linked to the chirality at C-1 and C-2.[59] Compound **1.37** was accordingly assigned to the *ent*-isocopalane series, which is commonly found in sponges (and has recently been isolated from the nudibranch *Hexabranchus sanguineus*).[58] Although a paucity of **2.46** precluded the use of the exciton chirality effect to determine the absolute configuration of this compound, biogenetic arguments suggested that **2.46** also belonged to the *ent*-isocopalane series.

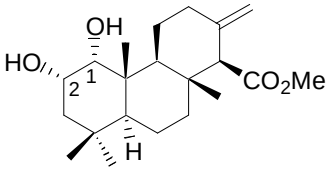

1.37

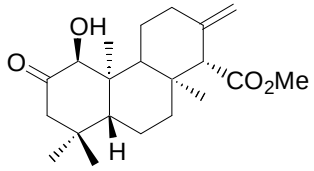

2.45

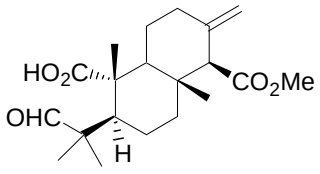

2.46

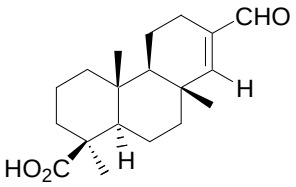

2.47

A further *ent*-norisocopalane (**2.47**) was isolated from the Micronesian sponge, *Coscinoderma mathewsi* in addition to four spongian metabolites.[80] The absolute configuration for **2.47** was based on the co-occurrence of this compound with related spongian diterpenes of known absolute configuration.

2.3 Selected syntheses of isocopalane and *ent*-isocopalane diterpenes

A number of different synthetic routes have been used to synthesize isocopalane and *ent*-isocopalane diterpenes.[*e.g.*60;61;63;64;70;75;81-83] As mentioned previously, the first synthesis of a naturally occurring isocopalane was by Imamura and Rúveda.[60] Other syntheses include that of Herz and Prasad[81] who synthesized *ent*-isocopalane compounds for use as standards to evaluate the presence of these compounds in crude oils. Although isocopalane-like compounds are routinely found in sediments and crude oils[*e.g.*84-86] they are thought to be either degradation products of naturally occurring resins or generated from kerogens.[85] Interestingly, the proportions of these tricyclic diterpenes are indicative of the conditions (*e.g*. temperature, pressure) to which the sedimentary rocks have been subjected and as a consequence they are regularly used as biomarkers.[81]

Since we report here the isolation of **2.2** and **2.3** from a Southern Ocean nudibranch and diterpene synthesis forms a major component of the research described in this thesis, we have decided to focus on the syntheses reported in the chemical literature for these two known compounds. Ungur *et al.*[83] first attempted a synthesis of **2.2** and **2.3** from cyclization of geranylgeranoic acid, (**2.46**, Scheme 2.2). From this superacid mediated cyclization they obtained racemic mixture of acids (**2.47** and **2.48**), which they converted *in situ* to the corresponding acid chlorides (**2.49** and **2.50**). The crude reaction mixture of **2.49** and **2.50** was then coupled with (–)-2,3-*O*-isopropylidene-*sn*-glycerol to yield a mixture of glycerides (**2.51** and **2.52**). Acid catalyzed hydrolysis of the acetonide protecting group afforded the diols (**2.53**) and **2.11**. The method for the coupling and deprotection steps had already been well-established.[87] Unfortunately, it was found that **2.53** and **2.11** were chromatographically inseparable (no details of attempted chromatographies were provided)[83] and an alternative route to **2.53** and **2.11** was required.

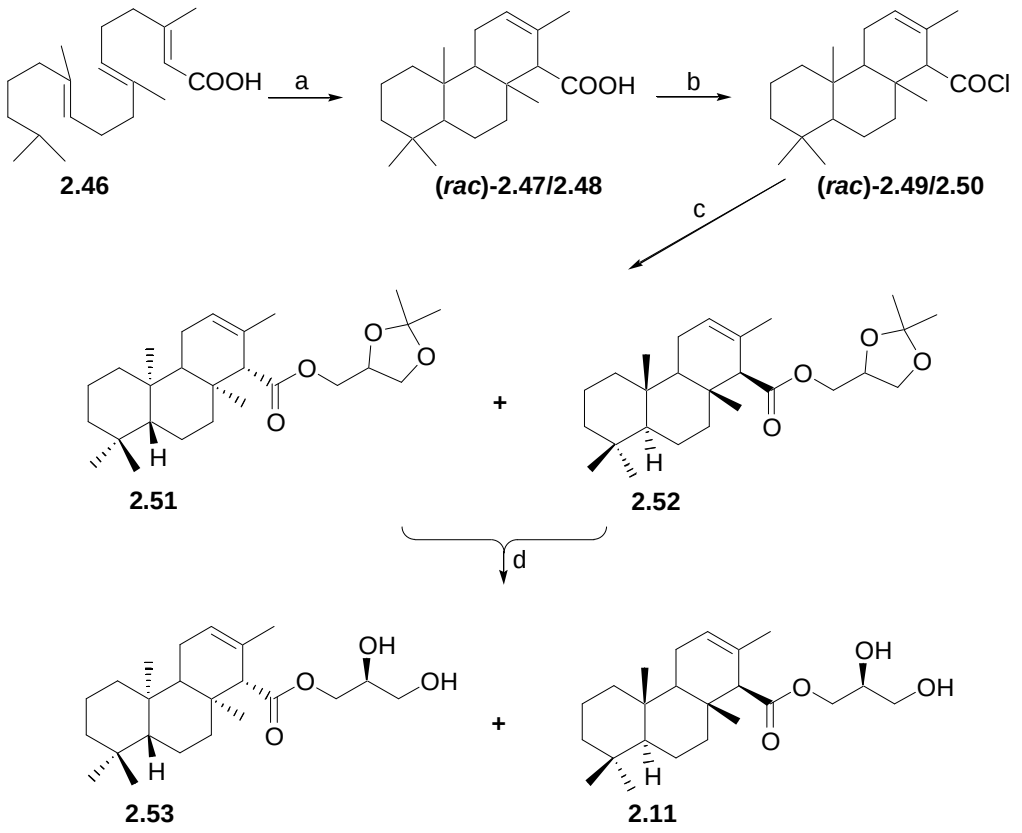

Scheme 2.2 Ungur *et al.'s* first attempt at the synthesis of acylglycerols **2.11** and **2.53** from geranylgeranoic acid, **2.46**.[83] *Reagents and conditions*: (a) FSO_3H, *i*-$PrNO_2$, -78 ℃, 40 min, then Et_3N; (b) $(COCl)_2$, C_6H_6, RT, 2 h, then 45 ℃, 0.5 h; (c) (–)-2,3-*O*-isopropylidene-*sn*-glycerol, NaH, dry CH_2Cl_2, 0 ℃, 20 min, then RT, 10 min h; (d) H_2SO_4, MeOH, RT, 4 h.

Since Ungur *et al.*[83] had failed to separate **2.53** and **2.11**, they required optically active precursors in their synthesis. To this end, they synthesized **2.47** (Scheme 2.3) from naturally occurring isocopalic acid (**2.54**), isolated from Copaiva Balsam.[70] Thereafter the same method as described in Scheme 2.2 (steps b-d) was followed to obtain (**2.53**).[83] Once **2.53** had been obtained, they used the established protocol of Fontana *et al.*[87] for the regioselective synthesis of diacylglycerides **2.2** and **2.3** (Scheme 2.4). Compound **2.2** was readily synthesized by preferentially acetylating the terminal primary alcohol of **2.53** with *N*-acetylimidazole, while **2.3** could be produced by selectively protecting the primary alcohol, acetylating the secondary alcohol and then removing the tertiary butyldimethylsilyl (TBDMS) protecting group.

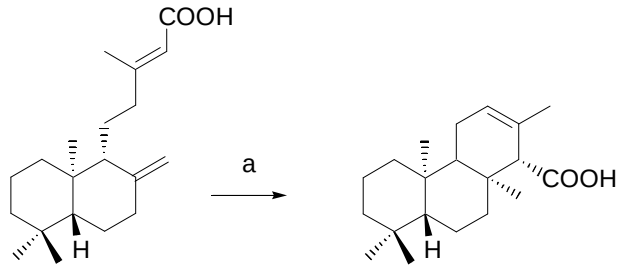

2.54 **2.47**

Scheme 2.3 Synthesis of isocopalic acid, **2.47**, from optically active **2.54**.[83] *Reagents and conditions*: (a) FSO_3H, *i*-$PrNO_2$, -78 ℃, 0.7 h, then Et_3N.

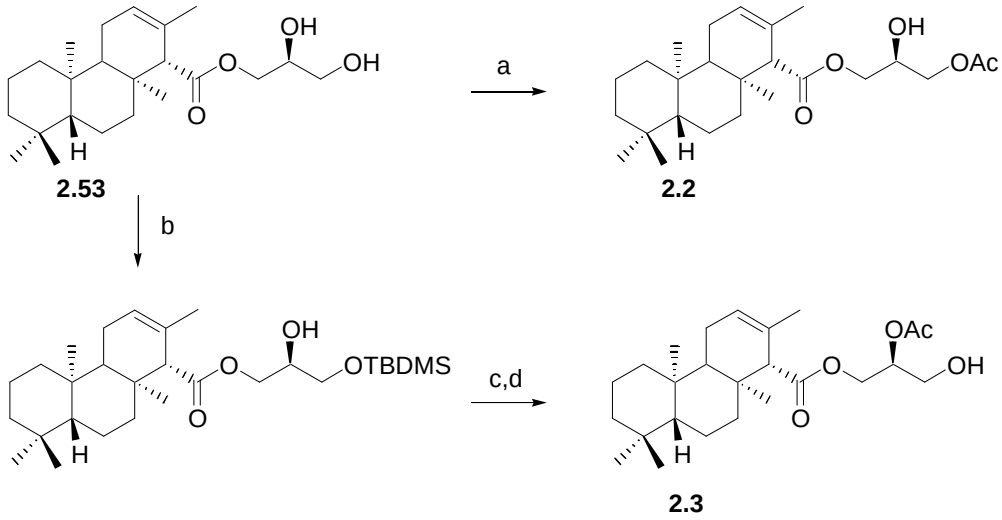

2.53 **2.2** **2.3**

Scheme 2.4 Method for the selective preparation of **2.2** and **2.3** from **2.53**.[83] *Reagents and conditions*: (a) *N*-acetylimidazole, DBU, C_6H_6, RT, 1 h; (b) TBDMSCl, dry pyridine, RT, 12 h; (c) Ac_2O, dry pyridine, RT, 12 h; (d) $PdCl_2(MeCN)_2$, RT, 1h.

2.4 Chemical ecology and bioactivity studies

Of all the isocopalane-type diterpenes isolated, the acylglycerides from nudibranchs have been the most extensively studied. While some nudibranchs sequester toxic compounds from their invertebrate prey (for example sponges or bryozoans),[88] and store these toxic metabolites in their mantle tissue as a feeding deterrent to predators, others have been shown to synthesize their allomones *de novo*.[89;90] The *de novo* biosynthesis of diterpene

diacylglycerides has been reviewed.[89] The general consensus is that the known 1'- and 2'-acylglycerols discussed in this chapter are synthesized *de novo* by the nudibranchs from which they have been isolated.[65;66;69;70;89;90]

In common with a general trend observed in diterpene acylglycerides,[17] many isocopalane acylglycerides (**2.2**-**2.3, 2.13**-**2.14**, **2.22**-**2.23**, **2.27**, **2.29**-**2.30** and **2.32**) have ichthyotoxic properties.[4;66;68;72] The first report that isocopalane acylglycerols were toxic to fish was published by Cimino *et al*.[72] who reported that **2.22** and **2.23** were toxic to the mosquito fish (*Gambusia affinis*) at concentrations between 1.0 and 0.1 *µ*g/mL respectively. Metabolites **2.13** and **2.14**, amongst the earliest isocopalanes isolated, were also found to be toxic to *G. affinis* at similar concentrations. Many of the verrucosins have been screened in a *Hydra* tentacle regeneration assay and have been shown to possess protein kinase C (PKC) stimulatory effects.[4;70;91]

Of all the isocopalanes isolated from sponges, only coelodiol and coeloic acid have any reported biological activity.[59] Both these compounds, **1.35** and **2.44**, were assayed against the MKN-45 cell line (human gastric adenocarcinoma) and were found to have moderate *in vivo* cell growth inhibition properties (20 µg/mL and 40 µg/mL) respectively.[59]

2.5 Known isocopalane diterpenes from an unidentified sub-Antarctic nudibranch

As part of an ongoing interdepartmental collaboration between the Southern Oceans Research Group and the Marine Natural Products Research Group at Rhodes University, we were fortunate enough to participate in the 2005 Marion Island re-supply expedition on board the *SA Agulhas* in April 2005 (Figure 2.1). The primary reason for this voyage was to transport a relief team of scientists to Marion Island, situated at 46°52'34" S, 37°51'32" E in the Southern Ocean (Figure 2.2), where South Africa maintains a base for meteorological and ecological research. During the re-supply of the South African base on Marion Island, the *SA Agulhas* was used for oceanographic research and we were permitted to dredge around the islands. Our interest in dredging around Marion Island lay in the fact that this island lies on the

border of the Polar Antarctic Convergence Zone and no marine natural product studies had previously been carried out around this island. Although we were specifically targeting sponge material as part of an ongoing anti-oesophageal cancer study, we were gratified to collect one large pale yellow nudibranch (Figure 2.1) from a dredge at a depth of *ca.* 115 m (Figure 2.3). The specimen was immediately frozen and stored at -20 ℃ until it could be extracted with acetone. The specimen was subsequently steeped in acetone for a period of four months, sonicated and the solvent removed, before again being steeped in acetone for a further week. The two acetone extracts were then combined and adsorbed onto a column of polystyrene-divinylbenzene stationary phase (HP-20), manufactured by Diaion and supplied by Supelco.

Figure 2.1 The *SA Agulhas* under anchor off the coast of Marion Island (top) and the unidentified nudibranch collected off the Marion Island coast (bottom).

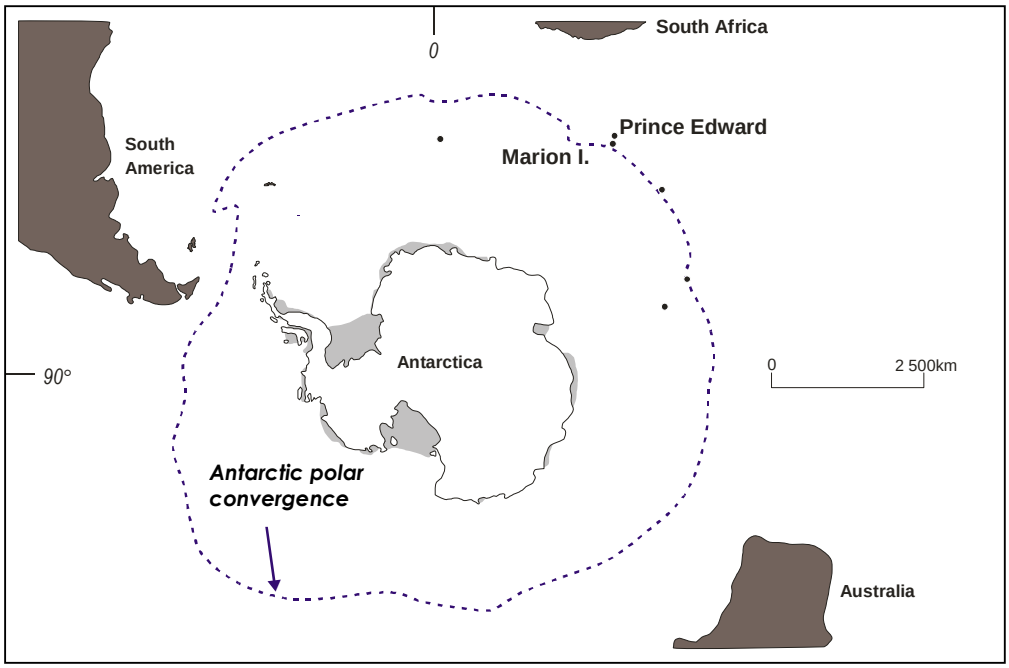

Figure 2.2 The position of Marion Island in the Southern Ocean.

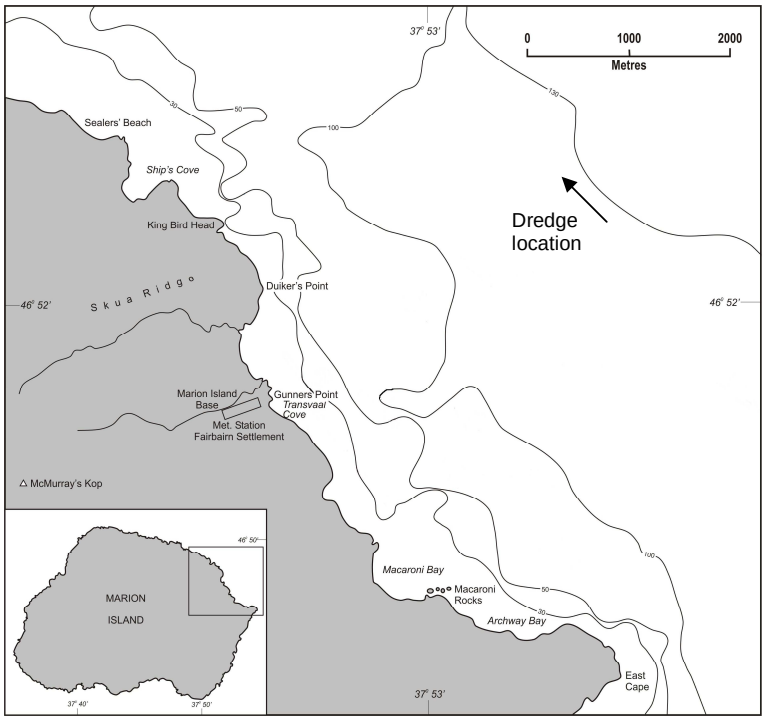

Figure 2.3 Collection site for the unidentified Marion Island nudibranch.

HP-20 chromatography is a reversed phase technique, in which the compounds being separated from one other are first adsorbed onto a polystyrene-divinylbenzene stationary phase before being sequentially stripped from the column with eluting solvents of decreasing polarity.[92] As a general rule, loading of an HP-20 column should not exceed 25 mg of crude extract per mL of HP-20 resin.[92] For our purposes, the marine organisms and terrestrial plant material (See Chapter Four) investigated were extracted with a water-miscible solvent (we used acetone for extraction and elution purposes in the research described in this thesis but methanol may also be used). The non-polar organic metabolites in the acetone extract were adsorbed onto the HP-20 resin beads by passing it through the column. The eluent was collected and diluted to approximately 50% of the original acetone concentration with water before being passed through the column a second time. Aqueous dilution of the acetone eluent facilitated the adsorption of semi-polar and polar organic metabolites onto the HP-20 beads.[92] This procedure was repeated until the final concentration of the acetone in the eluent passing through the column was deemed to be approximately 12.5%. At each stage, care was taken that no precipitate formed in the solution and if precipitation occurred, acetone would be added until the precipitate re-dissolved and this extract would then be passed through the column before continuing with the dilution as described above. Once the extract had reached a final concentration of 12.5% acetone and had been passed through the column, the HP-20 was washed with three column volumes of water to remove any salts remaining on the column and was then eluted with aliquots of aqueous acetone of decreasing polarity, beginning with 20% aqueous acetone and ending with 100% acetone, thus affording crude fractionation of the original acetone extract.[92] Details of the concentration of the eluting solvents used in all extractions are clearly indicated in the isolation scheme presented in this chapter (Scheme 2.5). Generally, any water-containing fractions once collected were diluted to about 30% of their original concentration with water and respectively passed through a second, smaller, HP-20 column to be re-adsorbed.[92] Once loaded, the second column was stripped with 100% acetone, thus avoiding the difficulty of *in vacuo* removal of an aqueous acetone solvent mixture using a rotary evaporator.

As the isolation procedures used in this thesis are described here for the first time, more detail will be presented. After stripping the HP-20 column sequentially with 20%, 40%, 60% and 80% aqueous acetone and, finally, with 100% acetone, the ^{1}H NMR spectra of each of these fractions were scrutinized for methyl singlets in the range 0.7-2.2 ppm. Of these five fractions, only the 80% aqueous acetone and 100% acetone fractions showed the methyl NMR resonances characteristic of diterpenes. These fractions were consequentially loaded onto a Diol column (transferred in 5% ethyl acetate in hexane) and were eluted with the eight increasingly polar aqueous acetone solvent combinations as indicated by Scheme 2.5.

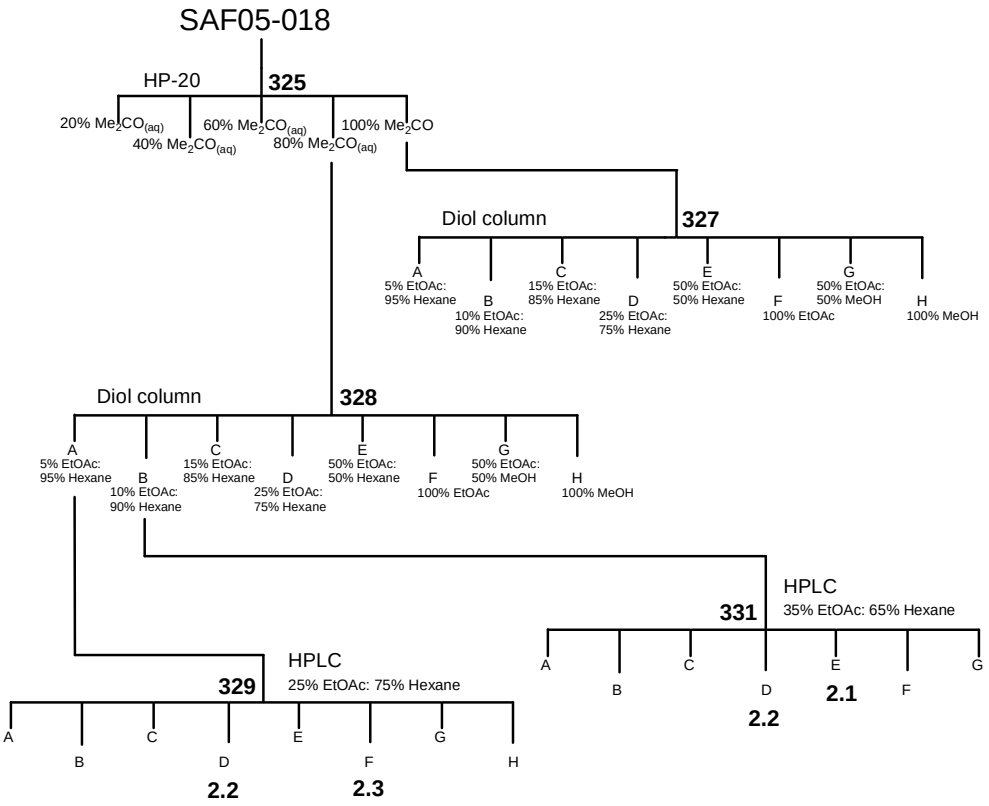

Scheme 2.5 Isolation scheme of compounds **2.2**, **2.3** and **2.1** from an acetone extract of the nudibranch (SAF05-018).

Diol is a derivatised silica based stationary phase that is suitable for elution with both polar and non-polar solvents. Dipole-dipole interactions between the solute and stationary phase in Diol chromatography are reduced (leading to fewer irreversible bindings between compounds and the stationary phase)[93] when compared with ordinary silica stationary phase making Diol superior to silica for many natural product isolations. The ^{1}H NMR spectra of each of the Diol chromatography fractions were analyzed again and two fractions, both originally from the 80% aqueous acetone fraction, 328-A (5% ethyl acetate, 95% hexane fraction) and 328-B (10% ethyl acetate, 90% hexane fraction) contained methyl singlet resonances characteristic of diterpenoid metabolites. Fraction 328-A was then subjected to normal phased semi-preparative HPLC (25% ethyl acetate, 75% hexane). Of the eight fractions collected, 329-D (19 mg, $[\alpha]_D$ = +10) and 329-F (10 mg, $[\alpha]_D$ = +21) were pure compounds and standard 1D and 2D data sets of each of these compounds were obtained. Through analysis of the ^{1}H and ^{13}C NMR spectra it was immediately apparent that the two isolates were closely related C-25 compounds, each containing two acetyl functionalities. This information, coupled with the presence of four methyl singlets and characteristic oxymethine and oxymethylene glycerides resonances (δ_H 4.23-4.35) allowed us to conclude that the compounds were either the isocopalane glycerides **2.2** and **2.3** or the ent-isocopalanes **2.13** and **2.14**. Since the ^{1}H NMR data for diastereomers **2.3** and **2.14** and both ^{1}H and ^{13}C NMR data for diastereomers **2.13** and **2.2** were available,[68] we were able to compare our NMR chemical shift and multiplicity data directly with the published data (Table 2.1 and Table 2.2) but were unable to draw any conclusions from the NMR data as to which enantiomeric series 329-D and 329-F belonged. Since only the *S* configuration at C-2' in the glyceryl side-chain has been found in marine acylglyceride diterpenes (reports of acylglycerols with an *R* configuration at C-2' have been erroneous),[2;4;47] application of the modified Mosher's method to determine the configuration at C-2' was not deemed necessary.

Table 2.1 ^{1}H and ^{13}C NMR data for compounds **2.2**[68], **2.13**[68] and 329-D.

	2.2[†]		**2.13**[†]		329-D[‡]	
Position	δ_C (mult.)	δ_H[§]	δ_C (mult.)	δ_H[§]	δ_C (mult.)	δ_H (int.,mult., *J*/ Hz)
1	39.9 (t)	0.80	39.8 (t)	0.80	39.9 (t)	0.79 (1H, m)
		1.62		1.61		1.62 (1H, m)
2	18.6 (t)	1.38	18.6 (t)	1.38	18.6 (t)	1.36 (1H, m)
		1.57		1.58		1.57 (1H, m)
3	41.8 (t)	1.14	41.8 (t)	1.14	41.8 (t)	1.11 (1H, m)
		1.38		1.38		1.36 (1H, m)
4	33.0 (s)	-	33.1 (s)	-	33.2 (s)	-
5	56.4 (d)	0.85	56.4 (d)	0.84	56.4 (d)	0.83 (1H, m)
6	18.5 (t)	1.38	18.4 (t)	1.38	18.5 (t)	1.35 (1H, m)
		1.57		1.58		1.57 (1H, m)
7	41.8 (t)	1.38	41.8 (t)	1.38	41.8 (t)	1.36 (1H, m)
		1.70		1.70		1.70 (1H, m)
8	37.5 (s)	-	37.4 (s)	-	37.4 (s)	-
9	54.2 (d)	1.16	54.2 (d)	1.16	54.3 (d)	1.14 (1H, dd, 11.1, 6.0)
10	36.5 (s)	-	36.6 (s)	-	36.6 (s)	-
11	22.7 (t)	1.95	22.6 (t)	1.95	22.7 (t)	1.94 (2H, m)
12	124.4 (d)	5.53	124.3 (d)	5.53	124.3 (d)	5.51 (1H, m)
13	128.5 (s)	-	128.5 (s)	-	128.5 (s)	-
14	62.5 (d)	2.96	62.5 (d)	2.96	62.5 (d)	2.95 (1H, m)
15	[⊥]	-	173.0	-	173.0 (s)	-
16	21.2 (q)	1.60	21.2 (q)	1.60	21.2 (q)	1.59 (3H, br s)
17	15.6 (q)	0.95	15.6 (q)	0.94	15.6 (q)	0.94 (3H, s)
18	21.6 (q)	0.81	21.6 (q)	0.81	21.7 (q)	0.80 (3H, s)
19	33.4 (q)	0.86	33.4 (q)	0.86	33.4 (q)	0.85 (3H, s)
20	15.7 (q)	0.90	15.7 (q)	0.90	15.7 (q)	0.90 (3H, s)
21	64.9 (t)	4.12	64.8 (t)	4.12	64.9 (t)	4.14 (2H, m)
		4.24		4.22		
22	68.4 (d)	4.12	68.4 (d)	4.10	68.4 (d)	4.08 (1H, m)
23	65.3 (t)	4.12	65.3 (t)	4.12	65.3 (t)	4.11 (1H, m)
		4.24		4.22		4.19 (1H, m)
OAc	[⊥]	-	[⊥]	-	171.0 (s)	-
	20.8 (q)	2.11	20.8 (q)	2.11	20.8 (q)	2.09 (3H, s)

[†] ^{1}H NMR (500 MHz, $CDCl_3$, referenced to C<u>H</u>Cl_3 at 7.26 ppm); ^{13}C NMR (125 MHz, $CDCl_3$, referenced to <u>C</u>DCl_3 at 77.0 ppm). [‡] ^{1}H NMR (400 MHz, $CDCl_3$, referenced to C<u>H</u>Cl_3 at 7.25 ppm); ^{13}C NMR (100 MHz, $CDCl_3$, referenced to <u>C</u>DCl_3 at 77.0 ppm); [§] Multiplicities not reported; [⊥] Not detected.

Table 2.2 ^{1}H NMR data for compounds **2.3**[68] and **2.14**[68] and ^{1}H and ^{13}C NMR data for 329-F.

	2.3†	**2.14**†	329-F‡	
Position	δ_H§	δ_H§	δ_C (mult.)	δ_H (int., mult., *J*/ Hz)
1	0.80	0.80	39.9 (t)	0.80 (1H, m)
	1.62	1.61		1.62 (1H, m)
2	1.38	1.38	18.7 (t)	1.37 (1H, m)
	1.57	1.58		1.55 (1H, m)
3	1.13	1.14	41.9 (t)	1.13 (1H, m)
	1.38	1.38		1.37 (1H, m)
4	-	-	33.2 (s)	-
5	0.85	0.84	56.4 (d)	0.84 (1H, dd, 11.1, 6.0)
6	1.38	1.38	18.5 (t)	1.37 (1H, m)
	1.57	1.58		1.55 (1H, m)
7	1.38	1.38	41.8 (t)	1.37 (1H, m)
	1.68	1.68		1.69 (1H, m)
8	-	-	37.4 (s)	-
9	1.15	1.15	54.3 (d)	1.16 (1H, m)
10	-	-	36.6 (s)	-
11	1.95	1.95	22.7 (t)	1.94 (2H, m)
12	5.52	5.53	124.3 (d)	5.51 (1H, m)
13	-	-	128.5 (s)	-
14	2.94	2.95	62.5 (d)	2.93 (1H, m)
15	-	-	172.8 (s)	-
16	1.60	1.60	21.2 (q)	1.59 (3H, br s)
17	0.93	0.93	15.6 (q)	0.93 (3H, s)
18	0.81	0.83	21.7 (q)	0.81 (3H, s)
19	0.86	0.86	33.4 (q)	0.85 (3H, s)
20	0.90	0.90	15.7 (q)	0.90 (3H, s)
21	4.23	4.27	61.7 (t)	4.21 (dd, 12.0, 5.8)
	4.35	4.34		4.34 (1H, dd, 12.0, 4.4)
22	5.10	5.07	72.4 (d)	5.08 (1H, apparent quintet, *J* = 5.1 Hz)
23	3.76	3.76	61.8 (t)	3.76 (2H, m)
OAc	-	-	170.6 (s)	-
	2.10	2.11	21.0 (q)	2.09 (3H, s)

† ^{1}H NMR (500 MHz, $CDCl_3$, referenced to $C\underline{H}Cl_3$ at 7.26 ppm); ‡ ^{1}H NMR (400 MHz, $CDCl_3$, referenced to $C\underline{H}Cl_3$ at 7.25 ppm); ^{13}C NMR (100 MHz, $CDCl_3$, referenced to $\underline{C}DCl_3$ at 77.0 ppm); § Multiplicities not reported.

Table 2.3 Specific rotations reported for previously isolated and synthesized **2.13**, **2.14**, **2.2** and **2.3** as well as 329-D and 329-F.

	Source			
Compound	*Archidoris montereyensis*	*Anisodoris fontaini*	Synthesis	Unidentified nudibranch
329-D	-	-		+10
329-F	-	-		+21
2.2	-	+21.9[68]	+13.9[83]	-
2.3	-	+66.9[68]	+10.2[87]	-
2.13	-53.7[66]	-	-47.7[83]	-
2.14	-33.0[66]	-	-41.8[83]	-

Zubia *et al*.[68] had ultimately made their determinations of whether their compounds were isocopalanes or *ent*-isocopalanes by comparison of the sign of the Cotton effect at 214 nm obtained from the circular dichroism spectra of **2.2**, **2.3**, **2.13** and **2.14**. Since circular dichroism (CD) facilities were unavailable in South Africa at the time this research was carried out, our first recourse to confirm the absolute configuration of the metabolites we had isolated was by comparison of the specific rotations of our compounds with those in the literature. A summary of comparative specific rotation data is given in Table 2.3. Fontana *et al.*[87] attributed the variation between the magnitude of the specific rotation of the synthetically produced **2.3** and the equivalent metabolite isolated from a natural source to the difficulties in accurately determining specific rotations of diminishing amounts (<3 mg) of a marine natural product. A general trend can nonetheless be inferred from the data presented in Table 2.3: the sign of the specific rotations of compounds **2.13** and **2.14** is always negative, while the sign of the specific rotation of **2.2** and **2.3** is always positive. We thus tentatively proposed that 329-D and 329-F belonged to the isocopalane series based on the positive sign of their specific rotations. Fortuitously, we were subsequently able to access CD facilities in the United States, and although we found that both 329-D and 329-F were unstable, we were able to reisolate a small amount of 329-D, sufficient to acquire the CD spectrum of this compound (Figure 2.4), from the original extract of SAF05-018. The positive CD curve at 216 nm was in accordance

with that reported for **2.2** and opposite to that recorded for **2.13**, and 329-D (and from biogenetic considerations 329-F) were thus allocated to the isocopalane series.

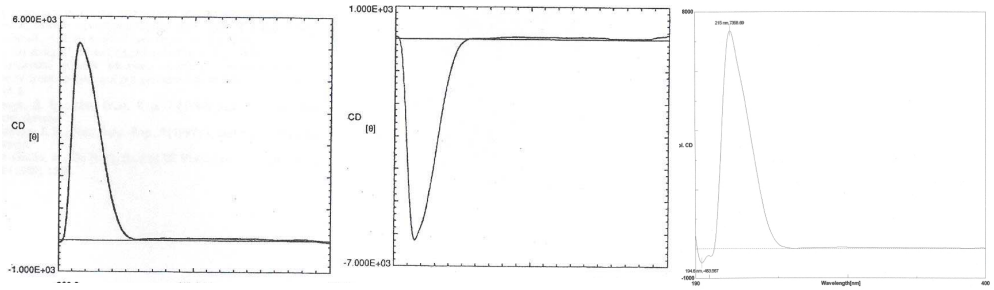

Figure 2.4 The CD curves of **2.2** (left)**,**[68] **2.13** (middle)[68] and 329-D (=**2.2**, right).

2.6 Identification of a new isocopalane diterpene from an unidentified sub-Antarctic nudibranch

A second diterpene-containing fraction from the Diol column (10% ethyl acetate, 90% hexane fraction) was subjected to normal phase semi-preparative HPLC (35% ethyl acetate, 65% hexane) and yielded two fractions of interest. The first of these was identified to be identical to 329-D, now determined to be **2.2**, but the second, minor fraction (**2.1**, 3 mg, $[\alpha]_D$ = +3) appeared to contain a new diterpene from analysis of its 600 MHz ^{1}H NMR spectrum.

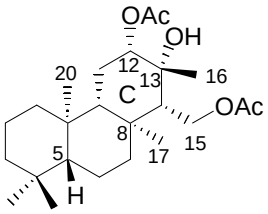

2.1

The molecular formula of **2.1** ($C_{24}H_{40}O_5$) was confirmed from HRFABMS data and implied five degrees of unsaturation. Analysis of the ^{13}C NMR data revealed the presence of two acetyl carbonyls (δ_C 169.3 and δ_C 169.7), which accounted for two of the degrees of unsaturation. Comparison of the ^{1}H and ^{13}C NMR data of **2.1** with those of **2.2** and **2.3** revealed that **2.1**

shared the same tricyclic skeleton as the former two compounds, which in turn accounted for the remaining three degrees of unsaturation. Further comparison of the NMR data for **2.1** with those of **2.2** and **2.3** indicated that the differences between **2.1** and **2.2** and **2.3** were limited to changes in the substitution pattern around ring C. The chemical shift assignments for rings A and B were thus initially made by analogy with those established for **2.2** and **2.3**, and further supported by extensive gCOSY and gHMBC correlations (Table 2.4). The most obvious difference in the NMR spectra of **2.1** when compared with those of **2.2** and **2.3** was the absence of the oxymethine and oxymethylene glyceride signals in addition to the loss of the Δ^{12} olefinic resonances in the ^{1}H and ^{13}C NMR spectra of the former compound. A three bond gHMBC correlation from H_3-17 (δ_H 1.41) to a methine carbon (δ_C 58.0) enabled assignment of the methine carbon as C-14 and hence the assignment of H-14 (δ_H 1.44) followed from gHSQC data. A gCOSY correlation between H-14 and two deshielded oxymethylene resonances (δ_H 4.15 and 4.27) allowed assignment of the oxymethylene carbon (δ_C 62.8) as C-15 from gHSQC data. Further confirmation of the assignment of C-15 was provided by three bond gHMBC correlations (Figure 2.5) between the oxymethylene protons H-15a (δ_H 4.15) and H-15b (δ_H 4.27) and both C-8 (δ_C 38.7) and an acetyl carbonyl (δ_C 169.7). A further three bond gHMBC correlation from the two C-15 oxymethylene proton resonances allowed placement of the deshielded quaternary carbon, C-13 (δ_C 74.6), the chemical shift of which was characteristic of an oxygenated quaternary carbon. A two bond gHMBC correlation from H_3-16 (δ_H 1.12 ppm) to C-13 confirmed the presence of the methyl group at this position, while a further three bond correlation from these methyl protons to C-14 further confirmed this assignment. An additional gHMBC correlation from H_3-16 to an oxymethine carbon (δ_C 78.3) led to the assignment of this carbon as C-12. The presence of the acetyl functionality at C-12 was provided by a three bond gHMBC correlation from H-12 (δ_H 5.01) to the remaining acetate carbonyl (δ_C 169.3).

Table 2.4 ^{1}H (600 MHz, C_6D_6), ^{13}C (150 MHz, C_6D_6) and 2D NMR data obtained for **2.1**.

Position	δ_C (mult.)	δ_H (int., mult., *J*/Hz)	gHMBC	gCOSY
1a	40.5 (t)	0.69 (1H, m)	20	1b, 2
1b		1.57 (1H, m)		1a, 2
2	18.9 (t)	1.32 (2H, m)	-	1a, 1b, 3a
3a	42.3 (t)	1.09 (1H, m)	2, 4	2, 3b
3b		1.34 (1H, m)	-	3a
4	33.5 (s)	-	-	-
5	57.2 (d)	0.73 (1H, dd, 12.0, 2.2)	6, 7, 9, 10, 20, 18, 19	6a, 6b
6a	18.7 (t)	1.48 (1H, m)	8, 7, 10, 17	5, 7a, 7b
6b		1.50 (1H, m)	-	5, 7a, 7b
7a	39.1 (t)	1.30 (1H, m)	17	6
7b		1.53 (1H, m)	-	6
8	38.7 (s)	-	-	-
9	52.6 (d)	1.35 (1H, m)	8, 10, 11, 12, 20, 17	11
10	38.0 (s)	-	-	-
11β	23.7 (t)	1.76 (1H, m)	8, 9, 12, 13, 14, 12-OAc	9, 12
11α		1.80 (1H, m)	8, 10, 11, 12, 20, 17	9, 12
12	78.3 (d)	5.01(1H, dd, 11.2, 5.0)	11, 12-OAc	11a, 11b
13	74.6 (s)	-	-	-
14	58.0 (d)	1.44 (1H, m)	8, 9, 12, 13, 15, 20	15a, 15b
15a	62.8 (t)	4.15 (1H, dd, 12.8, 3.8)	8, 13, 14, 15-OAc	14
15b		4.27 (1H, dd, 12.8, 2.5)	8, 13, 14, 15-OAc	14
16	27.2 (q)	1.12 (s, 3H)	12, 13, 14	-
17	26.1 (q)	1.41 (s, 3H)	8, 9, 14	-
18	21.7 (q)	0.80 (s, 3H)	3, 4, 5, 19	-
19	33.6 (q)	0.83 (s, 3H)	3, 4, 5, 18	-
20	16.6 (q)	0.82 (s, 3H)	1, 9, 10	-
12-OAc	169.3 (s)	-	-	-
	20.6 (q)	1.65 (s, 3H)	12-OAc	-
15-OAc	169.7 (s)	-	-	-
	20.6 (q)	1.72 (s, 3H)	15-OAc	-

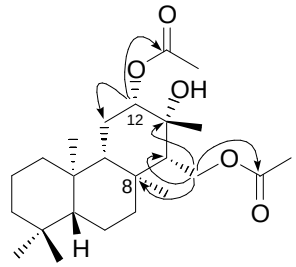

2.1

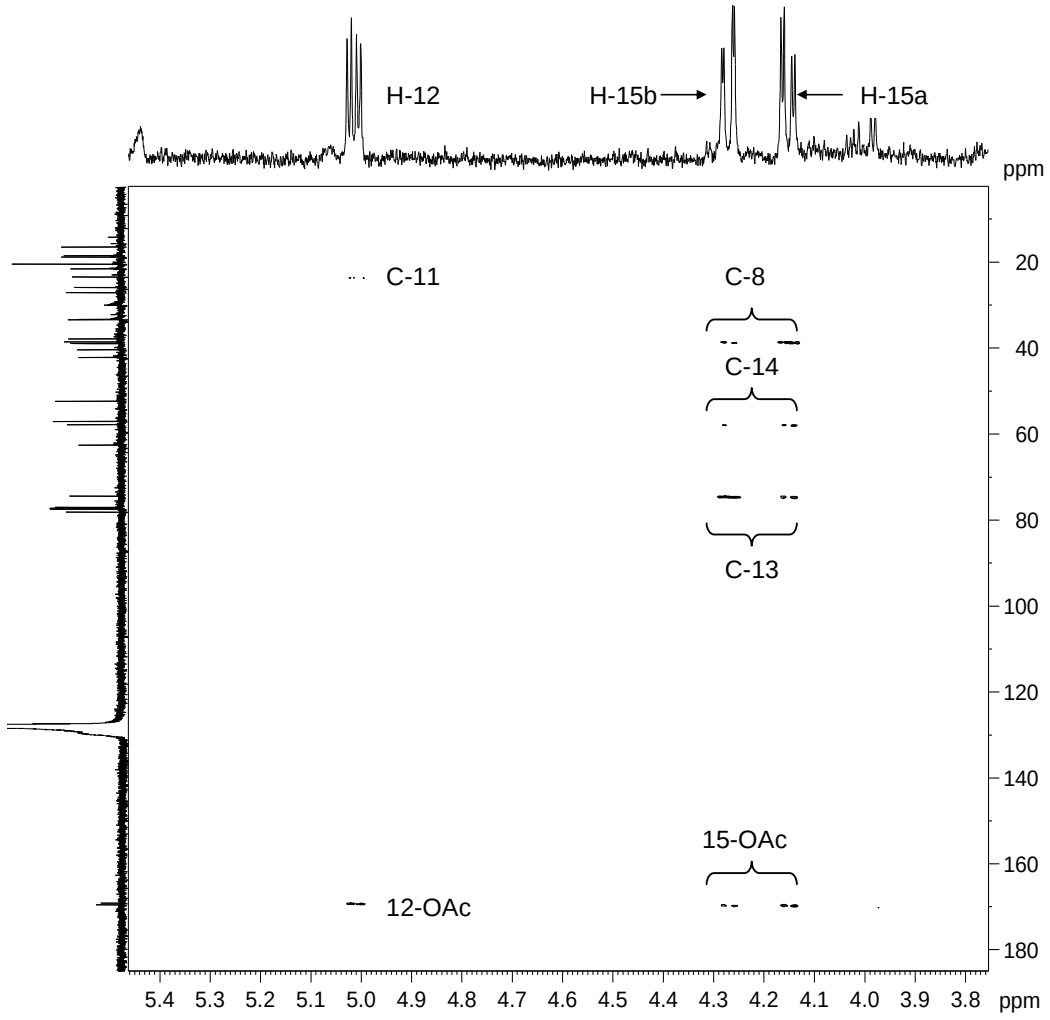

Figure 2.5 Downfield section (F1 = δ_C 10 – 180, F2 = δ_H 3.8 – 5.4) of the gHMBC spectrum (C_6D_6, 600 MHz) of **2.1**.

The relative configuration of **2.1** was determined from analysis of NOE data. Figure 2.6 indicates the key NOESY correlations used to determine the relative configuration of the molecule, while Figure 2.7 shows a section of the NOESY spectrum highlighting the correlations used to establish the relative configuration at C-12 and C-13 of **2.1**.

Vicinal coupling constants and NOESY correlations were used to assign the relative configuration of **2.1.** Of most importance were the NOESY correlations between H-5 (δ_H 0.73) and H-9 (δ_H 1.35), which in turn correlated to H-11β (δ_H 1.76). H-9 also correlated to both H-12 (δ_H 5.01) and H-14 (δ_H 1.44) while H-12 correlated with H-14 and H_3-16 (δ_H 1.12) implying a *cis* relationship between these three axial methine protons and Me-16. Further confirmation of the β-axial orientation of H-12 was derived from the large (axial-axial coupling to H-11α) and small (axial-equatorial coupling to H-11β) coupling values observed for H-12. A zero quantum coherence correlation between both H-11β (δ_H 1.76) and H-11α (δ_H 1.80) and H-12, was also present. These gCOSY-like peaks occasionally appear in NOESY spectra between *J*-coupled spin systems in small to mid-sized molecules.[94] The substituents at C-12 and C-14 were accordingly placed in α-equatorial positions while the hydroxyl functionality at C-13 could be assigned an α-axial position. An NOE correlation between axial H-11α (δ_H 1.80) and Me-17 (δ_H 1.41) and Me-20 (δ_H 0.82) in turn placed these methyl moieties in α-axial positions. Since **2.2** and **2.3** were isolated from the same organism they were determined to have an isocopalane tricyclic skeleton from CD data and biogenetic considerations. We have thus opted to show **2.1** as belonging to the same enantiomeric series as **2.2** and **2.3**.

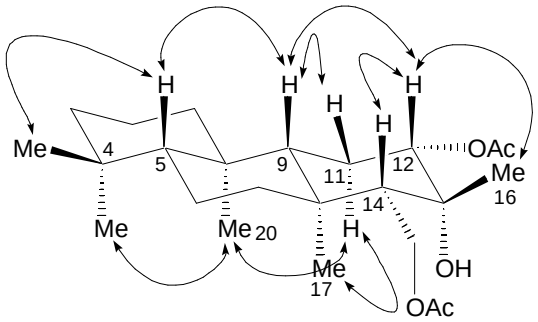

Figure 2.6 Key NOESY correlations in compound **2.1**.

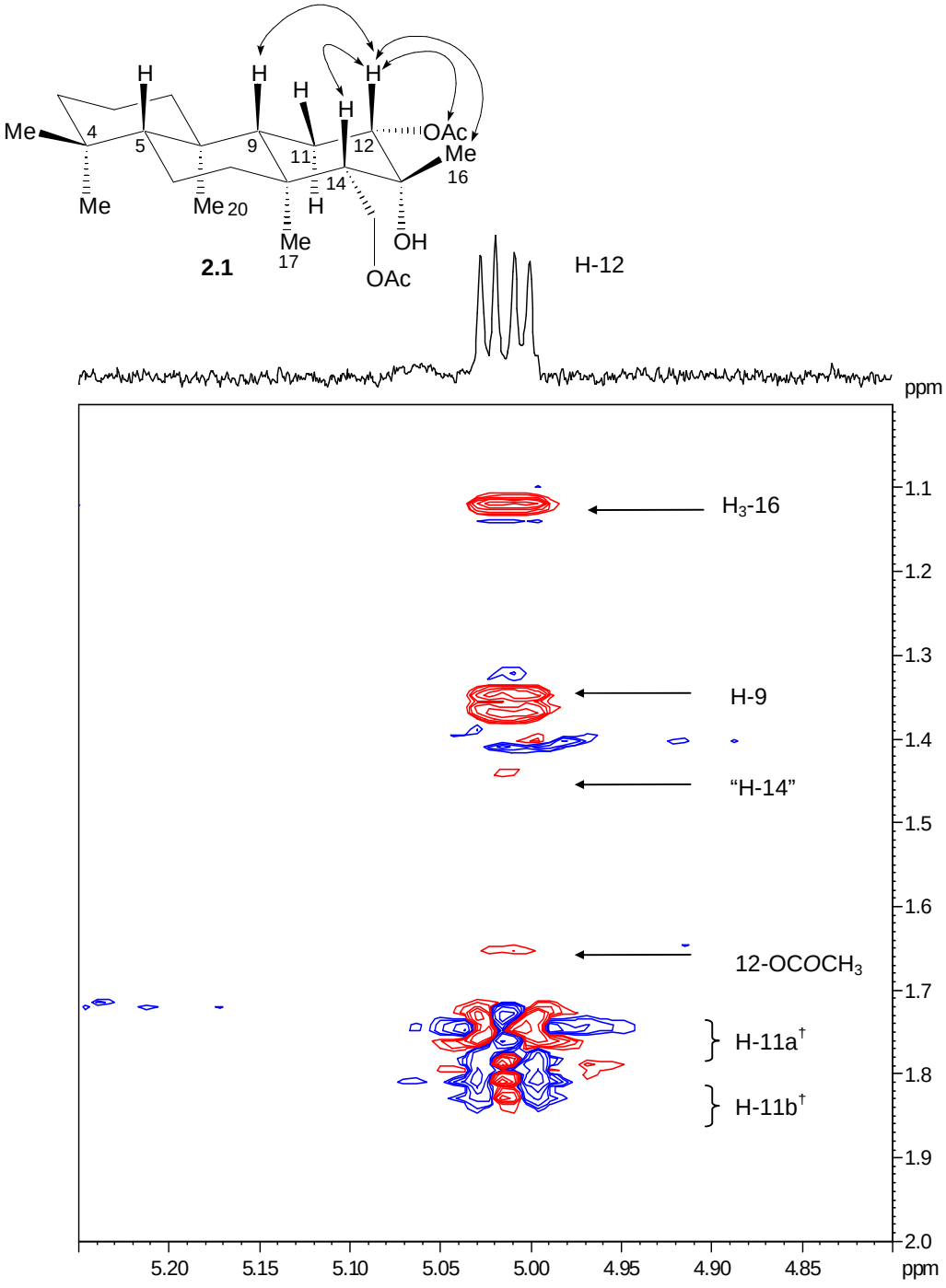

Figure 2.7 A section (F1 = δ_H 4.8 – 5.3, F2 = δ_H = 1.0 – 2.0) of the NOESY spectrum (C_6D_6, 600 MHz) of **2.1**. Red contours indicate positive peaks, blue contours indicate negative peaks. The accompanying figure shows the NOESY correlations to H-12 indicated in the spectrum.† Zero quantum coherences.[94]

2.7 Conclusions

Three rare isocopalane diterpenes, **2.2**, **2.3** and **2.1** were isolated from an unidentified sub-Antarctic nudibranch. The structures of the major components of the acetone extract of the nudibranch, **2.2** and **2.3**, were determined by comparison of ^{1}H and ^{13}C NMR data with those of known compounds. The absolute configuration of **2.2** was determined from the sign of the Cotton effect at 216 nm in comparison with the CD curves for known compounds **2.13** and **2.2**, allowing us to conclude that **2.2** was an isocopalane diterpene and **2.3** was hence assigned to the same series from biogenetic considerations. The minor component of the acetone extract of the nudibranch, **2.1**, was a new compound and was fully characterized spectroscopically. The relative configuration of **2.1** was determined from NOESY data and this compound was also proposed to have an isocopalane skeleton for biogenetic reasons.

Chapter Three

Labdane Diterpenes and Sterols from the South African Marine Pulmonate Mollusc, *Trimusculus costatus*

3.1 Introduction

Trimusculus costatus is an endemic, South African, intertidal, shell-less mollusc and the only known representative of the genus in Africa. Prompted by the successful reinvestigation of other *Trimusculus* species,[95-97] a reinvestigation of the secondary metabolites of *T. costatus* is presented in this chapter. The isolation, structure elucidation and antiproliferativer activity of two known 6β,7α-diacetoxylabda-8,13*E*-dien-15-ol (**3.1**) and 2α,6β,7α-triacetoxylabda-8,13*E*-dien-15-ol (**3.2**) and new 6β,7α,15-triacetoxylabda-8,13*E*-diene (**3.3**) labdane diterpenes, as well as new 3α,11-dihydroxy-9,11-seco-cholest-4,7-dien-6,9-dione (**3.4**) and cholest-7-en-3,5,7-triol (**3.5**) from *T. costatus* are described. The sterol, **3.5**, has never previously been isolated from a natural source. The introduction to this chapter provides an historical perspective of the chemistry, ecology and bioactivity studies of *Trimusculus* metabolites. The chiral derivatization strategies adopted to determine the relative and absolute configurations of the diterpenes isolated from *T. costatus* are also discussed.

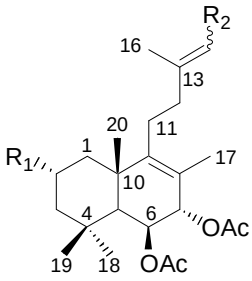

3.1 Δ^{13} *E* R_1 = H; R_2= CH_2OH
3.2 Δ^{13} *E* R_1 = OAc; R_2= CH_2OH
3.3 Δ^{13} *E* R_1 = H; R_2 = CH_2OAc
3.6 Δ^{13} *Z* R_1 = H; R_2 = CH_2OAc

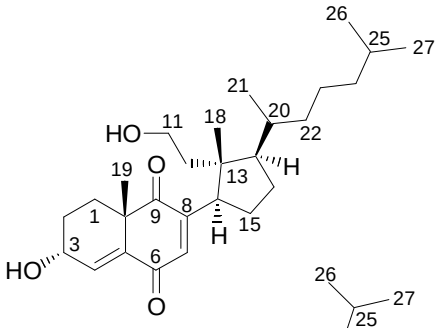

3.4

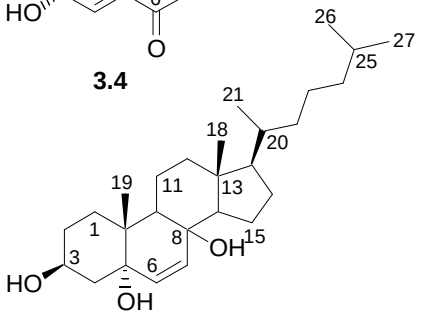

3.5

Diterpene **3.3** was determined to be the geometric isomer of the known diterpene (**3.6**), isolated from the Chilean *T. peruvianus*. The formation of the camphanate ester of **3.2** using (-)-camphanic acid and subsequent crystallization of this ester enabled the determination of the absolute configuration of **3.2** by X-ray crystallography. The structures of the steroidal metabolites **3.4** and **3.5** were determined using standard spectroscopic techniques, and the

relative configuration of these compounds was determined, where possible, from NOESY data. This chapter concludes with a discussion of the cytotoxicity of compounds **3.1**-**3.4** to oesophageal cancer cells.

3.1.1 Biology of Trimusculid molluscs

Members of the mollusc family Trimusculidae enjoy a global distribution and are generally found in the intertidal zone of rocky shores. As an adaptation to their intertidal habitat, trimusculids lack gills, instead relying on a modified mantle cavity to act as a lung.[98] They congregate in large colonies,[98] often living so closely together that their shells, with characteristically serrated edges, interlock like the pieces of a jigsaw puzzle. Trimusculids are prolific where they occur and, where population densities are high, they are often found living in layers on top of one another. Since the limpets live in shady rocky overhangs, algal growth is slow, reducing the significance of algae as a primary food source, typically exploited by other intertidal limpets.[11;98;99] *Trimusculus* species have, however, evolved a unique feeding method and use a mucous net, secreted by the mantle glands, to filter phytoplankton out of the water column.[98] The mucous net and trapped particles are ingested once the oral lobes detect the presence of food in the mucous net. A second form of mucous, distinct from that used for filter feeding has also been reported.[10;11;99-101] This milky white mucous, produced by numerous subepithelial glands situated in the mantle and sides of the foot,[98] is used as a chemical defence mechanism to deter predation and has developed as a direct consequence of the sessile, colonial lifestyle of these organisms.[10;11;99-101]

3.1.2 The natural products chemistry of Trimusculus species

Possibly prompted by Rice's[101] findings that the mucous secretions of *T. reticulatus* acted as a feeding deterrent for certain seastar species, Manker and Faulkner[99] performed the first investigation of the chemistry of the metabolites secreted by these pulmonates. Starting with 115 freeze-dried specimens of *T. reticulatus*, collected off the coast near San Diego, they were the first to isolate diterpene metabolites (**3.7** and **3.8**) from marine pulmonate molluscs.

The relative configuration of the B ring of **3.7** was determined through the reduction of **3.7** to the corresponding triol, followed by analysis of the $J_{5,6}$ and $J_{6,7}$ coupling constants. The *E* geometry of the Δ^{13} olefin in the alkenol side chain was presumably assigned from the ^{13}C NMR chemical shift of methyl C-16 (δ_C 16.2) and methylene C-12 (δ_C 39.1) in both **3.7** and **3.8**. An *E* configuration in similar olefins requires δ_C *ca*. 16 and *ca*. 39,[10;102] while a *Z* configuration requires δ_C *ca.* 24 and *ca.* 32).[97;100] The relative configuration of the B ring in **3.8** was assigned through comparison of the ^1H and ^{13}C NMR data of this compound with those of **3.7**, while the determination that H-2 was axial (from limited spectroscopic data) prompted the α-equatorial assignment of the acetyl functionality at C-2. The relative configuration of **3.7**, including the geometry of the exocyclic double bond was established *via* a synthesis of this compound by Gao *et al.*[102] A recent stereoselective synthesis of **3.7** (from *T. reticulatus*) by Pathak *et al.*[103] confirmed the absolute configuration of **3.7** and suggested that the metabolites secreted by *Trimusculus* species belong to the labdane, rather than the *ent*-labdane series of diterpenes. The respective syntheses of Gao and Pathak will be discussed later in this chapter.

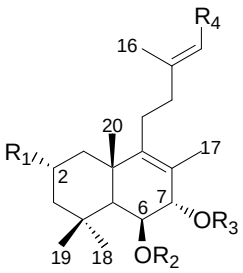

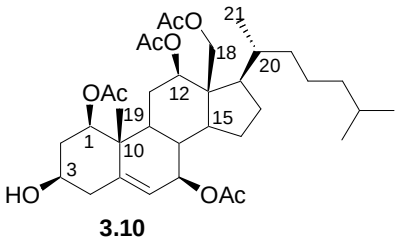

3.10

3.7 $R_1 = R_3 = H$; $R_2 = COCH_2CH(CH_3)_2$; $R_4 = CH_2OH$
3.8 R_1= OAc; $R_2 = COCH_2CH(CH_3)_2$; R_3 = Ac; $R_4 = CH_2OH$
3.9 $R_1 = H$; R_2 = Ac; $R_3 = COCH_2CH(CH_3)_2$; $R_4 = CO_2H$

Manker and Faulkner[11] returned to their investigations of *T. reticulatus* in 1996. Although their investigation was largely of an ecological nature, they also isolated two new compounds, (**3.9** and **3.10**), from another limpet, *T. conica*, collected in Anawhata Cove, North Island, New Zealand. Compound **3.9** was closely related to the compounds previously isolated from *T. reticulatus*, differing only in the presence of a carboxylic acid moiety in the side chain.

Compound **3.10**, however, was the first example of a steroidal metabolite isolated from *Trimusculus.*

The second species to be investigated, *T. peruvianus* has to date provided the largest diversity of secondary metabolites. The first specimens of this latter species, collected in El Tabo, V region, Chile, afforded (**3.11**).[104] San Martín *et al.*[97] later reported the isolation of (**3.6** and **3.12**-**3.14**) as well as a reisolation of **3.11**. Paradoxically, this time they assigned a *Z* geometry to the Δ^{13} olefin in **3.11**, in addition to the new diterpenes, **3.6** and **3.12**-**3.14**, suggesting a possible error in the second manuscript.[97] The diterpenes in the subsequent manuscript are indicated to be 17-norlabdane diterpenes,[97] but since ^{13}C NMR shift details for methyl C-17 are provided, we attribute this to poor editing and have included the C-17 methyl functionality in the structures provided (*vide infra*). The comparison of our ^{13}C NMR data for compounds **3.3** (isolation discussed later) and **3.2** with those reported for **3.6** has led us to conclude that **3.6** (and **3.12**-**3.14**) do indeed have a Δ^{13} *Z* olefin geometry (C-12: δ_C 32.3; C-16: δ_C 23.6),[100] and thus *Trimusculus* produces both Δ^{13} geometric isomers. Our attempts at synthesizing similar *Pleurobranchaea* metabolites (Chapter Five) have revealed that isomerisation around the Δ^{13} olefin does not occur (when a hydroxyl moiety at C-15 is present) under the conditions regularly used to isolate these unsaturated compounds and thus this possibility can be disregarded.

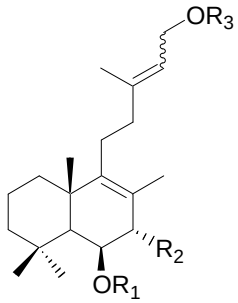

3.6 Δ^{13} *Z*; $R_1 = R_3 =$ Ac; R_2 = OAc
3.11 Δ^{13} *E*; R_1 = Ac; R_2 = OH; R_3 = H
3.12 Δ^{13} *Z*; R_1 = H; R_2 = OAc; R_3 = Ac
3.13 Δ^{13} *Z*; R_1 = Ac; R_2 = OAc; R_3 = H
3.14 Δ^{13} *Z*; R_1 = Ac; $R_2 = R_3$ = H

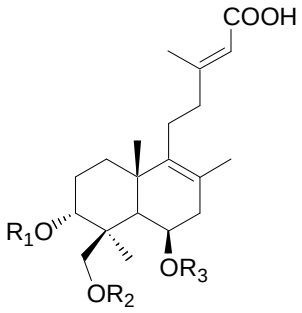

3.15 $R_1 = R_2 = R_3 =$ H
3.16 $R_1 = COCH_2CH(CH_3)_2$; $R_2 = R_3$ = H
3.17 $R_1 = R_3 = COCH_2CH(CH_3)_2$; R_2 = H;
3.18 $R_1 = R_2 = COCH_2CH(CH_3)_2$; R_3 = H

Another investigation of *T. peruvianus*, collected off the Antofagasta Coast, III Region, Chile, led to the isolation of four new compounds (**3.15**-**3.18**),[95] all of which possessed a carboxylic acid moiety at C-15, previously only found in **3.9**, isolated from *T. conica* metabolites *vide supra.*[11] Of further interest was that **3.15**-**3.18** were all oxygenated at C-3 and C-19, an oxygenation pattern not seen in any of the diterpene metabolites isolated previously from this genus. Unlike the reported metabolites isolated previously from specimens of *T. peruvianus*,[97] only the more common Δ^{13} *E* geometry was found. The *E* configuration was confirmed by the upfield shift (δ_C 17.5) of C-16, which the authors attributed to the shielding effect resulting from the *cisoid* relationship with the carboxylic acid, and the downfield shift (δ_C 41.2) of C-12.[95] An NOE relationship between H-14 and H_2-12 further corroborated this assignment. The axial orientation of the hydroxyl moiety of C-3 of **3.15** was made on the basis of the small coupling constants between H-3 and the vicinal protons of C-2. Base mediated hydrolysis of **3.16**-**3.18** to afford **3.15** revealed that compounds **3.15**-**3.18** possessed the same relative configuration. Furthermore, Díaz-Marrero *et al.* were able to determine the absolute configuration of the labdanes produced by *Trimusculus* through application of the modified Mosher's method to compound **3.18**. Interestingly, Díaz-Marrero *et al.* suggested that since the high degree of selectivity in oxidation sites was reminiscent of certain fungal modes of action on diterpene substrates, some symbiotic interaction between these phylletically distinct organisms might be plausible.

A subsequent publication from the same research group,[96] described the isolation of two new steroids, unusually hydroxylated at C-18 (**3.19** and **3.20**), from the original collection that yielded **3.16**-**3.18**. Apart from **3.10**, no steroidal compounds had previously been isolated from *Trimusculus*. What was of further interest was that **3.20** had a Δ^7-3α,5α,6β-triol substitution and unsaturation pattern, which, while unprecedented in marine steroidal metabolites,[96] was common in, amongst others, basidiomycete fungi, again tentatively suggesting a relationship between *Trimusculus* and fungal symbionts. The relative configuration of both **3.19** and **3.20** was determined from NOE data and comparative ^{13}C NMR chemical shift data.

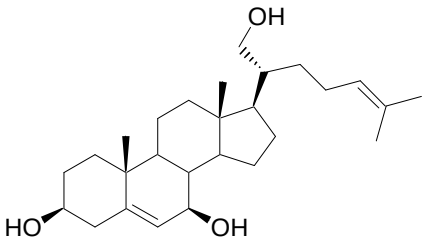

3.19

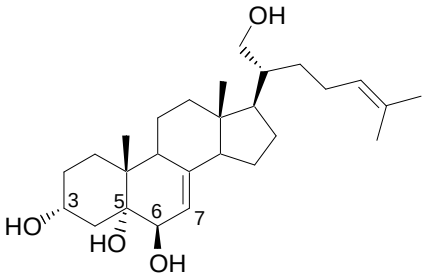

3.20

Gray *et al.*[10;100] conducted the first examination of the secondary metabolites of the endemic *T. costatus*, collected off the coast at Cintsa, near East London, South Africa and isolated the diterpene metabolites **3.1** and **3.2**. The 2α,6β,7α oxygenation pattern characteristic of *Trimusculus* diterpenes was established spectroscopically. Gray also attempted a synthesis of these compounds from a readily available diterpene precursor,[100] aspects of which will be discussed in Chapter Four.

Before continuing, it should be noted that in the papers published by Manker and Faulkner,[11;99] Rovirosa *et al.*[104] and San-Martín *et al.*[97] the numbering of carbons 18-20 differs from the standard trends in the diterpene literature. In order to achieve consistency with the labdane diterpene numbering system used elsewhere in this thesis, we have adopted the numbering system of Gray *et al.*[10;100] and Díaz-Marrero *et al.*[95] as indicated in the structures (*e.g.* **3.1**) at the beginning of this chapter.

3.1.3 Ecological and bioactivity studies of Trimusculus metabolites

The earliest studies of the defensive strategies of *T. reticulatus* were undertaken by Rice,[101] who found that the mucous secreted by these limpets stunned the feet of seastars, effectively reducing predation by these creatures. Rice noted that this form of defence was ideally suited to sessile animals such as *Trimusculus*, living in densely packed colonies, since stunning the tube feet of their seastar predators greatly increased the amount of time taken for the seastar to feed, thus reducing their predatory efficiency.

The first ecological study undertaken using purified *Trimusculus* metabolites was performed by Manker and Faulkner,[99] who were unable to determine whether either **3.7** or **3.8** deterred predation by seastars. They were, however, able to conclude that specimens of *T. reticulatus* taken from San Nicholas Island, Monterey, and San Diego showed no geographic variation in the diversity and relative quantities of metabolites secreted in the limpets' mucous. Nearly a decade later, Manker and Faulkner returned to their ecological study, this time including **3.9** and **3.10** in their investigations.[11] They found that compounds **3.7** and **3.8** were localized in the mantle, foot and mucous of *T. reticulatus*, while **3.9** and **3.10** were evident in the mantle and foot tissue of *T. conica* (no mucous from these limpets was collected for testing). None of the compounds were found in the viscera of either species. This finding supported the speculation that these metabolites were deployed externally and thus probably exhibited either interspecific anti-feedant or some unknown toxic effects. While they confirmed that the mucous from *T. reticulatus* was repugnant to the seastar *Astrometis* sp., they found that application of diol **3.7** alone did not elicit a response. A paucity of **3.8** precluded testing to confirm whether the lack of a mucous carrier or a possible synergistic effect could be the cause of lack of response for **3.7**. Although pellets treated with **3.7** and **3.8** did not deter feeding by the rainbow tropical wrasse (*Thallosoma lunare*), living specimens of *T. reticulatus*, as well as the mucous from these limpets, were found to be toxic to the larvae of the tubeworm, *Phragmatopoma californica*. Compound **3.7** was found to cause 100% mortality of these larvae at concentrations greater than 100 μgmL^{-1}, while compound **3.9** had no effect. The lack of toxicity of **3.9** to *P. californica* larvae is probably not unexpected as the source of this compound, *T. conica*, a native New Zealand species, would have co-evolved with different predators.

Gray *et al.*[10;100] used bioassay guided (*Artemia salina* assay) fractionation of *T. costatus* to isolate **3.1** and **3.2**. The difficulties described by Manker and Faulkner in performing ecologically significant assays using seastars coupled with a curiosity to determine why the *Trimusculus* metabolites apparently did not deter fish feeding prompted Gray *et al.*[10;100] to investigate whether **3.1** and **3.2** were repellent to *Pomadasys commersonni* (spotted grunter), a South African generalist predatory fish. Grey *et al.* found that **3.1** and **3.2** deterred feeding

by this species at sub-naturally occurring levels.[10;100] Although Gray did not perform any antifouling tests, his field observations of the extensive fouling of colonies of *T. costatus* in the South African intertidal zone led him to conclude that the compounds secreted did not have any significant antifouling activity.

Unfortunately, no ecological studies have been performed with *T. peruvianus*. However, **3.6** and **3.11**-**3.14** were tested for antibacterial activity. Only **3.6** showed modest activity (100 μgmL^{-1}) against both Gram positive and gram negative bacteria.[97] In later natural product investigations of *T. peruvianus*,[95;96] **3.17**-**3.20** were screened for activity against human colon carcinoma cell lines (H-119 and HT-29). Compounds **3.17**, **3.18** and **3.20** showed moderate activity (IC_{50} of 12.5 μgmL^{-1}), while **3.19** was significantly more cytotoxic (IC_{50} of 2.5 μgmL^{-1}). Gray[100] also screened **3.1** and **3.2** against four different cancer cell lines (LOX melanoma, OVCAR3 ovarian cancer, A549 non-small lung cancer and SNB19 CNS cancer) but found no significant activity (IC_{50} > 100 μgmL).

3.1.4 Synthetic approaches to Trimusculus metabolites

As mentioned previously, the first synthesis confirming the relative configurations of **3.7**, originally isolated by Manker and Faulkner, [99] was performed by Gao *et al.*,[102] in 22% overall yield (Scheme 3.1), nearly a decade after the initial isolation. Diol (**3.21**) was prepared from (±)-9-methoxycarbonyl-4,4,10-trimethyl-Δ^6-8-octalone (**3.22**) through a series of standard transformations. Routine selective protection of the primary alcohol moiety, followed by pyridinium chlorochromate (PCC) mediated rearrangement of the allylic tertiary alcohol introduced the desired enone functionality. After introducing the exocyclic olefin at C-9, the resultant ketone (**3.23**) was stereospecifically reduced with diisobutylaluminium hydride (DIBAH) to afford the desired 6β-hydroxyl epimer (**3.24**). Gao *et al.*[102] utilized 1,4-addition to diene (**3.25**) in combination with the reduced steric hindrance of the α-face of this compound to effect stereospecific addition of the 7α-acetoxy group using N-bromosuccinimide (NBS) in acetic acid.

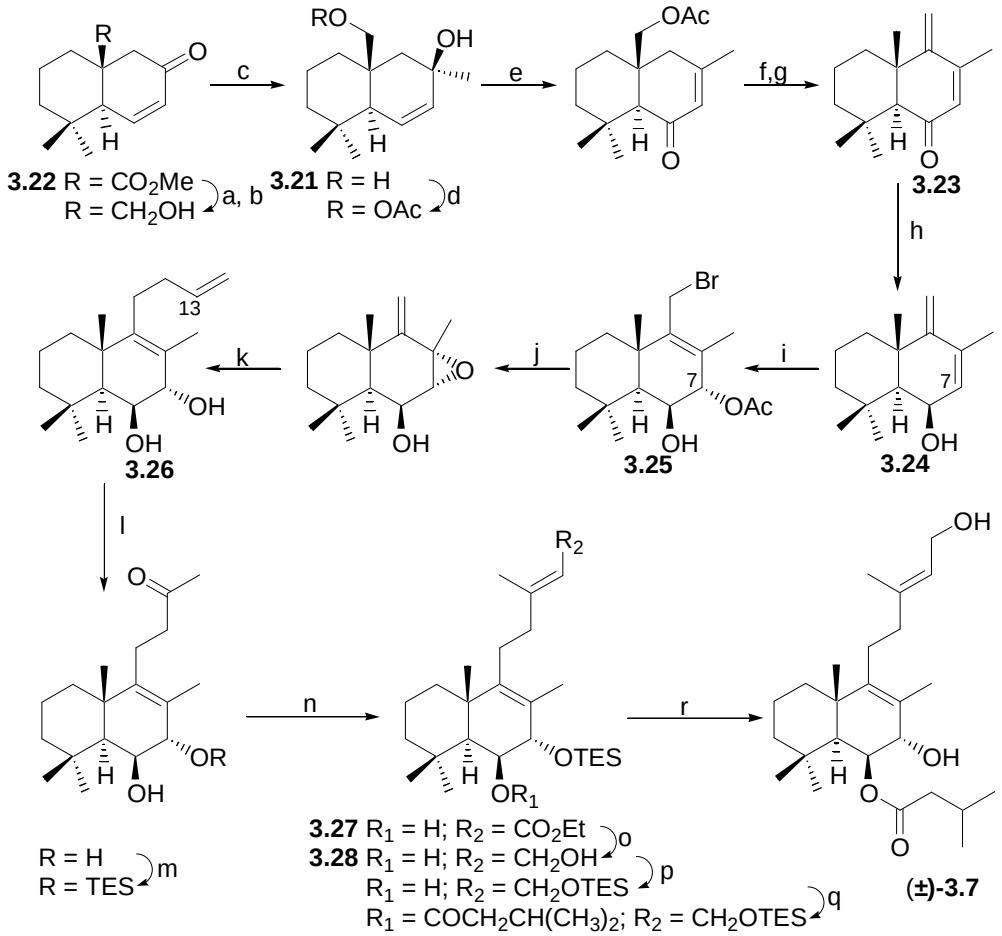

Scheme 3.1 Gao *et al.'s* synthesis of **(±)-3.7**.[102] *Reagents and conditions:* (a) LAH, Et_2O, 0℃, 2.5 h; (b) $BaMnO_4$, CH_2Cl_2, RT, 24 h; (c) MeLi, Et_2O, -78℃, 3 h; (d) Ac_2O, pyridine, RT, DMAP, RT, 24 h; (e) PCC, CH_2Cl_2, RT, 3 h; (f) K_2CO_3, MeOH, RT, 5 h; (g) *p*-TsOH, C_6H_6, Δ, 6 h; (h) DIBAH, CH_2Cl_2, -78℃, 3 h; (i) NBS (1 eq), AcOH, RT, 1 h; (j) K_2CO_3, MeOH, RT, 2 h; (k) CH_2=$CHCH_2MgBr$, CuBr-SMe_2 (cat), LiBr (cat), Et_2O, -78℃, 2 h; (l) $PdCl_2$, CuCl, DMF-H_2O, O_2, RT, 1 h; (m) TESCl, pyridine, 0℃ - RT, 6 h; (n) $(C_2H_5O)P(O)CH_2CO_2Et$, NaH, THF, 0℃-RT, 6 h; (o) DIBAH, CH_2Cl_2, -78℃, 3 h; (p) TESCl, pyridine, 0℃ - RT, 0.5 h; (q) isovaleric acid, DCC, DMAP, CH_2Cl_2, RT, 24 h; (r) TBAF, THF, RT, 6 h.

In continuation of the discussion of the synthesis of Gao *et al.*, intramolecular S_N2' epoxide formation, coupled with the introduction of the extended side chain through conjugate Grignard addition, resulted in the opening of the epoxide with concomitant rearrangement of the exocyclic olefin. Wacker oxidation of the terminal olefin in (**3.26**) allowed for further

elaboration of the alkenyl side chain. Introduction of the desired *E* geometry at C-13 was achieved using the Horner-Wadsworth-Emmons (HWE) modification of the Wittig reaction to yield the ester (**3.27**), which upon reduction with DIBAH yielded the allylic alcohol (**3.28**). Selective protection of the primary alcohol, followed by isovaleric acid esterification of the secondary alcohol and subsequent removal of the triethylsilyl (TES) protecting groups afforded the racemate **(±)-3.7**, confirming the relative configuration originally proposed by Manker and Faulkner.[99]

Although Gao *et al.*[102] had used synthesis to confirm the relative configuration of **3.7**, the absolute configuration of the *Trimusculus* diterpenes remained undefined. Pathak *et al.*[103] subsequently established the absolute configuration of **3.7** *via* synthesis from the readily available labdane diterpene (+)-larixol (**3.29**).The synthesis (Scheme 3.2) commenced with the isomerisation of the $\Delta^{8,17}$ olefin in **3.29**, affording a mixture of Δ^{7} (not shown in scheme) and Δ^{8} isomers. Since these isomers were difficult to separate, 2-iodobenzoic acid mediated oxidation was performed on the crude isomeric mixture and the desired ketone (**3.30**) isolated. Reduction of this ketone with lithium aluminium hydride (LAH) completed the inversion of configuration at C-6, affording the β-hydroxy moiety, which was then esterified with isovaleryl chloride. Allylic oxidation at C-7 with selenium dioxide occurred from the less sterically hindered α-face affording the 7α-hydroxy moiety, while palladium catalyzed allylic rearrangement of the side chain introduced the desired Δ^{13} *E* geometry and transposed the isovaleryl ester moiety at C-13 to C-15. Finally, selective saponification of the allylic isovaleryl ester (an unavoidable consequence of the earlier bisesterification) yielded **3.7** in 30% overall yield. Synthetic **3.7** was found to be identical to the natural product in all respects (^{1}H and ^{13}C NMR, IR and $[\alpha]_D$), suggesting that the diterpene natural products of *T. reticulatus* belong to the labdane series. This synthesis also provided a readily accessible source of **3.7** should any further biological activity studies of this compound be contemplated.

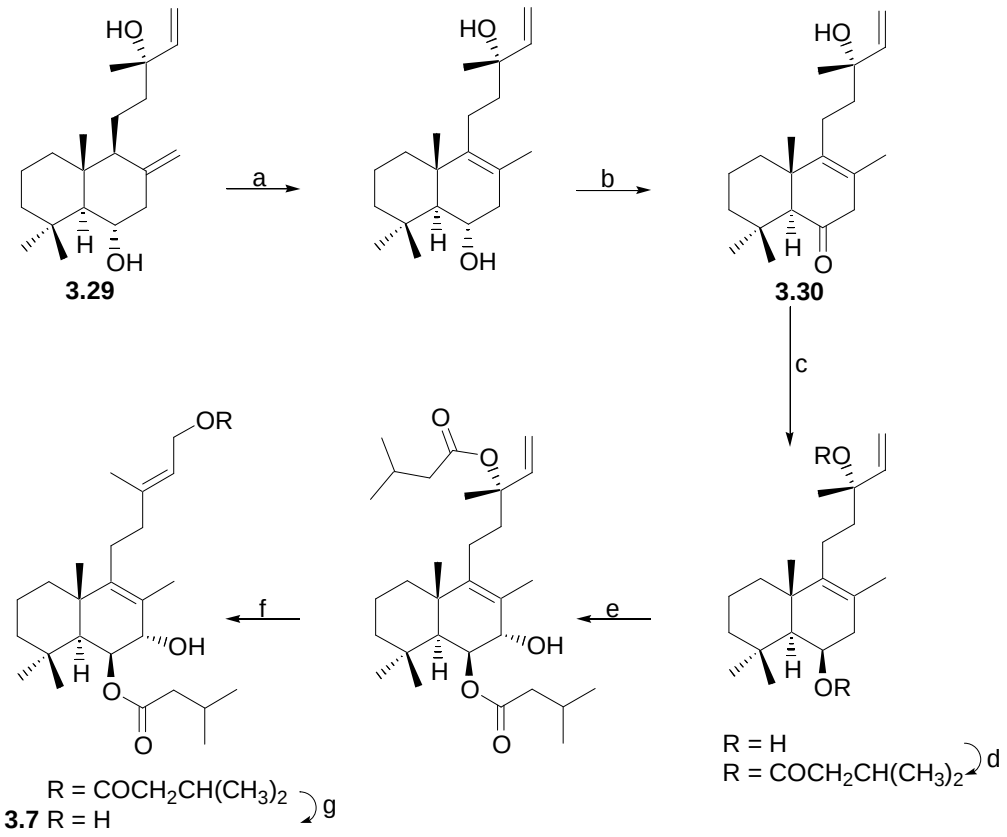

Scheme 3.2 Pathak *et al.'s*[103] synthesis of **3.7**. *Reagents and conditions:* (a) $NH_2CH_2CH_2NH_2$, Li, 100 ℃, overnight; (b) IBX (no further details given); (c) LAH, THF, 0℃; 1 h; (d) isovaleryl chloride, DMAP, pyridine, 0℃, overnight; (e) SeO_2, dioxane-H_2O, 60℃, 24 h; (f) $(PhCN_2)_2PdCl_2$, THF, RT, 3 h; (g) K_2CO_3, MeOH, 4℃ (1 h) then RT (9 h).

3.2 New secondary metabolites from *T. costatus*

3.2.1 Recollection of T. costatus

In May 2006, a collection of 1274 *Trimusculus costatus* specimens was made from the extensive and densely populated colonies of this mollusc occurring in the intertidal region of the rocky shore at Cinsta West, South Africa (Figure 3.1). Consistent with previous observations by Gray,[100] the limpets were growing in densely packed colonies, two to three

layers thick in the lower intertidal zone. The specimens collected were directly immersed in acetone and stored at -20℃ for a period of five mo nths.

Figure 3.1 The rocky shore at the collection site of *T. costatus*, Cintsa West.

3.2.2 Extraction and isolation of secondary metabolites

As a pilot study, a portion of the May 2006 collection (527 animals) in acetone (300 mL) was selected for the primary extraction. The isolation protocol is represented graphically in Scheme 3.3. The acetone was decanted from the specimens and the animals resuspended in acetone (300 mL) and returned to the freezer (-20℃). The acetone extract was loaded onto an HP-20 column and systematically eluted in the manner described in the previous chapter, to afford five fractions. Analysis of the ^{1}H NMR spectra of each of these fractions showed that the diterpene metabolites, **3.1** and **3.2**, occurred predominantly in the 60% and 80% acetone$_{(aq)}$ fractions. A portion (111 mg) of the 60% fraction (273 mg) was subjected to semi-preparative HPLC (60% ethyl acetate, 40% hexane) and **3.1** (30 mg) and **3.2** (41 mg) were isolated. These two metabolites were identical in all respects with those previously isolated by Gray *et al.*[10;100]

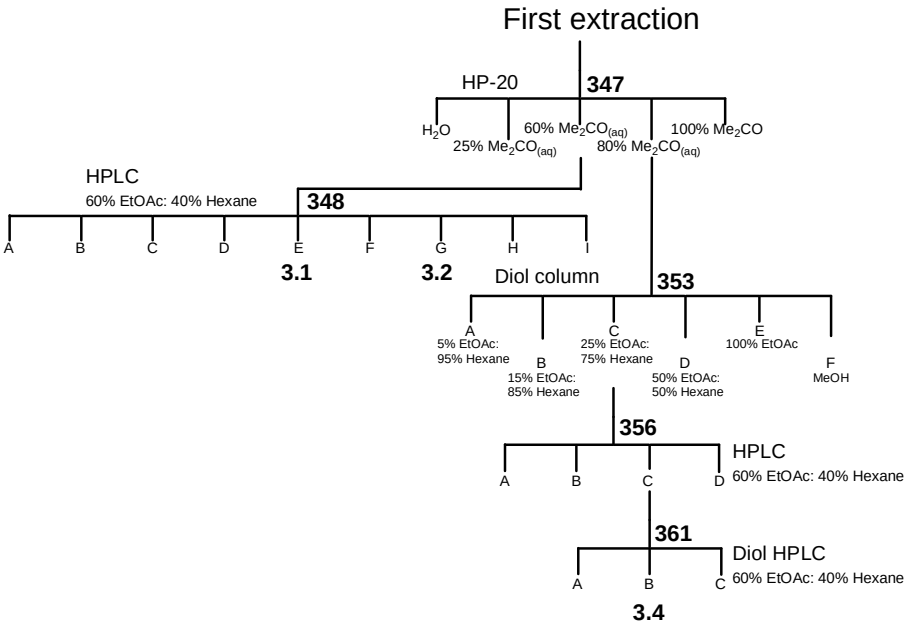

Scheme 3.3 First extraction from *T. costatus*.

Although the absolute configuration of the *T .reticulatus* metabolites had already been established conclusively by Pathak *et al.*[103] and the *T. peruvianus* metabolites by Díaz-Marrero *et al.*,[95] we wished to confirm that the diterpene metabolites from *T. costatus* also belonged to the labdane series. We accordingly chose to esterify both **3.1** and **3.2** with the chiral carboxylic acid chloride, (-)-1*S*-3-oxo-4,7,7-trimethyl-2-oxabicyclo[2.2.1]heptane-1-carbonyl chloride, or (-)-camphanic chloride (**3.31**). The camphanate esters of natural products are often crystalline and are thus regularly used in conjunction with X-ray crystallography to determine the absolute configuration of natural products.[*e.g.*105;106] Metabolites **3.1** and **3.2** were accordingly derivatized with (-)-camphanic chloride to yield the camphanate esters (**3.32** and **3.33**). The camphanate esters were purified by semi-preparative HPLC and crystallization attempted from a variety of solvents. Ultimately only **3.33** provided crystals suitable for X-ray crystallography from initial dissolution of **3.33** in ethyl acetate and allowing the slow diffusion of hexane into the solution over a period of weeks. Single crystal X-ray analysis of **3.33** (Figure 3.2) confirmed that **3.2**, as well as **3.1** and **3.3** (from biogenic considerations, isolation of **3.3** still to be discussed) shared a labdane configuration, in common with other *Trimusculus* diterpenes.

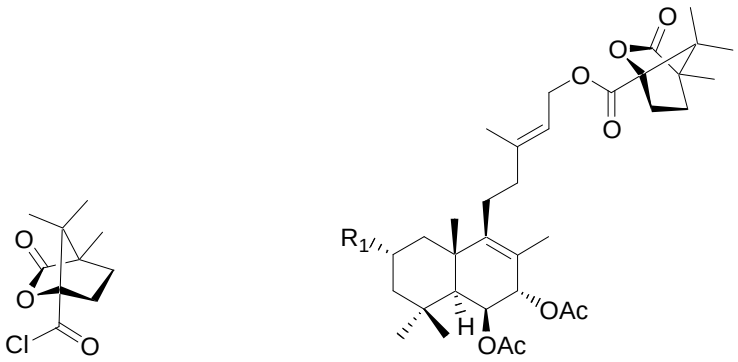

3.31

3.32 R_1 = H
3.33 R_1 = OAc

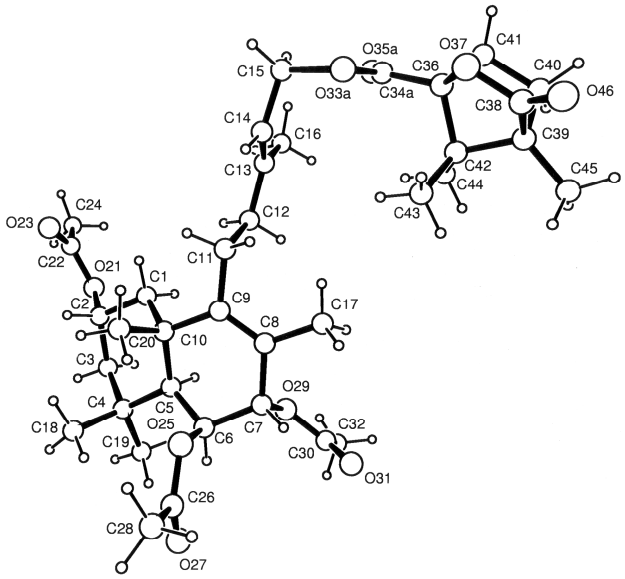

Figure 3.2 Perspective view of the major conformation adopted by molecules of **3.33**.

The ^{1}H NMR spectrum of the 80% acetone$_{(aq)}$ fraction (483 mg) revealed a complex mixture of metabolites. The fraction was thus resuspended in acetone and adsorbed onto Diol stationary phase and eluted with aliquots of solvents of increasing polarity, again as described in the previous chapter. Resonances characteristic of terpenoid compounds in the ^{1}H NMR spectrum of the 25% ethyl acetate, 75% hexane fraction prompted us to subject this fraction to semi-preparative normal phase HPLC (60% ethyl acetate, 40% hexane), affording compound **3.2** (58 mg) and an impure fraction (38 mg) containing other interesting

metabolites from ^{1}H NMR spectroscopy. The long retention time of peaks eluting from the normal phase column and the extensive "tailing" observed in the chromatogram necessitated a change in stationary phase in order to isolate the interesting metabolites in this fraction. Accordingly, Diol semi-preparative HPLC (40% ethyl acetate, 60% hexane) afforded 9,11-secosterol, **3.4**, as a yellow oil (30 mg). 9,11-Secosterols (*e.g.* **3.34**),[107] appear to be unique to the marine environment and to date have only been reported from soft corals,[e.g.108-116] sponges[e.g.117-122] and tunicates.[107] Therefore, the isolation of secosterol **3.4** from *T. costatus* is the first reported isolation of a 9,11-secosterol from a marine mollusc.

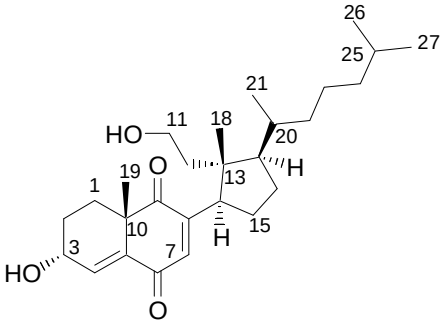

3.4

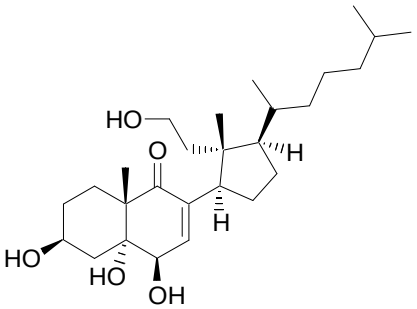

3.34

The molecular formula of **3.4**, established as $C_{27}H_{42}O_4$ by HRFABMS data, implied seven degrees of unsaturation. The presence of two α,β-unsaturated ketones (δ_C 187.5 and 201.8) and their corresponding two trisubstituted olefins [δ_C 135.2 (d), 140.4 (s), 138.7 (d) and 153.5 (s)] and one secondary hydroxyl functionality (δ_C 63.0) was further corroborated by the IR absorption bands at 1683 and 1624 cm^{-1} and a broad absorbance band at 3420 cm^{-1} respectively. The two α,β-unsaturated ketones accounted for four of the seven degrees of unsaturation required by the molecular formula, and the absence of any further carbonyl or olefinic functionalities thus suggested a tricyclic skeleton. Analysis of ^{13}C and DEPT NMR spectra confirmed the presence of twenty seven carbons, comprising two trisubstituted olefins, one oxymethylene, two conjugated ketones, one oxymethine, two quaternary, four methine and eight methylene carbons. The presence of twenty seven carbons suggested a steroidal structure, but the tricyclic nature of **3.4** implied rearrangement of the typical tetracyclic steroid skeleton, such as in a 9,11-secosterol, *e.g.* **3.34**.[107] Analysis of the ^{1}H NMR spectrum of **3.4** revealed the presence of two tertiary methyl groups (δ_H 0.75 and 1.37) as

well as three secondary methyl groups (δ_H 0.86, 0.86 and 0.96), consistent with the those reported for **3.34** (Table 3.1), suggesting a similar distribution of methyl groups in these two compounds. Additionally, two deshielded geminal resonances [δ_H 3.71 (H-11a) and δ_H 3.84 (H-11b)], mutually coupled to two other geminal protons [δ_H 1.15 (H-12a) and 1.71 (H-12b)] in an isolated spin system are characteristic of a 9,11-secosterol skeleton with a primary hydroxyl group at C-11.[107] The ^{13}C NMR chemical shifts of C-11 (δ_C 59.0) and C-12 (δ_C 41.3) from gHSQC correlations also compared favourably with analogous chemical shifts in similar compounds.[107-110;122] Finally, a ketone moiety at C-9 is also typical of a 9,11-secosterol, in which oxidative cleavage of the C-9, C-11 bond of a steroid precursor has occurred. The position of the carbonyl at C-9 was supported by gHMBC correlations from H_3-19 (δ_H 1.37) to C-9 (δ_C 201.8). Further ^{1}H and ^{13}C NMR assignments were made from gHMBC correlations from H_3-19 to quaternary carbons C-10 (δ_C 49.2) and C-5 (δ_C 140.4), as well as to methylene carbon C-1 (δ_C 25.0). A two bond gHMBC correlation from the olefinic methine proton H-7 (δ_H 6.69) to the remaining carbonyl carbon (δ_C 187.5), in addition to a three bond gHMBC correlation from the olefinic proton H-4 (δ_H 6.70) to the same carbon placed the second ketone at C-6. A gCOSY correlation between H-4 and oxymethine proton H-3 (δ_H 4.34) allowed for the assignment of C-3 (δ_C 63.0) from gHSQC data. gCOSY correlations between oxymethine H-3 (δ_H 4.34) and between H_2-2 (δ_H 1.89) followed to allow for the assignment of C-2 (δ_C 27.2) from gHSQC data. Two and three bond gHMBC correlations from H-3 (Figure 3.3) to both C-2 and C-4 (δ_C 135.2) and both C-1 and C-5 confirmed the assignments made for the A ring. As the spectroscopic differences between **3.4** and the secosterol **3.34** were limited to the substitution pattern around the A and B rings the remaining assignments in the right hand hemisphere were made by comparison of the ^{1}H and ^{13}C NMR data of these two compounds (Table 3.1) and were supported by exhaustive gHMBC and gCOSY correlations where necessary.

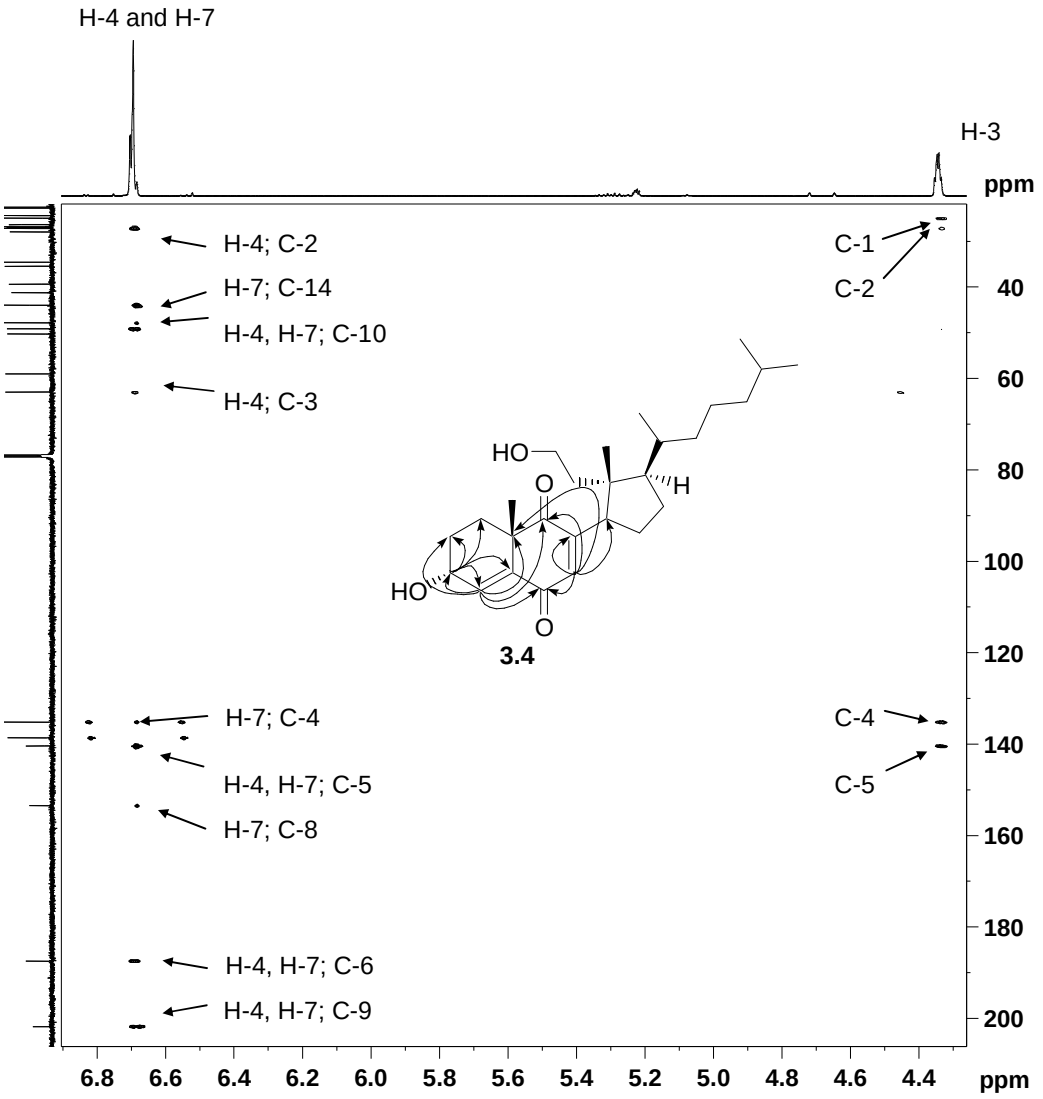

Figure 3.3 A region of the gHMBC spectrum ($CDCl_3$, 600 MHz; F1 = δ_C 20 – 205; F2 = δ_H 4.3 – 6.9) of **3.4** showing the key correlations used to assign the carbons of the A and B rings. The accompanying diagram summarizes the gHMBC correlations indicated in the spectrum.

Table 3.1 Comparison of the ^{1}H (600 MHz) and ^{13}C (150 MHz) NMR data ($CDCl_3$) obtained for **3.4** with ^{1}H (500 MHz) and ^{13}C (125 MHz) NMR data ($CDCl_3$) reported for **3.34**.[107]

	3.4		**3.34**	
Position	δ_C (mult.)	δ_H (int., mult., *J*/Hz)	δ_C (mult.)[†]	δ_H (int.[†], mult.,[‡] *J*/Hz)
1β	25.0 (t)	1.77 (1H, m)	28.6	1.52
1α		2.17 (1H, ddd 13.5, 13.4, 3.6)		2.00
2	27.2 (t)	1.89 (2H, m)	31.0	1.49
				1.89
3	63.0 (d)	4.34 (1H, m)	68.3	4.02 (m)
4	135.2 (d)	6.70 (1H, dd, 4.0, 0.9)	39.2	2.31 (dd, 12.9, 12.9)
				1.95
5	140.4 (s)	-	77.0	-
6	187.5 (s)	-	72.4	4.44 (d, 4.9)
7	138.7 (d)	6.69 (1H, s)	138.2	6.49 (d, 4.9)
8	153.5 (s)	-	137.3	-
9	201.8 (s)	-	202.8	-
10	49.2 (s)	-	47.0	-
11a	59.0 (t)	3.71 (1H, ddd, 10.7, 9.4, 5.8)	59.1	3.69 (m)
11b		3.84 (1H, ddd, 10.7, 10.0, 5.6)		3.81 (m)
12a	41.3 (t)	1.15 (1H, m)	40.5	1.15
12b		1.71 (1H, m)		1.63
13	47.9 (s)	-	46.1	-
14	44.0 (d)	3.54 (1H, dd, 11.1, 8.7)	43.5	3.50 (bt, 9.5)
15	27.0 (t)	1.68 (2H, m)	27.2	1.68
16a	26.4 (t)	1.50 (1H, m)	29.6	1.46
16b		1.89 (1H, m)		1.85
17	50.3 (d)	1.74 (1H, m)	49.8	1.83
18	17.7 (q)	0.75 (3H, s)	17.4	0.75 (s)
19	26.8 (q)	1.37 (3H, s)	21.0	1.47 (s)
20	34.6 (d)	1.43 (1H, m)	38.5	1.43
21	18.8 (q)	0.96 (3H, d, 6.7)	19.2	0.97 (d, 6.8)
22a	35.5 (t)	1.02 (1H, m)	35.3	1.01 (m)
22b		1.35 (1H, m)		1.33
23a	24.4 (t)	1.15 (1H, m)	24.5	1.11
23b		1.35 (1H, m)		1.31
24	39.4 (t)	1.12 (2H, m)	39.4	1.09
25	28.0 (d)	1.52 (1H, m)	28.0	1.51
26	22.8 (q)	0.86 (3H, d, 6.6)	22.8	0.85 (d, 7)
27	23.0 (q)	0.86 (3H, d, 6.6)	23.0	8.85 (d, 7)

[†] Not provided; [‡] Where provided.

The relative configuration of the A-ring was determined through NOE correlations (Figure 3.4). A correlation between H_3-19 (δ_H 1.37) and both H-1β (δ_H 1.77), and H-3 (δ_H 4.34) implied these were all on the same face of the ring. The configuration indicated in the

cyclopentane ring in the right hand hemisphere of the molecule and at C-20 was determined from biogenetic considerations.

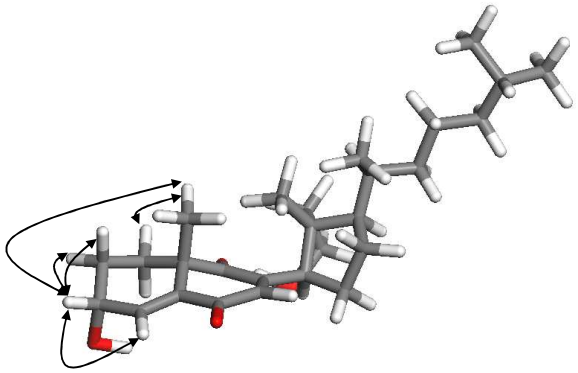

Figure 3.4 Key NOESY correlations used in the determination of the C-3 configuration of **3.4**.

In order to investigate the absolute configuration of **3.4** by chemical means, more material needed to be isolated. To do this the remainder of the May 2006 collection of *T. costatus* (753 animals) was worked up in the usual manner. The limpets were immediately resuspended in acetone (300 mL) and returned to the freezer along with the original extract. After one week, the second extract from both the first and the second isolation was pooled with the first extract from the second isolation. Concentration *in vacuo* of these combined extracts commenced until the total volume was approximately 300 mL. The isolation procedure is depicted graphically in Scheme 3.4.

The pure secosterol **3.4** was found in (380-E and 390-B) providing a total yield (including the 29.5 mg from the first isolation) of 122 mg from 1274 animals (or 0.096 mg/animal). A further new compound, **3.3**, the acetylated product of **3.1** (and Δ^{13} geometric isomer of **3.6**) was isolated in small quantities (2 mg, 0.002 mg/animal) from semi-preparative HPLC of 379-C. The structure of **3.3** was readily confirmed as the Δ^{13} *E* geometric isomer of **3.6** through the comparison of ^{1}H and ^{13}C NMR data of the two compounds, particularly the ^{13}C NMR chemical shift of C-12 and C-16 (δ_C 39.2 and 16.6 respectively, Table 3.2).[99;102] Based on analysis of the 2D NMR data sets acquired for **3.3**, we believe that the ^{13}C NMR chemical shifts for C-6 and C-7 have been incorrectly assigned in **3.6**.[97] As a final confirmation of the

structure of **3.3**, a portion of **3.1** was acetylated by stirring a portion of this compound with pyridine and acetic anhydride (16 h). The specific rotations and ^{1}H and ^{13}C NMR spectra of the naturally occurring and semi-synthesized **3.3** were identical.

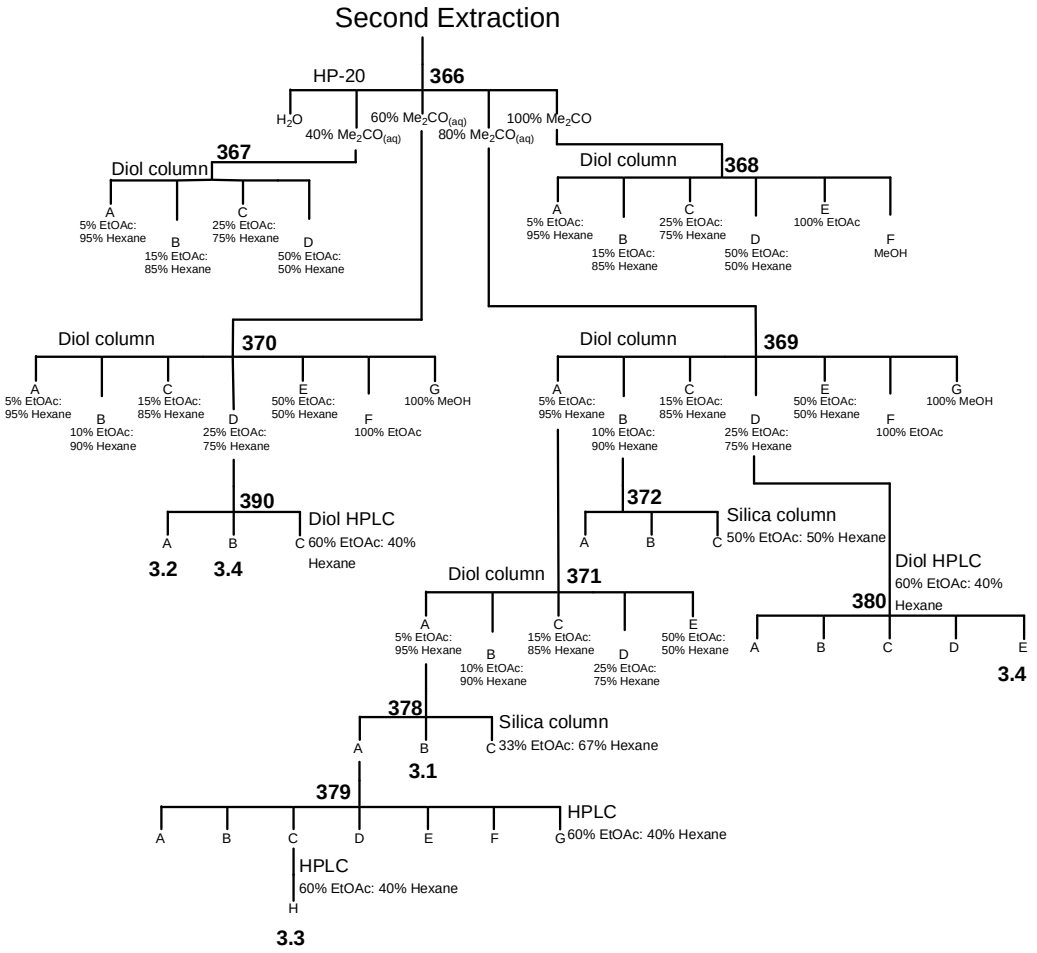

Scheme 3.4 Second isolation procedure for the May 2006 *T. costatus* collection.

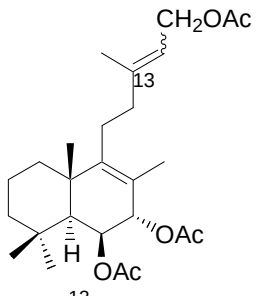

3.3 Δ^{13} *E*

3.6 Δ^{13} *Z*

Table 3.2 Comparison of the ^{1}H (600 MHz) and ^{13}C (150 MHz) NMR data obtained for **3.3** with those reported for **3.6** by San-Martín *et al.*[97] (^{1}H: 300 MHz; ^{13}C: 75 MHz; $CDCl_3$).

	Diterpene **3.3**		Diterpene **3.6**	
Position	δ_C (mult.)	δ_H (int., mult., *J*/Hz)	δ_C (mult.)	δ_H (int., mult., *J*/Hz)
1a	38.9 (t)	1.21 (1H, m)	39.1 (t)	†
1b		1.80 (1H, m)		
2a	19.0 (t)	1.54 (1H, m)	19.2 (t)	†
2b		1.69 (1H, m)		
3a	43.1 (t)	1.19 (1H, m)	43.3 (t)	†
3b		1.42 (1H, m)		
4	33.4 (s)	-	33.4 (s)	-
5	49.2 (d)	1.47 (1H, d, 1.1)	49.3 (d)	1.50 (1H, br s)
6	69.6 (d)	5.31 (1H, br s)	73.6 (d)	5.32 (1H, br s)
7	73.4 (d)	4.97 (1H, br s)	69.4 (d)	4.98 (1H, br s)
8	121.7 (s)	-	122.1 (s)	-
9	147.7 (s)	-	147.8 (s)	-
10	39.5 (s)	-	39.6(s)	-
11	26.8 (t)	2.21 (2H, m)	27.2 (t)	2.05 (2H, m)
12	39.2 (t)	2.11 (2H, m)	32.3 (t)	2.10 (2H, m)
13	142.3 (s)	-	143.1 (s)	-
14	118.1 (d)	5.37 (1H, t, 6.9)	119.3 (d)	5.36 (1H, t, 7.3)
15	61.3 (t)	4.50 (2H, d, 7.1)	61.1 (t)	4.59 (1H, d, 7.3)
16	16.6 (q)	1.74 (3H, s)	23.6 (q)	1.73 (3H, br s)
17	17.0 (q)	1.61 (3H, s)	17.3 (q)	1.58 (3H, s)
18	33.0 (q)	0.97 (3H, s)	33.2 (q)	0.97 (3H, s)
19	23.1 (q)	0.95 (3H, s)	23.3 (q)	0.98 (3H, s)
20	21.0 (q)	1.28 (3H, s)	21.7 (q)	1.30 (3H, br s)
6-OAc	169.7 (s)	-	169.7 (s)	-
	21.5 (q)	2.03 (3H, s)	21.5 (q)	2.04 (3H, s)
7-OAc	171.1 (s)	-	171.1 (s)	-
	21.1 (q)	2.08 (3H, s)	21.1 (q)	2.09 (3H, s)
15-OAc	169.9 (s)	-	169.9 (s)	-
	21.2 (q)	2.06 (3H, s)	21.2 (q)	2.05 (3H, s)

† No values reported.

We next attempted the modified Mosher's method[123] to determine the absolute configuration of the secondary alcohol moiety in **3.4**. Although the Mosher's method is routinely used to determine the absolute configuration of natural products, the difficulty in this case rested on the fact that there were two sites available for esterification with α-methoxy-α-trifluoromethylphenylacetic acid (MTPA). This problem was eventually circumvented through the selective acetylation of the primary alcohol utilizing Ishihara *et al.*'*s* method.[124] The procedure involved dissolving **3.4** in dichloromethane and reacting the solution with acetyl chloride in the presence of a sterically hindered base (collidine) at -78℃. Although the procedure did produce some of the diacetylated product (**3.35**, 9%), we were able to isolate the monoacetate (**3.36**) as the major product (27%) through semi-preparative HPLC. The diacetylated product was identified by the presence of two deshielded methyl singlets (δ_H 2.02 and 2.01) but not further characterized. Confirmation of the selective acetylation of the primary alcohol was provided by two bond gHMBC correlations from H-11a and H-11b to the acetyl carbonyl carbon, as well as the significant downfield shift of these two resonances in the ^{1}H NMR spectrum of **3.36** (Figure 3.5).

With **3.36** in hand we were able to make use of the modified Mosher's method[123] to determine the absolute configuration at C-3. Dale and Mosher[125] postulated that the most stable conformation of the α-methoxy-α-trifluoromethylphenylacetic acid (MTPA) moiety in solution is when the ester, carbinyl and trifluoromethyl substituents are *syn*-periplanar (Figure 3.6).

In this *syn*-periplanar conformation, the diamagnetic effect of the phenyl substituent shields the protons of the alkyl chain on the side of this moiety, while the protons of the other alkyl chain are deshielded by the methoxy functionality. This spectroscopic method was first developed prior to the advent of Fourier transform NMR when most NMR spectrometers were operating in the 60-100 MHz range, making complete assignments of the protons in complex molecules impossible.

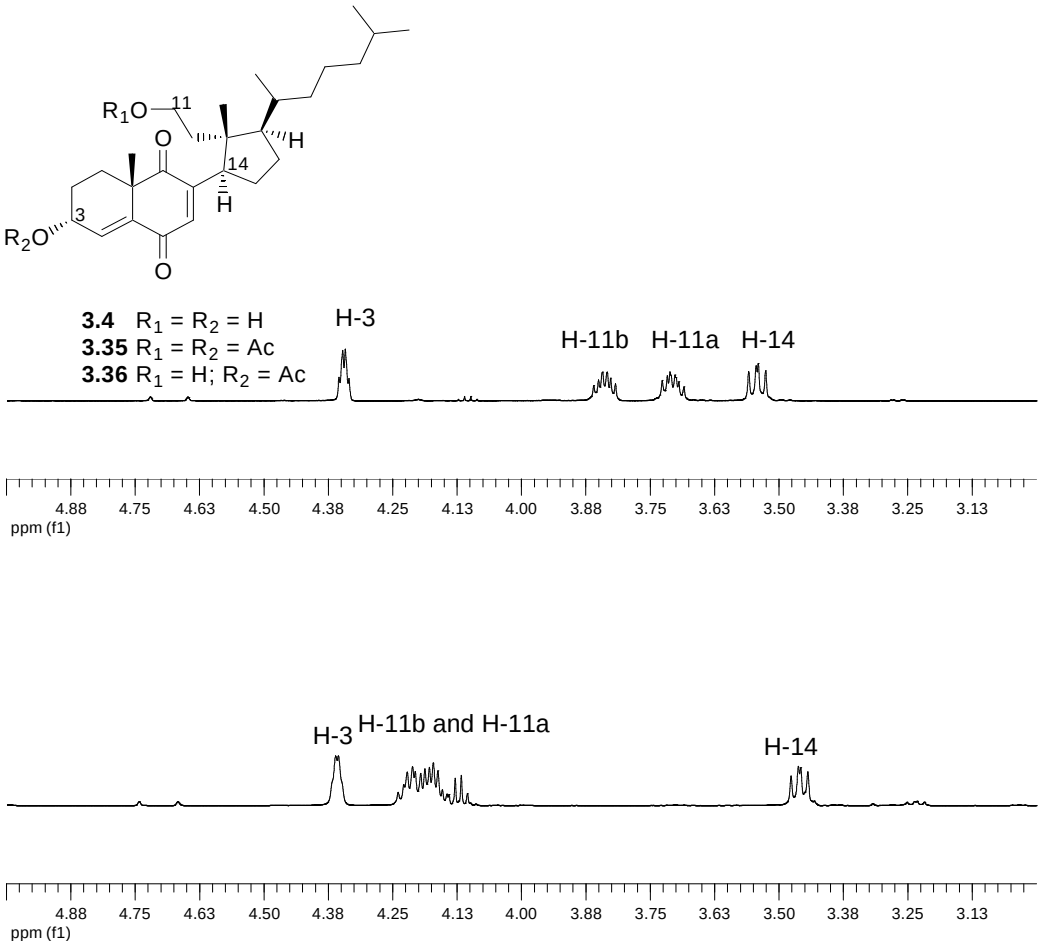

Figure 3.5 The downfield ^{1}H NMR (600 MHz, $CDCl_3$) spectra of **3.4** (top) and **3.36** (bottom) showing the deshielding of H-12a and H-12b after monoacetylation.

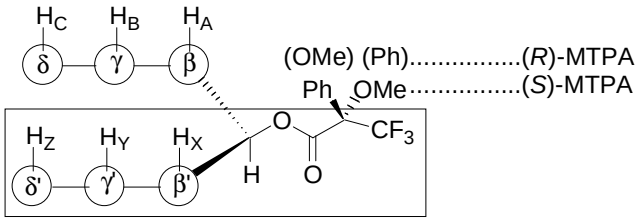

Figure 3.6 The conformation adopted by the (*R*)- and (*S*)-MTPA esters of a secondary alcohol.[123]

In the early days, when Mosher and Dale invented this method, lanthanide and ^{13}F NMR shift reagents, exploiting the chemical shift differences of the CF_3 (^{19}F) or OMe (^{1}H) moieties, were used. The configuration of the secondary alcohol in question was thus determined on the basis of only two data points, reducing the reliability of the method. Fortunately, the advent of high field, Fourier Transform NMR spectrometers has made it possible to completely assign the ^{1}H chemical shifts of complex molecules, greatly increasing the number of data points available, and forming the basis of the modified Mosher's method.[123] Once all protons have been assigned for both the (*R*)- and (*S*)-MTPA esters respectively, the change in chemical shift ($\Delta\delta = \delta_S - \delta_R$) for all protons in the (*R*)- and (*S*)-MTPA esters can be calculated. As indicated (Figure 3.7), when protons with positive $\Delta\delta$ values are placed on the right hand side of the MTPA functionality and those with negative values on the left, the model can be used to determine the absolute configuration of the compound in question.

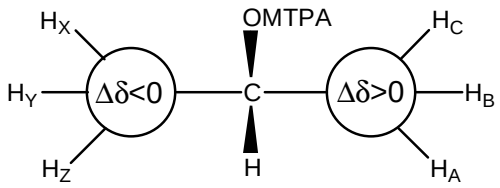

Figure 3.7 Model for absolute configuration determination in the MTPA esters of secondary alcohols.[123]

The (*S*)- and (*R*)-MTPA esters of **3.36** (**3.37** and **3.38)** were accordingly prepared and the ^{1}H and ^{13}C NMR resonances of each ester fully assigned with the aid of gCOSY, gHMBC and gHSQC NMR data. The change in chemical shift ($\Delta\delta = \delta_S - \delta_R$) for all protons was calculated and is summarized in Figure 3.8. Ohtani *et al.*[123] had cautioned that sterically hindered hydroxyl moieties could cause anomalies in the sign of some of the values obtained. Although some anomalies in the values obtained were seen (in the right hand hemisphere of **3.36**), these anomalies were sufficiently distant from the MTPA ester moiety to be disregarded and thus we were able to determine that the configuration at C-3 of the parent secosterol **3.4** is *R*, with the alcohol functionality α-axial to the ring.

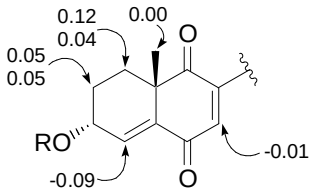

R = MTPA

	S- MTPA ester **3.37**	*R*-MTPA ester **3.38**	
^{1}H number	δ_H	δ_H	$\Delta\delta$
1a	1.83	1.79	0.04
1b	2.1	1.98	0.12
2	2.04	1.99	0.05
3	5.61	5.61	0.00
4	6.56	6.65	-0.09
5	-	-	-
6	-	-	-
7	6.67	6.68	-0.01
8	-	-	-
9	-	-	-
10	-	-	-

Figure 3.8 Proton chemical shifts and calculated Δδ values obtained from the application of the modified Mosher's method to **3.36** (600 MHz, $CDCl_3$).

During the second isolation procedure, methyl resonances, similar to those observed in the ^{1}H NMR spectrum of **3.4**, were noted in the ^{1}H NMR spectra of some of the minor fractions. To investigate the source of these methyl resonances in addition to isolating more of **3.4** for configuration and bioactivity studies, a second collection of *T. costatus* was made from the same location as previously. A collection (1658 specimens) of *T. costatus* was immediately steeped in acetone (600 mL) and stored at -20℃ for one week. One week later, this acetone was decanted, combined with the first fraction, concentrated to approximately 300 mL and loaded onto HP-20 (Scheme 3.5).

The secosterol **3.4** was isolated after exhaustive chromatography and was found in fractions 388-B, 389-B, 394-C and 394-D (303 mg, 0.183 mg/animal). Cholest-7-en-3,5,7-triol, **3.5**, was ultimately isolated through semi-preparative HPLC (50% EtOAc, 50% hexane) of 393-B (16 mg, 0.010 mg/animal).

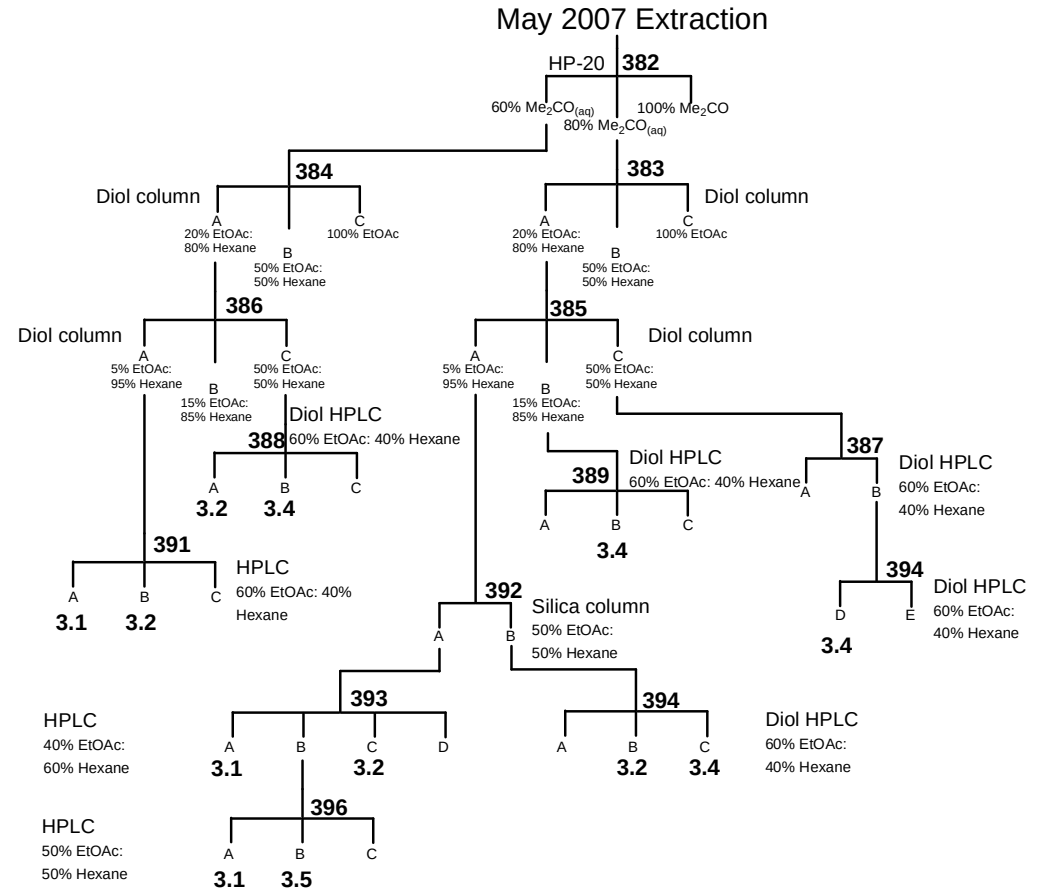

Scheme 3.5 Isolation scheme for May 2007 extraction of *T. costatus* metabolites.

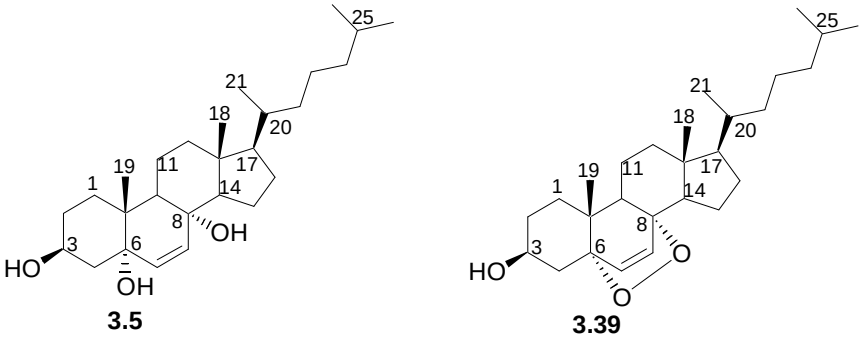

The molecular formula of **3.5** established as $C_{27}H_{46}O_3$ by HRFABMS data, implied five degrees of unsaturation. One degree of unsaturation was accounted for by a disubstituted olefin [δ_C 130.7 (d) and 135.4 (d)], evident in the ^{13}C and DEPT135 spectra of **3.5**. The absence of further unsaturated functionalities led us to deduce a tetracyclic skeleton for **3.5**. A

closer inspection of the ^{13}C and DEPT NMR spectra suggested the presence of twenty seven carbons, comprising one trisubstituted olefin, four quaternary, eight methine (one oxygenated) and ten methylene carbons. The twenty seven carbons and tetracyclic nature of **3.5** suggested a steroid. Analysis of the ^{1}H NMR spectrum of **3.5** revealed the presence of two tertiary methyl groups (δ_H 0.78 and 0.86) as well as three secondary methyl groups (δ_H 0.84, 0.85 and 0.88), similar to those found in **3.4** and consistent with a steroid nucleus. The right hand hemisphere of **3.5** (rings C and D and the side chain) were assigned through analogy with known steroidal compounds, as well as **3.4**, and confirmed by exhaustive gHMBC and gCOSY correlations (Table 3.3). A two bond gHMBC correlation from the remaining methyl functionality H_3-19 (δ_H 0.86), not found in the side chain of **3.5**, allowed for the assignment of quaternary C-10 (δ_C 36.92). Further, three bond gHMBC correlations, from H_3-19 tentatively allowed us to assign methylene carbon C-1 (δ_C 34.7) and methine carbons C-9 (δ_C 51.6) and C-5 (δ_C 82.1). gHMBC correlations between both of two vicinal olefinic methines (δ_H 6.49 and 6.22) in an isolated spin system to C-5 (δ_C 82.1) and another oxygenated quaternary carbon (δ_C 79.4) placed the disubstituted olefin between these two quaternary carbons. The ^{1}H and ^{13}C chemical shifts for C-6 and C-7 were reminiscent of epidioxy sterols, (*e.g.* **3.39**),[126;127] however, the HRFABMS data [*m/z* 419.3525 (calcd for $C_{27}H_{47}O_3$ $[(M + H)^+]$, 419.3525)] supported the structure **3.5**. The mass spectrum of the sterol (Figure 3.9) also revealed no peak corresponding to the loss of molecular oxygen (M – 32), expected for an epidioxy sterol.[128] We thus suggested hydroxyl functionalities at C-6 and C-8. Another three bond gHMBC correlation from H-9 (δ_H 1.54) to δ_C 79.4 allowed us to assign C-8. A three bond gHMBC correlation from the more deshielded of the olefinic resonances (H-7, δ_H 6.49) to C-14 (δ_C 51.0) enabled us to assign C-7 (δ_C 130.7) and suggested that the remaining olefinic resonance was C-6 (δ_C 135.4). A three bond correlation between H-6 and C-4 provided the assignment of C-4 (δ_C 36.89), which was confirmed by a gCOSY correlation between H-3 (δ_H 3.95), and both H-4β (δ_H 1.88) and H-4α (δ_H 2.09). A two bond gHMBC correlation from H-3, as well as gCOSY correlations between H-3 and both H-2β (δ_H 1.51) and H-2α (δ_H 1.82), allowed us to assign C-2 (δ_C 30.1).

Table 3.3 ^{1}H (600 MHz), ^{13}C (150 MHz) and 2D NMR data obtained for **3.5** in $CDCl_3$.

Position	δ_C (mult.)	δ_H (int., mult., *J*/Hz)	gHMBC	gCOSY
1β	34.7 (t)	1.67 (1H, ddd, 13.5, 6.9, 3.5)	C-2, C-3, C-4, C-5, C-19	H-1b, H-2a, H-2b
1α		1.95 (1H, m)	C-2, C-19	H-1a, H-2a, H-2b
2β	30.1 (t)	1.51 (1H, m)	C-3	H-1a, H-1b, H-2b, H-3
2α		1.82 (1H, m)	C-3	H-1a, H-1b, H-2a, H-3
3	66.4 (d)	3.95 (1H, m)	C-1, C-2, C-4	H-2a, H-2b, H-4a, H-4b
4β	36.89 (t)	1.88 (1H, dd, 13.8, 11.7)	C1, C-2, C3, C-5, C-6	H-3, H-4b
4α		2.09 (1H, ddd, 13.8, 5.0, 1.9)	C1, C-2, C3, C-5, C-6	H-3, H-4a
5	82.1 (s)	-	-	-
6	135.4 (d)	6.22 (1H, d, 8.5)	C-4, C-5, C-8, C-9	H-7
7	130.7 (d)	6.49 (1H, d, 8.5)	C-4, C-5, C-8, C-9, C-14	H-6
8	79.4 (s)	-	-	-
9	51.6 (d)	1.54 (1H, dd, 12.2, 4.6)	C7, C-8, C-11	H-11a, H-11b
10	36.92 (s)	-	-	-
11a	20.6 (t)	1.42 (1H, m)	C-8	H-9, H-12a, H-12b
11b		1.61 (1H, m)	C-9	H-9
12a	39.4 (t)	1.17 (1H, m)	C-13	H-11a, H-12b
12b		1.95 (1H, m)	C-9, C-10, C-14	H-11a, H-12b
13	44.7 (s)	-	-	-
14	51.0 (d)	1.48 (1H, m)	C-15	H-15a
15a	23.4 (t)	1.20 (1H, m)	C-12, C-14, C-18	H-14, H-15b, H-16b
15b		1.48 (1H, m)	-	H-15a
16a	28.2 (t)	1.36 (1H, m)	-	H-15a, H-16b, H-17
16b		1.92 (1H, m)	-	H-16a, H-17
17	56.4 (d)	1.17 (1H, m)	C-13, C-16, C-18, C-20	H-16a, H-16b
18	12.6 (q)	0.78 (3H, s)	C-17, C-14, C-13, C-12	-
19	18.1 (q)	0.86 (3H, s)	C-1, C-2, C-5, C-9, C-10	-
20	35.2 (d)	1.36 (1H, m)	C-17	H-17, H-22a
21	18.6 (q)	0.88 (3H, d, 6.5)	C-17, C-22	-
22	35.9 (t)	1.01 (1H, m)	-	H-22b, H-23b
		1.32 (1H, m)	-	H-22a, H-23a
23	23.8 (t)	1.14 (1H, m)	C-25	H-22b, H-23b
		1.32 (1H, m)	-	H-22a, H-23a, H_2-24
24	39.4 (t)	1.14 (2H, m)	C-25, C-26, C-27	H-23b, H-25
25	28.0 (d)	1.51 (1H, m)	C-24, C-26, C-27	H_2-24, H_3-26, H_3-27
26	22.8 (q)	0.85 (3H, d, 6.6)	C-24, C-25, C-27	H-25
27	22.5 (q)	0.84 (3H, d, 6.6)	C-24, C-25, C-26	H-25

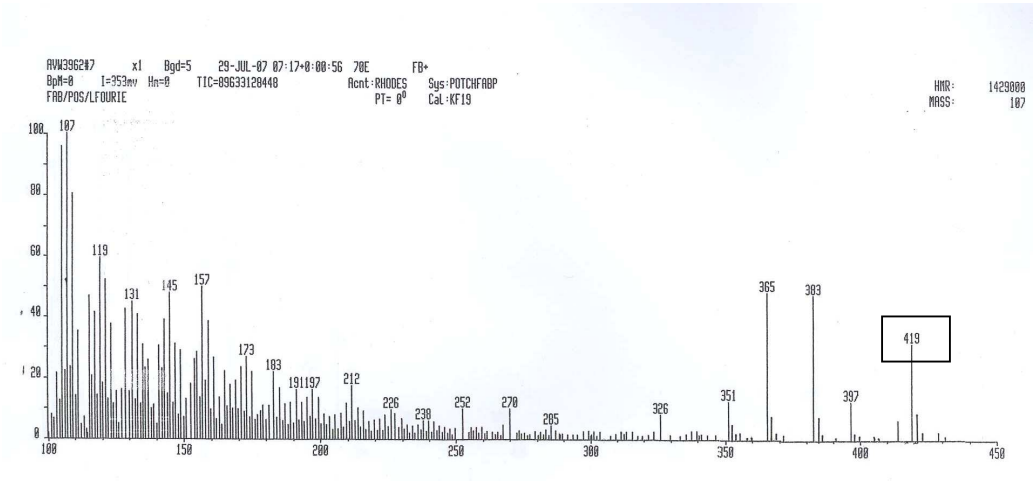

Figure 3.9 FAB mass spectrum of **3.5** showing the $(M + H)^+$ peak at 419 amu.

The relative configuration of the A ring of **3.5** was determined spectroscopically (Figure 3.10). NOESY correlations between H_3-19 (δ_H 0.86) and all three of H-1β (δ_H 1.67), H-2β (δ_H 1.51) and H-4β (δ_H 1.88) suggested that these protons were all on the same face of **3.5**. Similarly, NOESY correlations between H-3 (δ_H 3.95) and all three H-1α (δ_H 1.95), H-2α (δ_H 1.82) and H-4α (δ_H 2.09) but not to any of the β protons suggested that the hydroxyl functionality at C-3 was in a β-equatorial orientation. The congruency between the ^{13}C NMR chemical shifts of C-8 and C-9 in **3.5** and the analogous chemical shifts reported for the epidioxy sterol **3.39**[126;127] would suggest the same configuration at C-8 and C-9 in **3.5**.

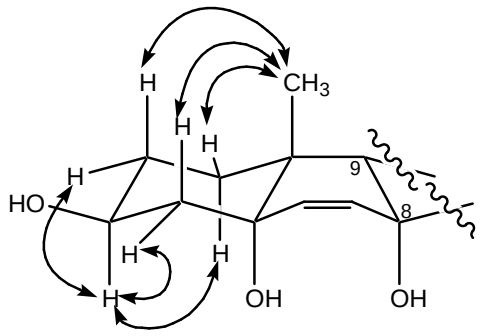

Figure 3.10 Key NOESY correlations used in the determination of the relative configuration of the A ring of trihydroxysterol **3.5**.

3.3 Activity of *Trimusculus* metabolites against oesophageal cancer

As part of an ongoing collaborative research product between the Department of Medicinal Biochemistry at the University of Cape Town and the Marine Natural Products Research Group at Rhodes University, we assayed four of the metabolites (**3.1**-**3.4**) isolated from *T. costatus* as well as the ester, **3.32**, for their activity against oesophageal cancer. Globally, oesophageal cancer is the eighth most devastating form of this disease, with a five year survival rate of lower than 10% after diagnosis.[129] The incidence of the cancer is generally higher in males than in females and is increasing globally. Aetiological studies of this disease are complicated by the number and inconsistency of external factors associated with the disease.[130-132] In the South African context, oesophageal cancer is the second most common cancer,[133] with studies in Soweto revealing that residents there had a five fold higher risk of developing the cancer than the world average.[134] High incidence rates have also been reported in the former Transkei,[131] particularly amongst Xhosa males. Although a wide range of factors have been linked to the disease, oesophageal cancer has traditionally been associated locally with low socio-economic status, poor nutrition (including maize contaminated with *Fusarium*), and particularly the use of alcohol and tobacco.[131;132;134;135] A recent study has, however, concluded that the consumption of home-brewed beer (and the associated intake of excessive dietary iron) could not directly be related to an increased risk of development of oesophageal cancer once adjustment for sex, age and tobacco usage had been made.[136] Prompted by the extraordinarily high incidences of this form of cancer, Bohr *et al*. detected a strong correlation (approximately 50%) between patients with bacteria of the family *Heliobacteracea* and oesophageal carcinomas, implying that these bacteria may be involved in the initiation of the cancer of the oesophagus.[134] Similarly, the Human Papilloma Virus (HPV) has been detected in 15 -75% of oesophageal tumours studied.[135]

Although the survival rate of patients with oesophageal cancer has improved over the past few decades, long term prognoses are not good.[137] Adjuvant radiotherapy has also been shown not to improve chances of survival and although chemoradiation has shown promising results, the extended treatment periods may lead to poor compliance and proper localization

of the treatment has proven problematic.[137] A comprehensive strategy consisting of treatment with combined cisplatin (**3.40**) and 5-fluorouracil (**3.41**) based chemotherapy, in addition to surgery, is currently the most commonly used and effective treatment.[135]

At the Department of Medicinal Biochemistry, University of Cape Town, activity of the pure secondary metabolites isolated (and those modified in the course of absolute configuration determination) against the oesophageal cancer cell line WHCO1 was determined. A dose response curve was determined from the (MTT) assay and IC_{50} values hence determined. The MTT [3-(4,5-dimethylthiazol-2-yl)-2,5-diphenyltetrazolium bromide] assay is a colorimetric assay, based on the action of a mitochondrial dehydrogenase enzyme on the tetrazolium rings of MTT (pale yellow), to form formazan crystals (dark blue).[135;138] Viable cells can be detected by the accumulation of the cell membrane impermeable formazan crystals within them. After solubilisation of the cells by the addition of a detergent, the number of cancerous cells surviving in the presence of the potentially cytotoxic compound being tested is directly proportional to the level of the formazan crystals present.[135;138] A mulitiwell scanning spectrophotometer (ELISA reader) is used for the determination of the level of formazan present. The IC_{50} values of metabolites **3.1**-**3.4** and **3.32** (as well as comparison compounds **3.40** and **3.42**) against the oesophageal cancer cell line WHCO1 are summarized in Table 3.4.

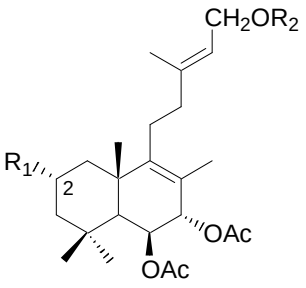

3.1 $R_1 = R_2 = H$;
3.2 $R_1 = OAc$; $R_2 = H$
3.3 $R_1 = H$; $R_2 = Ac$
3.32 $R_1 = H$; R_2 = camphanate

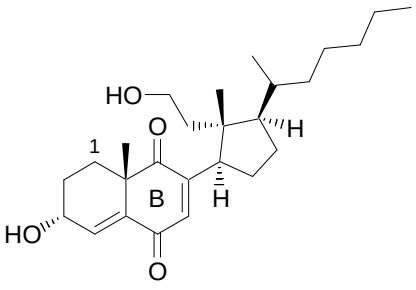

3.4

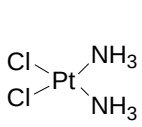

3.40

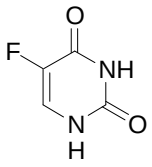

3.41

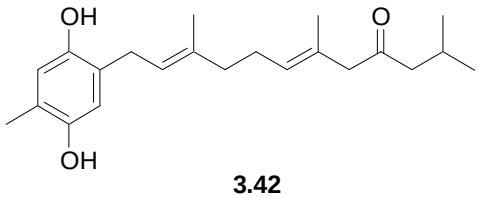

3.42

Table 3.4 Summary of the IC_{50} values of compounds against the WHCO1 cell line.

	Compound tested						
	3.1	**3.3**	**3.32**	**3.2**	**3.4**	**3.40**	**3.42**
IC_{50} (μM)	25.1	84.2	77.2	23.7	3.2	13.0	9.5

Since only a few compounds were screened against the oesophageal cancer cells (Table 3.3), we are able to draw only tentative conclusions regarding structure-activity relationships. The first conclusion is that oxygenation at C-2 appears to have little effect on the IC_{50} value (**3.1** and **3.2**). Secondly, the primary alcohol on the alkenyl chain appears to be of some importance, since esterification of **3.1** (**3.3** and **3.32**) brings about a significant increase in the IC_{50} value of the diterpenes. Furthermore, the bulkiness of the moiety esterified to **3.1** appears to have little influence on the IC_{50} value, since **3.3** and **3.32** have comparable values. Of the four naturally occurring metabolites (**3.1-3.4**), only **3.4** had a lower IC_{50} value than cisplatin (**3.40**). Another triprenylated toluhydroquinone compound (**3.42**) used for comparative purposes has been included since it has been the subject of some interest in our laboratory. A collaborative effort between the Department of Medicinal Chemistry and our own research group has revealed that **3.42** (and related analogous diterpenes from the same natural product source) induces apoptosis through the generation of reactive oxygen species (ROS) as the result of the oxidation of the hydroquinone moiety to a quinone.[135] Since ring B of **3.4** is structurally similar to a quinone, the possibility exists that this secosterol may have a similar mode of action. Naturally further studies would be required to support this supposition.

3.3 Conclusions

The known diterpenes **3.1** and **3.2**, as well as one new diterpene, **3.3** were isolated from the pulmonate mollusc, *T. costatus.* The absolute configuration of **3.2**, and hence **3.1** and **3.3** was determined through X-ray diffraction of a single crystal of the camphanate ester of **3.2**. The new 9,11-secosterol**, 3.4**, was also isolated and the relative configuration determined by spectroscopic means. The modified Mosher's method was employed to determine the absolute configuration of the secondary hydroxyl at C-3. The new trihydroxylated sterol, **3.5**, was also isolated and the relative configuration in ring A determined from NOESY data. The activity of compounds **3.1**-**3.4** and **3.32** against an oesophageal cancer cell line was investigated, with **3.4** exhibiting modest activity.

Chapter Four

Semi-synthesis of Nitrile-containing Labdane Diterpenes with Agrochemical Potential

4.1 Introduction

This chapter describes an extension of the PhD thesis research of Gray[100] and includes a comprehensive investigation of the agrochemical properties of a trio of unusual labdane diterpene nitriles 9α-cyano-15,16-epoxy-7β-hydroxylabda-13(16),14-dien-6-one (**4.1**), 9α-cyano-15,16-epoxy-7-hydroxylabda-7,13(16),14-trien-6-one (**4.2**) and 9α-cyano-15,16-epoxy-6β,7β-dihydroxylabda-13(16),14-diene (**4.3**). Nitriles **4.1**, **4.2** and **4.3** were derived from the readily available South African terrestrial plant metabolite hispanolone (**4.4**). The introduction to this chapter provides a synopsis of Gray's original synthesis of **4.1** and a discussion of the relevance of his work to the molluscan chemistry described in Chapter Three. The introduction is followed by a detailed account of how Gray's initial findings were extended to provide firstly, more of **4.1** for *in planta* studies at Dow AgroSciences in the USA, secondly a new minor product, **4.2**, from the Michael addition reaction that afforded **4.1** and, thirdly, a reduced analogue of **4.1**, **4.3**, for a limited structure-activity relationship (SAR) study of the fungicidal properties of labdane diterpene nitriles. Surprisingly, the promising initial activity of **4.1** against the economically important plant fungicidal pathogen, *Phytophthora infestans* (potato late blight) could not be reproduced. Fortuitously, **4.1**, **4.2** and **4.3** exhibited significant activity in the secondary screening against *Magnaporthea grisea* (rice blast) and *Puccinia recondita* (wheat brown rust) at levels sufficient to warrant further *in planta* testing. The details of the *in planta* tests performed on **4.1**, **4.2** and **4.3** by Dow AgroSciences conclude this chapter.

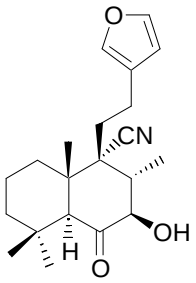

4.1

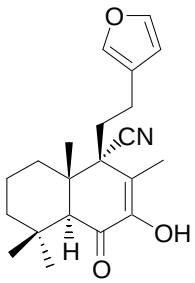

4.2

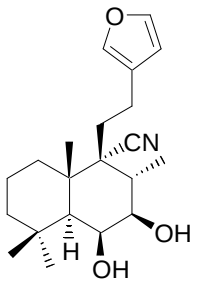

4.3

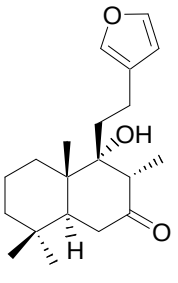

4.4

4.1.1 A summary of Gray's original synthesis of the labdane nitrile, ***4.1***

At the time that Gray *et al*.[10;100] first isolated compounds **3.1** and **3.2** from *Trimusculus costatus*, only the relative configuration of the *Trimusculus* diterpene metabolites had been established *via* a non-stereoselective synthesis of **4.5** (Scheme 3.1, Chapter Three).[102] As a consequence Gray *et al.* attempted a stereoselective semi-synthesis (Scheme 4.1) of **3.1** from optically active rhinocerotinoic acid (**4.5**) to unambiguously determine the absolute configuration of the *Trimusculus* metabolites.

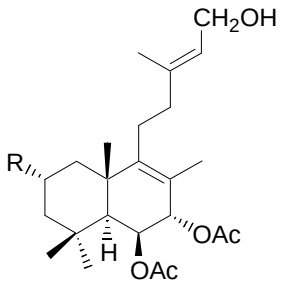

3.1 R = H
3.2 R = OAc

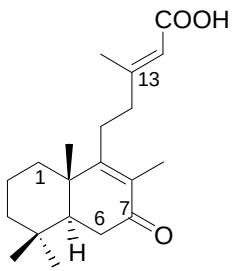

4.5

Diterpene **4.5** was selected as a synthetic precursor to **3.1** for a number of reasons, the most obvious being that a typical labdane configuration at C-5 and C-10 was already in place and a ketone functionality at C-7 not only provided oxygenation at this position but also a means to direct further oxygenation to C-6. The positioning of the Δ^8 and Δ^{13} olefins and the requisite *E* geometry of the Δ^{13} olefin in the side chain of **4.5** were also the same as in **4.1**. Finally, the report that rhinocerotinoic acid had been isolated from a South African plant *Elytropappus rhinocerotis*,[139] a species common in the veld around Grahamstown, meant that a potential source of **4.5** existed close at hand.

Unfortunately, preliminary screening of extracts of *E. rhinocerotis* collected near Grahamstown revealed that local specimens of this plant did not contain any **4.5**. Consequently, the semi-synthesis of **4.5** from sclareol (**2.21**) described by Dekker,[139] which had provided the absolute configuration of rhinocerotinoic acid was modified by Gray *et al.*[100] and **4.5** obtained in an improved 32% overall yield (Scheme 4.1).[100;140]

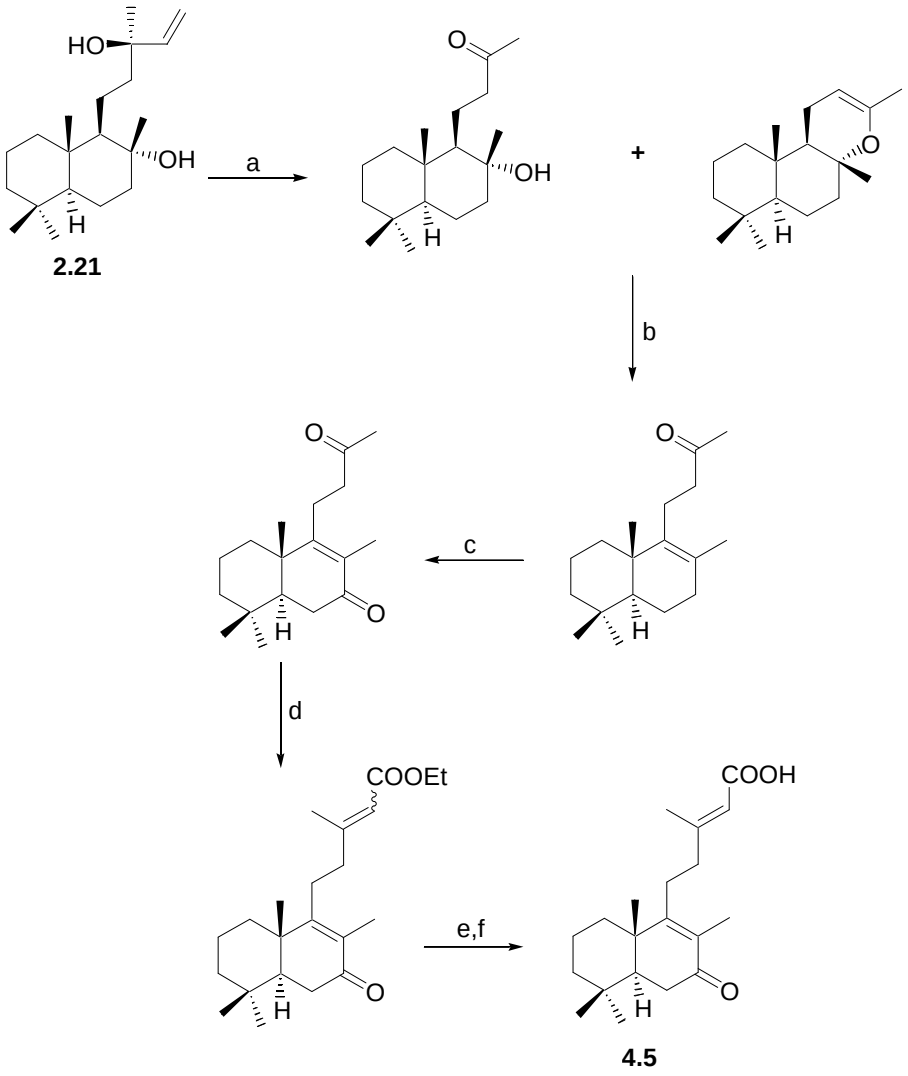

Scheme 4.1 Stereoselective synthesis of **4.5** from (-)-sclareol (**2.21**).[100;140] *Reagents and conditions*: (a) $KMnO_4$, Me_2CO, 15 ℃, 18 h; (b) I_2 (cat.), benzene, Δ, 6 h; (c) CrO_3-Py_2, CH_2Cl_2, RT, 72 h; (d) $(C_2H_5O)_2P(O)CH_2CO_2Et$, NaH, THF, RT, 2 h; (e) H_2SO_4, AcOH, 100 ℃, 4 h; (f) Trituration from hexane.

Although a reliable route to a supply of **4.5** was now available,[100;140] synthesizing large quantities would prove both time consuming and costly if this material was also going to be used to explore various methodologies for stereoselective oxygenation at C-6 and subsequent reduction of the C-7 ketone moiety. A similar diterpene, hispanone (**4.6**), which contains the same A and B ring substitution pattern as **4.5**, was therefore chosen as a model

compound for oxygenation studies. Hispanone had previously been isolated by members of the same research group[141] from the local plant, *Ballota africana* (Figure 4.1). Although **4.6** was isolated as a minor component from *B. africana* (and may be an artefact of the isolation procedure)[141] transformations of the major component, **4.4**, to **4.6** were well established.[142-144]

Figure 4.1 The southern African plant, *B. africana*.

Gray *et al.* thus isolated **4.4** from *B. africana* and quantitatively converted this compound to **4.6** (Scheme 4.2) *via* an iodine mediated dehydration reaction. Various methods for introducing the desired oxygenation at C-6 in **4.6** were attempted, including manganic acetate oxidation to give an epimeric mixture of the C-6 acetates of **4.6** (**4.7** and **4.8**) and eventually the stereoselective Rubottom procedure to give 6α-hydroxy hispanone (**4.9**).

The epimers **4.7** and **4.8** could be readily separated by semi-preparative HPLC, however, both compounds proved surprisingly susceptible to acid hydrolysis, yielding a complex inseparable mixture of products. Saponification of **4.7** and **4.8** (Scheme 4.3) was similarly unsuccessful, yielding only a small amount of the required saponification product, (**4.9**, 4%) as well as the enols (**4.10**, 26%) and (**4.11**, 30%).

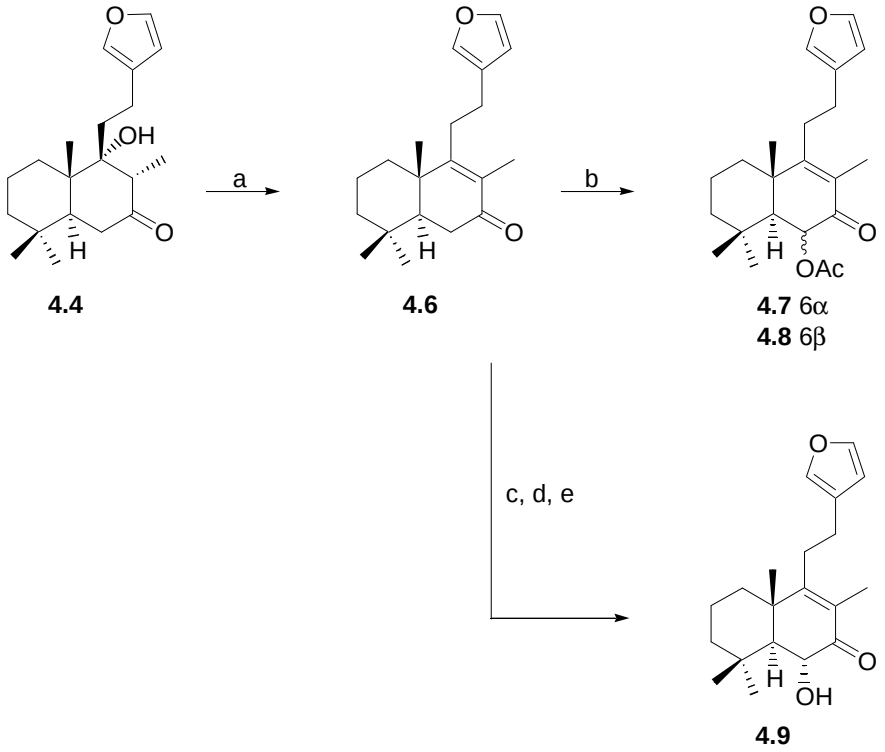

4.4 **4.6** **4.7** 6α **4.8** 6β **4.9**

Scheme 4.2 Gray *et al.*'s[100] approaches to oxygenation at C-6. *Reagents and conditions*: (a) I_2 (cat.), C_6H_6, Δ; (b) $Mn(OAc)_3$, C_6H_6, Δ; (c) LDA, TMSCl, THF, -78℃-RT, 5 h; (d) *m*-CPBA, CH_2Cl_2, 0℃-RT, 1 h; (e) HCl wash.

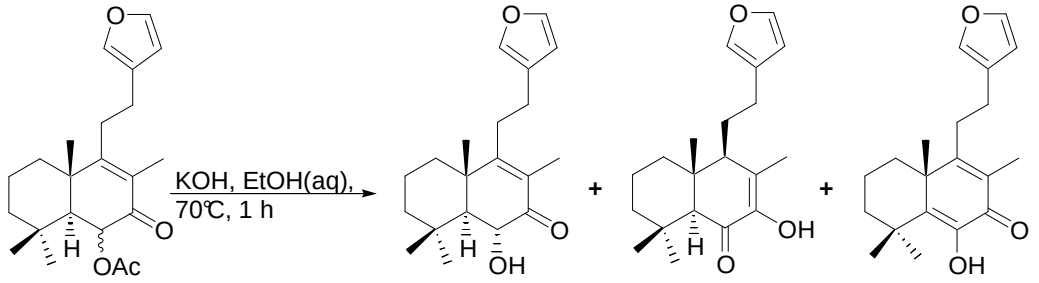

4.7 6α **4.8** 6β **4.9** **4.10** **4.11**

Scheme 4.3 Saponification of **4.7** and **4.8**.[100]

Gray[100] consequently attempted Mori's potassium cyanide catalyzed transesterification reaction (Scheme 4.4),[145] which yielded the required **4.9** in low yield (15%) and surprisingly the Michael adduct **4.1** as the major product (43%). It is this latter product which was of interest to us (*vide infra)*.

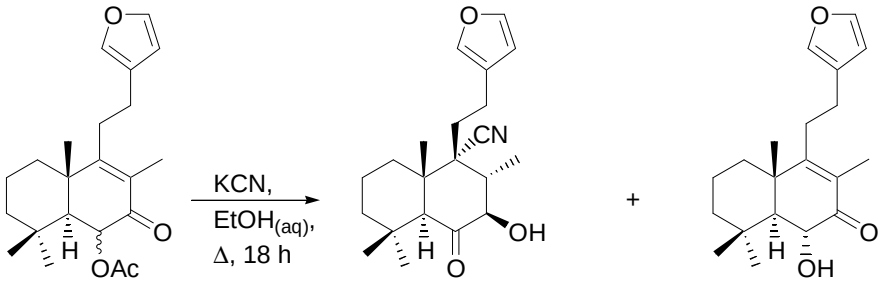

4.7 6α
4.8 6β
4.1
4.9

Scheme 4.4 Compounds resulting from Gray's[100] attempts at KCN mediated transesterification.

As part of an ongoing screening program with Dow AgroSciences (Indianapolis, USA), twelve compounds (**4.1**, **4.4**, **4.6**-**4.9** and **4.12-4.17**) from Gray's model studies on **4.4** were subjected to two insecticidal (beet army worm and tobacco worm), four fungicidal (potato late blight, wheat glume blotch, maize smut and wheat leaf blotch) and two herbicidal (bent grass and duckweed) tests. Of all these compounds only the nitrile, **4.1**, was found to be active, specifically against potato late blight.

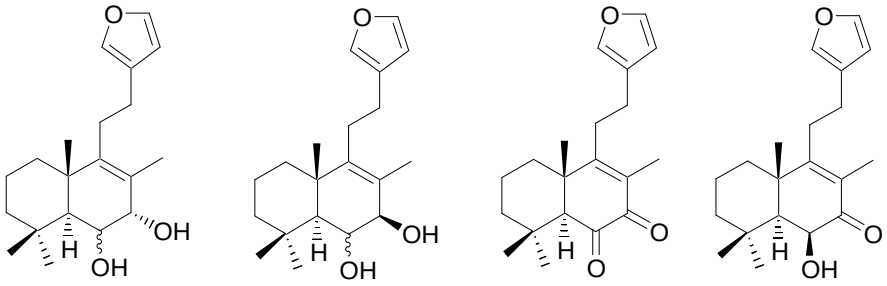

4.12 6α
4.13 6β
4.14 6α
4.15 6β
4.16
4.17

Potato late blight is caused by the pathogenic fungus *Phytophthora infestans* and has been ranked as the most devastating disease in world agriculture.[146] The pathogen acts quickly and is capable of laying waste to entire plantings of potatoes within one week of infection. In the late 1840's this plant pathogen laid waste to the potato crops in Ireland, leading to widespread starvation (over one million people died) and forcing an equivalent number of Irish citizens to migrate to other countries.[146] Today, potato late blight is just as devastating, especially in countries such as Russia, where the potato is a staple food. New, more virulent strains are emerging and even with modern fungicides, crop losses due to the pathogen are estimated at around 15%.[146] A need therefore exists for novel fungicides active against *P. infestans* and since **4.1** showed some potential in this regard, Dow AgroSciences were interested in performing further *in planta* assays. Unfortunately, as **4.1** was only produced as an unexpected side product, supplies were limited and more material needed to be provided in order for the *in planta* tests to be carried out. Although time constraints prevented Gray from synthesizing more of **4.1**, the potential of the diterpene as an agrochemical warranted further investigation, particularly since only three reaction steps were required to produce the novel compound from a readily available plant natural product derivative, **4.4**.

Our aim was, therefore, to extend Gray's preliminary discovery to:

- provide sufficient amounts of **4.1** for *in planta* trials at Dow AgroSciences
- explore more efficient procedures for extracting **4.4** from *B. africana*
- investigate the Michael addition in more detail to discover possible nitrile minor products
- establish unequivocally the α position of the C-9 nitrile substituent in this series of compounds implied from NOE studies
- synthesize analogues of **4.1** for structure-activity relationship studies

4.2 Collection of plant material and isolation procedures

4.2.1 Collection of B. africana and extraction and isolation of hispanolone, ***4.4***

A collection of *B. africana* was made in November 2003 at Woodbury Lodge, Amakhala Game Reserve, situated along the N2 between Grahamstown and Port Elizabeth, Eastern Cape, South Africa. The aerial parts of the collected plants were air-dried for two months before being steeped in acetone for three days. The acetone extract was subsequently decanted, filtered and concentrated *in vacuo* to a tenth of its original volume. Overnight decolourization of the dark green extract with activated charcoal, followed by filtration through celite afforded a gold coloured solution. At the same time that we were isolating **4.4** from *B. africana*, we were experimenting with a new chromatographic medium (HP-20) in our laboratory (see Chapter Two for more details). We decided to attempt to use this chromatographic stationary phase and compare the results with those reported for the isolation of **4.4** by Davies-Coleman *et al*.,[141] involving standard silica gel chromatography. The decolourized extract concentrate was thus loaded onto an HP-20 column in the manner described in Chapter Two and sequentially stripped with aliquots of aqueous acetone in a sequence of decreasing polarity in the normal manner. As we routinely "back loaded" the $60\%_{(aq)}$ acetone fraction onto a second, smaller HP-20 column as a facile method for removal of water (metabolites are re-adsorbed onto the HP-20 column and eluted with pure acetone), we diluted this fraction to 1.5L with water and were gratified to notice small crystalline plates in solution that we suspected to be **4.4**. We allowed this chromatographic fraction to stand for four days at 4℃, before filtering off the resulting white crystalline plates (3.82 g, 1.5%). The plates were confirmed to be **4.4** by comparison of the ^{1}H and ^{13}C NMR data of the crystalline material with reported data.[141] Most importantly, this method also gave nearly double the yield (1.52%) of **4.4** from *B. africana* over that reported (0.8%) for the isolation of this compound using standard normal phase chromatographic methods.[141]

4.3 Semi-synthesis of a diterpene based agrochemical from hispanolone

Although an established protocol[142-144] for the dehydration of **4.4** using thionyl chloride already existed, Gray[100] had had difficulty duplicating their reported yields and instead opted for Mangoni and Bellardini's iodine catalysed dehydration reaction[147] for the conversion of **4.4** to **4.6**.[148] Accordingly **4.4** was refluxed with catalytic quantities of molecular iodine in anhydrous benzene under a Dean-Stark trap. Initially unable to achieve the same degree of conversion (87%) reported by Gray, we attempted the same method but using toluene sulfonic acid as the dehydrating agent. After work-up of the toluene sulfonic acid dehydration reaction, only the starting material **4.4** was evident by analysis of the ^{1}H NMR spectrum. The presence of **4.6** would have been discernable by the appearance of a vinylic methyl singlet at δ_H 1.79 and the disappearance of the methyl doublet of **4.4** (δ_H 1.11). Ultimately the difficulties with using molecular iodine as the catalyst for dehydration were solved by placing 3Å molecular sieves in the collecting vessel of the Dean-Stark trap and we were able to achieve almost quantitative dehydration (by NMR) after refluxing for 24 hours. Standard silica flash chromatography (5% ethyl acetate, 95% hexane) afforded pure **4.6** (84%) as crystals (from methanol), whose data were identical in all respects to those reported for this compound.[100;141] The mechanism for the iodine catalyzed reaction is not fully understood, although Reeve and Doherty[149] suggested that the dehydration may proceed *via* a carbonium ion.

Initial attempts at the α'-acetoxylation of **4.6** using manganic acetate were relatively low yielding compared with those reported in the literature.[150;151] Bush and Finkbeiner[152] had suggested that the method of preparation of the manganic acetate might influence the yield obtained and we thus decided to compare the yields obtained from commercial manganic acetate with those from manganic acetate which we had prepared from manganese diacetate.[153] The α'-acetoxylation reaction was replicated four times, varying either the solvent or reagent as presented in Table 4.1.

Table 4.1 Summary of conditions for the α'-acetoxylation of **4.6**.

Source of manganic acetate	Solvent	Time refluxed	% Yield (by NMR)
Aldrich	benzene	48 hours	100%
Self-prepared	benzene	48 hours	19%
Aldrich	toluene	48 hours	61%
Self-prepared	toluene	48 hours	0%

As can be seen from Table 4.1, the problem lay with the source of the manganic acetate, with material bought from Aldrich proving superior, regardless of the solvent used, for the α'-acetoxylation reaction. Our reasoning for using toluene as an alternative solvent lay in the higher boiling point of this solvent (111℃ as compared with 80℃ for benzene), which would enable the solution to be refluxed at a higher temperature. At the same time, we surmised that since the reaction requires the removal of water by means of a Dean-Stark trap, benzene's ability to form an azeotropic mixture with water (which toluene lacks) might facilitate this removal and thus improve the yields (Table 4.1). From the results presented in Table 4.1, benzene proved to be the better solvent for the α'-acetoxylation reaction.

After workup of the reaction in which commercial manganic acetate and benzene were used to achieve the α'-acetoxylation of **4.6**, **4.7** and **4.8** were successfully separated (in a 5:2 ratio) using normal phase HPLC (10% ethyl acetate, 90% hexane) in 66% overall yield. Later attempts at α'-acetoxylation of **4.6**, in which acetic acid was added to the reaction mixture prior to refluxing, failed to improved the yields obtained in this reaction. Reportedly,[150] acetic acid increases the solubility of manganic acetate in organic solvents. Our overall yield of 66% is nonetheless a substantial improvement over the 19% overall conversion of **4.6** to **4.7** and **4.8** reported previously.[142]

Williams and Hunter[153] proposed two mechanisms for the α'-acetoxylation of enones using manganic acetate. The first of these is based on the ligand transfer mechanism similar to that proposed for the lead tetraacetate mediated oxidation of enones (Scheme 4.5).

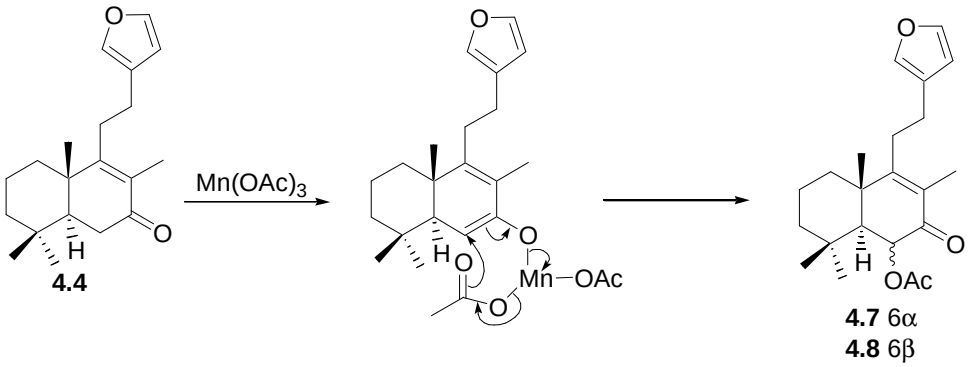

Scheme 4.5 Ligand transfer mechanism for α'-acetoxylation of **4.6** by manganic acetate.[153]

The second mechanism proposed (Scheme 4.6) proceeds *via* ligand transfer to an α-keto radical. This radical based mechanism currently appears to be more widely accepted than the ligand transfer mechanism.[150;154]

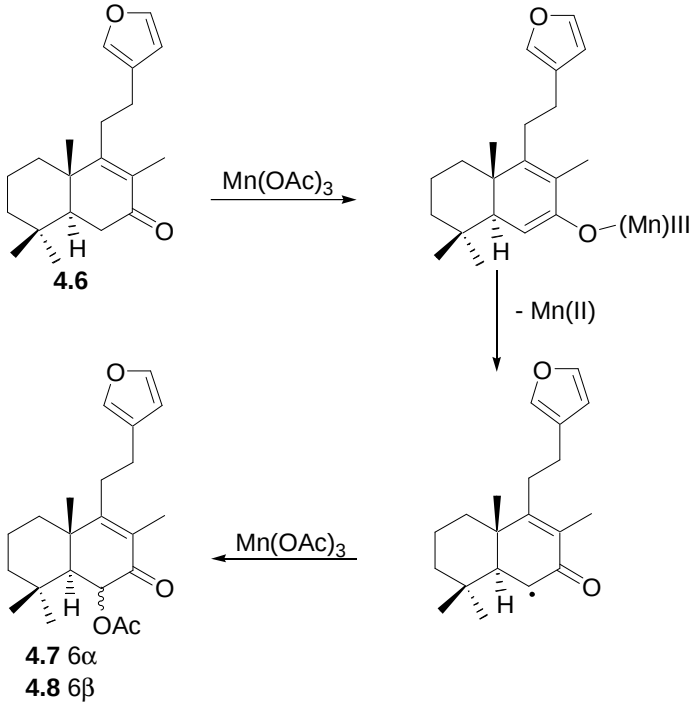

Scheme 4.6 Radical based mechanism for α'-acetoxylation of enones.[154]

The final step in the synthesis of **4.1** involved the unexpected Michael addition of a cyanide nucleophile to an enone during Mori's[145] mild transesterification procedure (Scheme 4.7).

Accordingly, a mixture of **4.7** and **4.8** was dissolved in 95% aqueous ethanol in the presence in potassium cyanide and refluxed for 24 hours until the starting material could no longer be detected by TLC. After workup, the reaction mixture was subjected to normal phase semi-preparative HPLC (10% ethyl acetate, 90% hexane) to give 9α-cyano-15,16-epoxy-7β-hydroxylabda-13(16),14-dien-6-one, **4.1** (45%), 9α-cyano-15,16-epoxy-7-hydroxylabda-7,13(16),14-trien-6-one, **4.2** (9%), 6-hydroxy-15,16-epoxylabda-5,8,13(16),14-tetraene-7-one, **4.11** (2%) and 6α-hydroxy-15,16-8,13(16),14-trien-7-one, **4.9** (1%). The data for **4.1**, **4.9** and **4.11** were identical in all respects to those reported by Gray.[100] The structure of the new minor product, **4.2**, was determined from comparison of ^{1}H and ^{13}C NMR data of this compound with those of **4.1** as well as by application of standard 2D NMR techniques as follows.

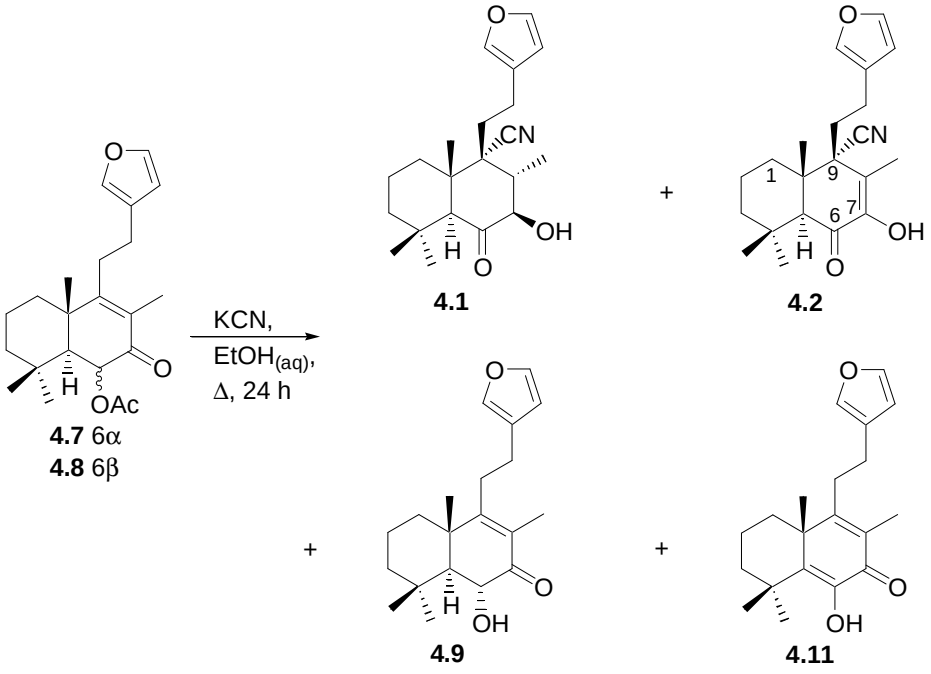

Scheme 4.7 The Michael addition and transesterified products resulting from refluxing **4.7** and **4.8** with KCN in $EtOH_{(aq)}$.

The molecular formula ($C_{21}H_{29}O_3$) of **4.2**, which differed from that of **4.1** by the loss of two hydrogen atoms, was established by HRFABMS data and implied nine degrees of

unsaturation, five of which were accounted for by the decalin and furan ring systems. The presence of a nitrile moiety [δ_C 119.5 (Figure 4.2), supported by an IR stretching band at 2222 cm^{-1} and a ketone functionality (δ_C 193.6) accounted for a further three degrees of unsaturation, leaving one degree of unsaturation unaccounted for.

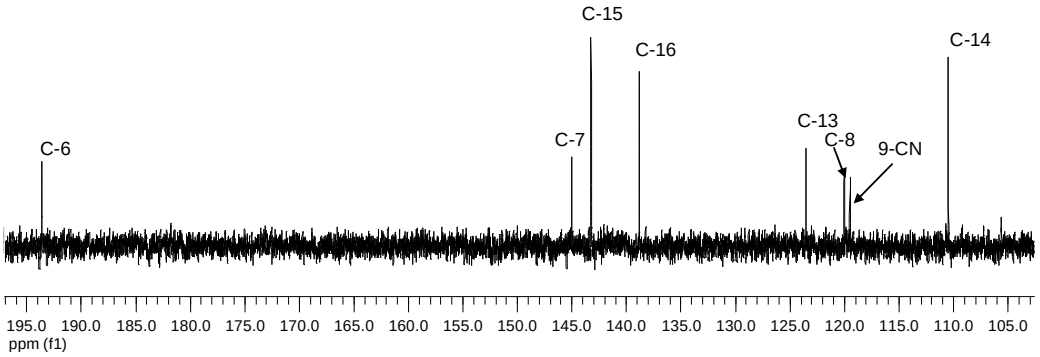

Figure 4.2 Downfield ^{13}C NMR spectrum (400 MHz, $CDCl_3$) of **4.2**.

Comparison of the ^1H and ^{13}C NMR data of known **4.1** with that of new **4.2** indicated that the changes in substitution pattern were limited to ring B. The disappearance of the signals for C-7 and C-8 (δ_C 77.3 and 47.1) and the appearance of the two resonances of a tetrasubstituted olefin (δ_C 145.0 and 120.0) implied that these could be assigned to C-7 and C-8 and accounted for the outstanding double bond equivalent. The upfield shift of carbonyl C-6 (δ_C 193.6) was consistent with that of an α,β-unsaturated ketone, supporting the Δ^7 placement of the double bond. The position of the nitrile moiety at C-9 (δ_C 46.0) was confirmed by three bond gHMBC correlations from H-11a and H-11b (δ_H 1.85 and 1.99) and Me-17 (δ_H 2.01) to the carbon of the nitrile moiety (9-CN, δ_C 119.5). The 1,2-transposition of the carbonyl functionality from C-7 in **4.7** and **4.8** to C-6 in **4.2** (similar to that observed in **4.1**) was confirmed by a two bond gHMBC correlation from singlet H-5 (δ_H 2.75) to carbonyl C-6 (δ_C 193.6). The ^1H and ^{13}C NMR data and a summary of all gCOSY and gHMBC correlations for **4.2** is provided in Table 4.2. A NOESY correlation between H_3-20 (δ_H 1.00) and H-11a tentatively suggested an α-axial placement of the nitrile functionality at C-9. This configuration

was later confirmed by X-ray analysis of a single crystal of **4.2** grown from hexane/benzene (Figure 4.3).

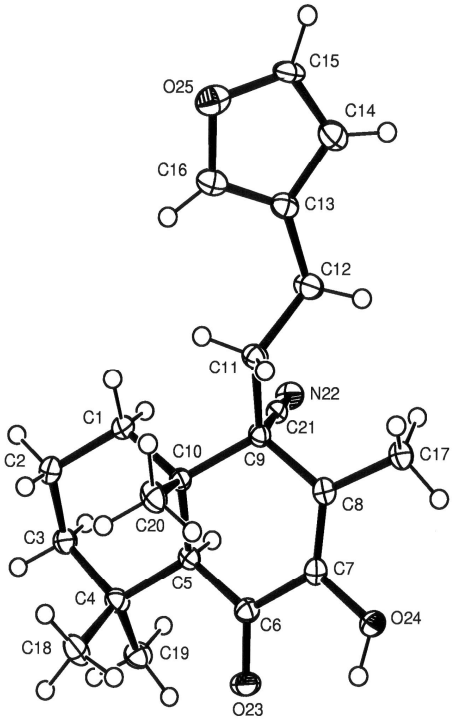

Figure 4.3 A view of a molecule of 9α-cyano-15,16-epoxy-7-hydroxylabda-7,13(16),14-trien-6-one, **4.2**.

We believe that the 1,2-transposition of the ketone functionality in **4.1** probably occurs after the saponification of **4.7** or **4.8** and may be an example of the Lobry de Bruijn-Alberda van Eckenstein rearrangement, best known in carbohydrate chemistry. As a small matter of interest, this already impressively named reaction is an abbreviation of the even more spectacularly named Cornelius Adriaan van Troostenbery Lobry de Bruijn and Willem Alberda van Eckenstein reaction.[155] The general mechanism for this rearrangement reaction in **4.1** is shown below (Scheme 4.8) and proceeds *via* an enolate.

Table 4.2 ^{1}H (400 MHz), ^{13}C (100 MHz) and 2D NMR data for 9α-cyano-15,16-epoxy-7-hydroxylabda-7,13(16),14-trien-6-one (**4.2**) in $CDCl_3$.

Position	δ_C (mult.)	δ_H (int., mult., *J*/Hz)	gHMBC	gCOSY
1	35.1 (t)	1.80 (2H, m)	C-2, C-3, C-10	H_2-2
2	17.8 (t)	1.60 (2H, m)	C-1, C-2	H-3a, H-3b, H_2-1
3	41.9 (t)	1.32 (1H, m)	C-1, C-2, C-4, C-5	H-3b, H_2-2
		1.45 (1H, dddd, 13.5, 3.5, 3.2, 1.1)	C-1, C-2, C-4, C-5	H-3a, H_2-2
4	32.8 (s)	-	-	-
5	58.6 (d)	2.75 (1H, s)	C-3, C-4, C-6, C-7, C-10, C-18	-
6	193.6 (s)	-	-	-
7	145.0 (s)	-	-	-
8	120.0 (s)	-	-	-
9	46.0 (s)	-	-	-
10	52.5 (s)	-	-	-
11	31.6 (t)	1.85 (1H, m)	C-8, C-9, C-10, C-12, C-13, 9-CN	H-11b, H_2-12
		1.99 (1H, m)	C-8, C-9, C-12, C-13,C-20, 9-CN	H-11a, H_2-12
12	24.7 (t)	2.82 (2H, m)	C-11, C-13, C-14, C-16	H-11a, H-11b
13	123.6 (s)	-	-	-
14	110.5 (d)	6.29 (1H, m)	C-13, C-15,C-16	H-15, H-16†
15	143.3 (d)	7.38 (1H, t, 1.7)	C-13, C-16	H-14, H-16†
16	138.8 (d)	7.28 (1H, m)	C-13, C-14,C-15	H-14†, H-15†
17	12.6 (q)	2.01 (3H, s)	C-7, C-9, C-10	-
18	33.4 (q)	1.16 (3H, s)	C-3, C-4, C-5, C-19	-
19	21.5 (q)	1.24 (3H, s)	C-3, C-4, C-5, C-18	-
20	15.7 (q)	1.00 (3H, s)	C-1, C-5, C-9, C-10	-
9-CN	119.5 (q)	-	-	-
7-OH		6.46 (br s)	C-6, C-7, C-8	-

†Weak gCOSY correlations.

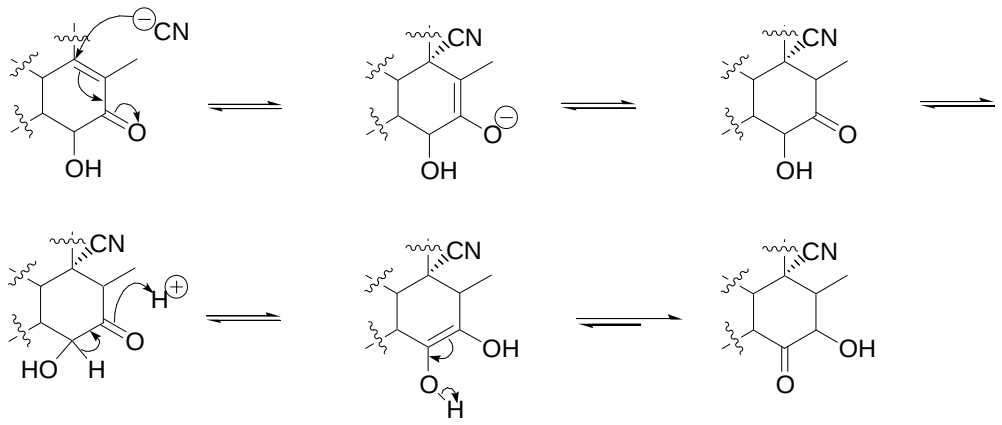

Scheme 4.8 Mechanism for the post saponification formation of **4.1**, incorporating the Lobry de Bruijn-Alberda van Eckenstein rearrangement adapted from Jones.[155]

Although we now had sufficient **4.1** available to perform *in planta* bioactivity studies, we theorized that a simple reduction of the ketone functionality would produce an additional analogue of **4.1** for structure-activity relationship studies and might also improve the hydrophilicity of the compound. Naturally, aqueous solubility would be a desirable trait in a fungicide as this would increase the ease of aqueous application of a fungicide to crops. Accordingly we attempted our first reduction of **4.1** (Scheme 4.9) in the standard manner at 0℃ with lithium aluminium hydride and succeeded in reducing the ketone functionality at C-6 to yield **4.3**. Analysis of the ^{1}H NMR spectrum of the crude reaction mixture also suggested a single product, later determined to be 9α-cyano-15,16-epoxy-6β,7β-dihydroxylabda-13(16),14-diene (**4.3**). The single peak in the HPLC trace during the purification process confirmed that only one product was formed. Computer modelling of **4.1** (Figure 4.4) revealed that the stereoselectivity of this reduction was probably due to steric hindrance from the axial Me-17 and equatorial alkyl side chain on the β-face of the ring leading to hydride delivery exclusively to the less hindered α-face of the molecule. Subsequent attempts at reduction of the nitrile moiety with lithium aluminium hydride in refluxing tetrahydrofuran (Scheme 4.9) led us to the conclusion that the nitrile functionality was stable under these conditions, probably as a result of being situated in a sterically hindered locale.

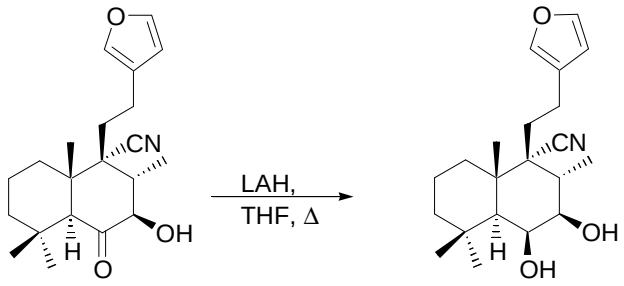

4.1 **4.3**

Scheme 4.9 Attempted reduction of the nitrile moiety of **4.1** with LAH in refluxing THF.

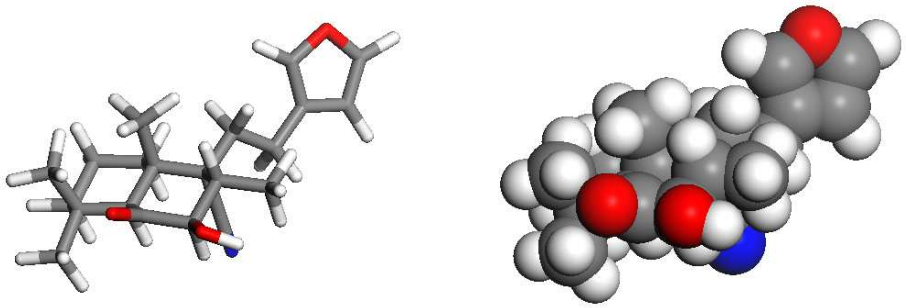

Figure 4.4 Stick and space filling representations of the global energy minimum of **4.1**.

The structure of **4.3** was readily deduced by comparison of the ^{1}H and ^{13}C NMR spectra with those of **4.1**. The reduction of the ketone functionality was confirmed by the absence of a carbonyl resonance in the ^{13}C spectrum of **4.3**, as well as the appearance of an additional oxymethine signal (δ_C 69.6 and 4.28) in the ^{1}H NMR spectrum. Additionally, the H-5 resonance that had appeared as a singlet in the ^{1}H NMR spectrum of **4.1** now appeared as a doublet in the ^{1}H NMR spectrum of **4.3**. Evidence that the nitrile functionality was still present was provided by the ^{13}C NMR resonance at δ_C 121.0, as well as the IR stretching band at 2221 cm^{-1}. Finally, the molecular formula of **4.3** ($C_{21}H_{30}NO_3$), established from HRFABMS data for this compound, confirmed the proposed structure.

The axial positioning of the hydroxyl moiety at C-6 was implied by the small values of the $J_{5,6}$ (1.9 Hz) and $J_{6,7}$ (3.2 Hz) coupling constants (Figure 4.5). Additionally, a NOESY correlation

between α-axial proton H-5 (δ_H 1.44) and H-6 (δ_H 4.28) supported the β-axial position of the hydroxyl at C-6.

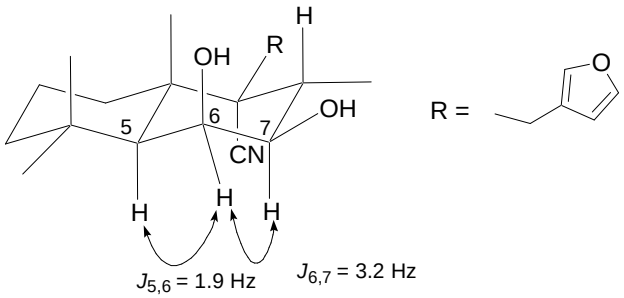

Figure 4.5 Schematic representation of the $J_{5,6}$ and $J_{6,7}$ coupling constants in diol **4.3**.

4.4 Investigating the agrochemical potential of the nitrile-containing furanolabdanes prepared from hispanolone

As mentioned earlier, Gray[100] screened twelve furanoditerpenes (**4.1**, **4.4**, **4.6**-**4.9** and **4.12**-**4.17**) produced during the course of his model synthetic studies on **4.4** for their agrochemical potential. Only **4.1** had evinced any significant activity (80% growth inhibition of potato late blight at 200 ppm, causative agent *P. infestans*) in these assays but the limited quantities of this compound available had precluded any further *in planta* screens. Having semi-synthesized sufficient quantities of **4.1**, as well as two further nitrile-containing analogues, **4.2** and **4.3**, we submitted these compounds to Dow AgroSciences (Indianapolis, USA) for further screening. All three compounds were first evaluated for *in vitro* inhibition of five plant pathogenic fungi (wheat germ blotch, potato late blight, rice blast, wheat leaf blotch and maize smut) and also brewers yeast. Paradoxically, compound **4.1** failed to show any significant activity against potato late blight in this *in vitro* screening process, but did show inhibition of rice blast (causative agent *Magnaporthea grisea*). All three compounds **4.1**, **4.2** and **4.3** were nonetheless still investigated for their *in planta activity* by application as one day protectant treatments for control of nine different plant pathogenic fungi (barley leaf blotch, cucurbit anthracnose, curcurbit powdery mildew, wheat powdery mildew, wheat glume blotch, potato late blight, wheat brown rust, rice blast and wheat leaf blotch). In these one day protective

assays, all three compounds were active against rice blast at the 200 ppm level. Nitrile **4.1** also inhibited the growth of wheat brown rust (causative agent *Puccinia recondita* f.sp. *tritici*) at the 200 ppm level.

Rice blast is generally held to be the most devastating global fungal rice disease.[156] The pathogen has been reported in 85 different countries (*i.e*. nearly every rice growing country in the world).[157] The disease is particularly prevalent in humid and temperate climates since spores are rapidly spread through contaminated water droplets.[158;159] Since rice blast has been estimated to account for 10-30% of the annual rice crop losses per annum by some[159] and even up to 50% by others,[157] the fungus is of considerable economic significance.

Wheat brown rust is also a devastating plant pathogen and the spores of this fungus are rapidly spread by wind and also water droplets.[160;161] An estimate in the Netherlands placed wheat contamination by wheat brown rust at 50%.[161] Although timely treatment can retard the growth of the sori (destructive fruiting bodies of the fungus) for a period of two to three weeks, crop losses in excess of 50% are not uncommon.[161]

The appearance of fungal strains resistant to existing fungicides creates the ongoing need for new fungicides.[156;162] As a result, further evaluations of the activity of compounds **4.1** and **4.3** at increasing dilution were made. Unfortunately, infection control with more dilute solutions of **4.1** and **4.3** (Table 4.3) was not as effective as the controls [tebuconazole (**4.18**) and azoxystrobin (**4.19**)]. The effect of dilution on the activity of **4.2** could not be measured due to insufficient quantities being available, but would presumably be similar.

Interestingly, the structure of azoxystrobin, **4.19**, a widely used fungicide active against rice blast, is based on the natural products strobilurin A (**4.20**), isolated from the fungus *Strobilurus*, and oudemansin A (**4.21**), from the fungus *Oudemansiella*.[156;163;164] Both **4.20** and **4.21** showed weak activity against rice blast prior to the synthesis of analogues such as **4.19**.[156;164] The mode of action of **4.19** is believed to be electron transfer inhibition in the mitochondrial complex III.[164] Tebuconazol, **4.18**, is believed to inhibit sterol 14α-

demethylation by a haem-thiolate enzyme of the cytochrome P450 superfamily in fungal systems.[165;166]

Table 4.3 One day protectant disease control of compounds **2, 3** and **4** against *M. grisea* and *P. recondita.*

Compound	Concentration (ppm)	% Control of *M. grisea*	% Control of *P. recondita*
4.1	200	90	80
	50	33	22
	12.5	21	22
4.2	200	91	-
4.3	200	83	56
	50	29	22
	12.5	13	0
Tebuconazole (**4.18**)	25	63	100
Azoxystrobin (**4.19**)	50	99	99
	25	99	100
	12.5	99	100

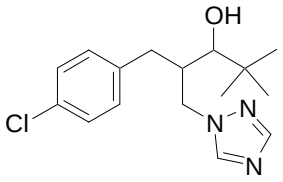

4.18

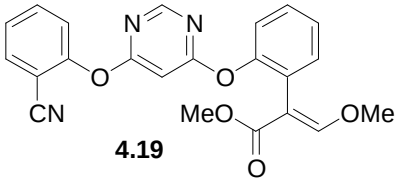

4.19

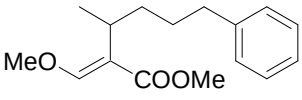

4.20

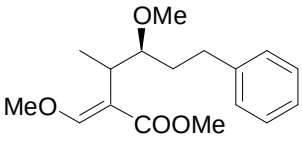

4.21

Compounds containing both nitrile functionalities and activity against rice blast are not unprecedented. In addition to **4.19,** compound **4.22** and related analogues,[167;168] as well as compound **4.23** and related analogues have proven to be effective agents for rice blast control in preliminary investigations.[169]

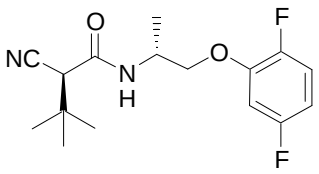

4.22

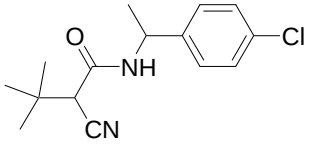

4.23

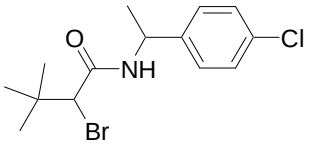

4.24

The activity of **4.22** was linked to its ability to inhibit scytalone dehydratase, the enzyme responsible for the production of fungal melanin in rice blast.[167;168] Rice blast spores bind to the rice plant's hydrophobic cuticle, after which they germinate in as little as two hours and then differentiate into appressoria.[158;159] These appressoria are the mechanism through which the fungus enters the host and this is achieved through the application of mechanical force resulting from the generation of immense turgor pressure within the appressoria.[158;169;170] Fungal melanin, produced by scytalone dehydratase, plays an important role in generating the turgor pressure within the appressoria, thus allowing infection to take place.[170] Inhibition of melanin production thus prevents infection and interrupts the fungal life cycle. Unfortunately, the fungicidal activity of **4.22** was not directly linked to the nitrile moiety. In the case of **4.23**, Manabe *et al.*[169] attributed the increased activity of the compound against *M. grisea* to the increased solubility afforded through the substitution of a bromine group in **4.24** for the more hydrophilic nitrile functionality so again, no further conclusions can be drawn as to the importance of the nitrile moiety in terms of fungicidal properties.

4.5 Summary and conclusions

An improved method for extracting hispanolone from *B. africana* using HP-20 resin was discovered, increasing yields by nearly 100% over those reported previously.[141] Hispanolone was successfully dehydrated using catalytic quantities of molecular iodine in yields comparable to those reported[148] and acetoxylated using manganic acetate. Commercially purchased manganic acetate gave superior results to that synthesized in-house following the method suggested by Williams and Hunter.[153] Interestingly, the addition of acetic acid to the reaction mixture during reflux as suggested by Demir[150] failed to produce the superior results claimed by these authors. Nonetheless, we were still able to report a substantial improvement in yield of **4.7** and **4.8** over those reported by Garcia-Alvarez *et* al.[142] The application of Mori's potassium cyanide mediated transesterification reaction procedure produced two Michael adducts (**4.1** and **4.2**) as the major components of the reaction mixture, one of which (**4.2**) had not previously been isolated by Gray, and two saponified products, **4.9** and **4.11**. Reduction of the major nitrile containing compound **4.1** yielded the diol **4.3**, the nitrile moiety proving to be resistant to lithium aluminium hydride reduction. Although the ability of compound **4.1** to prevent infection by potato late blight (*Phytophthora infestans* as indicated by preliminary screening) was not confirmed by subsequent screening, compounds **4.1**, **4.2** and **4.3** were found to have significant activity against rice blast (*M. grisea*) and **4.1** against wheat brown rust (*Puccinia recondita*). Unfortunately, the activity of these compounds declined at low concentrations, limiting their potential as commercial fungicidal agents.

Chapter Five

The Semi-synthesis of Two Isomeric Labdane Diterpene Aldehyde Metabolites from *Pleurobranchaea meckelii.*

5.1 Introduction

This chapter describes the semi-synthesis of two isomeric marine molluscan labdane diterpene aldehyde metabolites, labd-13*E*-ene-8β-ol-15-al (**5.1**) and labd-13*Z*-ene-8β-ol-15-al (**5.2**) from the commercially available, terrestrial plant derived, labdane diterpene manool (**5.3**). Diterpenes **5.1** and **5.2** were originally isolated from the Mediterranean nudibranch, *Pleurobranchaea meckelii*.[50] Selected synthetic diterpenes arising from the syntheses described in this chapter were also evaluated for their activity against an oesophageal cancer cell line (WHCO1), the details of which conclude the chapter.

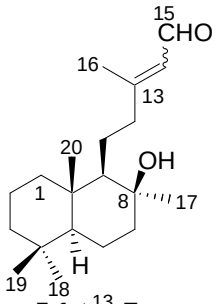

5.1 Δ^{13} *E*
5.2 Δ^{13} Z

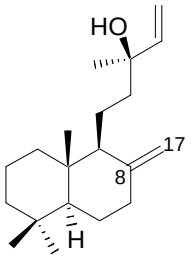

5.3

5.2 The isolation of 5.1 and 5.2 from *P. meckelii* by Ciavatta *et al*.[171]

Nudibranchs belonging to the Order Notaspidea, *e.g.* the Mediterranean nudibranch *Pleurobranchaea meckelii* (Figure 5.1), secrete a mucous as possible defence strategy to deter predation.[9;171] An acetone extract of several specimens of *P. meckelii*, collected by SCUBA from the Gulf of Naples, afforded the two isomeric labdane diterpene aldehyde metabolites **5.1** and **5.2**,[171] the syntheses of which are discussed in this chapter. Diterpene metabolites are commonly sequestered by marine opisthobranch molluscs from their marine invertebrate diet.[9;171] However, a dietary source of **5.1** and **5.2** could not be identified and their presence in the skin of *P. meckelii* seemed to suggest that these two compounds may be the products of *de novo* biosynthesis (See Chapter One). A defensive role for **5.1** and **5.2** in the chemical ecology of *P. meckelii* was not established experimentally but rather implied from the presence of α,β-unsaturated aldehyde moieties in these two compounds.[171]

Figure 5.1 The notaspidean mollusc, *P. meckelii* (reproduced with the permission of G. Cimino).

5.3 Rationale behind the synthesis of 5.1 and 5.2

Bioactivity studies of marine natural products are frequently hampered by the paucities of these compounds available for biological study.[172] As predators of other marine invertebrates, nudibranchs are positioned near the top of the marine invertebrate food chain.[44] Therefore, a large-scale removal of any nudibranch species, sufficient to supply sufficient quantities of bioactive metabolites for chemical ecology and/or other bioactivity studies, has obvious deleterious implications for the marine environment. The semi-synthesis of selected bioactive diterpene marine natural products from common terrestrial plant diterpenes provides one possible solution to the bioactive marine diterpene supply problem.

Ciavatta *et al.*[171] alluded to the instability of **5.1** and **5.2** and the implications this instability had for structure elucidation and further chemical ecology studies. The relative instability of many bioactive marine natural products through facile degradation processes, including isomerisation on exposure to sunlight and/or chromatographic media, is often problematic. Accordingly, a desirable semi-synthetic strategy would be one that can quantitatively deliver a relatively unstable marine natural product for bioactivity studies from a stable precursor without prior chromatographic purification. Ciavatta *et al.*[171] had determined the absolute stereochemistry of **5.1** by reducing the unstable aldehyde functionality with sodium borohydride to the stable labd-13*E*-ene-8β,15-diol (**5.4**). We determined that manganese

dioxide mediated oxidation of **5.4** and its geometric isomer, labd-13*Z*-ene-8β,15-diol (**5.5**) would provide a facile route to **5.1** and **5.2** respectively.

5.4 Attempted synthesis of 5.1 and 5.2 *via* a modification of Wisch's synthetic strategy

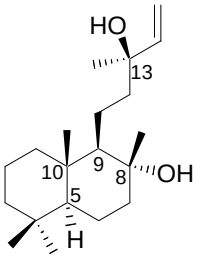

2.21

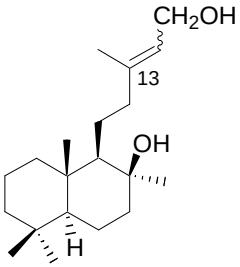

5.4 Δ^{13} *E*
5.5 Δ^{13} *Z*

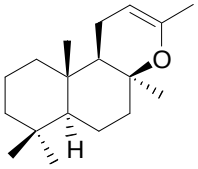

5.13

During his MSc studies in our laboratory, Wisch had previously synthesized **5.4** in low yield (3%) from the synthetic precursor, sclareol (**2.21**, Scheme 5.1).[173] This plant-derived diterpene served as a useful labdane precursor for the semi-synthesis of **5.1** and **5.2** as it was both commercially available and already possessed the correct configurations at C-5, C-9 and C-10. The major difficulty encountered by Wisch in his synthetic approach was the inversion of the configuration at C-8. This inversion was ultimately achieved through phosphorus oxychloride dehydration of the tertiary hydroxyl at C-8 in the selectively protected diols (**5.6** and **5.7**), to afford the 13-*tert*-butyldimethylsilanyloxy-14,15-bisnorlabd-8(17)-enes (**5.8** and **5.9**). These olefins were subsequently oxidized to 13*R*-*tert*-butyldimethylsilanyloxy-14,15,17-trisnorlabdan-8-one (**5.10**) and 13*S*-*tert*-butyldimethylsilanyloxy-14,15,17-trisnorlabdan-8-one (**5.11**) *via* ozonolysis, allowing for stereospecific nucleophilic addition of a β-equatorial methyl functionality at C-8. Deprotection of the tertiary butyldimethylsilyl protected C-13 hydroxyl moiety followed by Swern oxidation yielded a small amount of the ketol (**5.12**). A further problem in this synthesis was the facile intramolecular cyclization of **5.12** to afford 8β,13-epoxy-14,15-bisnorlabda-12-ene (**5.13**). The Δ^{13} olefin in **5.4** and **5.5** was introduced *via* a Horner-Wadsworth-Emmons (HWE) modification of the Wittig reaction.

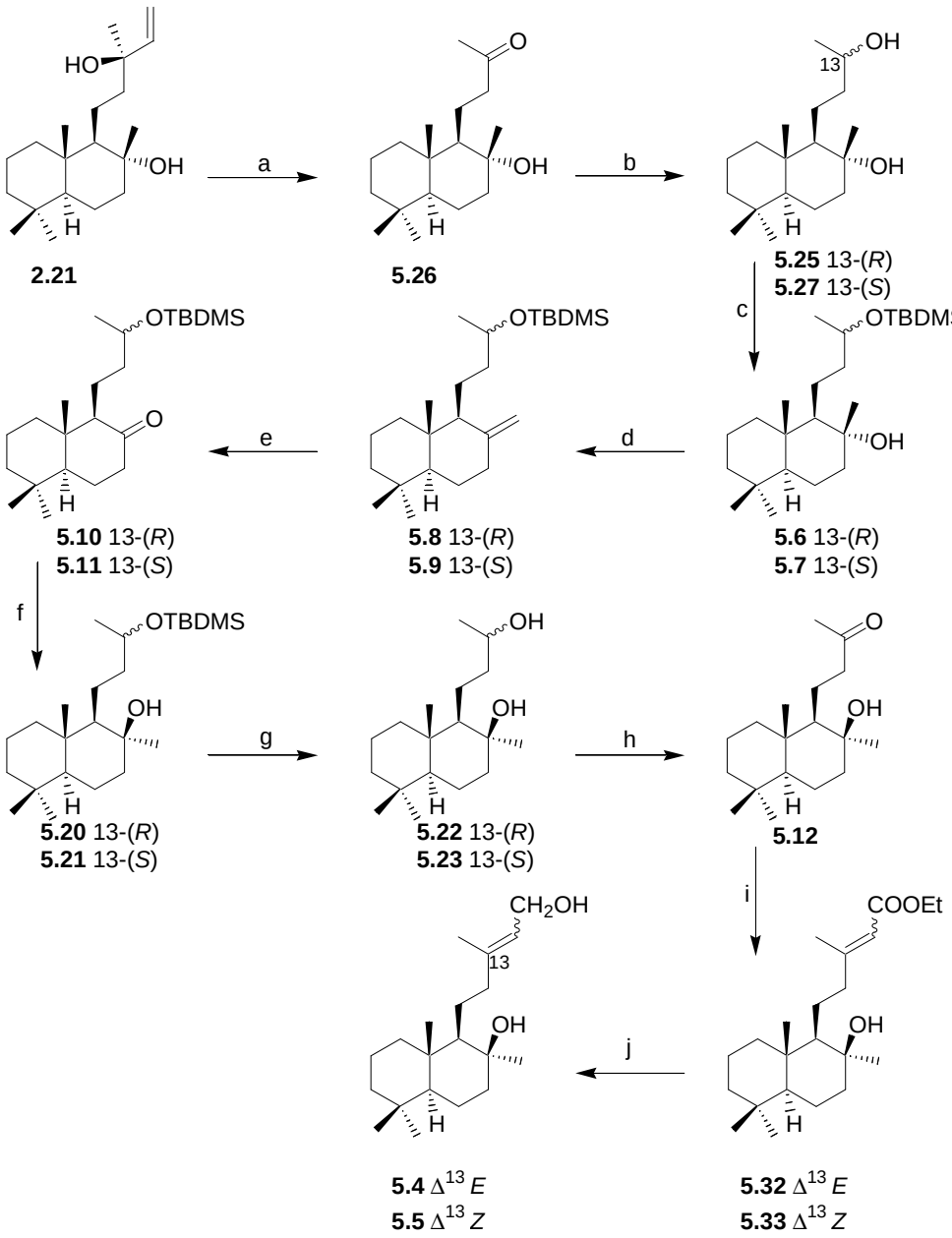

Scheme 5.1 Wisch's synthetic approach to compounds **5.4** and **5.5**.[173] *Reagents and conditions*: (a) $KMnO_4$, Me_2O, 15℃-RT, 48 h; (b) LAH, THF, 0℃-RT, 2 h; (c) 2, 6-lutidine, TBDMS triflate, CH_2Cl_2, -78℃, 2 h; (d) $POCl_3$, DMAP, pyridine, 0℃, 3 h; (e) O_3, CH_2Cl_2, -78℃, 0.5 h, then PPh_3, RT, 2 h; (f) MeLi, THF, -78℃-RT, 12 h; (g) TBAF, THF, Δ, 4 h, then RT 12 hours; (h) oxalyl chloride, DMSO, CH_2Cl_2 -78℃, 1h then Et_3N, 1 h, then RT 2 h; (i) $(C_2H_5O)_2P(O)CH_2CO_2Et$, NaH, THF, RT, 12 h; (j) DIBAH, CH_2Cl_2, 0℃, 4 h.

Time constraints resulted in the termination of Wisch's synthesis only one oxidation step short of the desired target, **5.1**, and we decided to repeat his synthesis, however, using **5.3** instead of **2.21** as a starting material. Manool, **5.3**, also a commercially available labdane diterpene, possessed a structure similar to **2.21** with the exception that the desired $\Delta^{8(17)}$ olefin was already in place. Starting with **5.3** thus eliminated the need for the non-selective phosphorus oxychloride dehydration step, which was one of the lower yielding steps in Wisch's synthetic route because three vinylic isomers were obtained. Cognizant of the facile intramolecular cyclization of **5.12** to **5.13** under Swern conditions, we anticipated that the milder conditions associated with Dess-Martin periodinane oxidation might reduce the tendency of **5.12** to cyclise to **5.13**.

Our modified synthesis (Scheme 5.2) was similarly initiated with potassium permanganate mediated oxidative cleavage of the terminal olefin of **5.3** to yield 14,15-bisnorlabd-8(17)-ene-13-one (**5.14**), which provided a ketone functionality at C-13, suitable for the later introduction of an olefin at this position. The ^{1}H NMR spectrum of the crude reaction mixture revealed a characteristic deshielded methyl ketone singlet (H_3-16, δ_H 2.08) and the retention of the $\Delta^{8(17)}$ olefinic resonances (δ_H 4.82 and 4.43), confirming the regioselective oxidative cleavage of the Δ^{14} olefin. Similarly, the ^{13}C NMR spectrum (Figure 5.2) revealed the appearance of a ketone carbon (δ_C 209.1, C-13) and the retention of two olefinic resonances attributable to C-8 [δ_C 148.4, (s)] and C-17 [δ_C 106.3, (t)]. Methyl ketone **5.14** was purified by silica flash chromatography (10% ethyl acetate, 90% hexane) and the ^{1}H and ^{13}C NMR data and specific rotation data for this compound were identical with published data.[174;175]

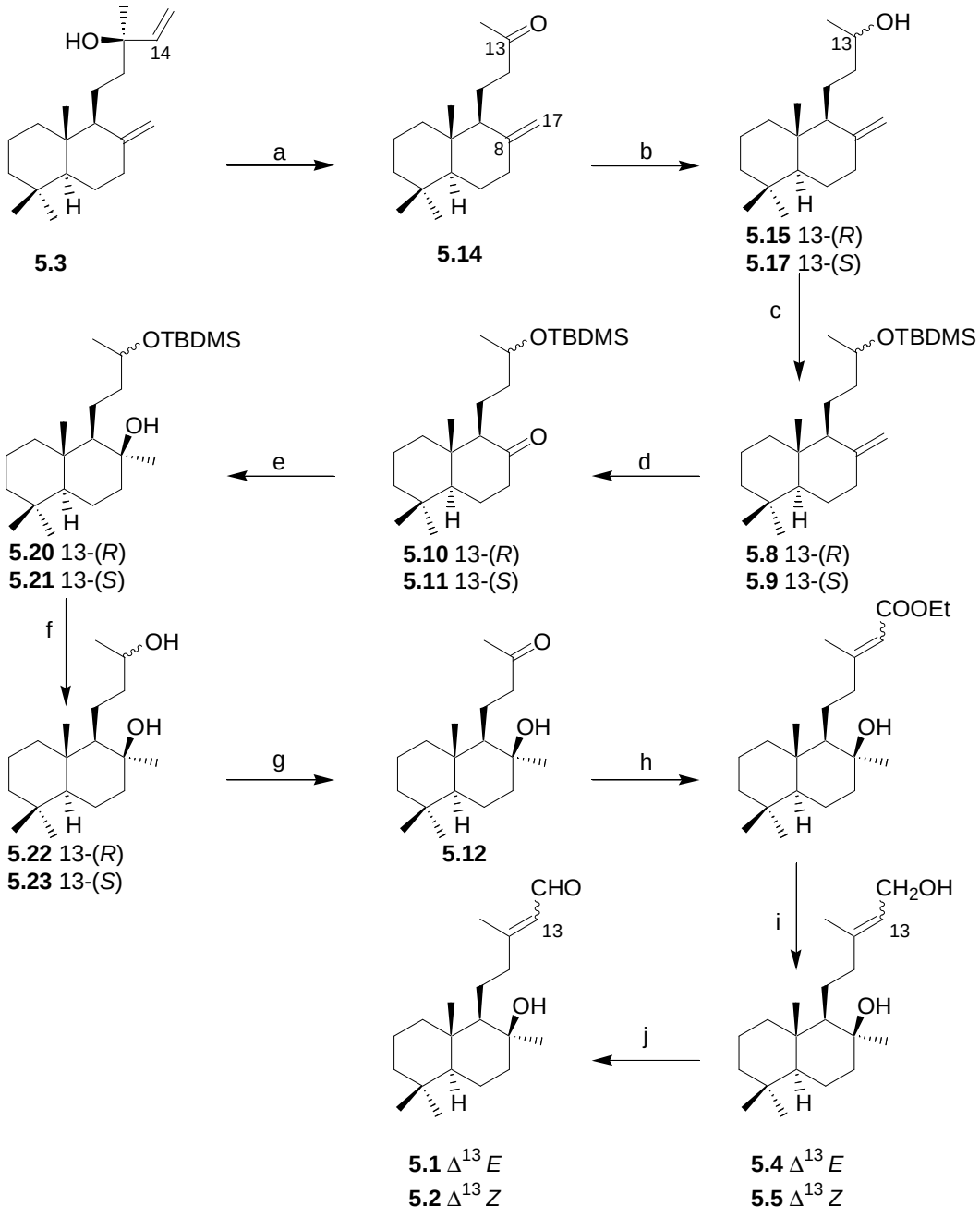

Scheme 5.2 Proposed synthesis of **5.1** and **5.2**. *Reagents and conditions*: (a) $KMnO_4$, PTEACl, CH_2Cl_2, 16℃-RT, 48 h; (b) LAH, THF, 0℃-RT, 3 h; (c) 2,6 lutidine, TBDMS triflate, CH_2Cl_2, -78℃, 2 h; (d) O_3, CH_2Cl_2, -78℃, 10 min, then PPh_3, RT, 4 h; (e) MeLi, THF, -78℃-RT, 14 h; (f) TBAF, THF, Δ, 4 h; (g) oxalyl chloride, DMSO, CH_2Cl_2 -78℃, 1h then Et_3N, 1 h, then RT 3 h; (h) $(C_2H_5O)_2P(O)CH_2CO_2Et$, NaH, THF, RT, 12 h; (i) DIBAH, CH_2Cl_2, 0℃, 4 h; (j) MnO_2, CH_2Cl_2.

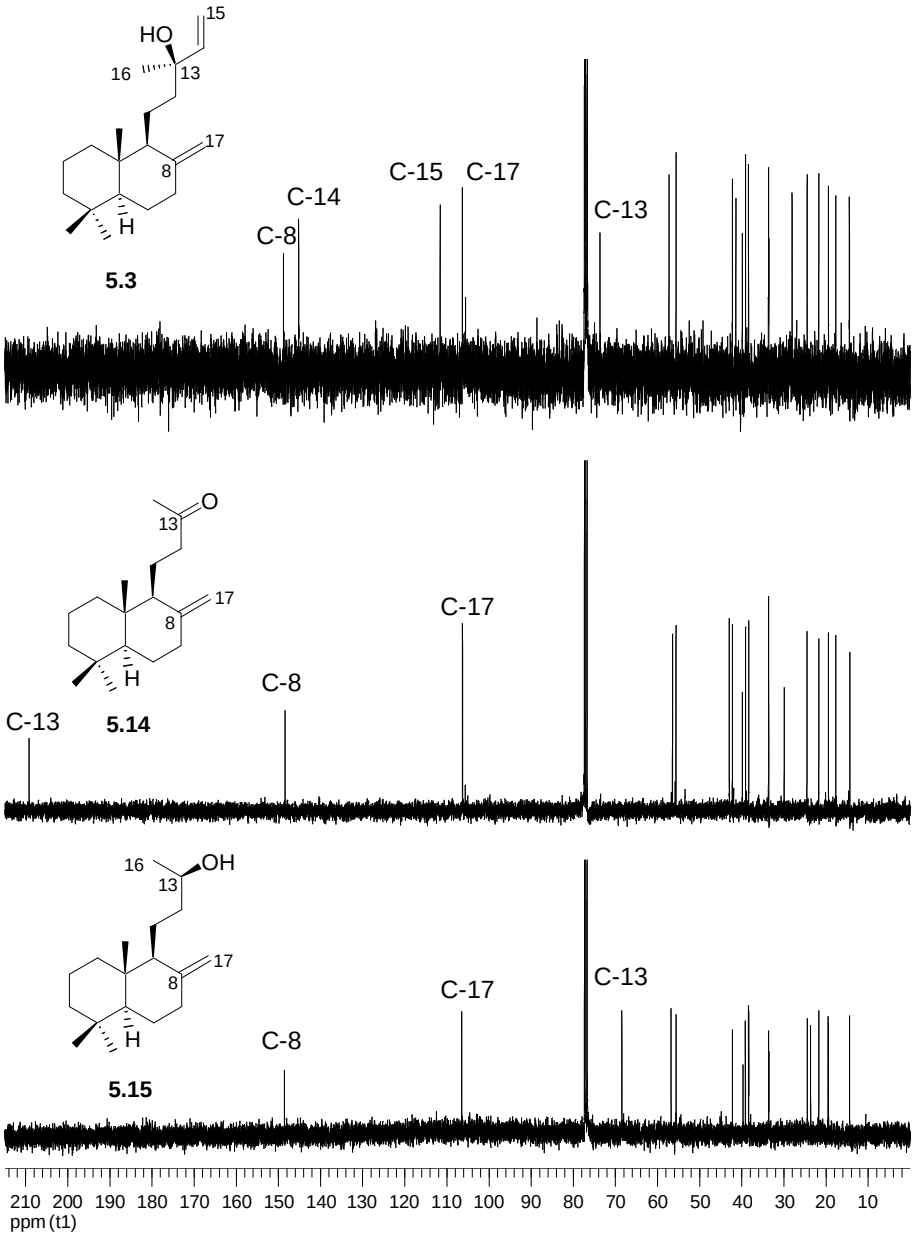

Figure 5.2 The ^{13}C NMR spectra (100 MHz, $CDCl_3$) of **5.3** (top), **5.14** (middle) and **5.15** (bottom).

Our initial attempts at the permanganate oxidation of **5.3** to afford **5.14** proved to be low yielding (36%). We thus decided to try and improve the workup by adsorbing the organic material from the manganese dioxide dominated reaction mixture onto HP-20 polystyrene beads. Attempted centrifugation to separate the HP-20 beads from the thick brown precipitate

of manganese dioxide produced by the reaction was unsuccessful. Further attempts to separate the HP-20 beads from the manganese dioxide *via* flushing the beads out with water were similarly ineffective. Reduction of the manganese dioxide with a solution of oxalic acid and sodium thiosulfate,[176] followed by extraction of the organic component in the usual manner, only resulted in a modest improvement (*ca.* 5%) to the isolated yield of **5.14**. A compromise between the different workup methods, *i.e.* first filtering the reaction mixture through celite and then reducing the remaining manganese dioxide did not improve the yield, although this method was preferred since it reduced the amount of oxalic acid and sodium thiosulphate required for the reduction. Finally, by changing the solvent employed in the reaction from acetone to dichloromethane and adding the phase transfer catalyst, phenyltriethylammonium chloride (PTEACl),[177] **5.14** was consistently obtained in 56% yield. This yield was in accordance with the yields reported for the oxidation of an analogous labdane diterpene, larixol (**3.29**) to the corresponding diketone (**5.16**),[176] but somewhat less than the 93% alluded to by do Céu Costa *et al*.[177]

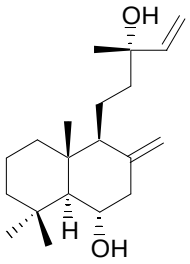

3.29

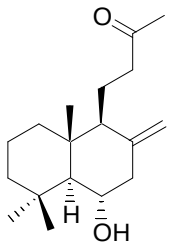

5.16

Although the C-13 ketone was required for later elaboration of the alkyl side chain, it was deemed necessary first to introduce the correct configuration at C-8. Oxidation of the $\Delta^{8(17)}$ olefin to a ketone would allow stereospecific alkylation with methyl lithium (Scheme 5.2, step e). Initially, we opted to protect the C-13 ketone and reduction of **5.14** with lithium aluminium hydride in anhydrous tetrahydrofuran afforded the C-13 epimers, 14,15-bisnorlabd-8(17)-ene-13*R*-ol (**5.15**) and 14,15-bisnorlabd-8(17)-ene-13*S*-ol (**5.17**) in an 8:7 ratio (93% combined isolated yield) after purification by semi-preparative HPLC (14% ethyl acetate, 86% hexane). The disappearance of the C-13 carbonyl resonance in the ^{13}C NMR spectrum of **5.14** and the

appearance of an NMR chemical shift attributable to an oxymethine at C-13 (δ_C 68.9 for **5.15**) is shown in Figure 5.2. Although compounds **5.15** and **5.17** had been reported previously in the chemical literature,[178;179] neither had been fully characterized (^{1}H and ^{13}C NMR data incomplete, specific rotation data not provided). The fully assigned ^{1}H and ^{13}C NMR data and specific rotations of both **5.15** and **5.17** are provided in Chapter Seven. We thus decided to determine the configuration at C-13 by means of the modified Mosher's method as described in Chapter Three and prepared the (*R*)- and (*S*)-MTPA esters (**5.18** and **5.19** respectively) of **5.17** in the usual manner.[123;125] Diterpene **5.17** also proved a useful model compound for the determination of the configuration of secondary alcohols and was used as a trial compound to practise the modified Mosher's method prior to the determination of the configuration at C-3 in **3.4** (Chapter Three). The ^{1}H and ^{13}C NMR data for each of these compounds were fully assigned using gCOSY, gHMBC and gHSQC experiments and a summary of the ^{1}H $\Delta(\delta_S-\delta_R)$ values is provided in Figure 5.3.

The protection of alcohols **5.15** and **5.17** was necessary to prevent an intramolecular cyclization from occurring subsequent to oxidation of the exocyclic $\Delta^{8(17)}$ olefin (*vide supra*). As Wisch had previously found a silyl ether protecting group to be stable to the reaction conditions employed later in the synthesis, yet readily removed by treatment with tetra-*n*-butylammonium fluoride (TBAF), we adopted the same protection strategy. Separation of the C-13 epimers **5.15** and **5.17** by semi-preparative HPLC proved time consuming, particularly at this early stage in the synthesis, and a mixture of **5.15** and **5.17** (purified by silica flash chromatography) was thus reacted with *t*-butyldimethylsilyl trifluoromethane sulfonate in anhydrous dichloromethane and the base 2,6-lutidine to yield the silyl ethers **5.8** and **5.9** in 81% combined isolated yield. Unfortunately, **5.8** and **5.9** proved inseparable by semi-preparative HPLC (hexane). The ^{1}H and ^{13}C NMR spectra (Figure 5.4) of the mixture of **5.8** and **5.9** revealed the characteristic signals at [δ_H 0.04 (6H) and 0.88 (9H)] and (δ_C -4.5, -4.7 and 25.9) of the tertiary butyldimethylsilyl ether and the molecular formula ($C_{24}H_{47}SiO$, $[M + H]^+$) of the protected epimers was confirmed by HRFABMS data.

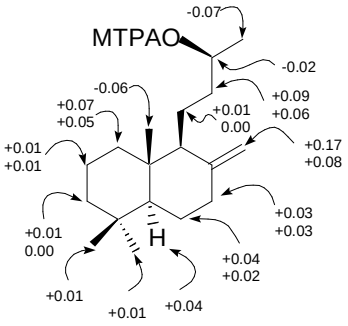

^{1}H number	δ_H (S)-MTPA ester (**5.18**)	δ (R)-MTPA ester (**5.19**)	$\Delta(\delta_S-\delta_{R)}$
H-1a	0.98	0.91	+0.07
H-1b	1.67	1.62	+0.05
H-2a	1.45	1.44	+0.01
H-2b	1.54	1.53	+0.01
H-3a	1.16	1.16	0.00
H-3b	1.38	1.37	+0.01
H-5	1.06	1.02	+0.04
H-6a	1.30	1.26	+0.04
H-6b	1.70	1.68	+0.02
H-7a	1.93	1.90	+0.03
H-7b	2.35	2.32	+0.03
H-9	1.58	1.48	+0.10
H-11a	1.24	1.23	+0.01
H-11b	1.37	1.37	0.00
H-12a	1.38	1.29	+0.09
H-12b	1.83	1.77	+0.06
H-13	5.10	5.12	-0.02
H_3-16	1.24	1.31	-0.07
H-17a	4.39	4.22	+0.17
H-17b	4.77	4.69	+0.08
H_3-18	0.86	0.85	+0.01
H_3-19	0.79	0.78	+0.01
H_3-20	0.63	0.57	+0.06

Figure 5.3 ^{1}H chemical shifts (600 MHz, $CDCl_3$) and calculated Δδ values obtained from the application of the Modified Mosher's method to **5.17**.

Following the successful protection of **5.15** and **5.17,** we were in a position to perform a reductive ozonolysis of the $\Delta^{8(17)}$ olefin of **5.8** and **5.9** to afford the ketones **5.10** and **5.11**. Accordingly, a constant stream of ozone was bubbled through a solution of **5.8** and **5.9** in anhydrous dichloromethane until the solution had changed to a deep blue colour, indicating that the solution was saturated with ozone. The reaction mixture was purged of ozone with nitrogen, triphenylphosphine added, and the solution stirred at room temperature. Once reduction of the ozonide intermediate had been confirmed by TLC, hydrogen peroxide was added to the solution to precipitate any remaining triphenylphosphine as triphenylphosphine

oxide, which could be removed by filtration through a silica plug. The C-13 epimers **5.10** and **5.11** were then separated by semi-preparative HPLC (5% ethyl acetate, 95% hexane) in an 89% combined isolated yield. Analysis of the ^{13}C NMR spectrum of **5.10** (Figure 5.4) revealed the disappearance of the $\Delta^{8(17)}$ olefinic resonances present in the ^{13}C NMR spectra of **5.8** and **5.9** and the appearance of the expected endocyclic ketone resonance (δ_C 212.0 in **5.10**). Further comparison of the ^{1}H and ^{13}C data of **5.10** and **5.11** with those reported for the corresponding compounds by Wisch[173] confirmed that the desired compounds had been obtained.

Having successfully synthesized compounds **5.10** and **5.11** we were now able to perform the stereospecific alkylation of the C-8 carbonyl to introduce the desired configuration at this position. After reviewing the literature pertaining to the nucleophilic addition of a methyl functionality to similar cyclohexanone-type systems,[180;181] Wisch concluded that methyl lithium would be the most effective alkylating agent, and later demonstrated by means of GLC analysis of the products from this reaction that the nucleophilic addition of the methyl functionality at C-8 using methyl lithium gave a single product. Subsequent NMR analysis confirmed a β-axial hydroxyl functionality at this stereocentre as described below.

Methyl lithium was thus added drop wise to a cooled (-78℃) solution of **5.10** or **5.11** in anhydrous tetrahydrofuran. After quenching the reaction, and subsequent workup, the reaction mixture was purified by semi-preparative HPLC (10% ethyl acetate, 90% hexane) to yield both the tertiary alcohols (**5.20** or **5.21)**, in the same isolated yield of 82%. The disappearance of the C-8 carbonyl resonance at *ca.* 212 ppm in the ^{13}C spectra and appearance of a downfield methyl singlet at *ca.* 1.12 ppm in the ^{1}H NMR spectra of both **5.20** and **5.21** relative to **5.10** and **5.11** respectively suggested that the addition of a methyl functionality at C-8 had been successful. The configuration at C-8 was confirmed by analysis of the ^{1}H and ^{13}C NMR spectra of **5.20** and **5.21**. The configuration at C-8 (β-axial hydroxyl and α-equatorial methyl functionalities) in **5.20** (and similarly for **5.21**) was supported by threefold spectroscopic evidence, which included the deshielding of the H_3-20 angular methyl protons (δ_H 0.94), the shielding of C-6 (δ_C 18.1) and downfield shift of the C-17 methyl carbon

resonance (δ_C 30.6).[171;182;183] The shielding of the C-6 resonance is attributed to a γ-gauche affect associated with a β-axially orientated hydroxyl functionality at C-8.[184] Conversely, an 8α-methyl substituent shields the H_3-20 protons (δ_H 0.80), the C-17 methyl carbon resonance is shifted upfield (δ_C 24.0) while the C-6 resonance is shifted downfield (δ_C 20.5).[171;185] The ^{13}C NMR spectrum of **5.20** is included in Figure 5.4.

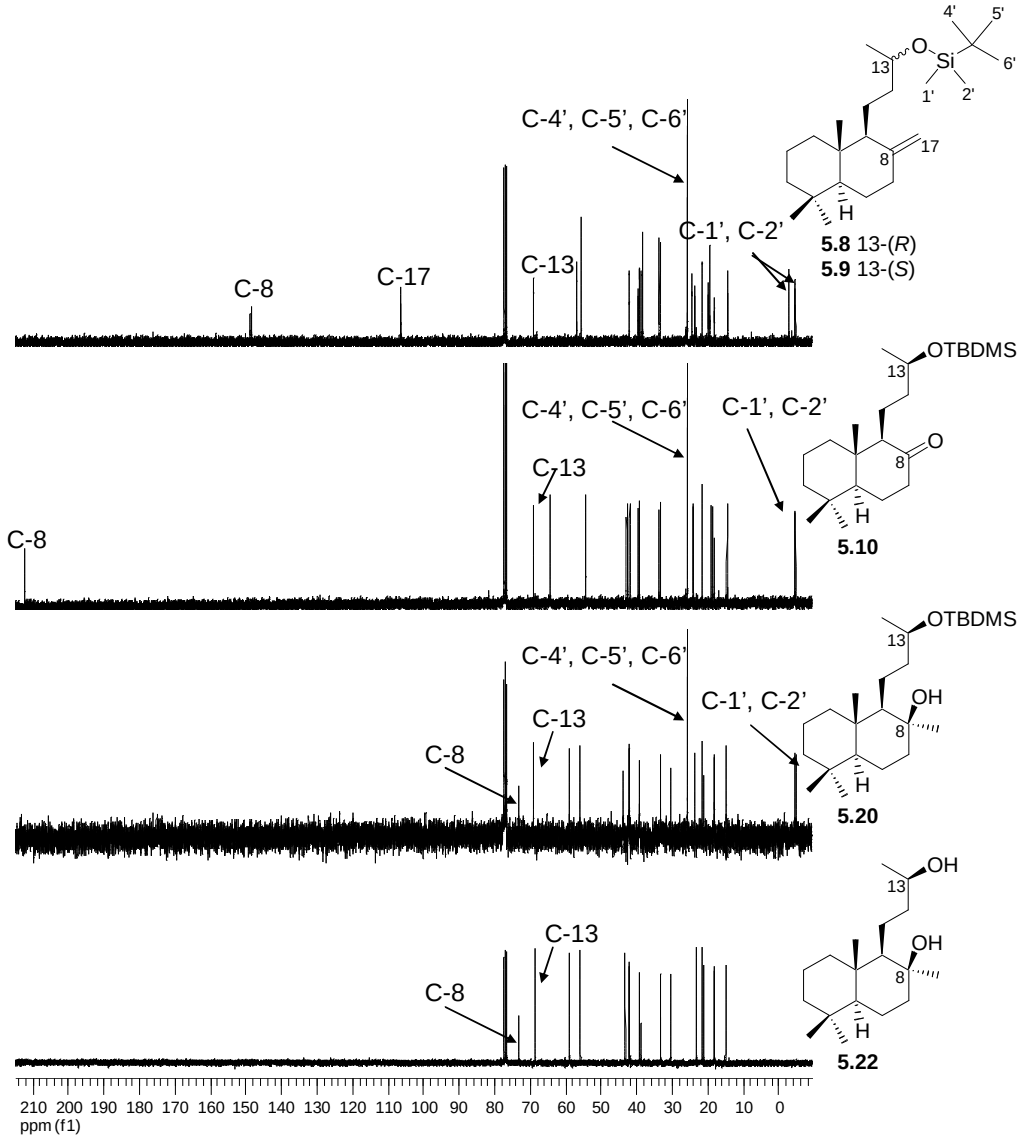

Figure 5.4 The ^{13}C NMR spectra (100 MHz, $CDCl_3$) of **5.8** and **5.9**, **5.10**, **5.20** and **5.22**.

The next step in our synthesis required the elaboration of the alkyl side chain with the correct bond geometry. To achieve this, the protecting group was removed by refluxing a

tetrahydrofuran solution of either **5.20** or **5.21** and tetra-*n*-butylammonium fluoride and purification of the reaction products by semi-preparative HPLC (50% ethyl acetate, 50% hexane) to afford diols (**5.22**) and (**5.23**) in 87% isolated yield. Analysis of the ^{13}C NMR spectra of **5.22** (Figure 5.5) and **5.23** revealed the disappearance of the characteristic methyl resonances of the protecting group at (δ_C 25.9, -4.4 and -4.7) in both compounds. After slow evaporation from ether, crystals of **5.22**, suitable for X-ray diffraction were obtained. The crystal structure of **5.22** (Figure 5.5) confirmed the absolute configuration at both C-8 and C-13. The secondary structure of **5.22** is of interest as it appears to comprise an infinite ribbon of hydrogen bonded molecules in which both C-8 and C-13 hydroxyl groups act as both a hydrogen bond donor and acceptor (Figure 5.6) and is reminiscent of a supramolecular zipper.[186] We were unable to crystallize **5.23**, which might suggest that a similar molecular zipper arrangement is not possible for this epimer.

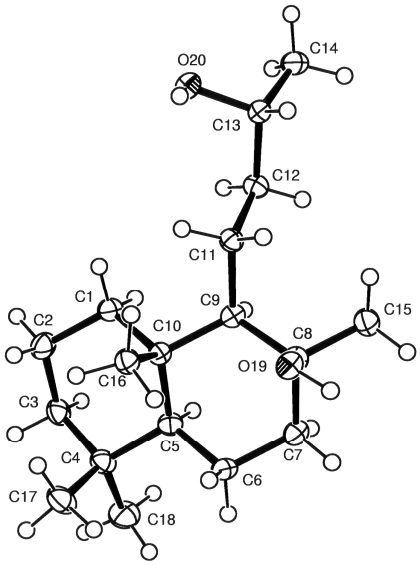

Figure 5.5 A view of a molecule of 14,15-bisnorlabd-8(17)-en-8β,13*R*-diol, **5.22**, from the crystal structure.

Swern oxidation of the secondary alcohol of **5.22** and **5.23** as described by Wisch,[173;187] failed to yield the desired ketone product, **5.12**, but instead resulted in a complex mixture of products as determined from inspection of the ^{1}H and ^{13}C NMR spectra of the reaction mixture. Monitoring of the reaction by TLC had shown that all the starting material had been

consumed, yet analysis of the ^{13}C NMR spectrum of the reaction mixture and testing for a ketone functionality in the reaction mixture with 2,4-dinitrophenol hydrazone (2,4-DNP reagent) confirmed that this functional group was not present. Wisch had only attempted this reaction once and we thus forced to conclude that his results were not reproducible.

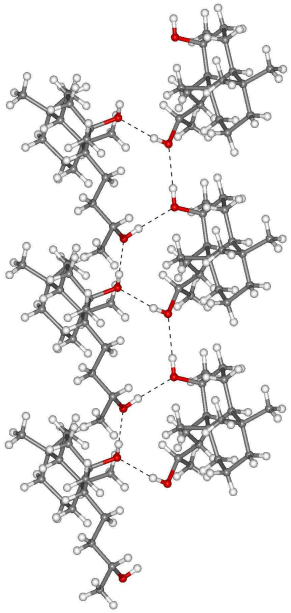

Figure 5.6 A portion of the infinite ribbon formed by molecules of **5.22** from the crystal structure.

An alternative oxidation procedure, using Dess-Martin periodinane (DMP),[188] had been contemplated from the outset of the synthesis in the hope of improving the yields from the Swern oxidation. Dess-Martin periodinane (**5.24**) is an efficient oxidizing agent, suitable for the oxidation of primary alcohols to aldehydes and secondary alcohols to ketones.[188;189] The oxidation occurs under mildly acidic to neutral conditions[188;189] and we thus hoped that by using this milder oxidizing agent, we would be able to isolate **5.12** as the major product from the oxidation of **5.22** or **5.23** and avoid the competing cyclization to (**5.13**).

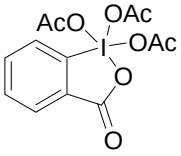

5.24

Since we had exhausted our supplies of **5.22** and **5.23** in our earlier attempts at the Swern oxidation, we instead used 14,15-bisnorlabda-8α,13*R*-diol (**5.25**, Scheme 5.3) as a model compound. Model compound **5.25** was readily obtained from the potassium permanganate oxidation of **5.21** to 8α-hydroxy-14,15-bisnorlabda-13-one (**5.26**, Scheme 5.1) and subsequent reduction of **5.26** with lithium aluminium hydride to yield 14,15-bisnorlabda-8α,13*R*-diol **5.25** and its C-13 epimer 14,15-bisnorlabda-8α,13*S*-diol (**5.27**). The attempted Dess-Martin oxidation of **5.25** in anhydrous tetrahydrofuran,[188] afforded the tricyclic ether (**5.28**, Scheme 5.3) as the major product. Further attempts at the Dess-Martin periodinane oxidation in acetonitrile at both 0℃ and 24℃ were similarly unsuccessful. Finally, a one pot oxidation and HWE reaction, using Dess-Martin periodinane as oxidant and either tetrahydrofuran or acetonitrile as solvent, was attempted. When tetrahydrofuran was used as a solvent, the oxidation procedure was allowed to run for one hour, before deprotonated triethylphosphonoacetate (in tetrahydrofuran) was added drop wise and stirring continued overnight. Conversely, when acetonitrile was used as a solvent, the oxidation was allowed to run for one hour, before 5% aqueous sodium bicarbonate was added and the organic and aqueous fractions separated. The organic fraction was dried with anhydrous magnesium sulfate and concentrated to dryness *in vacuo.* After further drying of the reaction mixture on a freeze dryer for two hours, this mixture was immediately taken up in anhydrous tetrahydrofuran, deprotonated triethylphosphonoacetate in tetrahydrofuran added, and the reaction allowed to stir overnight at ambient temperature. After workup of both the reaction mixtures, semi-preparative HPLC (33% ethyl acetate, 67% hexane) afforded **5.28**, from both the oxidation performed in tetrahydrofuran (46%) and acetonitrile (38%). Analysis of the ^{13}C NMR spectrum of **5.28** revealed the absence of any ester or carbonyl resonances, but the spectrum did contain resonances attributable to a trisubstituted olefin [δ_C 147.9 (s) and 94.6 (d)], which were consistent with those reported for **5.28**. Comparison of the remaining ^{1}H and ^{13}C NMR data of **5.28** as well as the specific rotation with those previously reported for the compound,[100] confirmed that we had isolated **5.28** from the reaction mixture. Bigley *et al*.[190] had also reported that **5.26** readily dehydrated to **5.28** in solution at room temperature and quantitatively in the presence of even trace amounts of acid. Since the mechanism (Scheme 5.3) proceeds *via* **5.26**, we deemed the oxidation to have been successful, but unfortunately

the concomitant cyclization appeared unavoidable. Although reportedly **5.28** can be hydrated to **5.26** (and by analogy **5.13** to **5.12**) using aqueous methanolic acetate or methanolic semicarbazide acetate,[191] Bigley *et al.*[190] had been unable to reproduce this hydration, and were only able to achieve partial hydration of **5.28** to **5.26** using aqueous methanolic acid at room temperature. Since partial conversion of **5.13** to **5.12** would not be adequate for our needs, we decided not to pursue this synthetic approach any further.

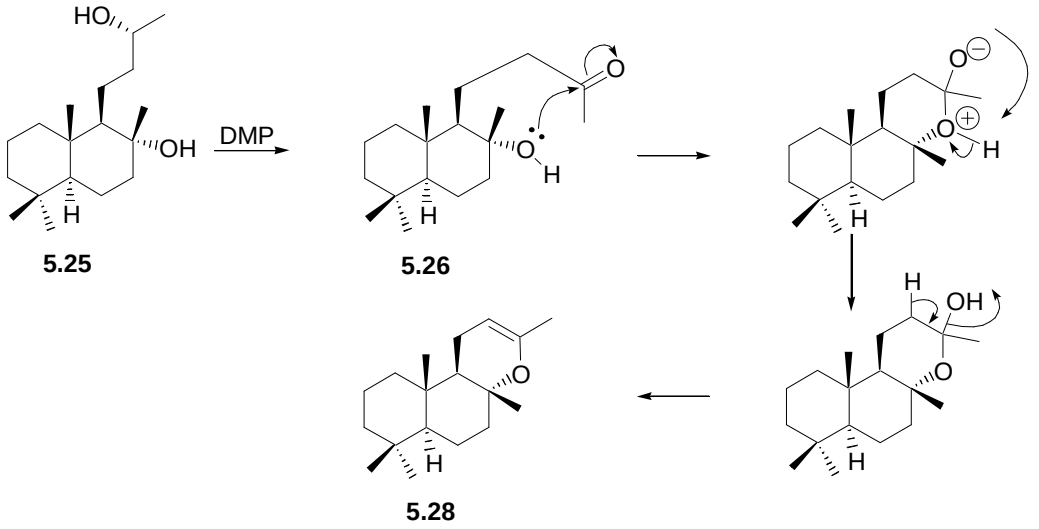

5.25 **5.26** **5.28**

Scheme 5.3 Tentative mechanism for the formation of **5.28** from **5.25**.[100]

Our failure to repeat Wisch's synthesis, even with some modification, required us to investigate another synthetic approach to **5.4** and **5.5**. Two non-stereoselective syntheses of **5.4** and **5.5** had been reported.[64;192] A racemic mixture of **5.4** had previously been obtained in good yield through the biomimetic cyclization of (*E*,*E*,*E*)-geranylgeranyl acetate in the presence of a mercury (II) triflate/N,N-dimethylaniline cyclization complex.[64] This method was deemed unsuitable as our goal was a stereoselective synthesis of **5.1** and **5.2**.

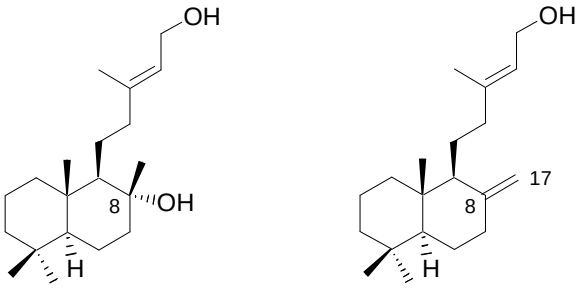

5.29 **5.30**

Popa *et al*.[192] had serendipitously synthesized **5.4** (and **5.29**, the 8α-hydroxy epimer of **5.4**) *via* a series of successive MnO_2 and Ag_2O oxidations of **5.3** to yield (**5.30**). The $\Delta^{8(17)}$ olefin of the final oxidation product, **5.30**, was subsequently epoxidised with perphthalic acid and reduced with lithium aluminium hydride to afford **5.4** and **5.29** as the minor and major products respectively. A search of the chemical literature revealed examples of epoxidation of the $\Delta^{8(17)}$ olefin in related diterpenes, where the formation of the α-epoxide is always favoured (75-80%) over the β-epoxide (20-25%).[178;193-195] As only the minor product, the β-epoxide, could be reduced to afford the desired configuration at C-8, this method was not viable.

5.5 Synthesis of 5.1 and 5.2 *via* a regioselective HWE reaction performed on 5.31

Having decided against a synthetic route involving the epoxidation of the $\Delta^{8(17)}$ olefin, we opted for a strategy (Scheme 5.4) dependent on a regioselective HWE reaction performed on 14,15,17-trisnorlabdane-8,13-dione (**5.31**). From past experience with labdane diterpenes, we knew that C-8 is sterically hindered by β-axial Me-20 and the β-equatorial alkyl chain at C-9, and we thus reasoned that this situation might lead to preferential attack at the less hindered ketone at C-13 of **5.31**. Although **5.31** could readily be accessed *via* reductive ozonolysis of **5.14** (or another suitable precursor, *vide infra*), it was hoped that by performing the HWE reaction on **5.31**, regioselective olefination at C-13 would occur to afford two Δ^{13} geometric isomers, ethyl 17-norlabd-13-*E*-en-8-one-15-oate (**5.32**) and ethyl 17-norlabd-13-*Z*-en-8-one-15-oate (**5.33**). At this stage there were two possible options, the first being to attempt a regioselective and stereospecific methylation of the C-8 ketone functionality. Reetz *et al*.[196] had demonstrated that a ketone could be preferentially methylated in the presence of an ester functionality using methyl titanium trichloride, generated by treating methyl lithium with titanium tetrachloride at -78℃. Should the methyl titanium chloride reaction prove effective in yielding the desired C-8 alcohols, ethyl labd-13-*E*-en-8β-ol-15-oate (**5.34**) and ethyl labd-13-*Z*-en-8β-ol-15-oate (**5.35**), facile reduction of the ester moiety would yield the desired diols, **5.4** and **5.5**. If the methyl titanium chloride reaction did not prove to be regioselective, the second option would be to protect the ketone at C-8 as an acetonide (**5.36** and **5.37**), reduce the ester moieties to the corresponding alcohols, (**5.38** and **5.39**) with lithium aluminium

hydride followed by deprotection to afford (**5.40** and **5.41**). A number of methods existed for this acetonide deprotection, including mild methods such as the addition of catalytic quantities of molecular iodine in acetone[197] or montmorillonite clay in acetone.[198] We would then be able to perform the methyl lithium reaction on **5.40** and **5.41** to afford **5.4** and **5.5**, without any competing reactions occurring.

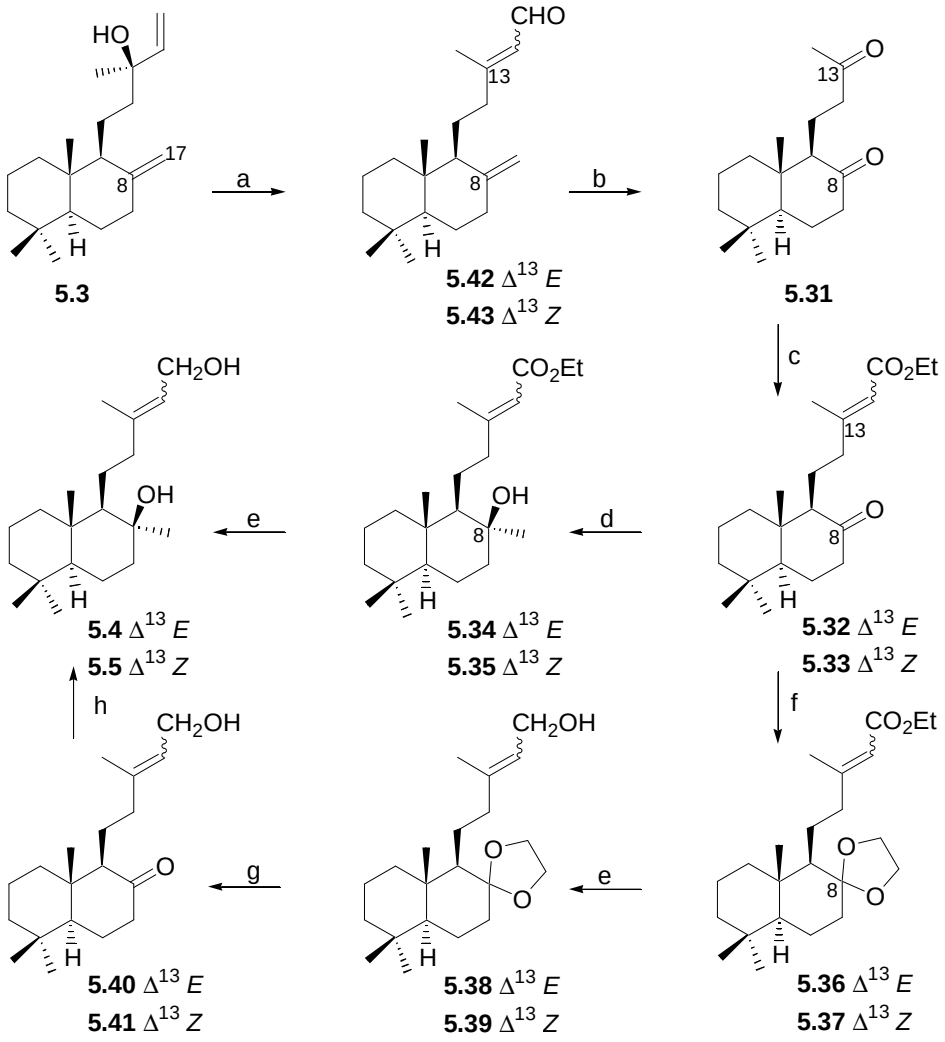

5.3

5.42 Δ^{13} *E*
5.43 Δ^{13} *Z*

5.31

5.4 Δ^{13} *E*
5.5 Δ^{13} *Z*

5.34 Δ^{13} *E*
5.35 Δ^{13} *Z*

5.32 Δ^{13} *E*
5.33 Δ^{13} *Z*

5.40 Δ^{13} *E*
5.41 Δ^{13} *Z*

5.38 Δ^{13} *E*
5.39 Δ^{13} *Z*

5.36 Δ^{13} *E*
5.37 Δ^{13} *Z*

Scheme 5.4 Proposed alternative route to **5.4** and **5.5**. *Reagents and conditions*: (a) PCC, CH_2Cl_2, RT; (b) O_3, CH_2Cl_2, -78℃ then PPh_3, RT; (c) $(C_2H_5O)_2P(O)CH_2CO_2Et$, NaH, THF, RT; (d) CH_3TiCl_3, Et_2O, -30℃ to -10℃ (e) LAH, THF, 0℃ to RT; (f) $HOCH_2CH_2OH$, *p*-TsOH, C_6H_6; (g) I_2 or montmorillonite clay, Me_2CO, RT; (h) MeLi, Et_2O, -78℃ to RT.

Diketone **5.31** could be accessed in a number of different ways. One of the earliest cited methods was to increase the temperature during the potassium permanganate oxidation of **5.3**, thus also increasing the proportion of **5.31** to **5.14** to a maximum reported yield of 36%.[174] Alternatively, we could use the known O_3/ triphenylphosphine reaction,[174;199-201] which we had already employed on the methyl ketone **5.14**, although this route provided **5.14** in low overall yield from **5.3** because of the initial low yielding (56%) potassium permanganate oxidation of **5.3**. Another reported method for the synthesis of the diketone involved the use of osmium tetroxide and periodic acid on manool at pH 6.[202] The high cost and toxicity of osmium tetroxide was a major deterrent for us and we consequently devised a new method to effect this transformation. A pyridinium chlorochromate oxidation of **5.3** (Scheme 5.4) was chosen as this reaction involves a migration of the Δ^{14} olefin to Δ^{13} with concomitant oxidation of the transposed alcohol functionality to yield (*E*)-labda-8(17)dien-15-al (**5.42**) and (*Z*)-labda-8(17)dien-15-al (**5.43**),[203] which could easily be converted to **5.31** by reductive ozonolysis.

Manool, **5.3**, was thus reacted with pyridinium chlorochromate to yield the aldehydes, **5.42** and **5.43**.[203;204] Analysis of the ^{1}H NMR spectrum of the reaction mixture immediately revealed the presence of two pairs of deshielded doublets (δ_H 9.97 and δ_H 9.82) which corresponded to the aldehyde protons of the *E* and *Z* isomeric aldehydes (ratio 2:1). The combined yield of **5.42** and **5.43** was 90% after silica flash chromatography (6% ethyl acetate, 94% hexane) of the reaction mixture. The remainder of the ^{1}H and ^{13}C NMR data of the column purified reaction mixture were consistent with those in the literature.[203;204] The aldehydes, **5.42** and **5.43**, were unstable, which required that the ozonolysis reaction was performed immediately after the purification step.

The ozonolysis procedure followed was identical to that previously discussed for the ozonolysis of **5.8** and **5.9**. After ozonolysis and reduction of the resultant ozonide with triphenylphosphine, the reaction mixture was purified by silica flash chromatography (50% ethyl acetate, 50% hexane) to afford **5.31** in 78% yield as the sole product. Diketone **5.31** could easily be distinguished from the mixture of aldehydes comprising the starting material, **5.42** and **5.43**, by the appearance of a deshielded methyl singlet in the ^{1}H NMR spectrum (δ_H

2.07, Figure 5.7), the absence of any olefinic and aldehyde resonances in the ^{13}C NMR spectrum of **5.31**.

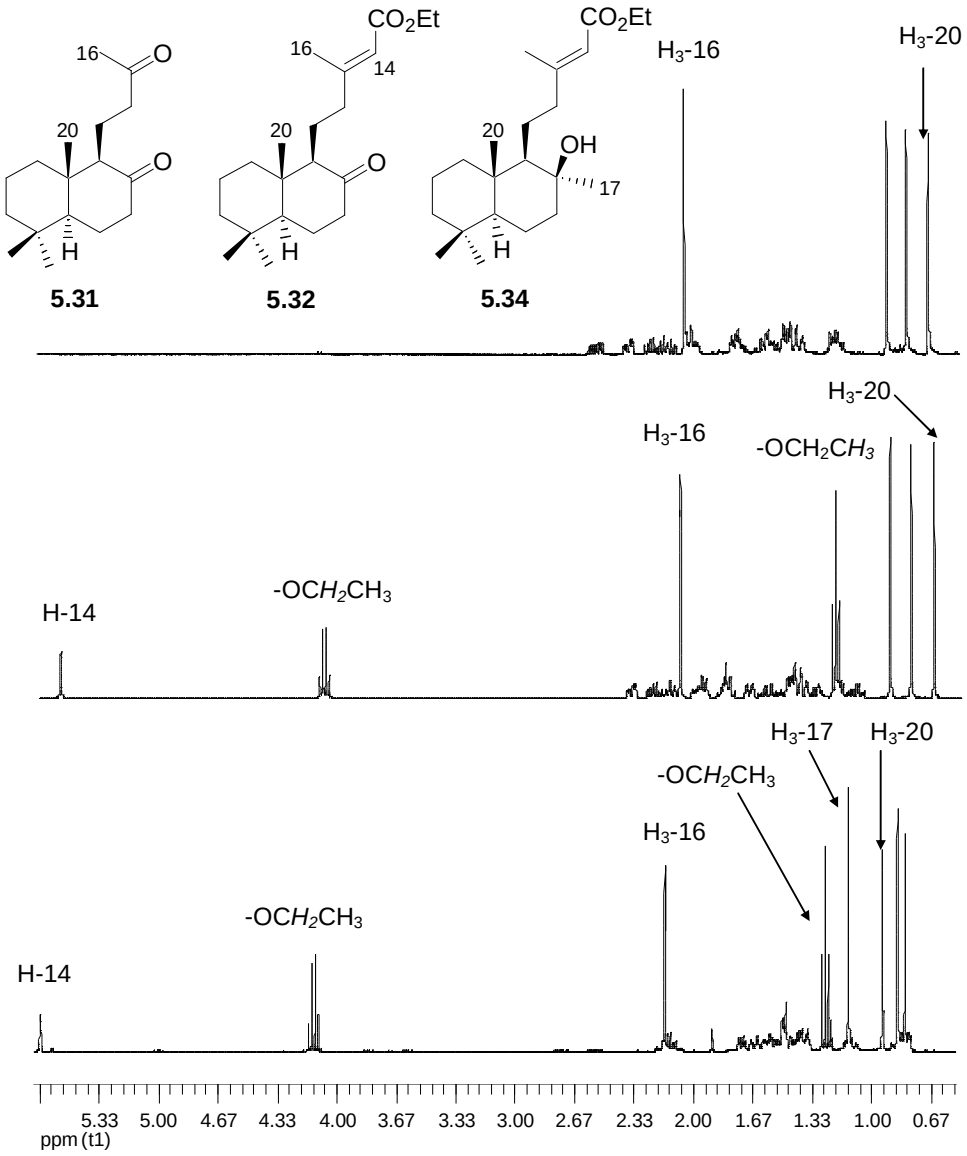

Figure 5.7 The ^{1}H NMR (400 MHz, $CDCl_3$) spectra of **5.31** (top), **5.32** (middle) and **5.34** (bottom).

With an efficient procedure for the synthesis of diketone **5.31** (71% overall yield from **5.3**) in place, we were able to attempt a regioselective olefination of the more accessible methyl ketone functionality of **5.31** *via* the HWE reaction (Scheme 5.5). The Horner-Wadsworth-Emmons modification of the Wittig reaction is an important tool for the preparation of alkenes

and utilizes resonance stabilized phosphonate anions (*e.g*. **5.44**), which react with ketones and aldehydes under mildly basic conditions to form intermediate betaines (*e.g*. **5.45** and **5.46**).[205;206] An irreversible decomposition of the betaine through the *syn* elimination of oxygen to the phosphorus atom *via* a four membered transition state (*e.g.* **5.47** and **5.48**) occurs to afford an olefin (*e.g.* **5.32** and **5.33**). The bond geometry of the olefin formed, for example, in the HWE reaction performed on **5.31** is determined by the relative stabilities of **5.47** and **5.48**. This stability is influenced by the degree of steric interaction between the ethoxycarbonyl functionality and the adjacent methyl or alkyl groups,[100;205;206] making the *trans*-diastereoisomer (**5.47**) more stable, and hence leading to preferential formation of the *E*-alkene. Resonance stabilized phosphonates are generally used to prepare *trans* olefins, although the degree of selectivity is diminished when ketones are used rather than aldehydes.[207] The preparation of *cis* olefins requires an aldehyde precursor and the use of customized HWE reagents at low temperatures (-78℃), a base *e.g.* potassium hexamethyldisilazane (KHMDS) and the expensive potassium chelating agent, crown ether 18C6.[208]

In our early attempts at using the HWE reaction using only one equivalent of triethylphosphonoacetate, we found that we were routinely reisolating unreacted **5.31** from the reaction mixture and we accordingly adjusted the proportion of reagents relative to **5.31**, ultimately finding that using three equivalents of triethylphosphonoacetate and two and a half equivalents of sodium hydride maximized yields of ethyl 17-norlabd-13-*E*-en-8-one-15-oate, **5.32**, and ethyl 17-norlabd-13-*E*-en-8-one-15-oate, **5.33**. The tricyclic isomeric compounds, ethyl 17-norabiet-13(15)-*E*-en-8β-ol-16-oate (**5.49**) and ethyl 17-norabiet-13(15)-*Z*-en-8β-ol-16-oate (**5.50**) were also isolated as minor products. The proportion of base to triethylphosphonoacetate was kept below 1:1 as we reasoned that **5.49** and **5.50** were forming from a base catalyzed aldol condensation of **5.31** to **5.51**, which subsequently underwent an HWE reaction at C-13. The structural elucidation of the tricyclic products, **5.49** and **5.50**, will be discussed later (Chapter Six, Section 6.2). The desired ethyl esters, **5.32** and **5.33**, were isolated from the reaction mixture in 74% combined overall yield (*E*/*Z* ratio 3:1) *via* normal phase HPLC (6% ethyl acetate, 94% hexane).

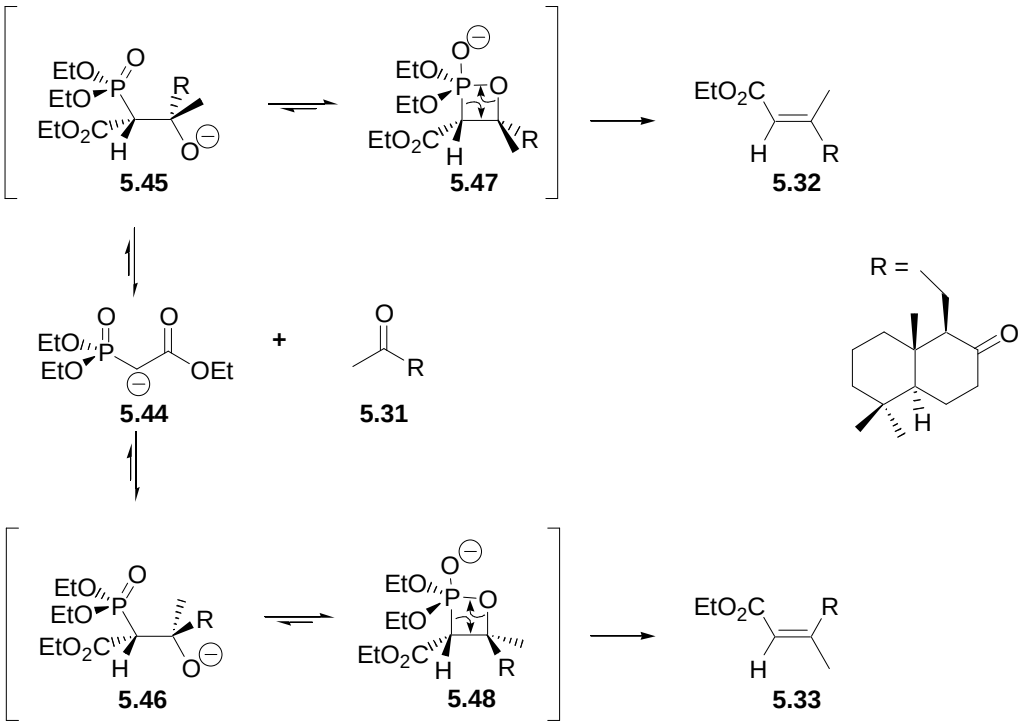

Scheme 5.5 Mechanism for the HWE reaction between triethylphosphonoacetate and **5.31**.[207]

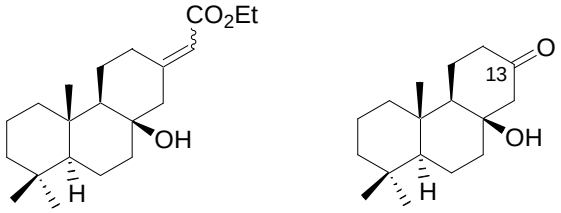

5.49 Δ^{13} *E*
5.50 Δ^{13}*Z*

5.51

The molecular formula ($C_{21}H_{36}O_3$) of **5.32** was established from HRFABMS data and implied five degrees of unsaturation, two of which could be attributed to an α,β-unsaturated ester, one to a carbonyl functionality and the remaining two to the decalin ring system of **5.32**. Preliminary analysis of the ^{13}C NMR spectrum **5.32** revealed the retention of one ketone functionality (δ_C 211.7) and the appearance of chemical shifts attributable to an unsaturated ethyl ester functionality [δ_C 166.8 (s), 160.1 (s), 115.7 (d), 59.4 (t), 14.3 (q)]. Comparison of the ^{1}H and ^{13}C NMR data of **5.31** and **5.32** (Figure 5.7) limited the differences to the alkenoate side chain of these two compounds. gHMBC correlations of **5.31** (see Table 5.1 and Figure 5.8) from each of H-7b (δ_H 2.41), H-7a (δ_H 2.27), H-9 (δ_H 1.99), H_2-11 (δ_H 1.36) and H-12a (δ_H

1.87) to C-8 (δ_C 211.7) confirmed that the ketone functionality remained at C-8, and hence that preferential olefination had occurred at C-13. The regioselective olefination at C-13 was also implied by a downfield chemical shift of H_3-16 (adjacent to C-13) from δ_H 2.07 to δ_H 2.13 from comparison of the ^{1}H NMR spectra of **5.31** and **5.32** (Figure 5.7). The gHMBC correlations used to confirm the structure of the alkenyl side chain are shown in Figure 5.8. The *E* bond geometry of the Δ^{13} olefin in **5.32** was determined from ^{13}C NMR chemical shifts of methyl C-16 and methylene C-12 (δ_C 18.7 and 40.2 respectively).[99;102] Similarly, the presence of a *Z* Δ^{13} olefin in **5.33** was determined from the ^{13}C NMR chemical shift of the vinylic Me-16 carbon resonance (δ_C 25.0) and the allylic methylene C-12 signal (δ_C 32.6). The two minor tricyclic products from the same HWE reaction (**5.49** and **5.50**), were isolated in 9% combined yield (*E*/*Z* ratio 7:2).

As mentioned in the earlier discussion of our new synthetic route to **5.4** and **5.5**, the ketoesters, **5.32** and **5.33**, were required to attempt a chemoselective alkylation of the ketone functionality at C-8 in the presence of the α,β-unsaturated ester in the alkenyl chain. Reetz *et al*.[196] had reported the preferential alkylation of a ketone moiety over that of an ester functionality using a non-basic methyl titanium trichloride reagent. This reagent is generated by ligand exchange between methyl lithium of methyl Grignard reagents and titanium tetrachloride.[196;209] In the transition state of carbonyl addition using titanium based alkylation agents, the reagent and substrate are bound tightly together, since the carbonyl-titanium bond is shorter than other metal-oxygen bonds.[196;209] This short carbonyl-titanium bond facilitates discrimination between various ketones and aldehydes and other different carbonyl containing functionalities *e.g.* esters based on steric factors.[196] We accordingly attempted to prepare the methyl titanium chloride under the conditions described by Reetz *et al*.[196] using methyl lithium and titanium tetrachloride in ether at -78℃, but a ll attempts at using this reagent on **5.32** were unsuccessful, yielding only starting material upon purification. We believe this was possibly due to water in either the distilled solvents or titanium tetrachloride, which prevented the formation of the methyl titanium chloride reagent at the small scale (0.06 mmol of **5.32**) at which the reaction was being performed.

Table 5.1 ^{1}H (400 MHz), ^{13}C (100 MHz), gCOSY and gHMBC NMR data for **5.32** in $CDCl_3$.

Position	δ_C (mult.)	δ_H (int., mult., *J*/Hz)	gHMBC	gCOSY
1a	39.3 (t)	1.14 (1H, ddd, 13.2, 12.2, 4.9)	2, 9, 10, 20	1b, 2
b		1.74 (1H, m)	2, 3, 10, 20	1a, 2
2	19.0 (t)	1.50 (2H, m)	1, 4, 10	1a, 1b, 3a, 3b
3a	41.9 (t)	1.23 (1H, m)	1, 2, 4, 18, 19	2, 3b, 18
b		1.44 (1H, m)	1, 18, 19	2, 3a
4	33.7 (s)	-	-	-
5	54.3 (d)	1.46 (1H, m)	1, 4, 6, 7, 9, 10, 20, 18, 19	6a, 6b
6a	24.1 (t)	1.64 (1H, dddd, 13.3, 13.1, 13.0, 5.0)	5, 7	5, 6b, 7a, 7b
b		2.05 (1H, m)	5, 7	5, 6a, 7a, 7b
7a	42.6 (t)	2.27 (1H, ddd, 13.3, 7.2, 6.8)	5, 6, 8	6a, 6b, 7b
b		2.41 (1H, ddd, 13.2, 4.8, 2.1)	5, 6, 8, 9	6a, 6b, 7b
8	211.7(s)	-	-	-
9	63.2 (d)	1.99 (1H, m)	1, 7, 8, 12, 20	11a, 12a
10	42.6 (s)	-	-	-
11	19.6 (t)	1.36 (2H, m)	8, 9, 12, 13	9, 12a, 12b
12a	40.2 (t)	1.87 (1H, m)	9, 11, 13, 14	9, 11, 12b
b		2.18 (1H, m)	11	11, 12a
13	160.1 (s)	-	-	-
14	115.7 (d)	5.61 (1H, dd, 2.1, 1.2)	12, 14, 16	14
15	166.8 (s)	-	-	-
16	18.7 (q)	2.13 (3H, d, 1.2)	12, 13, 15, 16	15
18	33.5 (q)	0.94 (3H, s)	3, 4, 5, 18	-
19	21.7 (q)	0.84 (3H, s)	3, 4, 5, 19	3a
20	14.7 (q)	0.71 (3H, s)	1, 5, 9, 10	1a, 9
-O$CH_2$$CH_3$	59.4 (t)	4.13 (2H, dq, 7.1, 0.5)	15, -O$CH_2$$CH_3$	-O$CH_2$$CH_3$
-O$CH_2$$CH_3$	14.3 (q)	1.26 (3H, t, 7.1)	-O$CH_2$$CH_3$	-O$CH_2$$CH_3$

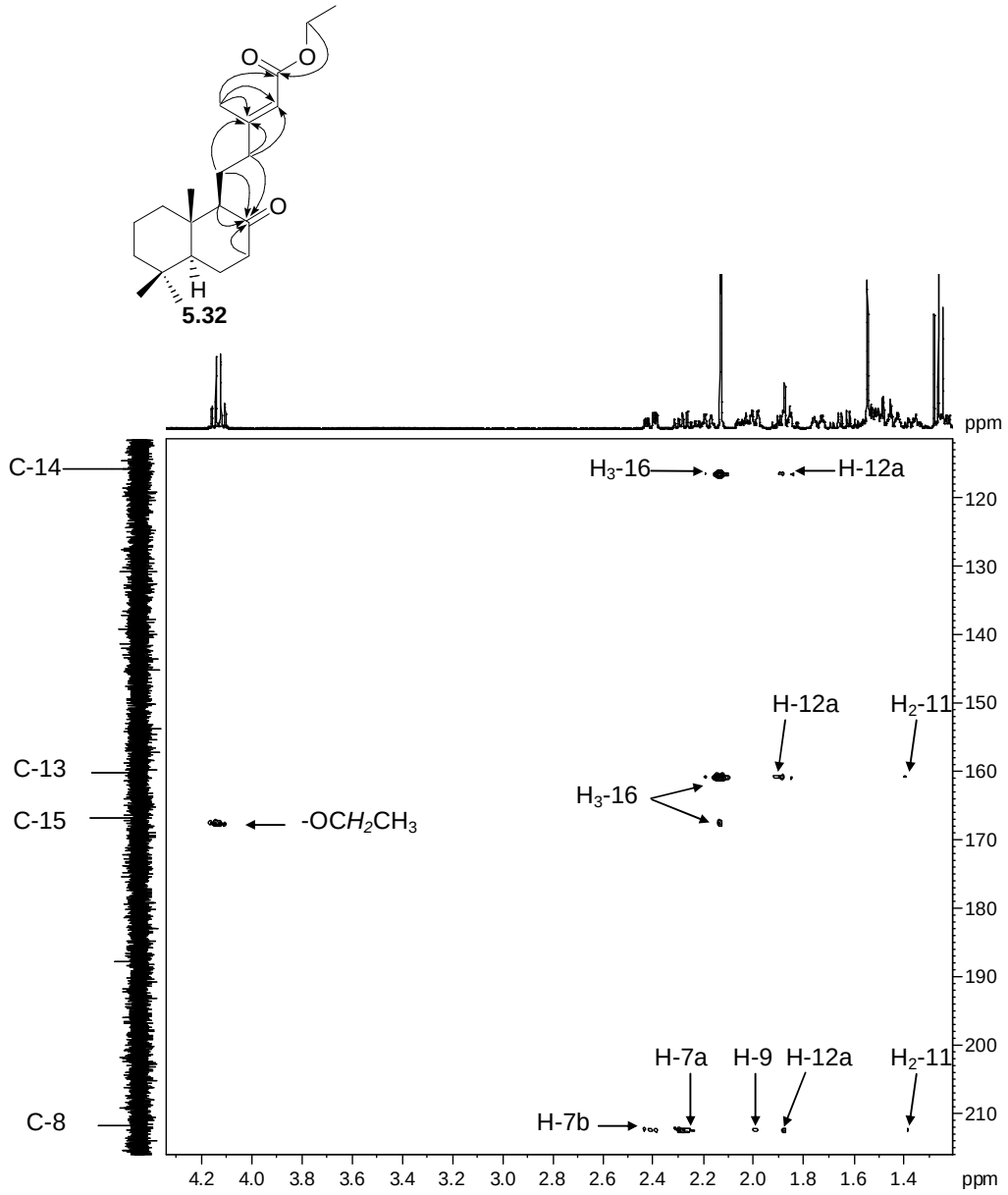

Figure 5.8 Upfield section (F1 = δ_C 100 – 210, F2 = δ_H 1.2 – 4.3) of the gHMBC spectrum (400 MHz, $CDCl_3$) of **5.32**. The accompanying figure indicates key correlations from the gHMBC spectrum of **5.32**.

Following the unsuccessful methyl titanium chloride reaction, we decided to attempt the reaction using only methyl lithium, methyl magnesium bromide or methyl magnesium chloride as alkylating agents, reasoning that the ketone at C-8 would probably be more reactive than the α,β-unsaturated ester in the alkenyl chain and thus be more susceptible to nucleophilic addition. Although methyl lithium mediated alkylation had been demonstrated to afford only the 8β-hydroxyl moiety,[173] we considered that using a less reactive alkylating reagent such as methyl magnesium bromide, or the even less reactive methyl magnesium chloride, might result in a higher proportion of C-8 addition products. For similar reasons, we decided to attempt the reaction at -78℃ to slow the reaction down. Gratifyingly, chemoselective methylation of the C-8 ketone in **5.32** (and also **5.33**, once the reaction protocol had been established) proceeded smoothly using all three alkylating agents. The methyl nucleophile attacked the endocyclic ketone with *Re*-facial selectivity to afford ethyl labd-13*E*-en-8β-ol-15-oate, **5.34**, and ethyl labd-13*Z*-en-8β-ol-15-oate, **5.35**, respectively. The reaction mixture was purified using semi preparative HPLC (14% ethyl acetate, 86% hexane) with none of the di-addition product or addition to the ester carbonyl being detectable (in the ^{1}H NMR spectrum of the crude reaction mixture). Although we were expecting the methyl lithium reaction to afford only the 8β-hydroxyl epimer, previous studies with Grignard reagents on various cyclohexanones had found that a mixture of the α- and β-epimers was to be expected.[180;181] Since molecular modelling of related diterpenes had shown that the β face of the molecule around C-8 was sterically hindered, delivery from the α-face of the ring system was probably favoured, accounting for the controlled formation of only the 8β-hydroxy epimers. We were encouraged to find that the yields of **5.34** and **5.35** were enhanced when methyl magnesium chloride (81%) was used, as opposed to either methyl magnesium bromide (70%) or methyl lithium (51%). Using the same method as used in **5.20** and **5.21**, the 8β-axial orientation of the alcohol substituent in **5.34** and **5.35** was supported by threefold spectroscopic evidence *viz.* the deshielding of the H_3-20 angular methyl protons (δ_H 0.94 in both), the shielding of C-6 (δ_C 18.1 and 18.3 respectively) and a downfield shift of the C-17 methyl carbon resonance (δ_C 30.6 in both) in the ^{1}H and ^{13}C NMR spectra of these two compounds, similar to **5.20** and **5.21**.[171;182;183] The ^{1}H NMR spectrum of **5.34** is shown in Figure 5.7.

Two different methods for the reduction of the ester functionalities of **5.34** and **5.35** were attempted. Reduction of **5.34** with diisobutylaluminium hydride (DIBAH) in tetrahydrofuran at 0℃ afforded labd-13*E*-ene-8β,15-diol, **5.4**, in 53% yield after purification with semi-preparative HPLC (50% ethyl acetate, 50% hexane). The yield of **5.4** was marginally improved to 66% by the use of lithium aluminium hydride in ether at 0℃, but no further improvement in yield could be made by altering either solvent (*e.g.*THF) or temperature (*e.g.* -20℃). The reduction of the ester was determined by analysis of the ^{1}H NMR spectrum of **5.4**, where the absence of the methyl triplet (δ_H 1.26) and methylene quartet (δ_H 4.13) of the ester functionality, in addition to the appearance of an oxymethylene doublet (δ_H 4.14), were immediately apparent. In the ^{13}C NMR spectrum of **5.4**, the retention of the vinylic resonances [δ_C 123.1 (d) and δ_C 140.4 (s)], the disappearance of the ester carbonyl resonance (δ_C 166.8) and the appearance of an additional oxymethylene resonance (δ_C 59.4) confirmed the loss of only the ester moiety. All other ^{1}H and ^{13}C NMR data were consistent with those in the literature for **5.4**, with the exception of the data published by Giang *et al*.[210] who we believe to have erroneously identified a diterpenoid compound, isolated from *Leonurus heterophyllus*, as **5.4**. Although the specific rotation of synthetic (+)-**5.4** ($[\alpha]_D$ + 21) was lower in magnitude than that established by Ciavatta *et al*.[171] ($[\alpha]_D$ + 32), for the reduction product of the nudibranch derived **5.1**, it was significantly different to the specific rotations reported for **5.4** isolated from terrestrial plants ($[\alpha]_D$ 0 and +99).[210;211] The negative specific rotation previously reported for *ent*-**5.4** ($[\alpha]_D$ -32)[182;212] is in agreement with the established labdane stereochemistry of semi-synthetic **5.4** and supports that proposed by Ciavatta *et al*. for marine-derived **5.4**.

The target aldehyde, labd-13*E*-ene-8β-ol-15-al **5.1** (^{1}H and ^{13}C NMR spectra shown in Figure 5.9) was quantitatively procured by stirring **5.4** in dichloromethane with manganese dioxide (10 eq) overnight. The ^{1}H NMR spectrum (in deuterated benzene) of **5.1** clearly revealed the appearance of an aldehyde doublet (δ_H 9.91) and the disappearance of an oxymethylene signal (δ_H 4.14) relative to **5.4**. Filtration through celite gave a 25:1 mixture of **5.1**:**5.2** (*i.e.* > 95% *E* isomeric purity from NMR analysis). The ratio of **5.1**:**5.2** changed substantially (15:1) after an attempt was made to remove the small amount of labd-13*Z*-ene-8β-ol-15-al, **5.2**, in the isomeric mixture using normal phase HPLC (20% ethyl acetate, 80% hexane) and this

isomerisation was suggestive of the instability of these α,β-unsaturated aldehyde compounds to silica chromatography. An analogous manganese dioxide oxidation of **5.5** gave **5.2**:**5.1** in a 50:1 ratio (*i.e.* > 98% *Z* isomeric purity from NMR analysis) which, after normal phase HPLC, also reverted to a mixture of 11:1 (Z:*E*) geometric isomers. The ^{1}H and ^{13}C NMR data of the 25:1 mixture of predominantly **5.1** (acquired in deuterated chloroform) was consistent in all respects with the spectroscopic data published for the corresponding *P. meckelii* metabolite (Table 5.3).[171] In our hands, the ^{1}H NMR spectrum of the isomeric mixture, containing almost exclusively **5.2**, showed evidence of initial partial isomerisation followed by total degradation (to form an inseparable mixture of products) on standing in a solution of deuterated chloroform (12 h). Accordingly, the NMR data for the *Z* isomer dominated mixture was obtained in deuterated benzene. We consequently also avoided using chloroform for recording the specific rotations of **5.1** and **5.2**. Paradoxically, Ciavatta *et al.*[171] reported negative specific rotations for chloroform solutions of **5.1** ($[\alpha]_D$ -35.2) and **5.2** ($[\alpha]_D$ -28.2) isolated from *P. meckelii*, which are opposite in sign to those obtained for our semi-synthetic **5.1** ($[\alpha]_D$ +26) and **5.2** ($[\alpha]_D$ +24) recorded in benzene but also opposite in sign and magnitude to the specific rotation (recorded in chloroform) of both the reduction product precursor, **5.4**, derived from **5.1** isolated from *P. meckelii*,[171] and our semi-synthetic **5.4**. Interestingly, a negative specific rotation ($[\alpha]_D$ -8.5) was reported for **5.29**, the 8α-epimer of **5.4**.[185] While epimerization at C-8 is an unlikely explanation for the discrepancy between the signs of the specific rotations of the naturally occurring and synthetic **5.1** and **5.2**, we believe that this discrepancy may be related to the facile isomerisation and instability of the α,β-aldehydes to both chromatographic media and solution in deuterated chloroform.

Table 5.2 Comparison of the ^{13}C NMR (125 MHz) of marine derived **5.1** and semi-synthetic **5.1** (150 MHz) in $CDCl_3$. The ^{1}H (600 MHz) and ^{13}C (150 MHz) data of synthetic **5.1** in C_6D_6 are also presented.

Marine **5.1**[171]		Synthetic **5.1**		
Position	δ_C [†] (mult.)	δ_C [‡] (mult.)	δ_C [§] (mult.)	δ_H [⊥] (int., mult., *J*/ Hz)
1a	39.3 (t)	39.3 (t)	39.3 (t)	0.65 (1H, m)
1b				1.48 (1H, m)
2a	18.2(t)	18.2 (t)	18.61 (t)	1.18 (1H, m)
2b				1.49 (1H, m)
3a	42.3 (t)	42.3 (t)	42.4 (t)	1.10 (1H, ddd, 14.2, 6.6, 3.8)
3b				1.37 (1H, ddd (11.8, 3.8, 1.4)
4	33.3 (s)	33.2 (s)	33.4 (s)	-
5	55.9 (d)	55.9 (d)	56.0 (d)	0.63 (1H, dd, 12.2, 2.4)
6a	18.1 (t)	18.1 (t)	18.62 (t)	1.23 (1H, m)
6b				1.33 (1H, m)
7a	42.0 (t)	41.9(t)	42.6 (t)	1.18 (1H, m)
7b				1.54 (1H, ddd, 13.5, 3.5, 3.3)
8	73.1 (s)	73.1 (s)	72.4 (s)	-
9	58.8 (d)	58.8 (d)	58.8 (d)	0.41 (1H, dd, 4.6, 2.6)
10	39.3 (s)	39.0 (s)	39.2 (s)	-
11a	23.3 (t)	23.3 (t)	23.5 (t)	1.20 (1H, m)
11b				1.43 (1H, m)
12a	44.3 (t)	44.3 (t)	44.4 (t)	1.80 (1H, m)
12b				1.84 (1H, m)
13	164.1 (s)	164.2 (s)	162.1 (s)	-
14	127.2 (d)	127.1 (d)	127.3 (d)	5.93 (1H, ddd (7.8, 2.5, 1.3)
15	191.4 (d)	191.4 (d)	190.0 (d)	9.91 (1H, d, 7.8)
16	17.6(q)	17.6(q)	17.0(q)	1.60 (1H, d, 1.3)
17	30.6 (q)	30.6 (q)	30.8 (q)	0.86 (3H, s)
18	33.4 (q)	33.4 (q)	33.7 (q)	0.88 (3H, s)
19	21.6 (q)	21.6 (q)	21.9 (q)	0.85 (3H, s)
20	15.1 (q)	15.1 (q)	15.3 (q)	0.95 (3H, s)

[†] 125 MHz, $CDCl_3$; [‡] 150 MHz, $CDCl_3$; [§] 150 MHz, C_6D_6; [⊥] 600 MHz, C_6D_6

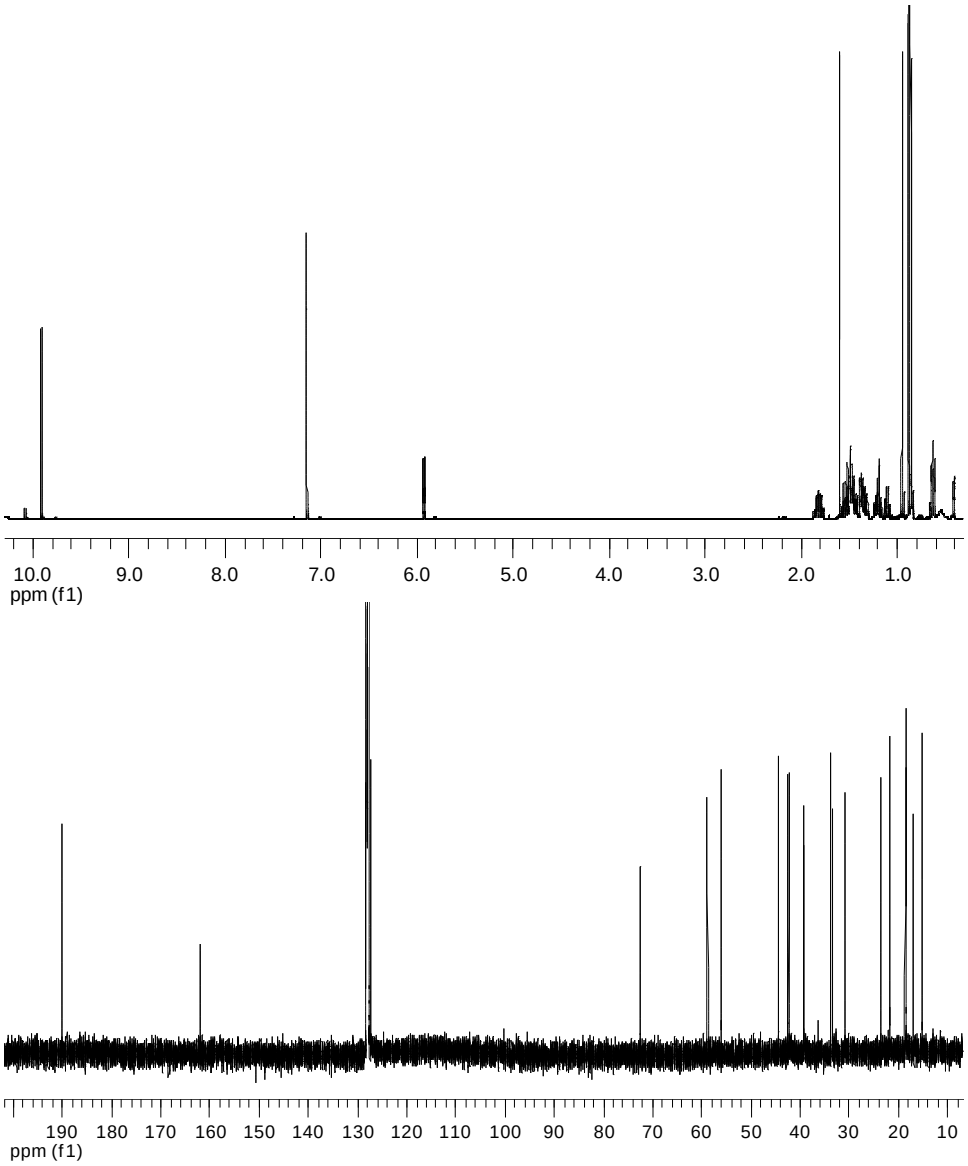

Figure 5.9 The ^{1}H (600 MHz) and ^{13}C (150 MHz) NMR spectra of **5.1** in C_6D_6.

5.6 The anti-oesophageal cancer activity of selected labdane diterpenes from this chapter

Seven of the diterpenes (**5.1**-**5.5**, **5.32**, **5.49** and **5.50**) discussed within this chapter were sent to the Department of Medicinal Biochemistry, at the University of Cape Town, as an extension of the previous evaluation of labdane diterpenes, isolated from *T. costatus* (Chapter Three, Section 3.3), for their activity against oesophageal cancer cell lines. A dose response curve

was obtained using the (MTT) assay and IC_{50} values (Table 5.4) determined against the WHCO1 oesophageal cancer cell line.

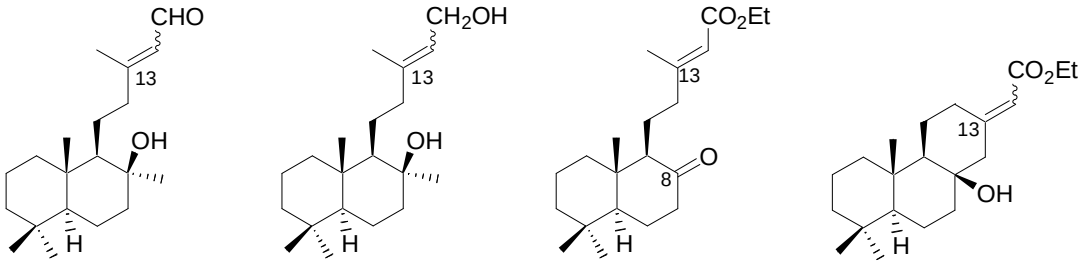

5.1 Δ^{13} *E*
5.2 Δ^{13} Z

5.4 Δ^{13} *E*
5.5 Δ^{13} *Z*

5.32

5.49 Δ^{13} *E*
5.50 Δ^{13}*Z*

Table 5.3 Summary of the IC_{50} values of compounds against the WHCO1 cell line.

	Compound tested						
	5.1	**5.2**	**5.4**	**5.5**	**5.32**	**5.49**	**5.50**
IC_{50} (μM)	5.4	16.7	49.6	121.6	No activity	48.5	No activity

Once again, the limited number of compounds assayed prevented us from drawing more than tentative conclusions regarding structure-activity relationships. In all cases, the Δ^{13} [or $\Delta^{13(15)}$] *E* isomers (**5.1**, **5.4** and **5.49**) had lower IC_{50} values than their *Z* isomeric counterparts, particularly in the case of **5.49** and **5.50**, where **5.49** revealed modest activity while **5.50** was inactive. The aldehydes, **5.1** and **5.2,** were significantly more active than the diols, **5.4** and **5.5**, with **5.1** possessing an IC_{50} value nearly an order of magnitude lower than that of the corresponding diol, **5.4**.

5.7 Conclusions

The target compounds, **5.1** and **5.2** were successfully synthesized in 19% and 6% overall yield respectively from a commercially available labdane diterpene precursor, **5.3**. The successful synthetic strategy (Scheme 5.6) depended on a regioselective HWE reaction on the diketone, **5.31**, which afforded **5.32** and **5.33**. The second obstacle in the successful synthetic strategy surrounded the stereospecific and chemoselective alkylation of the C-8

carbonyl moiety of **5.32** and **5.33**. Stereospecific and chemoselective alkylation was achieved with methyl lithium, methyl magnesium bromide and methyl magnesium chloride at -20℃ with the latter reagent proving to be the most efficient. Reduction of the esters, **5.34** and **5.35**, was best achieved using LAH. Facile oxidation of the primary alcohols, **5.4** and **5.5** to their corresponding aldehydes, **5.1** and **5.2** was achieved with manganese dioxide. The aldehydes **5.1** and **5.2** proved unstable in deuterated chloroform and degraded to an inseparable mixture of products within twelve hours. The aldehydes also isomerised when subjected to standard chromatographic procedures. The anti-oesophageal cancer activity of compounds **5.1-5.5**, **5.32, 5.49** and **5.50** was evaluated and the aldehydes **5.1** and **5.2** were found to be the most cytotoxic.

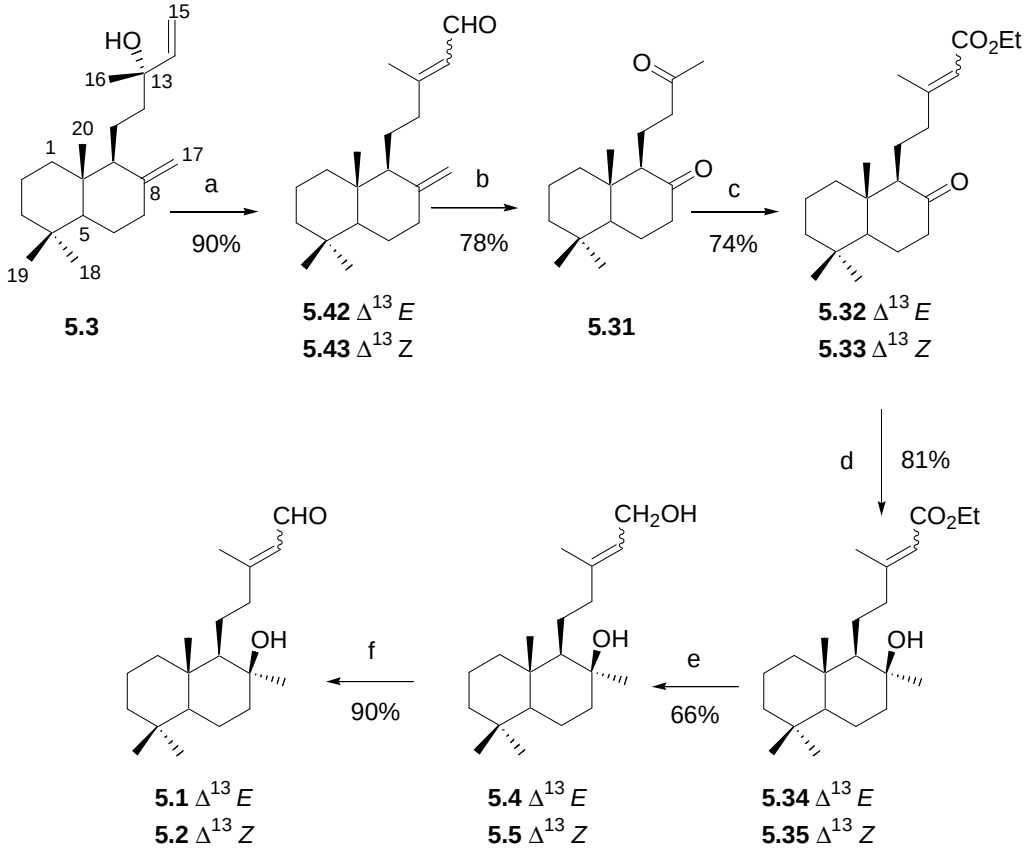

Scheme 5.6 The final synthetic route to **5.1** and **5.2**. *Regents and conditions:* (a) PCC, CH_2Cl_2, RT, 26 h (b) O_3, CH_2Cl_2, -78℃, 10 min, then PPh_3, RT, 4 h; (c) $(C_2H_5O)_2P(O)CH_2CO_2Et$, NaH, THF, 0 ℃ to RT, 16 h; (d) MeMgCl, Et_2O, -20 ℃ (1 h) to RT (3 h); (e) LAH, THF, 0℃ (0.5 h) to RT (2 h); f) MnO_2, CH_2Cl_2, RT, 16 h.

Chapter Six

The Semi-synthesis of Tricyclic Diterpenes with Anti-malarial Activity

6.1 Introduction

This chapter describes an extension of the research discussed in Chapter Five, where ethyl 17-norabiet-13(15)-*E*-en-8β-ol-16-oate (**5.49**) and ethyl 17-norabiet-13(15)-*Z*-en-8β-ol-16-oate (**5.50**) were isolated as the minor products of a regioselective HWE reaction performed on (**5.31**). An investigation of the natural product literature revealed reports of similar tricyclic compounds (**6.1-6.5**) with anti-malarial properties.[213;214] Since we are cognizant of the impact that malaria has on developing nations including our own (*vide infra*) and were in possession of a readily accessible starting material (**5.51**), from which analogues, **5.49**-**5.50**, as well as 17-norpimaran-13α-ethoxy-8,16-olactone (**6.6**), 17-norisopimar-15-ene-8β,13β-diol (**6.7**), 17-norisopimarane-8β,16-diol (**6.8**) and 17-norabiet-13(15)-ene-8β,16-diol (**6.9**) could be derived, we decided to further investigate the potential of analogous tricyclic norditerpenes as anti-malarial agents. This chapter thus consists of a discussion of the synthesis and structural elucidation of the semi-synthetic norditerpenes (**5.49**-**5.50** and **6.6**-**6.9**) and culminates in a critical evaluation of their anti-malarial potential from parasite inhibition and haemolytic studies.

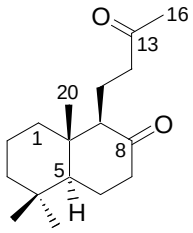

5.31

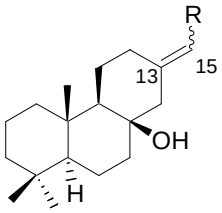

5.49 $\Delta^{13(15)}$ *E* R = CO_2Et
5.50 $\Delta^{13(15)}$ *Z* R = CO_2Et
6.9 $\Delta^{13(15)}$ *Z* R = CH_2OH

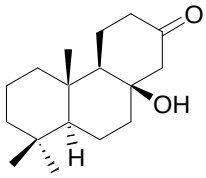

5.51

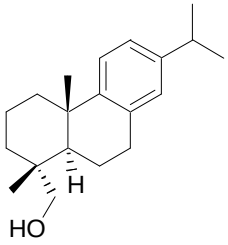

6.1

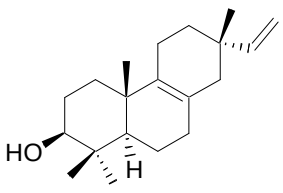

6.2

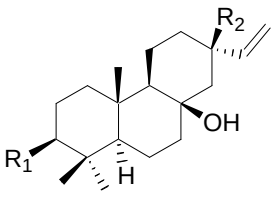

6.3 R_1 = OH; R_2 = CH_3
6.7 R_1 = H; R_2 = OH

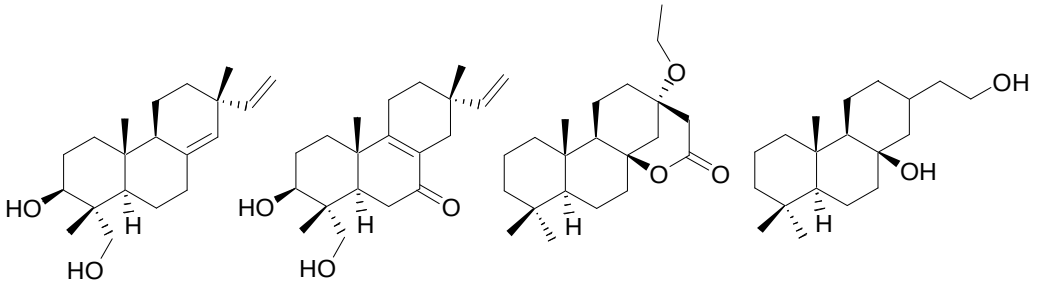

6.4 **6.5** **6.6** **6.8**

6.1.1 Natural products analogues as anti-malarial drug agents

Malaria is a parasitic disease, with between 300 and 660 million clinical cases reported each year.[215-217] Although statistics vary widely from source to source, approximately 70% of all cases appear to be concentrated on the African continent,[216] where at least one million deaths per annum are directly (and up to three million deaths indirectly) attributed to the disease.[218] More than 75% of the deaths recorded are of children under the age of five,[218] translating into the staggering figure that every forty seconds a child in Africa dies of malaria.[215;218]

Of the four different species of parasite that cause malaria (*Plasmodium falciparum, P. vivax, P. malariae* and *P. ovale*), *P. falciparum*, is the most virulent, prevalent and drug resistant species.[218;219] In Africa, the transfer of *P. falciparum* to its human host is greatly aided by the mosquito *Anopheles gambiae*.[215;218;219] The female *A. gambiae* is the most successful vector of malarial parasites as a result of both its affinity for biting humans and longevity, the latter being particularly important since a time period of 8-30 days, dependent on ambient temperature, is required for the parasite to complete that part of its lifecycle spent within the mosquito.[215;218;219] The global concentration of malaria in tropical regions has been directly linked to the shortened gestation period required by the parasite within the mosquito at sustained temperatures over 18℃. [215;218;219]

Although nearly two billion people are exposed to malaria every year,[216-219] the countries where malaria is most prevalent are also amongst the poorest worldwide and thus can afford neither proper treatment nor management of the disease for their citizens.[215;218-220] As a result,

large pharmaceutical companies have been reluctant to take the financial risk of developing anti-malarial treatments[219] and resistance to existing malarial prophylactics is increasing.[215;218-223]

The low cost of chloroquine (**6.10**) and its related analogues [*e.g.* amodiaquine (**6.11**) and halofantrine (**6.12**)] have made them the most common treatment for malaria in Africa. Chloroquine has been used as an anti-malarial in Africa since the late 1970's and has its structural roots in quinine (**6.13**),[220;222] a natural product derived from the bark of the Peruvian *Cinchona* tree, brought to Europe in the seventeenth century.[220;222] Resistance to chloroquine was first reported in 1986 and has since become widespread.[222] The malarial *Plasmodium* produces large amounts of free Fe(II) haem during its lifecycle through degradation of the host erythrocyte's haemoglobin.[219-221] This free Fe(II) haem is toxic to the parasite and is accordingly oxidized to Fe(III) haematin, which is then stored within vacuoles as a crystalline pigment (called haemozoin), rendering it harmless to the parasite. Chloroquine and its analogues are concentrated within the same vacuole, preventing crystallization of the haematin, and thus killing the malarial parasites once lethal concentrations of haematin have been reached.[219-221]

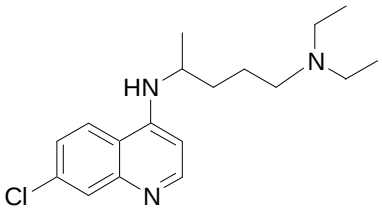

6.10

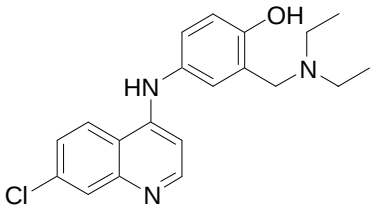

6.11

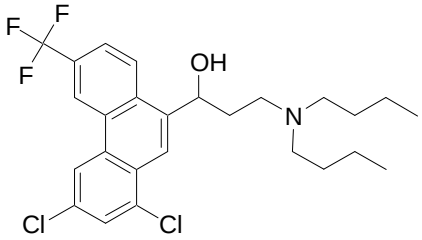

6.12

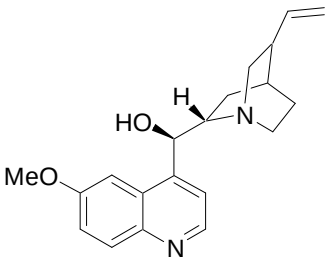

6.13

The alternative cost-effective treatment available to combat chloroquine resistance is the combination of pyrimethamine (**6.14**) and sulfadoxine (**6.15**).[219-221] Unfortunately, this

treatment targets the enzymes dihydrofolate reductase (DHFR) and dihydropteroate synthase, the alleles coding for which are susceptible to point mutations, thus enabling the malarial parasites to evolve rapid resistance to this combination treatment.[219-222]

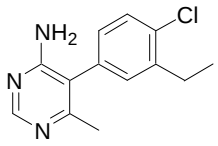

6.14

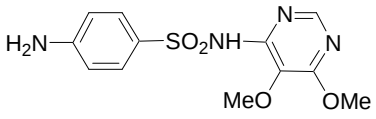

6.15

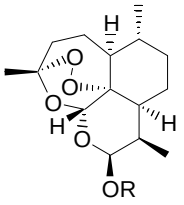

6.16 R = $CO(CH_2)_2CO_2H$
6.17 R = Me
6.18 R = Et
6.20 R = H

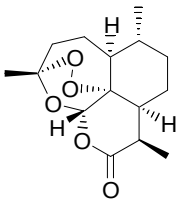

6.19

The most promising new natural product derived anti-malarials to date are the artemesinins (**6.16**-**6.18**),[219;220] all of which are structural analogues of the active component of artemesinin (**6.19**), isolated from the Chinese herb "qinhao" (*Artemesia annua*)[224] with an endoperoxide bridge. The artemesinins are rapidly converted to the active form dihydroartemesinin (**6.20**) in the human body. Dihydroartemesinin is active against the gametocytes that comprise the sexual reproduction stage and infect the mosquito.[220] Unfortunately, the artemesinins have short half lives in the human body and must thus be administered continually over five to seven days, and this can be problematic in the African context where poor health care structures lead to poor compliance.[219;220] Additionally, although the artemesinins are relatively inexpensive by global standards, they are still considerably more expensive than the quinoline and pyrimethamine-sulfadoxine alternatives and beyond what many developing nations can afford.[219;220]

Although the vogue over the last decade or so has been to focus on target-based drug discovery (*i.e.* where a specific "gene, gene product or molecular mechanism" has been

targeted),[225] the number of new compounds reaching the market has been decreasing, despite large investments into research and development by pharmaceutical companies.[225] As can be seen (*vide supra*) from the brief overview of current anti-malarial agents in use, two of the main groups, *viz.* the chloroquines and artemesinins are analogues of naturally occurring bioactive compounds. We thus proposed to investigate the anti-malarial properties of analogues of a naturally occurring series of tricyclic diterpenes **6.1**-**6.5**. Although Asili and coworkers[213;214] had reported anti-plasmodial activity for **6.1**-**6.5**, they considered the weak anti-plasmodial activity of these diterpenes to be an indirect consequence of echinocytic and stomatocytic changes to the erythrocyte cell membrane, leading to compromised cell function and death of the malarial parasites through indirect destruction of their host cells. Our objective was thus to investigate the effects of synthetically produced analogues of **6.1**-**6.5** in the hopes of better understanding or even obviating the apparent erythrocyte modifying behaviour of this class of compounds.

6.2 Semi-synthesis of potential anti-malarial compounds

As mentioned previously (Chapter Five, Section 5.5), we serendipitously synthesized compounds **5.49** and **5.50** in low (9%) combined isolated yield while performing an HWE reaction on **5.31**. We postulated that excess sodium hydride (acting as a base) initiated an intramolecular aldol condensation of **5.31** to **5.51**, which in turn reacted with the HWE reagent affording **5.49** and **5.50** (Scheme 6.1). Our observation of this initial intramolecular cyclization was not without precedent, since 8-hydroxy-13-podocarpanone, **5.51**, had previously been prepared by stirring either a solution of **5.31** in methanolic potassium hydroxide or ethanolic sodium ethoxide to afford **5.51** in 68% and 80% yield respectively,[174;202] To confirm that sodium hydride was inducing an intramolecular cyclization of **5.31**, we attempted the cyclization of **5.31** directly by adding sodium hydride to an anhydrous solution of this compound in tetrahydrofuran and established that two equivalents of sodium hydride provided **5.51** in almost quantitative yield (by NMR). The reaction was also closely monitored by TLC (TLC plate developed with iodine). Once all starting material appeared to have been converted to a single product, **5.51**, the reaction was halted by the addition of a few drops of

dilute HCl and the reaction mixture washed with water. Analysis of the ^{1}H NMR spectrum of the reaction mixture clearly showed the disappearance of the diagnostic deshielded methyl singlet (δ_H 2.07) in **5.31**, while the ^{13}C NMR spectrum revealed the disappearance of the methyl ketone resonance (δ_C 209.2) and the appearance of a new ketone carbonyl resonance (δ_C 210.7) and an oxygenated quaternary carbon resonance (δ_C 75.5). Analysis of the ^{13}C NMR spectrum of **5.51** also revealed that the reaction was stereospecific as no duplication of ^{13}C NMR resonances was observed (Figure 6.1). In our hands, **5.51** was unstable and rapidly degraded at room temperature in deuterated chloroform solution, preventing us from obtaining a full 2D NMR data set or a crystal structure of the compound. We were thus unable to determine conclusively whether the hydroxyl at C-8 was β-axial or α-equatorial. However, from a conformational perspective, a *trans* B/C ring junction would be favoured over the alternative *cis* B/C ring junction. Hugel *et al*.[182] had also proposed the β-axial orientation of the hydroxy at C-9 on the basis of a CD spectrum consistent with a *trans* B/C ring junction. The subsequent X-ray diffraction analysis of **5.50**, synthesized from **5.51** (*vide infra*) provided further confirmation of the β-axial orientation of the C-8 hydroxyl functionality.

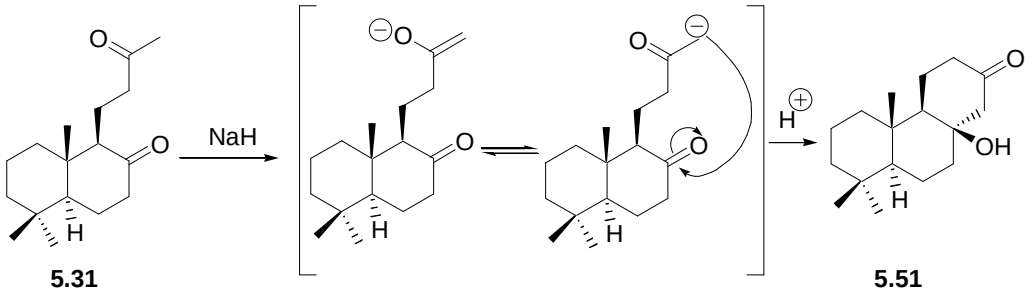

5.31 **5.51**

Scheme 6.1 Mechanism of the sodium hydride mediated intramolecular aldol condensation of **5.31** to **5.51**.

At the time that we first identified **5.49** and **5.50**, Jaroszewski and coworkers'[213] paper reporting the anti-malarial activity of compounds **6.2**-**6.5** came to our attention. We reasoned that the C-13 carbonyl functionality would prove a versatile scaffold for producing norabietane, norpimarane and norisopimarane analogues of these compounds, especially

since **5.51** could be accessed in approximately 71% yield from manool (**5.3**) by our established methodology.

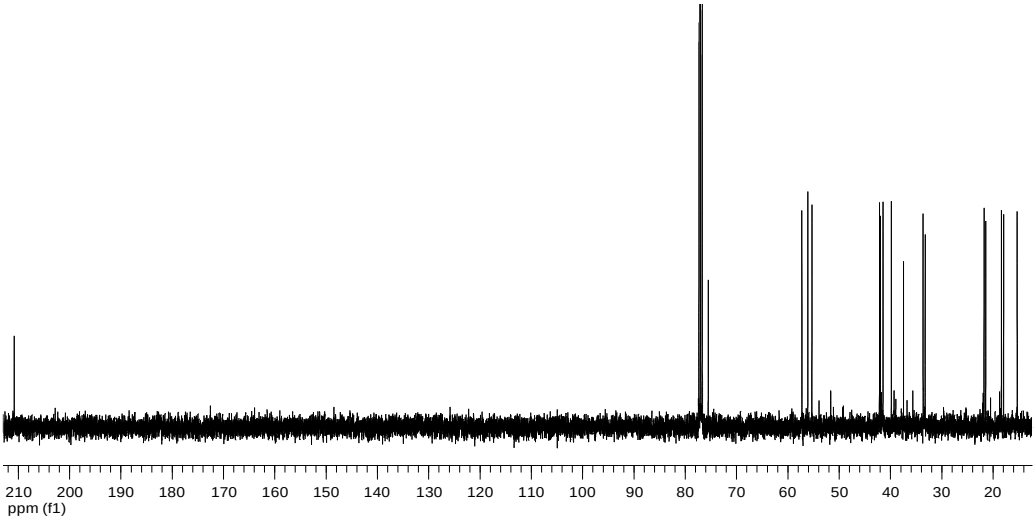

Figure 6.1 The ^{13}C NMR spectrum of **5.51**, demonstrating the absence of duplicated resonances.

Since Jaroszewski and coworkers[213] had reported the anti-plasmodial activity of isopimarane diterpenoids, we decided to synthesize **6.7**, differing only from **6.3** in the replacement of the methyl group at C-13 with a hydroxyl functionality and the absence of a secondary alcohol moiety at C-3. An established procedure for the preparation of nor-isopimarane **6.7** existed,[202] and **5.51** was accordingly reacted with vinyl magnesium bromide in tetrahydrofuran to yield 17-norisopimar-15-ene-8β,13β-diol, **6.7**, which was subsequently purified by normal phase semi-preparative HPLC (75% ethyl acetate, 25% hexane). Although no optical rotation data were available, comparison of the ^{13}C NMR data and melting points of **6.7** with those reported by Buckwalter *et al*.[202] confirmed our product to be identical to theirs.

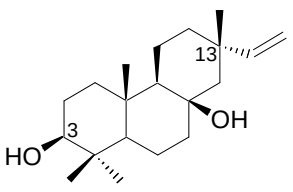

6.3

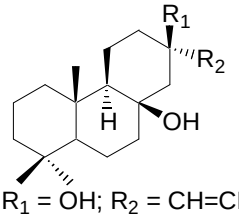

6.7 R_1 = OH; R_2 = CH=CH_2
6.21 R_1 = CH=CH_2; R_2 = OH

Extensive overlap in the methyl envelope of the ^{1}H NMR spectrum of **6.7** (in both deuterated chloroform and deuterated benzene) prevented us from confirming the configuration at C-13. However, molecular modelling of the starting material, **5.51** (Figure 6.2) revealed that the *Si*-facial selectivity may be due to reduced steric hindrance in the α-face of the molecule. The alternative C-13 epimer (**6.21**), with the hydroxyls *trans* to one another, would also presumably lead to an unfavourable 1,3-diaxial interaction between the C-8 hydroxyl and C-13 ethene functionality (Figure 6.2).

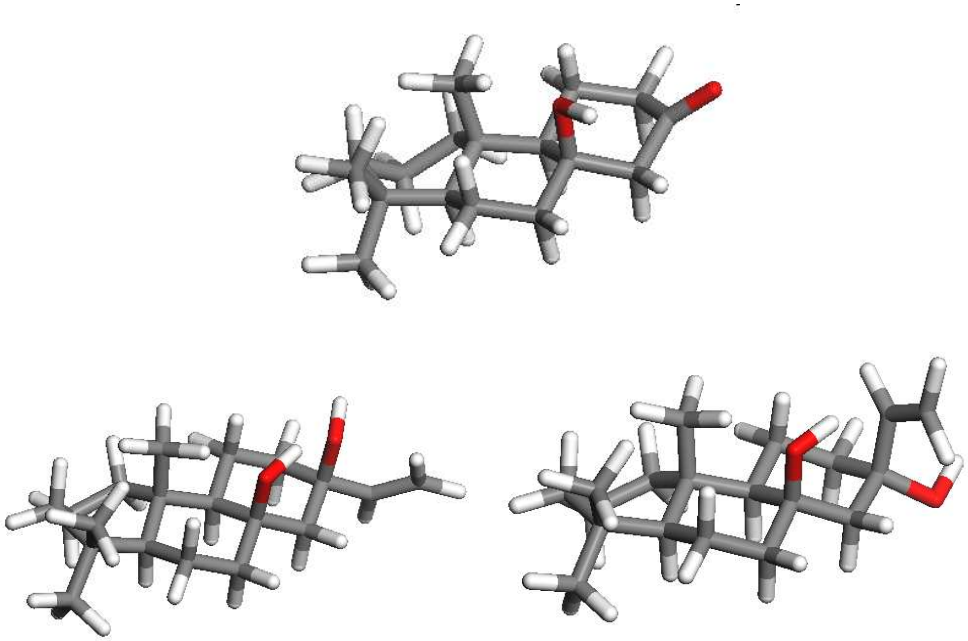

Figure 6.2 Stick molecular model representation of **5.51** (top) and stick representations of the two possible C-13 epimers **6.7** (bottom left) and **6.21** (bottom right).

Although we had previously isolated the minor products, **5.49** and **5.50**, from the HWE reaction of **5.31** with triethylphosphonoacetate, more of each of these needed to be synthesized in an attempt at obtaining crystal structures of one of these compounds to confirm the *Re*-facial selectivity of the intramolecular aldol condensation reaction. The HWE reaction, using **5.51** as a starting material, was thus reattempted and a mixture of the *E* and *Z* trisubstituted olefins obtained. Semi-preparative normal phase HPLC (10% ethyl acetate, 90% hexane) of the isomeric mixture afforded the pure *E* and *Z* isomers in a 4:3 ratio in 70%

overall isolated yield. As mentioned previously, while the HWE reaction is used to preferentially prepare either the *E* or *Z* geometric isomer, the stereoselectivity of the reaction is diminished when ketones are used as opposed to aldehydes,[207] and thus similar proportions of both geometric isomers were not unexpected. The spectroscopic determination of the structure of **5.49** is discussed below.

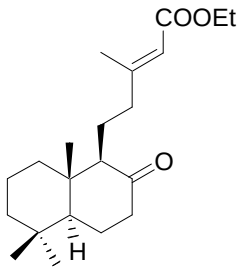

5.32

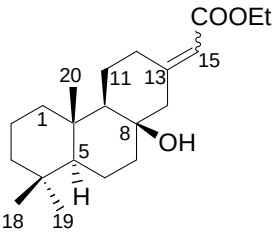

5.49 $\Delta^{13(15)}$ *E*
5.50 $\Delta^{13(15)}$ *Z*

The molecular formula ($C_{21}H_{34}O_3$) of **5.49** was determined from accurate mass data and was found to be consistent with **5.32**. The retention of resonances in the ^{13}C spectrum of **5.49** attributable to the α,β-unsaturated ethyl ester functionality [δ_C 166.3 (s), 159.4 (s), 116.1 (d) 59.6 (t) and 14.3 (q)] was noted. The HRFAB mass data implied five degrees of unsaturation, two of which were accounted for by the unsaturated ester moiety and in the absence of any other evidence for further unsaturation suggested that **5.49** was tricyclic. The absence of the methyl resonance in **5.32** (δ_H 2.13) in the ^1H NMR spectrum of **5.49**, coupled with the appearance of a deshielded oxygenated quaternary carbon (δ_C 73.9) and the discrepancy of two hydrogen atoms between the molecular formulae further supported a tricyclic skeleton similar to that of **6.7**. Comparison of our ^1H and ^{13}C NMR data for **5.49** (Table 6.1) with those of other tricyclic norditerpene compounds (e.g. **6.7**) allowed us to assign the majority of the A and B rings of **5.49**. gCOSY correlations (Table 6.1) between H-9 (δ_H 1.17) and H-11a (δ_H 1.43) and H-11b (δ_H 1.79) supported by gHSQC data allowed us to assign C-11 (δ_C 22.4). Similarly C-12 (δ_C 29.6) was assigned through gCOSY correlations between both the protons of C-11 to both H-12a (1.76) and H-12b (δ_H 3.92). Three bond gHMBC correlations from H-9, H-12a and H-12b allowed us to assign C-14 (δ_C 53.3), while a two bond gHMBC correlation from H-12a and H-12b to a quaternary carbon as well as three bond gHMBC correlations from

H-11a and H-11b to the same quaternary carbon, allowed us to assign C-13 (δ_C 159.4). A two bond gHMBC correlation (Figure 6.3) from H-15 (δ_H 5.60) to C-13 allowed us to place the unsaturated ester moiety at this position, which was subsequently confirmed by gHMBC correlations from H-12a, H-12b, H-14a (δ_H 2.05) and H-14b (δ_H 2.20) to C-15. The quaternary C-8 (δ_C 73.9) was assigned on the basis of gHMBC correlations from H-6a (δ_H 1.40), H-7a, (δ_H 1.44), H-7b (δ_H 1.75), H-9, H-11a, H-11b and H-14b. Crystallization of **5.49** from ether produced crystals suitable for X-ray diffraction analysis (Figure 6.4) and indirectly confirmed the *Si*-facial selectivity of the Grignard reaction in the synthesis of **5.51** (*vide supra*), the β-axial orientation of the C-8 hydroxyl functionality, and hence the *Re*-facial selectivity of the intramolecular aldol condensation reaction in both **5.49** and **5.51**. The structure of **5.49** was therefore unequivocally established as 17-norabiet-13(15)-*E*-en-8β-ol-16-oate. Norditerpenes **5.49** and **5.50** were assigned to the abietane series because the C_2 substituent at C-13 (*i.e.* the $\Delta^{13(15)}$ olefin) had neither a *syn* nor *anti* relationship with the angular methyl group at C-10 required for membership to either the pimarane or isopimarane diterpene series respectively.[226]

A cursory comparison of the ^{1}H and ^{13}C NMR spectra of **5.50** and **5.49** revealed these two compounds to be structurally similar. The only major differences in the ^{13}C NMR spectra of **5.49** and **5.50** were the chemical shifts of C-12 (δ_C 29.6 and 37.9) and C-14 (δ_C 53.3 and 45.3) respectively, which we attributed to **5.49** and **5.50** being $\Delta^{13(15)}$ isomers of each another. The HRFAB mass data of the two compounds were also identical, further confirming this assessment.

Table 6.1 The ^{1}H (400 MHz), ^{13}C (100 MHz), gHMBC and gCOSY data ($CDCl_3$) of **5.49**.

Position	δ_C (mult)	δ_C (Int., Mult, *J*/Hz)	gHMBC	gCOSY
1a	39.7 (t)	0.87 (1H, m)	2, 10, 20	1b, 2
1b		1.67 (1H, m)	2, 3	1a, 2
2a	18.4 (t)	1.38(1H, m)	1	1a, 1b
2b		1.59 (1H, m)	1	1a, 1b
3a	42.1 (t)	1.14 (1H, m)	1, 2, 3, 6, 19	2, 3b
3b		1.39 (1H, m)	4, 5	2a
4	33.3 (s)	-	-	-
5	56.3 (d)	0.91 (1H, d, 3.5)	1, 4, 6, 7, 9, 10, 20	6
6a	18.3 (t)	1.40 (1H, m)	3, 4, 5, 7, 8, 10	5, 7b
6b		1.58 (1H, m)	3, 4, 7, 8, 10	5, 7b
7a	41.5 (t)	1.44 (1H, m)	5, 8	7b
7b		1.75 (1H, m)	5, 6, 8	6, 7a
8	73.9 (s)	-	-	-
9	56.4 (d)	1.17 (1H, m)	5, 8, 10, 11, 12, 14, 20	11a, 11b
10	37.4 (s)	-	-	-
11	22.4 (t)	1.43 (1H, m)	8, 9, 12	11b, 12a, 12b
		1.79 (1H, m)	8, 9, 12, 13, 15	11a, 12a, 12b
12	29.6 (t)	1.76 (1H, m)	9, 11, 13, 15	11a, 11b, 12b,
		3.92 (1H, m)	9, 11, 13, 14, 15	11a, 11b, 12a
13	159.4 (s)	-	-	-
14	53.3 (t)	2.05 (1H, dd, 13.1, 2.3)	7, 8, 9, 12, 13, 15	14b
		2.20 (1H, ddd, 13.1, 1.6, 0.7)	7, 8, 9, 12, 13, 15	14a
15	116.1 (d)	5.60 (1H, t, 1.4)	12, 13, 14, 16	14a
16	166.3 (s)	-	-	-
17	-	-	-	-
18	33.6 (q)	0.87 (3H, s)	3, 4, 5, 19	-
19	21.7 (q)	0.84 (3H, s)	4, 3, 5, 18	-
20	15.4 (q)	0.94 (3H, s)	1, 9, 10	-
-O*CH*$_2$CH$_3$	59.6 (t)	4.13 (2H, q, 7.1)	15, -OCH$_2$*C*H$_3$	-OCH$_2$*CH*$_3$
-OCH$_2$*CH*$_3$	14.3 (q)	1.26 (3H, t, 7.1)	-O*C*H$_2$CH$_3$	-O*CH*$_2$CH$_3$

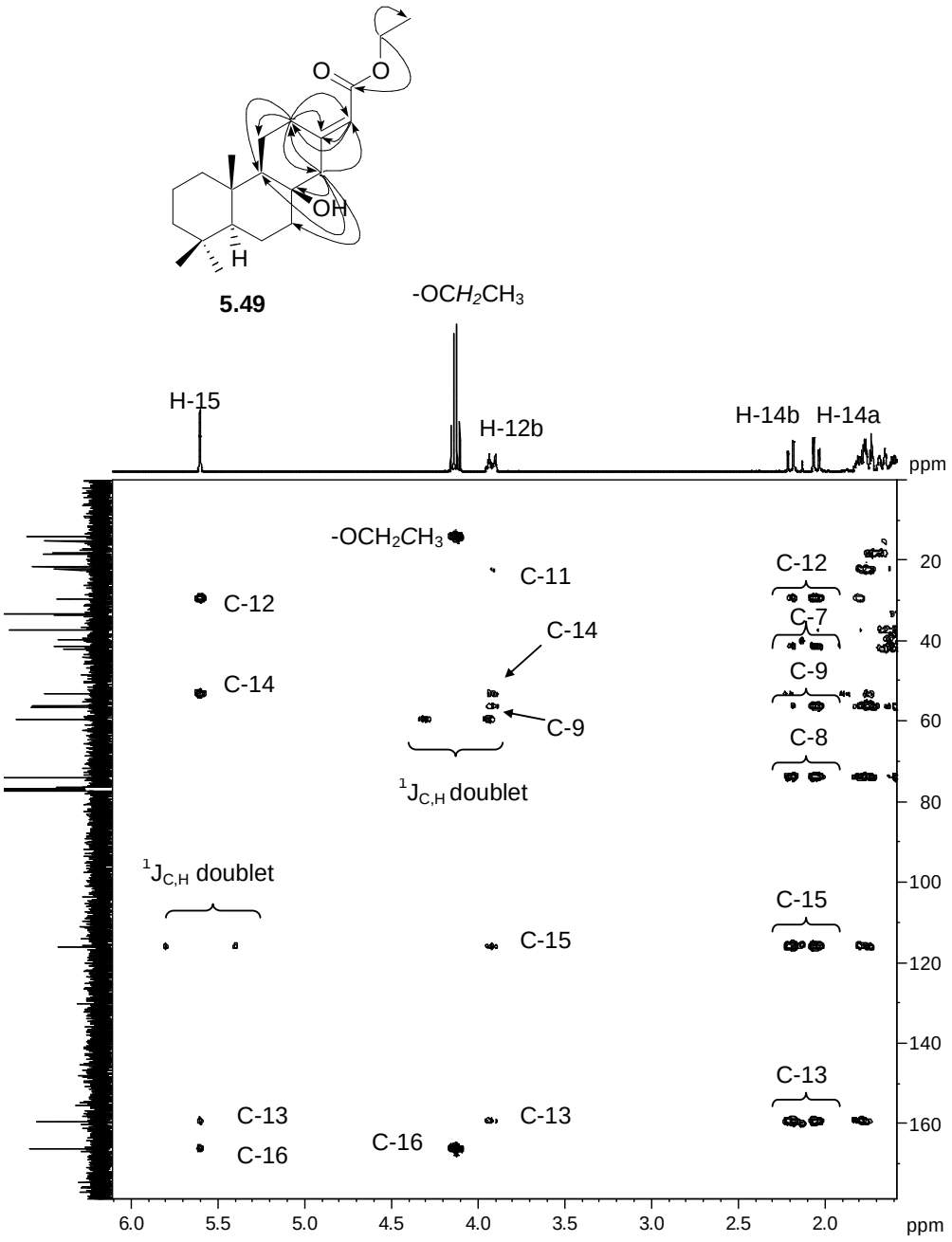

Figure 6.3 Downfield section (F1 = δ_C 0 – 180; F2 = δ_H 1.5 – 6.0) of the gHMBC spectrum (400 MHz, $CDCl_3$) of **5.49**. The accompanying structure summarizes the gHMBC correlations indicated in the spectrum. (Reference for $^1J_{C,H}$ doublets).[227]

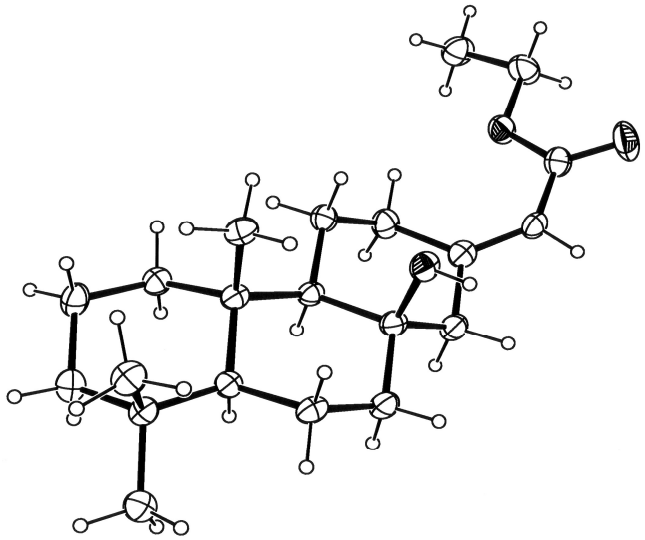

Figure 6.4 A view of a molecule of ethyl 17-*nor*abiet-13(15)-*E*-en-8β-ol-16-oate (**5.49**) from the crystal structure.

In an attempt to save time and circumvent the problems associated with the facile degradation of **5.51**, we also attempted a one-pot cyclization and HWE reaction on **5.51**. Accordingly, **5.51** was prepared in the standard manner and once all starting material was consumed (monitored by TLC), the deprotonated HWE reagent was added drop wise to the reaction mixture *via* a cannula. After the standard workup and purification by semi-preparative HPLC (10% ethyl acetate, 90% hexane), we observed both a reduction in overall yield of the two geometric isomers, **5.49** and **5.50** (32% as opposed to 70% by the previous method) and, curiously, a change in the *E*/*Z* ratio (2:1 as opposed to 4:3). Subsequent reattempts at improving the yields from the one pot reaction were unsuccessful, but on one occasion a minor crystalline compound, **6.6**, was isolated from the reaction mixture in low yield (10%).

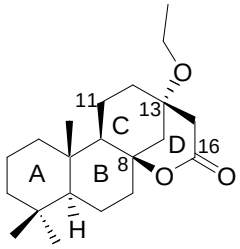

6.6

The molecular formula ($C_{21}H_{34}O_3$) of **6.6** was established by HRFABMS and implied five degrees of unsaturation, only one of which could be accounted for by an unsaturated functionality *i.e.* carbonyl resonance (δ_C 170.7). Comparison of the ^{1}H and ^{13}C NMR spectra of **6.6** with those of **5.49** and **5.50** suggested that **6.6** shared a similar tricyclic norditerpene skeleton, accounting for three degrees of unsaturation, and initially indicating that differences between **6.6** and **5.49** were confined to the substitution pattern around ring C and the presence of an additional ring. Further analysis of ^{1}H, ^{13}C and DEPT135 NMR spectra revealed the presence of four methyls (δ_C 33.6, 21.7, 16.0 and 14.8), nine methylenes, one oxymethylene, two methine, four quaternary carbons and one carbonyl functionality. A combination of gHSQC data and gCOSY correlations between H-9 (δ_H 1.06) and H-11a (δ_H 1.20) and H-11b (δ_H 1.80) allowed us to assign C-11 (δ_C 18.6) from gHSQC correlations. We similarly assigned C-12 (δ_C 35.6) from gCOSY correlations between H-11a and H-11b and H-12a (δ_H 1.57) and H-12b (δ_H 1.94). A three bond gHMBC correlation from H-11b allowed us to assign the quaternary C-8 resonance (δ_C 83.0), the deshielded nature of which implied oxygenation at this centre. The assignment of C-8 was confirmed by a two bond correlation from H-7a (δ_H 1.52) and H-7b (δ_H 1.96), The upfield shift of H_3-20 (δ_H 0.94) suggested an axial oxygenated moiety at C-8.[171] A further three bond gHMBC correlation from H-11b allowed us to assign quaternary C-13 (δ_C 71.6), and this assignment was further supported by gHMBC correlations from H-12a and H-12b to C-13. A two bond gHMBC correlation (Figure 6.5) from the oxymethylene protons (δ_H 3.44 and δ_H 3.45) of an ethoxy functionality also allowed us to place this moiety at C-13. Three bond gHMBC correlations (Figure 6.5) between H-12b and H-9 (δ_H 1.06) to a further methylene carbon resonance (δ_C 44.4) enabled the assignment of this carbon as C-14. Three bond gHMBC correlations from the two protons (δ_H 2.58 and 2.66) of a methylene carbon (δ_C 41.1) to both C-12 and C-14 allowed us to assign C-15. Confirmation of the assignment of C-14 was given by gHMBC correlations from both H-14a (δ_H 1.67) and H-14b (δ_H 1.75) to C-8 and C-9. A two bond gHMBC correlation from H-15a (δ_H 2.58) and H-15b (δ_H 2.66) to a shielded carbonyl functionality (δ_C 170.7) provided the assignment of C-16 as part of a lactone ring, which thus accounted for the fourth ring. A lactone ring also explained the deshielded nature of C-8 (δ_C 83.0), which was greater than

that expected when a tertiary alcohol was present at this carbon (*i.e.* 73.9, see Table 6.1). The fully assigned ^{1}H and ^{13}C NMR data for **6.6** are presented in Table 6.2.

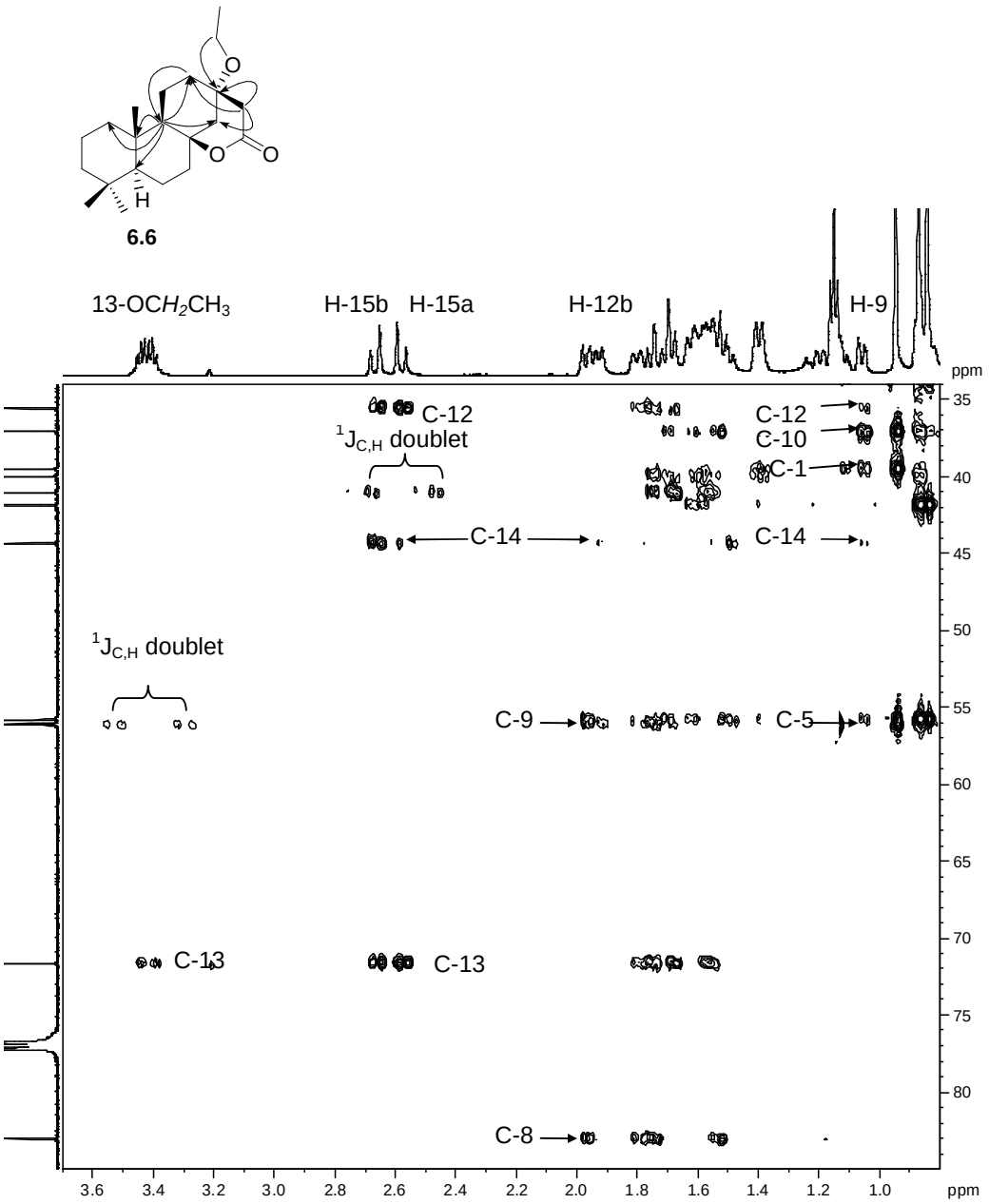

Figure 6.5 A section (F1 = δ_C 34 – 85; F2 = δ_H 0.8 – 3.7) of the gHMBC spectrum (600 MHz, $CDCl_3$) of **6.6**. The accompanying structure shows the key correlations indicated in the spectrum.

Table 6.2 ^{1}H (600 MHz), ^{13}C (150 MHz), gCOSY and gHMBC NMR data for **6.6** in $CDCl_3$.

Position	δ_C (mult)	δ_H (int., mult., J/Hz)	gHMBC	gCOSY
1a	39.5 (t)	0.85 (1H, m)	2, 10, 20	1b, 2a
1b		1.62 (1H, m)	2	1a, 2a, 2b
2a	18.4 (t)	1.39 (1H, m)	1, 3, 4, 10	1a, 2b, 3a
2b		1.60 (1H, m)	1, 3	1a, 2a, 2b, 3b
3a	41.9 (t)	1.12 (1H, m)	2, 3, 18	2a, 2b, 3b
3b		1.40 (1H, m)	1, 2, 4, 10	2b, 3a
4	33.2 (s)	-	-	-
5	55.8 (d)	0.87 (1H, dd, 12.2, 1.9)	6, 10	6
6a	17.7 (t)	1.54 (1H, m)	7	5, 7b
6b		1.70 (1H, m)	†	†
7a	40.0 (t)	1.52 (1H, m)	6, 8, 9, 13	7b
7b		1.96 (1H, m)	5, 6, 8, 13	6, 7a
8	83.0 (s)	-	-	-
9	56.1 (d)	1.06 (1H, dd, 12.5, 3.9)	1, 10, 11, 12, 14	11a, 11b
10	37.1 (s)	-	-	-
11a	18.6 (t)	1.20 (1H, m)	10, 12	11b, 12a, 12b
11b		1.80 (1H, m)	8, 9, 13	11a, 12a
12a	35.6 (t)	1.57 (1H, m)	13, 15	11a, 11b, 12b, 15a‡
12b		1.94 (1H, m)	9, 13, 14	11a, 12b
13	71.6 (s)	-	-	-
14a	44.4 (t)	1.67 (1H, dd, 12.8, 2.4)	8, 9, 13, 15	14b, 15b
14b		1.75 (1H, dd 12.8, 3.0)	8, 9, 13, 15	14a
15a	41.1 (t)	2.58 (1H, dd, 18.0, 1.8)	12, 13, 14, 16	12a‡, 15b
15b		2.66 (1H, dd, 18.0, 2.3)	12, 13, 14, 16	15a
16	170.7 (s)	-	-	-
17	-	-	-	-
18	33.6 (q)	0.87 (3H, s)	3, 4, 5, 19	-
19	21.7 (q)	0.84 (3H, s)	3, 4, 5, 19	-
20	14.8 (q)	0.94 (3H, s)	9, 10, 18	-
-O*C*H_2CH$_3$	56.2 (t)	3.44 (1H, q, 8.5)	-OCH$_2$*C*H$_3$, 13	-OCH$_2$C*H*$_3$
		3.45 (1H, q, 7.0)	-OCH$_2$*C*H$_3$, 13	-OCH$_2$C*H*$_3$
-OCH$_2$*C*H_3	16.0 (q)	1.15 (3H, t, 7.0)	-O*C*H$_2$CH$_3$	-O*C*H_2CH$_3$

† No correlations detected; ‡ W coupling

Final confirmation of the structure of **6.6** as 17-norpimaran-13α-ethoxy-8,16-olactone was provided by X-ray analysis of a single crystal of this compound (crystallized from hexane, Figure 6.6). The two independent molecules A and B in the asymmetric unit adopt essentially the same conformation except for the slightly different orientation of the ethoxy groups. A putative mechanism for the formation of **6.6** from **5.31** during the HWE reaction is presented in Scheme 6.2.

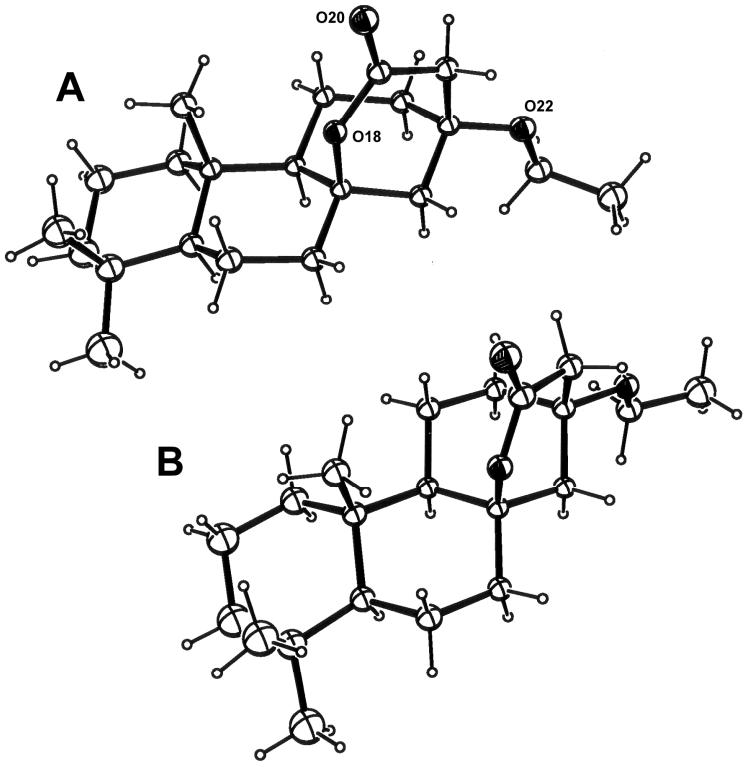

Figure 6.6 Perspective view of the two molecules of 17-norpimaran-13α-ethoxy-8,16-olactone, **6.6**, comprising the crystallographic asymmetric unit.

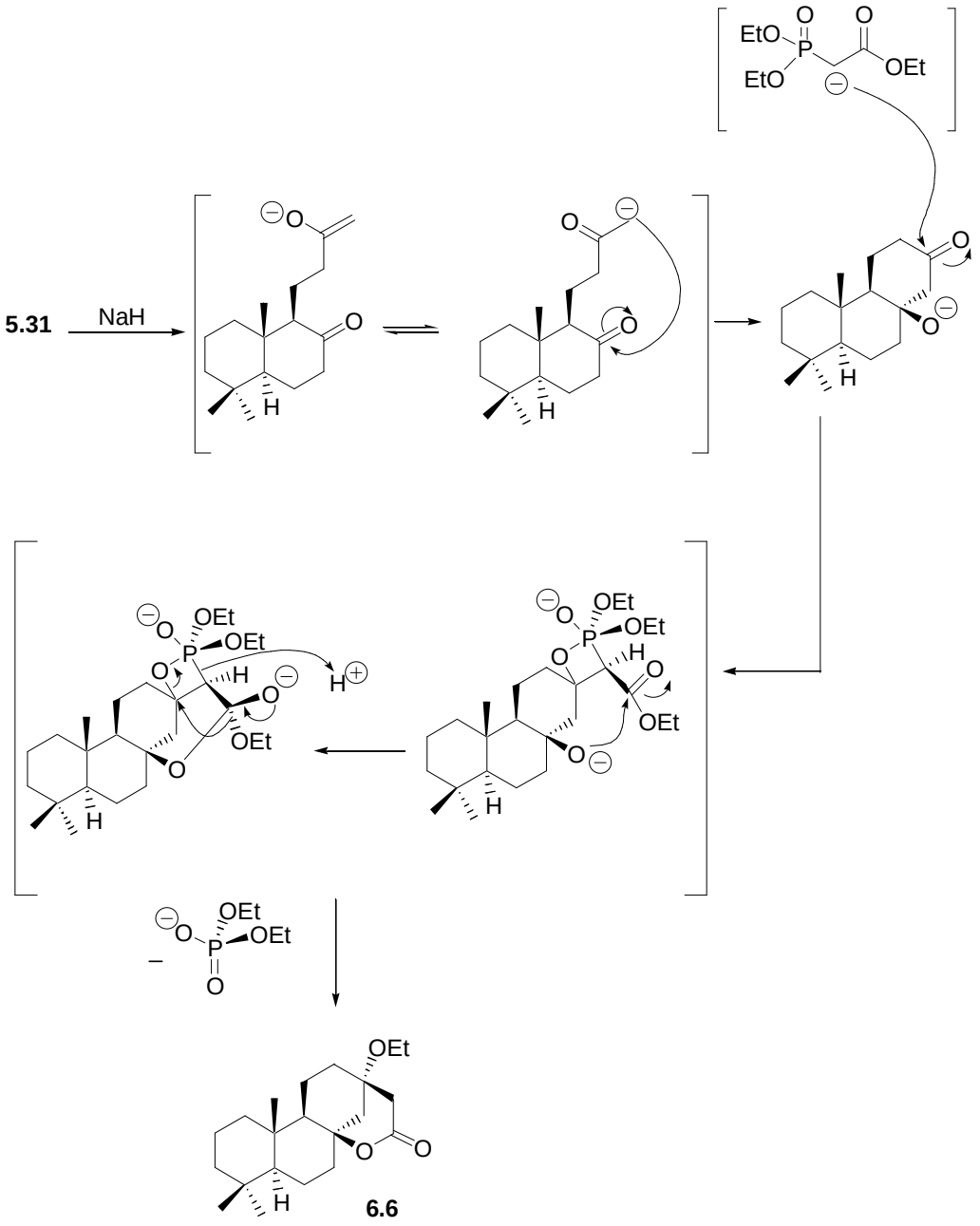

Scheme 6.2 Putative mechanism for the formation of **6.6** from **5.31** during the HWE reaction.

In the original publication that prompted the research described in this chapter, Jaroszewski and co-workers[213;214] suggest that compounds with polar functionalities concentrated on one side (ring A in their case) of the molecule initiated changes to the shape of the erythrocyte. Since we wished to further investigate the structure-activity relationships using analogous compounds, we decided to reduce the ethyl esters **5.49** and **5.50** with lithium aluminium

hydride to determine if a similar trend was evident in our compounds when a polar substituent was situated at C-8 instead of C-3. Accordingly, we simultaneously reduced the *E* and *Z* ethyl esters **5.49** and **5.50** with lithium aluminium hydride in tetrahydrofuran in separate reaction vessels but under the same conditions. Upon workup and subsequent normal phase semi-preparative HPLC (100% ethyl acetate) of the respective reduction mixtures of **5.49** and **5.50**, it was immediately apparent from the HPLC chromatogram that while the reduction of the *E* ethyl ester **5.49** yielded a single product, 17-norisopimarane-8β-16-diol (**6.8**), the reduction of the *Z* ethyl ester **5.50** yielded two products, 17-norabietane-13(15)-ene-8β,16-diol (**6.9**) and **6.8**.

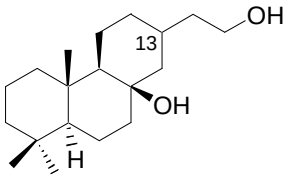

6.8

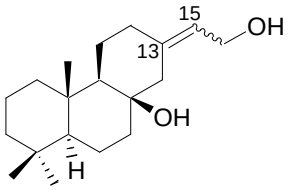

6.9 $\Delta^{13(15)}$ Z
6.22 $\Delta^{13(15)}$ *E*

Comparison of the ^{1}H and ^{13}C spectra of the reduction product **6.8** with those of the parent compound **5.49** revealed that the olefinic resonances (δ_H 5.60, δ_C 159.4 and δ_C 116.1) had disappeared, while an additional oxymethylene (δ_C 60.3) and methylene carbon (δ_C 40.4) evident in the DEPT135 spectrum, indicated that not only had the ethyl ester been reduced to a primary alcohol as expected, but an unexpected 1,4-Michael addition of hydride to the exocyclic olefin had also occurred. The molecular formula ($C_{19}H_{34}O_2$) of **6.8** was established by HRFABMS and confirmed the proposed tricyclic structure. Extensive overlap of the resonances (in both deuterated chloroform and benzene) in the methyl envelope of the ^{1}H NMR spectrum (Figure 6.7) of **6.8** prevented us from determining the configuration at C-13 by spectral means. However, scrutiny of the ^{13}C NMR spectrum of **6.8** (Figure 6.8) revealed no doubling of the ^{13}C resonances expected from a mixture of diastereomers and this information, coupled with the single peak in the HPLC chromatogram of **6.8** lead us to conclude that only one C-13 epimer had formed. It should be reiterated that this 1,4-hydride addition was unexpected as the hydride ion is an example of a hard nucleophile and would

thus be expected to react preferentially with the carbonyl functionality (a hard electrophile), yielding a product such as (**6.22**).[228]

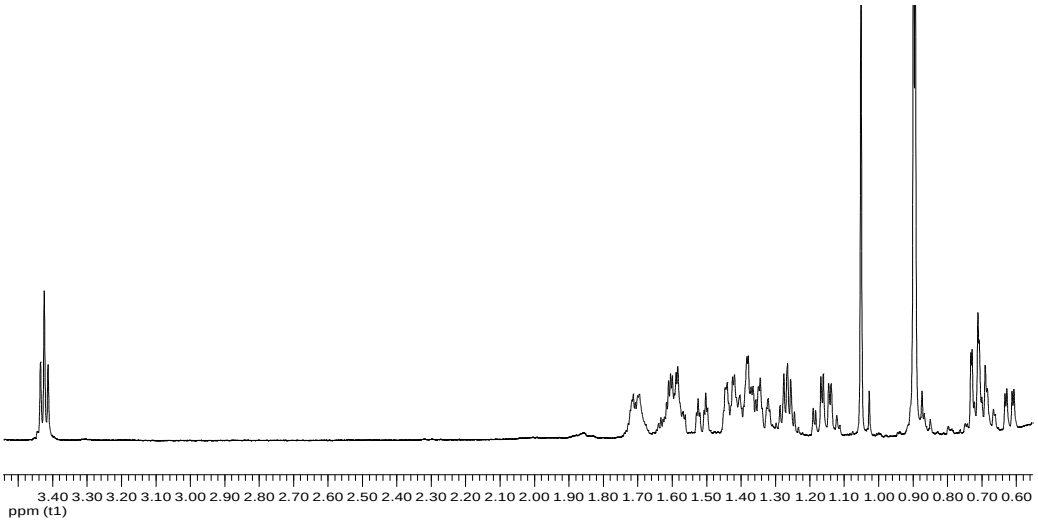

Figure 6.7 The ^{1}H NMR (600 MHz, C_6D_6) spectrum of **6.8**.

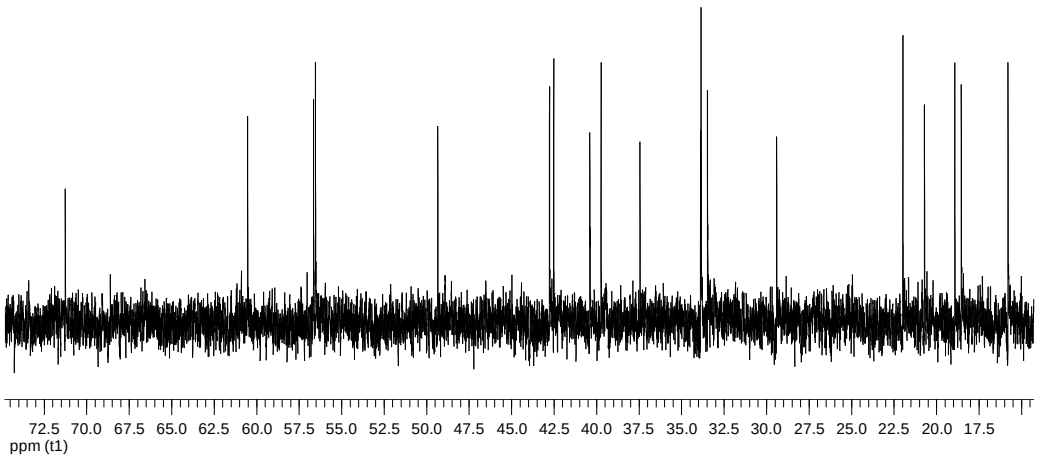

Figure 6.8 The ^{13}C NMR (150 MHz, C_6D_6) spectrum of **6.8**.

A cursory examination of the ^{1}H and ^{13}C NMR spectrum of one of the products from the lithium aluminium hydride reduction of **5.50** revealed it to be identical in all respects to **6.8**. The ^{1}H and ^{13}C NMR spectra of a second product from the reduction of **5.50** revealed that, while the

ethyl ester [δ_H 4.12 and 1.25; δ_C 167.2 (s), 59.7 (t) and 14.3 (q)] resonances had disappeared, the olefinic resonances [δ_H 5.65, δ_C 142.1 (s) and 123.5 (d)] had been retained. The appearance of additional oxymethylene resonances (δ_H 4.12 and 3.92 and δ_C 57.5) in the ^{1}H and ^{13}C NMR spectrum suggested that **6.9** was the expected reduction product of **5.50**. Final confirmation of the 17-norabiet-13(15)-ene-8β,15-diol structure of **6.9** was provided by the molecular formula ($C_{19}H_{32}O_2$) established from HRFABMS data.

6.3 The anti-plasmodial activity of the tricyclic norditerpenes

In continuation of our ongoing research on the activity of tricyclic norditerpenes against *P. falciparum* parasites and our interest in a possible correlation between this activity and echinocytic and stomatocytic erythrocyte membrane modifying effects, semi-synthetic analogues **5.49**-**5.50** and **6.6**-**6.9** were sent to the Division of Pharmacology, University of Cape Town (UCT), where they were assayed for both parasite inhibitory and haemolytic properties (results provided in Table 6.3). The inhibition studies were performed by transferring parasite-infected erythrocytes to microtitre plates and treating these with varying concentrations of the semi-synthetic compounds, using chloroquine as a control. After incubating the cells at 37℃ for forty eight hours, parasite viability was measured by determining parasite lactate dehydrogenase activity, relative to solvent controls (wells containing 0.5% DMSO). The haemolytic activity of the tricyclic norditerpenes was determined relative to uninfected cells, which had also been incubated for forty eight hours and measured by determining the absorbance at 405 nm, relative to saponin treated wells, used as 100% haemolysis controls. Changes in the erythrocyte shape were monitored by both light and phase contrast microscopy. The shape changing effects of the tricyclic norditerpenes on erythrocytes at sub-haemolytic concentrations were monitored by incubating erythrocytes in the presence of the norditerpenes at 100, 50 or 25 μgmL^{-1} for forty eight hours and were then assessed by light microscopy.

Table 6.3 Parasite-inhibitory and haemolytic properties of **5.49**-**5.50** and **6.6**-**6.9** compared to chloroquine (CQ, **6.10**).

	5.49	**5.50**	**6.6**	**6.7**	**6.8**	**6.9**	**CQ**
IC50 (μgmL^{-1}) ± SD[†]	5.7 ±4.6	3.9 ±1.2	19.6 ±6.6	10.7 ±5.3	13.3 ±5.1	10.6 ±3.3	0.0103 ±0.0023
% Haemolysis[‡] 200 μgmL^{-1}	17	34	0	0.2	5	102	ND
% Haemolysis 100 μgmL^{-1}	3	9	0	0.6	0	2	ND
% Stomatocytes[§] 100 μgmL^{-1}	8	17[⊥]	0	1	3	64	ND
% Echinocytes 100 μgmL^{-1}	0	0	9	2	2	0	ND
% Stomatocytes 50 μgmL^{-1}	2	11	1	1	1	5	ND
% Echinocytes 50 μgmL^{-1}	2	0	2	3	3	1	ND

[†]Mean IC_{50} values and standard deviations (SD) were derived from IC_{50} determinations carried out on four separate occasions for **5.49**-**5.50** and **6.6**-**6.9** and on three occasions for chloroquine (CQ). [‡]Percentage haemolysis was calculated relative to that obtained with 0.2% saponin. [§]The percentages of malformed erythrocytes (stomatocytes and echinocytes) present in erythrocyte samples incubated with the various compounds for forty eight hours are also indicated. [⊥]Mixture of knizocytes and stomatocytes. ND = not determined.

Jaroszewski and coworkers[213;214;229;230] had proposed that the apparent activity of many natural products and synthetic compounds e.g. **6.2**-**6.5** could be linked to the incorporation of these compounds into the erythrocyte membrane, which in turn caused shape changes in the erythrocyte. Such shape changes disrupted erythrocyte function and therefore the inhibition of parasite growth subsequently observed was not a reflection of compound toxicity, but rather a measure of the destruction of the parasites' host cell. Compounds that ultimately destroy erythrocytes cannot be considered true anti-malarial agents. After structure activity studies of six betulinic acid analogues,[230] **6.23**-**6.28**, they determined that **6.23**-**6.25** with hydrogen donating functional groups (-CO_2H, -CH_2OH and -$CONH_2$) caused the erythrocytes to

transform into echinocytes, while analogues **6.26**-**6.28** (containing -CHO, -Me and -CO_2Me functional groups) caused stomatocytes to form. Jaroszewski and coworkers subsequently concluded that in both cases the "anti-malarial" activity of these compounds could be ascribed to the shape changes induced in the erythrocyte host at subhaemolytic concentrations.

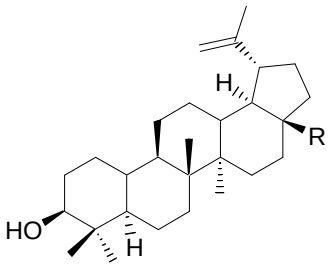

6.23 R = CO_2H
6.24 R = CH_2OH
6.25 R = $CONH_2$
6.26 R = CHO
6.27 R = Me
6.28 R = CO_2Me

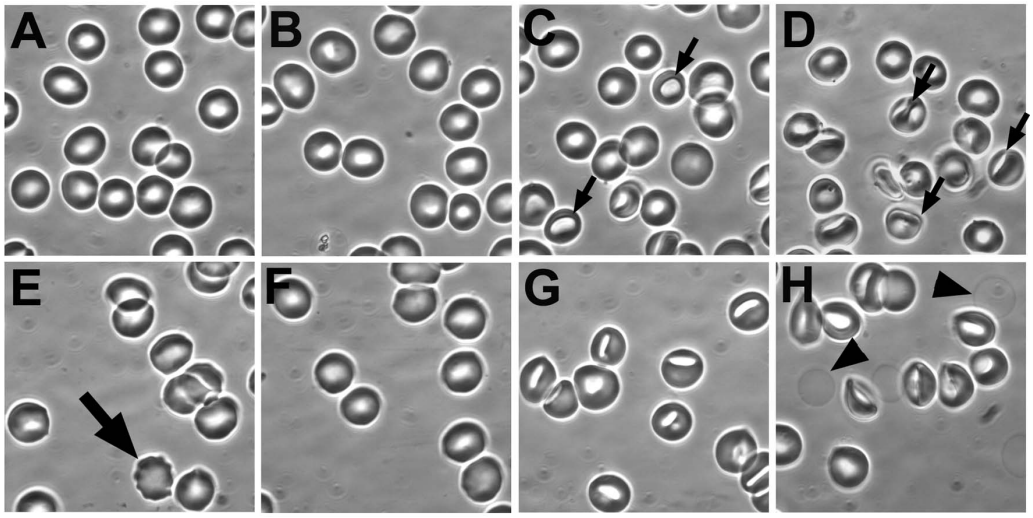

Figure 6.9 Phase-contrast micrograph of erythrocytes incubated with medium alone (A) or 100 μgmL^{-1} of compounds **6.6** (B), **5.49** (C), **5.50** (D), **6.6** (E), **6.8** (F) and **6.9** (G, H). Small arrows indicate type II stomatocytes in C and knizocytes in D. The large arrow denotes a type I echinocyte in E, and arrowheads in H indicate erythrocyte ghosts.

Three of our semi-synthetic compounds, **5.49**, **5.50** and **6.9**, showed haemolytic activity similar to that observed by Jaroszewski and coworkers at concentrations in the 100–200

μgmL^{-1} range (Table 6.3), suggesting that these compounds may accumulate in the erythrocyte bilayer. Haemolysis was negligible in this concentration range for compounds **6.6**-**6.8**. At a concentration of 100 μgmL^{-1}, **6.9**, the most haemolytic compound, induced the formation of stomatocyte type III shapes (Table 6.9, Figures 6.9G, 6.9H), despite possessing the -CH_2OH functionality that Jaroszewski and coworkers[230] had suggested was responsible for echinocytic shape changes. Interestingly, occasional erythrocyte ghosts were also present in the culture containing **6.9** (Figures 6.9G and 6.9H). The second most haemolytic compound, **5.50**, caused a mixture of knizocytes and type III stomatocytes to form (Table 6.3, Figure 6.9D) at the 100 μgmL^{-1} level, and only a small number of type II stomatocytes formed when incubated with **5.49** (Figure 6.9C). Only a modest increase in type I echinocytes was found for **6.6** (Table 6.3, Figure 6.9E), since control cultures contained 3-4% echinocytes, while the remaining compounds **6.7** and **6.8** displayed neither significant haemolytic effects nor erythrocyte shape modification effects. Although the compounds with the highest haemolytic effects (**5.49**, **5.50** and **6.9**) had the lowest IC_{50} values, and those with negligible haemolytic and erythrocyte shape changing effects (**6.6**-**6.8**) had the highest IC_{50} values (Table 6.3), it could be argued that the parasite inhibitory activity of the latter three compounds was not a consequence of erythrocyte shape changes. It may therefore tentatively be concluded that compounds **6.6**-**6.8** potentially affect either a parasite-specific target, or may possibly bind to the erythrocyte membrane at sub-haemolytic concentrations and somehow compromise the function of the erythrocyte and hence parasite viability. In the intra-erythrocytic development stages of the malarial parasites, a decrease in membrane deformability has been reported and linked to the release of several parasite proteins and their interaction with the erythrocyte plasma cell membrane and sub-membranous protein skeleton, resulting in a modification of cell function and structure.[231] During the early stages (*i.e.* the first twenty four hours), erythrocytes maintain their usual biconcave shape, permitting normal circulation in the blood stream, while in the final forty eight hours, the deformation of erythrocyte cell membranes is decreased and the erythrocytes adhere to other cells to allow microvascular sequestration into the post-capillary venules of various organs.[231-233] It is thus possible that the binding of **6.6**-**6.8** to the erythrocyte cell membrane interferes with the interaction of the parasite proteins with this membrane and prevents this stage of the parasite

lifecycle from being successfully completed. Further studies focused on the binding of compounds **6.7**-**6.8** binding to the erythrocyte cell membrane could thus possibly better allow us to understand the mode of action of these three norditerpenes.

6.4 Conclusions

Six analogues (**5.49**-**5.50** and **6.6**-**6.9**) of naturally occurring tricyclic norditerpenes (**6.1-6.5**) with anti-plasmodial activity were semi-synthesized from commercially available **5.3** *via* the common intermediate, **5.51**. Norditerpenes **5.49** and **5.50** had previously been isolated as minor components of an HWE reaction on **5.31**, and the combined yield of these compounds was increased to 70% through first performing an intramolecular aldol condensation of **5.31** to **5.51** before reacting with the HWE reagent. Since **5.51** was unstable, a one pot cyclization-HWE was attempted but resulted in reduced yields (32%) of **5.49** and **5.50** and a change in the *E*/*Z* ratio from 4:3 (from the two step reaction) to 2:1 (in the one-pot reaction). On one occasion **6.6** was isolated as a minor product from the one pot reaction. X-ray diffraction analysis of **5.49** and **6.6** established the absolute configuration of these norditerpenes, and by extrapolation the *Re*-facial selectivity of the intramolecular aldol condensation of **5.31**. Lithium aluminium hydride reduction of **5.49** exclusively yielded the unexpected 1,4-hydride addition product, **6.8**, while simultaneous reduction of **5.50** under identical reaction conditions yielded both **6.9** and **6.8**. Reacting **5.51** with vinyl magnesium bromide afforded the final analogue, **6.7**.

Tricyclic norditerpenes **5.49**-**5.50** and **6.6**-**6.9** were screened for anti-plasmodial activity and exhibited IC_{50} values in the concentration range of 3.9-19.6 μgmL^{-1}. Compounds **5.49**, **5.50** and **6.9** caused haemolysis over a range of concentrations (100-200 μgmL^{-1}) and also erythrocyte shape changes. Compounds **6.6**-**6.8** had the highest IC_{50} values but induced little to no haemolysis or erythrocyte shape changes. Further investigations should be performed to determine whether the binding of these compounds at concentrations too low to induce erythrocyte shape changes compromises erythrocyte function and hence parasite viability or whether these compounds affect a parasite-specific target.

Chapter Seven

Experimental

7.1 General experimental procedures

7.1.1 Analytical

Melting points were determined using a Reichert hot-stage microscope and are uncorrected. Optical rotations were measured on a Perkin-Elmer 141 polarimeter calibrated at the sodium-D line (589 nm) and the concentration of solutions used is expressed in g/100 mL. Circular dichroism spectra were collected on a Jasco J720 spectropolarimeter in MeOH by Ms. L. Cartner of the Natural Products Chemistry Group, National Cancer Institute, Frederick, United States of America. Infrared spectra were recorded on a Perkin-Elmer Spectrum 2000 FT-IR spectrometer with compounds as films (neat) on NaCl disks. NMR spectra were acquired on Bruker 400 MHz Avance and 600 MHz Avance II spectrometers using standard pulse sequences. Chemical shifts are reported in ppm, referenced to residual solvent resonances ($CDCl_3$ δ_H 7.25, δ_C 77.2, C_6D_6 δ_H 7.15, δ_C 128.0) Coupling constants are reported in Hz directly from the NMR spectra and corresponding coupling constants have not been matched. Low resolution mass spectra were recorded on a Finnigan GCQ spectrometer at 70 eV. High resolution fast atom bombardment mass spectra (Micromass 70-70E spectrometer) were obtained by Prof. L. Fourie of the Mass Spectrometry Unit, Northwest University, Potchefstroom, South Africa.

7.1.2 Chromatography

General laboratory solvents were distilled from glass before use. Analytical normal phase thin layer chromatography was performed on DC-Plastiekfolien Kieselgel 60 RP18 F_{254} plates. Plates were viewed under UV light (254 nm) and developed either with I_2 or by spraying with 10% H_2SO_4 in MeOH followed by heating. HP-20 beads used were manufactured by Diaion and supplied by Supelco. Open column chromatography was performed using Machery-Nagel Chroma-Bond OH Diol (0.45 μm) and flash chromatography was performed using Kieselgel 60 (230-400 mesh) silica gel. Normal phase semi-preparative HPLC separations were performed on a Whatman Magnum 9 Partisil 10 column using a Spectra-Physics Spectra-

Series P100 isocratic pump and a Waters 410 Differential Refractometer. Diol semi-preparative HPLC separations were performed on a Machery-Nagel VP 250/10 Nucleosil 100-7 OH column using a Spectra-Physics Spectra-Series P100 isocratic pump and a Waters 410 Differential Refractometer.

7.1.3 Synthesis

All reactions requiring anhydrous conditions were conducted in flame-dried apparatus either under a dry argon atmosphere or using an anhydrous calcium chloride drying tube. Dry solvents were prepared by standard procedures as described by Perrin and Amarego[234] and stored over the appropriate drying agent under an atmosphere of dry nitrogen. Immediately prior to their use in anhydrous reactions, Et_2O, THF and C_6H_6 were distilled from Na/benzophenone ketyl, while CH_2Cl_2, CH_3CN and Et_3N were distilled from calcium hydride. DMSO was distilled at reduced pressure from calcium hydride and stored over 4Å molecular sieves under nitrogen. Organic extracts were dried over anhydrous $MgSO_4$. All reactions were magnetically stirred.

7.1.4 Molecular modelling

Molecular modelling was performed using the Cerius^2 (version 4.5) software package developed by BIOSYMM/Molecular Simulations Inc. running on a Unix-based platform and using the default Universal Force Field.[235] Charges were included *via* the charge equilibration method[236] by applying the Qeq_charged 1.0 parameter set. The local minimum conformer was then subjected to a molecular dynamics routine (constant n, V, E) of 500 annealing cycles (300 to 500 K). The lowest energy conformer was then selected and transferred to the MaterialsStudio 2.2 package of Accelrys Inc., on Linux-based Pentium IV computers where it was optimized and subjected to full frequency analysis (zero imaginary frequencies) in DMol^3 (Accelrys Inc.) using the PW91 functional with the double numeric and polarization (DNP) basis set.

7.2 Chapter Two Experimental

7.2.1 Collection and extraction

A single yellow nudibranch specimen (6 x 8 cm) was dredged from a depth of 115m near Marion Island (46° 52' S, 37° 54'E) during early Au tumn, 2005 and immediately frozen and stored at -20℃ until it could be transferred to Me_2CO (250 mL). The nudibranch was exhaustively extracted with Me_2CO and the extracts combined. The Me_2CO extract was subjected to HP-20 and open column Diol chromatography, followed by normal phase semi-preparative HPLC (as described by Scheme 2.5 and Chapter Two Sections 2.4 and 2.5) to afford 12*S*,13*R*,14*S*-isocopalan-13-ol-12,14-diacetate (**2.1**, 3 mg), 3-(14*S*)-isocopal-12-ene-15-oyl-1-acetyl-*sn*-glycerol (**2.2**, 29 mg) and 3-(14*S*)-isocopal-12-ene-15-oyl-2-acetyl-*sn*-glycerol (**2.3**, 10 mg).

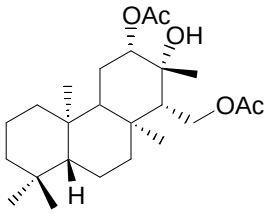

2.1

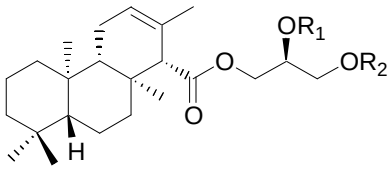

2.2 R_1 = H; R_2 = Ac
2.3 R_1 = Ac; R_2 = H

12S,13R,14S-Isocopalan-13-ol-12,14-diacetate (2.1): yellow oil; $[\alpha]_D^{25}$ +3 (*c* 0.2, $CHCl_3$); ^1H and ^{13}C NMR data, see Table 2.4; HRFABMS *m*/*z* 409.2953 (calcd for $C_{24}H_{41}O_5$ [$(M + H)^+$], 409.2954).

3-(14*S*)-Isocopal-12-ene-15-oyl-1-acetyl-*sn*-glycerol (2.2): yellow oil; $[\alpha]_D^{25}$ +10 (*c* 2.0, $CHCl_3$), lit.[68;83] +13.9, +21.9; $[\theta]_{216}$ 7359, lit.[68] 5412; ^1H and ^{13}C NMR data, see Table 2.1; HRFABMS *m*/*z* 421.2954 (calcd for $C_{25}H_{41}O_5$ [$(M + H)^+$], 421.2954).

3-(14*S*)-Isocopal-12-ene-15-oyl-2-acetyl-*sn*-glycerol (2.3): yellow oil; $[\alpha]_D^{25}$ +23 (*c* 1.0, CHCl3), lit.[68;87] +10.2, +66.9; ^{1}H and ^{13}C NMR data, see Table 2.2; HRFABMS *m*/*z* 421.2956 (calcd for $C_{25}H_{41}O_5$ [(M + H)$^+$], 421.2954).

7.3 Chapter Three Experimental

7.3.1 Collection and extraction

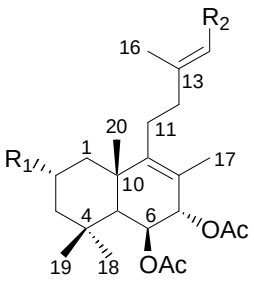

3.1 R_1 = H; R_2= CH_2OH
3.2 R_1 = OAc; R_2= CH_2OH
3.3 R_1 = H; R_2 = CH_2OAc

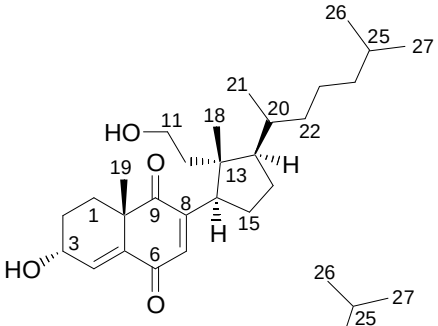

3.4

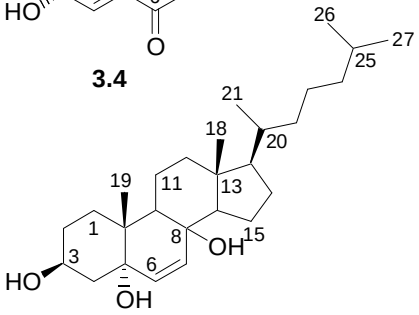

3.5

Two separate collections of *Trimusculus costatus* were made from the densely populated colonies of this mollusc at Cintsa west, South Africa. The first collection was made in May, 2006 and comprised 1274 specimens. The Me_2CO extract was subjected to HP-20 and open column Diol chromatography, followed by normal phase and/or Diol semi-preparative HPLC (as described in Schemes 3.4 and 3.5 and Chapter Three, Section 3.3) to afford 6β,7α-diacetoxylabda-8,13*E*-dien-15-ol (**3.1**, 30 mg), 2α,6β,7α-triacetoxylabda-8,13*E*-dien-15-ol (**3.2**, 41 mg), 6β,7α,15-triacetoxylabda-8,13*E*-diene (**3.3**, 2 mg, 0.002 mg/animal) and 3α,11-dihydroxy-9,11-seco-cholest-4,7-dien-6,9-dione (**3.4**, 122 mg, 0.096 mg/animal). It should be noted that **3.1** and **3.2** were not isolated exhaustively, so the mass per animal is not reported. The second collection was made in May 2007 from the same location, comprised 1658 animals, and was extracted exhaustively with Me_2CO. The Me_2CO extract was subjected to HP-20 and open column Diol chromatography, followed by normal phase and/or Diol semi-

preparative HPLC (as described by Scheme 3.6 and Chapter Three, Section 3.3) to afford **3.4** (303 mg, 0.183 mg/animal) and cholest-7-en-3,5,7-triol (**3.5**, 16 mg, 0.010 mg/animal).

6β,7α-Diacetoxylabda-8,13*E*-dien-15-ol (3.1): pale yellow oil; $[\alpha]_D^{24}$ +93 (*c* 1.6, $CHCl_3$), lit.[10;100] +93; IR (film) ν_{max} 3461, 2924, 2872, 1742, 1365 cm^{-1}; ^1H NMR ($CDCl_3$, 400 MHz) δ 5.43 (1H, dt, *J* = 6.7, 0.9 Hz, H-14), 5.31 (1H, m, H-6), 4.96 (1H, d, *J* = 1.1 Hz, H-7), 4.16 (2H, d, *J* = 6.8 Hz, H_2-15), 2.15 (2H, m, H_2-11), 2.09 (2H, m, H_2-12), 2.07 (3H, s, 7-OAc) 2.02 (6-OAc), 1.81 (1H, ddd, *J* = 12.5, 4.4, 3.4 Hz, H-1b), 1.71 (3H, s, H_3-16), 1.66 (1H, m, H-2b), 1.61 (3H, s, H_3-17), 1.54 (1H, m, H-2a), 1.47 (1H, m, H-5), 1.41 (1H, m, H-3b), 1.27 (3H, s, H_3-20), 1.22 (2H, m, H-1a and H-3a), 0.96 (3H, s, H_3-18), 0.95 (3H, s, H_3-19); ^{13}C NMR ($CDCl_3$, 100 MHz) δ 169.9 (s, 7-OAc), 169.7 (s, 6-OAc), 147.8 (s, C-9), 139.8 (s, C-13), 123.1 (d, C-14), 121.6 (s, C-8), 73.4 (d, C-7), 69.6 (d, C-6), 59.3 (t, C-15), 49.2 (d, C-5), 43.1 (t, C-3), 39.5 (s, C-10), 39.2 (t, C-12), 38.9 (t, C-1), 33.4 (s, C-4), 33.0 (q, C-18), 27.0 (t, C-11), 23.0 (q, C-19), 21.5 (q, 6-OAc), 21.1 (q, 7-OAc), 21.0 (q, C-20), 18.9 (t, C-2), 17.0 (q, C-17), 16.4 (q, C-16); HRFABMS *m/z* 406.2718 (calcd for $C_{24}H_{38}O_5$ [M^+], 406.2719).

2α,6β,7α-Triacetoxylabda-8,13*E*-dien-15-ol (3.2): colourless oil; $[\alpha]_D^{24}$ +60 (*c* 1.7, $CHCl_3$), lit.[10;100] +62; IR (film) ν_{max} 3450, 2942, 2863, 1742, 1716 cm^{-1}; ^1H NMR ($CDCl_3$, 400 MHz) δ 5.43 (1H, dt, *J* = 6.7, 0.9 Hz, H-14), 5.31 (1H, m, H-6), 5.11 (1H, tt, *J* = 11.7, 4.1 Hz, H-2), 4.98 (1H, d, *J* = 1.0 Hz, H-7), 4.16 (2H, d, *J* = 6.8 Hz, H_2-15), 2.21 (2H, m, H_2-11), 2.12 (1H, m, H-1b), 2.10 (2H, m, H_2-12), 2.07 (3H, s, 6-OAc), 2.02 (3H, s, 7-OAc), 2.00 (3H, s, 2-OAc), 1.79 (1H, ddd, *J* = 12.2, 4.2, 1.9 Hz, H-3b), 1.70 (3H, s, H_3-16), 1.61 (3H, s, H_3-17), 1.51 (1H, d, *J* = 1.4 Hz, H-5), 1.35 (3H, s, H_3-20), 1.26 (1H, m, H-3a), 1.25 (1H, m, H-1a), 1.02 (6H, s, H_3-18, H_3-19); ^{13}C NMR ($CDCl_3$, 100 MHz) δ 170.5 (s, 7-OAc), 169.7 (s, 6-OAc), 169.5 (s, 2-OAc), 146.7 (s, C-9), 139.4 (s, C-13), 123.4 (d, C-14), 122.2 (s, C-8), 73.3 (s, C-7), 69.0 (d, C-6), 68.5 (d, C-2), 59.3 (t, C-15), 48.8 (d, C-5), 47.7 (t, C-3), 43.9 (t, C-1), 40.5 (s, C-4), 39.1 (t, C-12), 34.3 (s, C-10), 33.0 (q, C-18), 26.8 (t, C-11), 23.7 (q, C-19), 21.9 (q, C-20), 21.4 (q, 7-OAc), 21.1 (q, 6-OAc), 17.0 (q, C-17), 16.4 (q, C-16), 14.1 (q, 2-OAc); HRFABMS *m/z* 464.2760 (calcd for $C_{26}H_{40}O_7$ [M^+], 464.2772).

6β,7α,15-Triacetoxylabda-8,13*E*-diene (3.3): pale yellow oil; $[\alpha]_D^{24}$ +48 (*c* 0.2, $CHCl_3$); IR (film) ν_{max} 2957, 2871, 1737, 1679, 1622 cm^{-1}; ^1H and ^{13}C NMR data, see Table 3.2; HRFABMS *m/z* 449.2909 (calcd for $C_{26}H_{41}O_6$ $[(M + H)^+]$, 449.2903).

3α,11-Dihydroxy-9,11-seco-cholest-4,7-dien-6,9-dione (3.4): bright yellow orange oil; $[\alpha]_D$ +32 (*c* 1.5, $CHCl_3$); IR (film) ν_{max} 3420, 2957, 1683, 1624, 1462 cm^{-1}; ^1H NMR and ^{13}C NMR see Table 3.1; HRFABMS *m/z* 430.3082 (calcd for $C_{27}H_{42}O_4$ $[M^+]$, 430.3083).

Cholest-7-en-3,5,7-triol (3.5): white amorphous solid; $[\alpha]_D^{24}$ +4 (*c* 1.5, $CHCl_3$); IR (film) ν_{max} 3401, 2953, 1459, 1377, 1228 cm^{-1}; ^1H and ^{13}C NMR data, see Table 3.3; HRFABMS *m/z* 419.3525 (calcd for $C_{27}H_{47}O_3$ $[(M + H)^+]$, 419.3525).

7.3.2 Synthetic aspects

7.3.2.1 Preparation of the camphanate esters of **3.1** and **3.2**

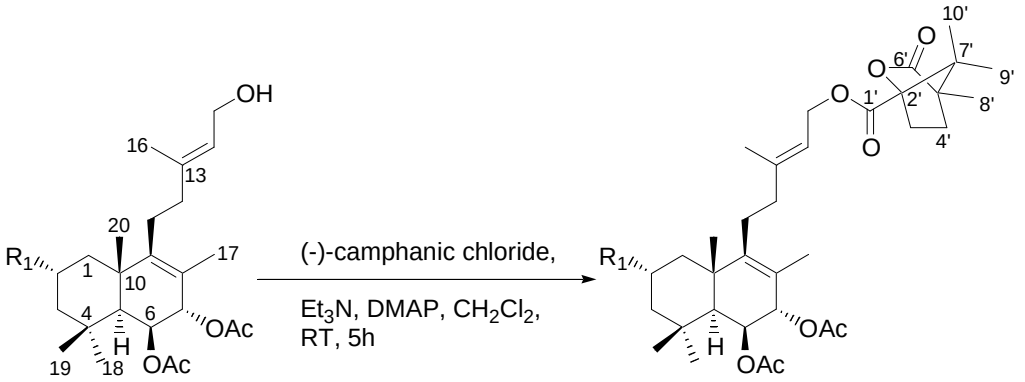

3.1 R_1 = H
3.2 R_1 = OAc

3.32 R_1 = H
3.33 R_1 = OAc

This method is representative. Diterpene **3.1** (30 mg, 0.07 mmol), camphanic chloride (34 mg, 0.16 mmol, 2.1 eq), Et_3N (60 µL, 7.05 mmol, 6 eq) and DMAP (5 mg, 0.04 mmol, 0.5 eq) were dissolved in anhydrous CH_2Cl_2 (2 mL) under an Ar atmosphere and stirred at ambient temperature (5 h). The reaction mixture was concentrated to dryness, taken up in Et_2O (5 mL) and washed with 1M HCl (1 mL) followed by H_2O (2 x 5 mL). The organic partition was dried ($MgSO_4$) and concentrated to an amorphous solid (69 mg). Normal phase HPLC (33%

EtOAc, 67% hexane) afforded the camphanate ester **3.32** (35 mg, 81%) as a yellow oil. The camphanate ester of **3.2** (**3.33**, 83%) was similarly prepared. Several attempts at growing crystals of **3.32** using a variety of solvents (*e.g.* propane, hexane, C_6H_6, EtOH, MeOH, Et_2O, EtOAc) and mixtures of these solvents failed to yield any crystals. Crystals of **3.33**, suitable for X-ray diffraction, were grown using the slow diffusion method (hexane/EtOAc).

Camphanate ester (3.32): pale yellow oil; ^{1}H NMR ($CDCl_3$, 400 MHz) δ 5.39 (1H, t, *J* = 7.2 Hz, H-14), 5.29 (1H, m, H-6), 4.95 (1H, d, *J* = 1.1 Hz, H-7), 4.73 (2H, d, *J* = 6.8 Hz, H_2-15), 2.42 (1H, ddd, *J* = 13.5, 10.8, 4.2 Hz, H-3'b), 2.17 (2H, m, H_2-11), 2.11 (2H, m, H_2-12), 2.07 (3H, s, 7-OAc) 2.02 (6-OAc), 2.02 (1H, m, H-3'a), 1.91 (1H, ddd, *J* = 13.2, 10.8, 4.6 Hz, H-4'b), 1.81 (1H, ddd, *J* = 12.5, 4.4, 3.4 Hz, H-1b), 1.75 (3H, br s, H_3-16), 1.68 (1H, ddd, *J* = 13.2, 9.2, 4.2 Hz, H-4'a), 1.66 (1H, m, H-2b), 1.59 (3H, s, H_3-17), 1.52 (1H, m, H-2a), 1.47 (1H, m, H-5), 1.41 (1H, m, H-3b), 1.26 (3H, s, H_3-20), 1.22 (2H, m, H-1a and H-3a), 1.09 (3H, s, H_3-8'), 1.03 (3H, s, H_3-10'), 0.95 (3H, s, H_3-18), 0.94 (3H, s, H_3-19), 0.93 (3H, s, H_3-9'); ^{13}C NMR ($CDCl_3$, 100 MHz) δ 178.1 (s, C-6'), 169.9 (s, 7-OAc), 169.6 (s, 6-OAc), 167.5 (s, C-1'), 147.5 (s, C-9), 143.5 (s, C-13), 121.6 (s, C-8), 117.4 (d, C-14), 91.1 (s, C-2'), 73.3 (d, C-7), 69.5 (d, C-6), 62.2 (t, C-15), 54.7 (s, C-7'), 54.2 (C-5'), 49.2 (d, C-5), 43.0 (t, C-3), 39.4 (s, C-10), 39.2 (t, C-12), 38.9 (t, C-1), 33.4 (s, C-4), 33.0 (q, C-18), 30.5 (t, C-3'), 28.9 (t, C-4'), 26.7 (t, C-11), 23.0 (q, C-19), 21.5 (q, 6-OAc), 21.1 (q, 7-OAc), 21.0 (q, C-20), 18.9 (t, C-2), 17.0 (q, C-17), 16.74 (q, C-9'), 16.68 (q, C-10'), 16.6 (q, C-16), 9.7 (q, C-8'); HRFABMS *m/z* 587.3584 (calcd for $C_{34}H_{51}O_8$ [$(M + H)^+$], 587.3584).

Camphanate ester (3.33): colourless plates (from hexane/EtOAc); mp 154-155°C; ^{1}H NMR ($CDCl_3$, 600 MHz) δ 5.40 (1H, dt, *J* = 7.1, 0.9 Hz, H-14), 5.31 (1H, m, H-6), 5.12 (1H, tt, *J* = 11.7, 4.1 Hz, H-2), 4.98 (1H, d, *J* = 0.8 Hz, H-7), 4.74 (2H, m, H_2-15), 2.42 (1H, ddd, *J* = 13.5, 10.8, 4.2 Hz, H-3'b), 2.19 (1H, m, H-11b), 2.13 (1H, m, H-11a), 2.10 (2H, m, H-1b and H-12b), 2.09 (1H, m, H-12a), 2.08 (3H, s, 7-OAc), 2.03 (3H, s, 6-OAc), 2.02 (3H, s, 2-OAc), 2.02 (1H, m, H-3'a), 1.91 (1H, ddd, *J* = 13.2, 10.8, 4.6 Hz, H-4'b), 1.80 (1H, ddd, *J* = 12.3, 4.1, 1.8 Hz, H-3b), 1.76 (3H, br s, H_3-16), 1.68 (1H, ddd, *J* = 13.2, 9.2, 4.2 Hz, H-4'a), 1.62 (3H, s, H_3-17), 1.51 (1H, d, *J* = 1.2 Hz, H-5), 1.36 (3H, s, H_3-20), 1.27 (1H, dd, *J* = 11.9, 7.0 Hz, H-3a), 1.25

(1H, dd, *J* = 11.9, 7.8 Hz, H-1a), 1.10 (3H, s, H_3-8'), 1.04 (3H, s, H_3-10'), 1.03 (6H, s, H_3-19 and H_3-20), 0.94 (3H, s, H_3-9'); ^{13}C NMR ($CDCl_3$, 150 MHz) δ 178.1 (s, C-6'), 170.5 (s, 2-OAc), 169.7 (s, 7-OAc), 169.5 (s, 6-OAc), 167.5 (s, C-1'), 146.5 (s, C-9), 143.2 (s, C-13), 122.4 (s, C-8), 117.6 (d, C-14), 91.1 (s, C-2'), 73.2 (d, C-7), 69.0 (d, C-6), 68.4 (d, C-2), 62.2 (t, C-15) 54.7 (s, C-7'), 54.2 (s, C-5'), 48.8 (d, C-5), 47.8 (t, C-3), 43.9 (t, C-1), 40.5 (s, C-4), 39.2 (t, C-12), 34.3 (s, C-10), 33.0 (q, C-18), 30.6 (t, C-3'), 29.0 (t, C-4'), 26.7 (t, C-11), 23.7 (q, C-19), 22.0 (q, C-20), 21.5 (q, 2-OAc), 21.4 (q, 6-OAc), 21.1 (q, 7-OAc), 17.0 (q, C-17), 16.8 (q, C-9'), 16.72 (q, C-10'), 16.67 (q, C-16), 9.7 (q, C-8'); HRFABMS *m/z* 646.3718 (calcd for $C_{36}H_{54}O_{10}$ [M^+], 646.3717).

Crystal data for 3.33: $C_{36}H_{52}O_{10}$, *M* = 644.78, 0.12 x 0.12 x 0.09 mm^3, monoclinic, space group $P2_1$ (No. 4), *a* = 10.4893(2), *b* = 7.7835(2), *c* = 21.1003(5) Å, *β* = 93.518(1)°, *V* = 1719.46(7) Å^3, *Z* = 2, D_c = 1.245 g/cm^3, F_{000} = 696, MoKα radiation, λ = 0.71073 Å, *T* = 113(2)K, $2\theta_{max}$ = 51.3°, 6480 reflections collected, 6480 unique (R_{int} = 0.0000). Final *GooF* = 1.045, R_1 = 0.0606, wR_2 = 0.1508, *R* indices based on 5199 reflections with I >2sigma(I) (refinement on F^2), 429 parameters, 1 restraint. Lp corrections applied, μ = 0.090 mm^{-1}. Absolute structure parameter = 0.1(13)[237] Tables of atomic co-ordinates and interatomic bond angles and bond lengths have not been deposited with the Cambridge data base and are provided in Appendix I.

7.3.2.2 Acetylation of **3.1**

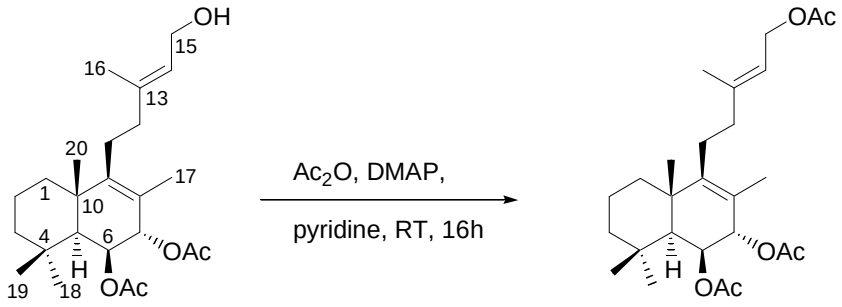

3.1 **3.3**

A solution of **3.1** (65 mg, 0.13 mmol) in pyridine (1 mL) and acetic hydride (1 mL) was stirred at ambient temperature overnight (16 h). The pyridine and acetic anhydride were removed *in vacuo* (0.5 mm Hg) and the remaining pale yellow oil (68 mg) purified by normal phase HPLC

(50% EtOAc, 50% hexane) to afford **3.3** (53 mg, 90%) as a pale yellow oil: $[\alpha]_D^{24}$ +52 (*c* 4.8, $CHCl_3$), **3.3** from *T. costatus* $[\alpha]_D^{24}$ +48; ^1H and ^{13}C NMR data consistent with those of the natural product; HRFABMS *m/z* 449.2909 (calcd for $C_{26}H_{41}O_6$ [$(M + H)^+$], 449.2903).

7.3.2.3 Selective acetylation of **3.4**[124]

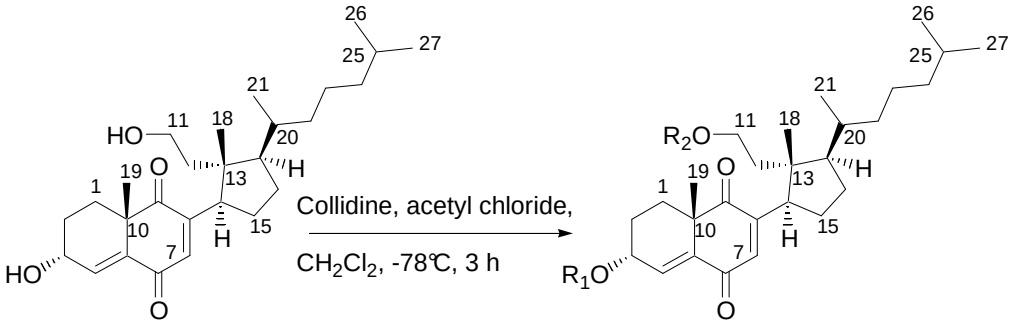

3.4

3.35 $R_1 = R_2 = Ac$
3.36 $R_1 = H$, $R_2 = Ac$

Anhydrous conditions. The 9,11 secosterol **3.4** (62 mg, 0.14 mmol) and collidine (0.28 mmol, 2 eq) were taken up in anhydrous CH_2Cl_2 (1 mL) and cooled to -78℃ under an Ar atmosphere. A solution of acetyl chloride (0.19 mmol, 2 eq.) in anhydrous CH_2Cl_2 (120 *μ*L) was added in a drop wise fashion and stirred at -78℃ (3 h). The solution was quenched with H_2O (1 mL) and concentrated to dryness *in vacuo* (0.5 mmHg). The resultant yellowish solid (103 mg) was taken up in EtOAc and passed through a Teflon micropore filter to remove the whitish precipitate that formed and the yellow filtrate concentrated to a yellow oil (71 mg). The yellow oil was subjected to Diol HPLC (40% EtOAc, hexane 60%) to afford both **3.35** (6 mg, 9%) and 3α-hydroxy-11-acetoxy-9,11-seco-cholest-4,7-dien-6,9-dione (**3.36,** 17 mg, 27%). Analysis of the ^1H NMR spectrum of each of the two fractions suggested that **3.35** was the diaceylated product (not further characterized) and that **3.36** was the desired 11-OAc product.

3α-Hydroxy-11-acetoxy-9,11-seco-cholest-4,7-dien-6,9-dione (3.36): yellow oil; $[\alpha]_D^{34}$ +19 (*c* 0.6, $CHCl_3$); ^1H NMR ($CDCl_3$, 600 MHz) δ 6.69 (1H, dd, *J* = 4.0, 0.9 Hz, H-4), 6.66 (1H, s, H-7), 4.33 (1H, m, H-3), 4.19 (1H, m, H-11b), 4.15 (1H, m, H-11a), 3.44 (1H, dd, *J* = 11.2, 8.4

Hz, H-14), 2.18 (1H, ddd, *J* = 13.5, 13.3, 3.4 Hz, H-1b), 2.01 (3H, s, 11-OAc), 1.89 (1H, m, H-16b), 1.87 (2H, m, H_2-2), 1.76 (1H, m, H-1a), 1.73 (2H, m, H-12b and H-17), 1.66 (2H, m, H_2-15), 1.50 (2H, m, H-16a and H-25a), 1.43 (1H, m, H-20), 1.35 (2H, m, H-22b and H-23b), 1.35 (3H, s, H_3-19), 1.26 (1H, m, H-12a), 1.14 (1H, m, H-23a), 1.13 (2H, m, H_2-24), 1.01 (1H, m, H-22a), 0.97 (3H, d, *J* = 6.7 Hz, H_3-21), 0.85 (3H, s, H_3-27), 0.85 (3H, s, H_3-26), 0.77 (3H, s, H_3-18); ^{13}C NMR ($CDCl_3$, 150 MHz) δ 200.4 (s, C-9), 187.5 (s, C-6), 171.0 (s, 11-OAc), 153.4 (s, C-8), 140.5 (s, C-5), 138.2 (d, C-7), 135.3 (d, C-4), 63.1 (d, C-3),), 61.0 (t, C-11), 50.7 (d, C-17), 49.1 (s, C-10), 47.7 (s, C-13),), 43.7 (d, C-14), 39.4 (t, C-24), 37.2 (t, C-12), 35.4 (t, C-22), 34.6 (d, C-20), 27.9 (d, C-25), 27.3 (t, C-15), 27.2 (t, C-2), 26.7 (q, C-19), 26.3 (t, C-16), 25.0 (t, C-1), 24.4 (t, C-23), 22.7 (q, C-26), 22.5 (q, C-27), 21.1 (q, 11-OAc), 18.9 (q, C-21), 17.5 (q, C-18); HRFABMS *m/z* 472.3188 (calcd for $C_{29}H_{44}O_5$ [M^+], 472.3189).

7.3.2.4 Preparation of the (*R*)- and (*S*)-MTPA esters of **3.36**

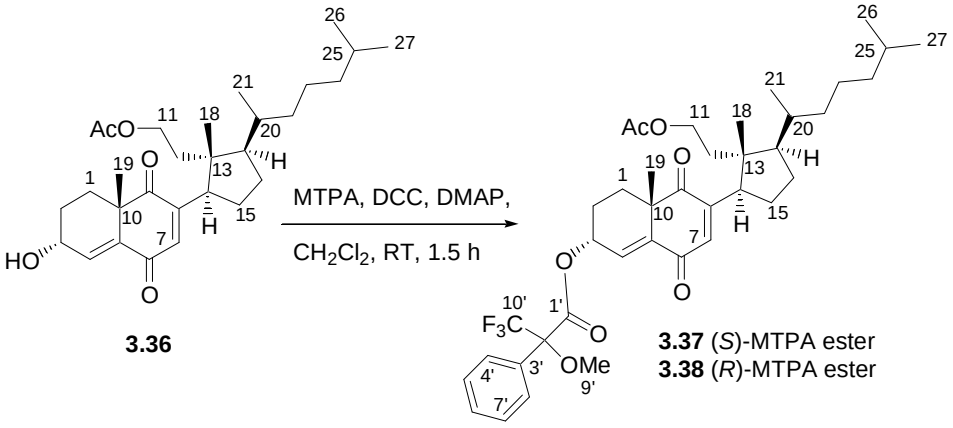

This method is representative. *R*-α-methoxy-α-trifluoromethylphenylacetic acid (6 mg), DCC (48 mg) and DMAP (7 mg) were added to a solution of **3.36** in anhydrous CH_2Cl_2 (2 mL). The solution was shaken periodically over period of 1.5 hours at ambient temperature, diluted with EtOAc (3 mL) and H_2O (1 mL) and filtered. The resulting solution was washed with 1M HCl (1 mL), H_2O (1 mL), saturated aqueous $NaHCO_3$ (1 mL) and once more with H_2O (1 mL) in the order presented. The resulting colourless oil (7 mg) was purified by semi-preparative HPLC (25% EtOAc, 75% hexane) to afford **3.38** (6 mg). The (*S*)-MTPA ester, **3.37**, was similarly prepared from **3.36**, using *S*-α-methoxy-α-trifluoromethylphenylacetic acid.

(S)-MTPA ester (3.37): yellow oil; ^{1}H NMR ($CDCl_3$, 600 MHz) δ 7.46 (2H, m, H-4' and H-8'), 7.37 (3H, m, H-5', H-6' and H-7'), 6.67 (1H, s, H-7), 6.56 (1H, dd, *J* = 4.3, 0.9 Hz, H-4), 5.61 (1H, m, H-3), 4.21 (1H, m, H-11b), 4.16 (1H, m, H-11a), 3.43 (3H, s, H_3-9'), 2.10 (1H, m, H-1b), 2.04 (2H, m, H_2-2), 2.01 (3H, s, 11-OAc), 1.89 (1H, m, H-16b), 1.83 (1H, H, H-1a), 1.74 (1H, m, H-12b), 1.73 (1H, m, H-17), 1.67 (2H, m, H_2-15), 1.52 (1H, m, H-16a), 1.49 (1H, m, H-25), 1.43 (1H, m, H-20), 1.37 (1H, m, H-22b), 1.36 (1H, m, H-23a), 1.24 (1H, m, H-12a), 1.17 (1H, m, H-23a), 1.14 (2H, m, H_2-24), 1.01 (1H, m, H-22a), 0.98 (3H, d, *J* = 6.7 Hz, H_3-21), 0.86 (3H, d, *J* = 6.6 Hz, H_3-27), 0.86 (3H, d, *J* = 6.6 Hz, H_3-26), 0.77 (3H, s, H_3-18); ^{13}C NMR ($CDCl_3$, 150 MHz) δ 199.7 (s, C-9), 186.6 (s, C-6), 170.1 (s, 11-OAc), 165.6 (s, C-1'), 153.6 (s, C-8), 143.2 (s, C-5), 138.1 (d, C-7), 132.5 (s, C-3'), 129.7 (d, C-7'), 129.7 (d, C-7'), 129.6 (d, C-4), 128.5 (d, C-6'), 127.2 (d, C-8'), 127.2 (d, C-4'), 124.1 (s, C-10'), 122.2 (s, C-2'), 67.7 (d, C-3), 60.9 (t, C-11), 55.4 (q, C-9'), 50.7 (d, C-17), 48.9 (s, C-10), 47.8 (s, C-13), 43.8 (d, C-14), 39.4 (t, C-24), 37.3 (t, C-12), 35.4 (t, C-22), 34.6 (d, C-20), 28.0 (d, C-25), 27.4 (t, C-15), 26.5 (q, C-19), 26.3 (t, C-16), 25.4 (t, C-1), 24.4 (t, C-23), 24.4 (t, C-2), 22.5 (q, C-27), 22.5 (q, C-26), 21.1 (q, 11-OAc), 19.0 (q, C-21), 17.6 (q, C-18).

(*R*)-MTPA ester (3.38): yellow oil; ^{1}H NMR ($CDCl_3$, 600 MHz) δ 7.45 (2H, m, H-4' and H-8'), 7.37 (3H, m, H-5', H-6' and H-7'), 6.68 (1H, s, H-7), 6.65 (1H, dd, *J* = 4.4, 0.9 Hz, H-4), 5.61 (1H, m, H-3), 4.20 (1H, m, H-11b), 4.16 (1H, m, H-11a), 3.49 (3H, s, H_3-9'), 3.43 (1H, dd, *J* = 11.1, 8.2 Hz, H-14), 2.01 (3H, s, 11-OAc), 1.99 (2H, m, H_2-2), 1.98 (1H, m, H-1b), 1.89 (1H, m, H-16b), 1.79 (1H, m, H-1a), 1.74 (1H, m, H-17), 1.72 (1H, m, H-12b), 1.67 (2H, m, H_2-15), 1.53 (1H, m, H-16a), 1.51 (1H, m, H-25), 1.45 (1H, m, H-20), 1.37 (2H, m, H-22b and H-23b), 1.37 (3H, s, H_3-19), 1.26 (1H, m, H-12a), 1.14 (3H, m, H-23a and H_2-24), 1.01 (1H, m, H-22a), 0.98 (3H, d, *J* = 6.7 Hz, H_3-21), 0.86 (3H, d, *J* = 6.6 Hz, H_3-27), 0.86 (3H, d, *J* = 6.6 Hz, H_3-26), 0.77 (3H, s, H_3-18); ^{13}C NMR ($CDCl_3$, 150 MHz) δ 199.7 (s, C-9), 185.6 (s, C-6), 171.0 (s, 11-OAc), 165.8 (s, C-1'), 153.7 (s, C-8), 143.4 (s, C-5), 138.1 (d, C-7), 132.5 (s, C-3'), 129.7 (d, C-4), 129.6 (d, C-7'), 129.6 (d, C-5'), 128.5 (d, C-6'), 127.1 (d, C-8'), 127.1 (d, C-4'), 124.1 (s, C10'), 122.2 (s, C-2'), 67.5 (d, C-3), 60.9 (t, C-11), 55.5 (q, C-9'), 50.8 (d, C-17), 48.9 (s, C10), 47.8 (d, C-13), 43.8 (d, C-14), 39.4 (t, C-24), 37.3 (t, C-12), 35.4 (t, C-22), 34.6 (d, C-

20), 28.0 (d, C-25), 27.4 (t, C-15), 26.4 (q, C-19), 26.3 (t, C-16), 25.2 (t, C-1), 24.5 (t, C-23), 24.1 (t, C-2), 22.8 (q, C-26), 22.5 (q, C-27), 21.1 (q, 11-OAc), 19.0 (q, C-21), 17.6 (q, C-18).

7.3.3 Activity of Trimusculus metabolites against oesophageal cancer

7.3.3.1 Cell lines and screening protocol

Assays were performed at the Department of Medicinal Biochemistry at the University of Cape Town by Dr C. Whibley and Dr O. Osoniyi. The protocol described here has been taken from the thesis of Dr C. Whibley[133] and is presented in truncated form.

The human oesophageal cancer cell line (WHCO1) screened against was obtained as a gift from Prof. R. Veale, University of the Witwatersrand, South Africa and derived from South African patients with squamous cell carcinoma of the oesophagus.[238] Samples for the MTT assay[138] were plated in 96 well plates to a final volume of 100 μL. MTT reagent (10 μL, Roche cat # 1465007) was added and the cells incubated (4 h, 37℃). Solubilisation reagent (100 μL) was added to each well and incubation continued (16 h, 37℃). Upon completion of the incubation time, plates were read (595 nm) on an Anthos microplate reader 2001. To determine IC_{50} values, 1500 cells per well were seeded in 90 μL Dulbecco/Vogt Modified Eagle's Minimal Essential Medium (DMEM) in Cellstar 96 well plates. After incubation (24 h), test samples were plated at a range of concentrations in 10 μL medium, with a final concentration of 0.2% DMSO and again incubated (48 h). Observations were made and processed in the manner described for the MTT assay. A dose-response curve was analyzed by non-linear regression analysis [non-linear regression (sigmoidal dose response with variable slope)] using the GraphPad Prism 4.00 package of GraphPad Software, San Diego, USA to determine the specific IC_{50} value for the compound tested against the WHCO1 cell line. The formula used was $Y = bottom + [(top-bottom)/(1 + 10^{(logIC50 - X) \times hillslope})]$, where Y is the absorbance at 595nm, X is the concentration of the test compound, bottom is the minimum absorbance (also the absorbance of the medium blank) and the hillslope is the slope of the curve.

7.4 Chapter Four Experimental

7.4.1 Isolation of hispanolone using HP-20 Chromatography

The aerial parts of *B. Africana* were collected from Woodbury Lodge, Amakhala Game Reserve, situated on the N2 between Grahamstown and Port Elizabeth in the Eastern Cape of South Africa in November 2003 and air dried for two months. Once dry, the leaves (250 g) were steeped in Me_2CO (2.5 L) for four days, the Me_2CO was decanted, filtered and concentrated *in vacuo* (250 mL). The resulting dark green liquid was treated with activated charcoal (20 g), stirred overnight, and filtered through a Celite plug to remove the particulate charcoal. This extract was diluted to a volume of approximately 1 L and passed through an HP-20 column (500 mL). The collected eluent was diluted with H_2O until the solution began to take on a cloudy appearance, whereupon this solution was again passed through the column. This method was repeated until a final concentration of approximately 20% Me_2CO was achieved. The column was stripped with a 40% Me_2CO solution (1.5 L) and the eluent discarded. The fraction obtained from a successive 60% Me_2CO stripping was collected, diluted to 30% Me_2CO in H_2O and allowed to stand at 4℃ for 4 days. The resu lting white plates (3.82 g, 1.5%) were collected by filtration and confirmed to be **4.4** by comparison of acquired ^{13}C NMR data with those in the chemical literature.[141]

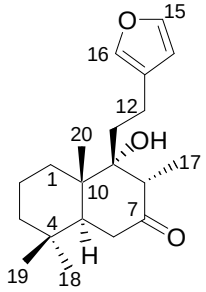

4.4

Hispanolone (4.4): white plates (from Me_2CO/H_2O); mp 133-135℃, lit.[141] 147-148℃; $[\alpha]_D^{32}$ -19 (*c* 6.4, $CHCl_3$), lit.[141] -18.7; IR (film) ν_{max} 2919, 2863, 1697, 1469, 1116 cm^{-1}; ^{13}C NMR ($CDCl_3$, 100 MHz) δ 211.8 (s, C-7), 143.0 (d, C-15), 138.6 (d, C-16), 124.8 (s, C-13), 110.7 (d, C-14), 81.7 (s, C-9), 50.9 (d, C-8), 46.4 (d, C-5), 43.3 (s, C-10), 41.3 (t, C-3), 39.2 (t, C-6),

34.8 (t, C-11), 33.6 (q, C-18), 33.1 (s, C-4), 31.9 (t, C-1), 21.6 (t, C-12), 21.4 (q, C-19), 18.5 (t, C-2), 16.2 (q, C-20), 8.2 (q, C-17).

7.4.2 Dehydration of hispanolone

Method A: Attempted dehydration of **4.4** using *p-TsOH* in C_6H_6

Hispanolone (**4.4**, 200 mg, 0.63 mmol) and p-TsOH (12 mg, 0.06 mmol, 0.1 eq.) were taken up in anhydrous C_6H_6 (30 mL) and refluxed under a Dean-Stark trap for (48 h). This solution was then washed with 5% $NaCO_3$ (1.2 mL), followed by H_2O (3 x 15 mL). The aqueous fractions were backwashed with CH_2Cl_2 (3 x 20 mL), all organic fractions were pooled, dried with $MgSO_4$, filtered and concentrated *in vacuo* to afford a yellowish oil (168 mg). Analysis of the ^1H NMR spectrum of the reaction mixture revealed that no dehydration of the starting material had taken place.

Method B: Dehydration of **4.4** using I_2 in C_6H_6[147]

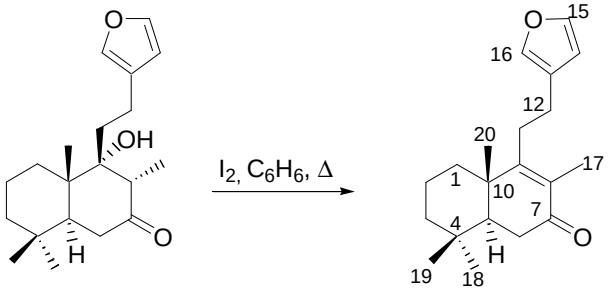

4.4 **4.6**

This method is representative. Hispanolone (**4.4,** 199 mg, 0.63 mmol) was taken up in anhydrous C_6H_6 (10 mL), and I_2 (10 mg, 40 mmol) added, turning the solution a bright pink colour. This solution was refluxed (24 h) under a Dean-Stark trap, into which 3Å molecular sieves had been placed. The process had been monitored by TLC and was stopped when no further conversion to hispanone was noticed. The C_6H_6 solution was washed with 5% aqueous $Na_2S_2O_3$ (3 x 5 mL) followed H_2O (1 x 20 mL). The aqueous partition fractions were pooled and backwashed with EtOAc (3 x 20 mL). The C_6H_6 and EtOAc partitions were pooled, dried with $MgSO_4$, filtered and concentrated *in vacuo* to afford a brownish oil (175 mg). Silica

flash column chromatography (5% EtOAc, 95% hexane) followed, to afford hispanone (159 mg, 84%) as pale yellow needles (crystallized from MeOH).

Hispanone (4.6): pale yellow needles (from MeOH); mp 65-66℃, lit. [141] 69-70℃; $[\alpha]_D^{32}$ +34 (*c* 2.2, $CHCl_3$), lit.[141] +43.3; IR (film) ν_{max} 2930, 2855, 1661, 1607, 1470 cm^{-1}; ^1H NMR ($CDCl_3$, 400 MHz) δ 7.36 (1H, t, *J* = 1.4 Hz, H-15), 7.26 (1H, m, H-16), 6.30 (1H, d, *J* = 0.9 Hz, H-14), 2.52 (2H, m, H_2-12), 2.48 (1H, m, H-6b), 2.45 (2H, m, H_2-11), 2.36 (1H, m, H-6a), 1.96 (1H, ddd, *J* = 12.3, 4.8, 2.8 Hz, H-1b), 1.79 (3H, s, H_3-17), 1.71 (1H, dd, *J* = 14.2, 3.8, H-5), 1.68 (1H, m, H-2b), 1.58 (1H, m, H-2a), 1.48 (1H, ddd, *J* = 13.2, 4.8, 3.7 Hz, H-3b), 1.42 (1H, ddd, *J* = 13.4, 12.9, 3.9 Hz, H-1a), 1.23 (1H, m, H-3a), 1.09 (3H, s, H_3-20), 0.92 (3H, s, H_3-19), 0.89 (3H, s, H_3-18); ^{13}C NMR ($CDCl_3$, 100 MHz) δ 200.3 (s, C-7), 167.0 (s, C-9), 143.0 (d, C-15), 138.6 (d, C-16), 130.4 (s, C-8), 124.5 (s, C-13), 110.6 (d, C-14), 50.3 (d, C-5), 41.3 (t, C-3), 40.9 (s, C-10), 35.9 (t, C-1), 35.2 (t, C-6), 33.1 (s, C-4), 32.5 (q, C-18), 30.2 (t, C-11), 24.2 (t, C-12), 21.3 (q, C-19), 18.6 (t, C-2), 18.1 (q, C-20), 11.5 (q, C-17); HRFABMS *m/z* 301.2167 (calcd for $C_{20}H_{29}O_2$ $[(M + H)^+]$, 301.2168).

*7.4.3 Acetoxylation of **4.6** using $Mn(OAc)_3.2H_2O$ in C_6H_6*[150;151;153]

7.4.3.1 Preparation of $[(Mn(OAc)_3.2H_2O]$[153]

This method is representative. Powdered $KmnO_4$ (2.5 g, 18 mmol) was added to a solution of $Mn(OAc)_2.4H_2O$ (14.6 g, 59.6 mmol) in glacial acetic acid (174 mL), which had first been heated under reflux for 30 minutes, following which the entire solution was refluxed for a further 30 minutes. The dark brown solution was stirred at room temperature overnight (16 h), forming a dark brown precipitate. This precipitate was collected by gravity filtration, washed with cold water (50 mL) and dried in a vacuum desiccator in the presence of KOH to yield manganic acetate (14.9 g, 94%) as a dark brown powder.

7.4.3.2 Acetoxylation of **4.6** using $Mn(OAc)_3.2H_2O$ in C_6H_6[150;151;153]

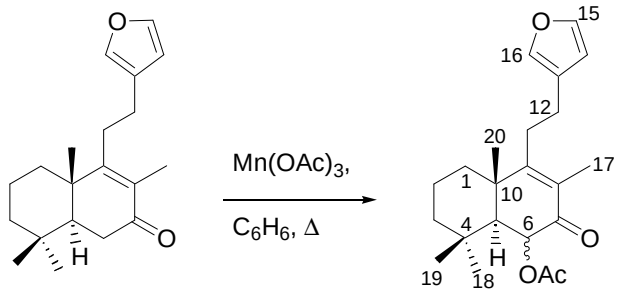

4.4

4.7 6α
4.8 6β

This method is representative. Proportionally equivalent volumes of toluene and quantities of self-prepared $Mn(OAc)_3.H_2O$ were used in the optimization attempts, the results of which are summarized in Table 4.1. Prior to the addition of **4.6**, the $Mn(OAc)_3.2H_2O$ (1.77 g, 1.5 g per mmol of hispanone) was refluxed in anhydrous C_6H_6 (3 h) under a Dean-Stark trap, into which 3Å molecular sieves had been placed. After this, hispanone (357 mg, 1.18 mmol) was taken up in anhydrous C_6H_6 (2 mL) and transferred to the reaction vessel *via* cannula. Refluxing continued (24 h) and the reaction was monitored by TLC. Once no further conversion of the starting material was noted, the reaction solution was concentrated (50 mL) *in vacuo* and washed with 5% aqueous $Na_2S_2O_7$ (30 mL), stirring until the dark brown manganese precipitate had been reduced. This mixture was acidified with conc. HCl (0.5 mL) and subsequently neutralised (5% $NaHCO_3$, 6.0 mL). The organic and aqueous phases were then separated. The aqueous phase was back extracted with CH_2Cl_2 (3 x 50 mL) and all organic partition fractions combined, dried ($MgSO_4$), concentrated *in vacuo* to yield a brownish oil and partially purified by silica flash chromatography (5% EtOAc, 95% hexane), to afford a yellow oil (337 mg, 80%). Analysis of ^1H NMR data indicated a 5:2 mixture of the α- and β-acetoxylated products. These isomers were separated using semi-preparative HPLC (10% EtOAc, 90% hexane) to afford 6α-acetoxy-14,15-epoxylabda-8,13(16),14-trien-7-one (**4.7**, 200 mg, 0.56 mmol, 47% yield) and 6β-acetoxy-14,15-epoxylabda-8,13(16),14-trien-7-one (**4.8**, 79 mg, 0.22 mmol, 19% yield) as yellow oils.

6α-Acetoxy-14,15-epoxylabda-8,13(16),14-trien-7-one (4.7):[148] yellow oil; $[\alpha]_D^{19}$ +50 (*c* 2.4, $CHCl_3$), lit.[148] +51; IR (film) ν_{max} 2932, 2871,1747, 1674, 1616 cm^{-1}; ^1H NMR ($CDCl_3$, 400 MHz) δ 7.36 (1H, br s, H-15), 7.25 (1H, br s, H-16), 6.29 (1H, br s, H-14), 5.63 (1H, d, *J* = 13.4 Hz, H-6), 2.52 (2H, m, H_2-12), 2.49 (1H, m, H-11b), 2.43 (1H, m, H-11a), 2.18 (3H, s, 6-OAc), 2.04 (1H, d, *J* = 13.4 Hz, H-5), 1.98 (1H, m, H-1b), 1.80 (3H, s, H_3-17), 1.67 (1H, dddd, *J* = 13.6, 13.6, 4.2, 2.9 Hz, H-2b), 1.57 (1H, m, H-2a), 1.44 (1H, m, H-3b), 1.42 (1H, m, H-1a), 1.27 (1H, m Hz, H-3a), 1.27 (3H, s, H_3-20), 1.05 (3H, s, H_3-18), 1.00 (3H, s, H_3-19); ^{13}C NMR ($CDCl_3$, 100 MHz) δ 194.6 (s, C-7), 170.3 (s, 6-OAc), 166.9 (s, C-9), 143.1 (d, C-15), 138.6 (d, C-16), 128.9 (s, C-8), 124.2 (s, C13), 110.5 (d, C-14), 74.7 (d, C-6), 53.8 (d, C-5), 42.7 (d, C-3), 42.5 (s, C-10), 36.4 (t, C-1), 35.5 (q, C-18), 33.5 (s, C-4), 30.4 (t, C-11), 24.1 (t, C-12), 21.9 (q, C-19), 21.3 (q, 6-OAc), 19.9 (q, C-20), 18.4 (t, C-2), 11.6 (q, C-17); HRFABMS *m/z* 359.2222 (calcd for $C_{22}H_{31}O_4$ $[(M + H)^+]$, 359.2222).

6β-Acetoxy-14,15-epoxylabda-8,13(16),14-trien-7-one (4.8):[148] white amorphous solid; $[\alpha]_D^{19}$ -66 (*c* 1.1, $CHCl_3$), lit.[148] -61; IR (film) ν_{max} 2932, 2855, 1667, 1606, 1471 cm^{-1}; ^1H NMR ($CDCl_3$, 400 MHz) δ 7.37 (1H, t, *J* = 1.6 Hz, H-15), 7.27 (1H, br s, H-16), 6.31 (1H, br s, H-14), 5.79 (1H, d, *J* = 3.2 Hz, H-6), 2.58 (2H, m, H_2-12), 2.53 (1H, m, H-11b), 2.50 (1H, m, H-11a), 2.06 (3H, s, 6-OAc), 1.96 (1H, m, H-1b), 1.85 (3H, s, H_3-17), 1.77 (1H, m, H-2b), 1.76 (1H, d, *J* = 3.2 Hz, H-5), 1.61 (1H, m, H-2a), 1.45 (1H, m, H-3b), 1.42 (3H, s, H_3-20), 1.36 (1H, ddd, *J* = 13.5, 13.1, 3.4 Hz, H-1a), 1.24 (1H, ddd, *J* = 13.8, 13.5, 3.1 Hz, H-3a), 1.05 (3H, s, H_3-18), 1.04 (3H, s, H_3-19) ; ^{13}C NMR ($CDCl_3$, 100 MHz) δ 193.5 (s, C-7), 169.6 (s, 6-OAc), 168.5 (s, C-9), 143.1, d, C-15), 138.6 (d, C-16), 129.3 (s, C-8), 124.4 (s, C-13), 110.5 (d, C-14), 70.2 (d, C-6), 53.0 (d, C-5), 43.5 (t, C-3), 41.1 (s, C-10), 37.6 (t, C-1), 33.8 (s, C-4), 32.5 (q, C-18), 30.7 (t, C-11), 23.0 (q, C-19), 21.8 (q, C-20), 21.4 (q, 6-OAc), 18.6 (t, C-2), 11.7 (q, C-17); HRFABMS *m/z* 359.2222 (calcd for $C_{22}H_{31}O_4$ $[(M + H)^+]$, 359.2222).

*7.4.4 Michael addition of cyanide to **4.7** and **4.8***[100;145]

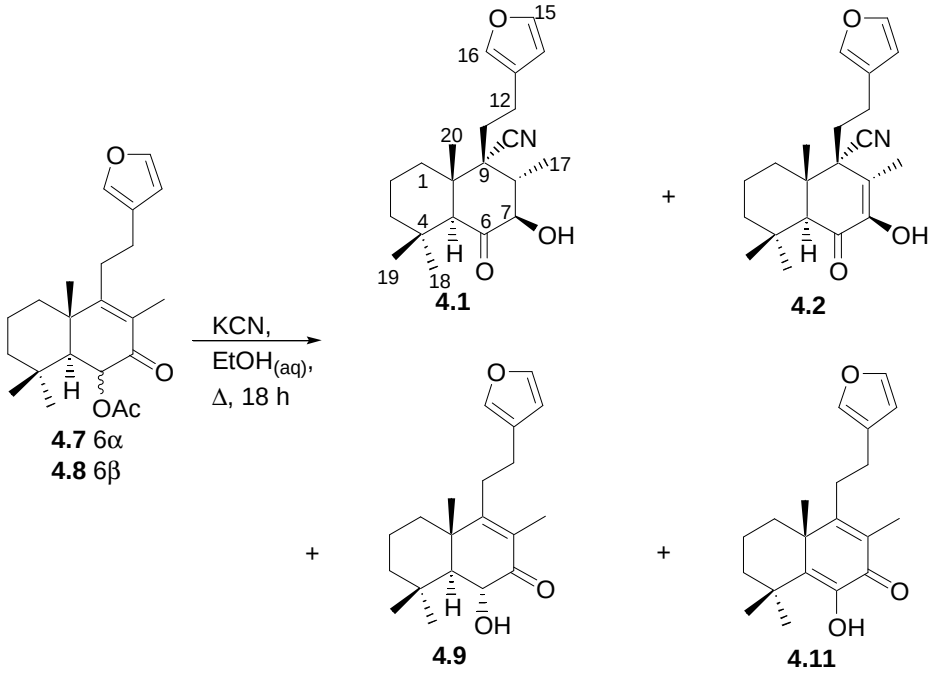

A 5:2 mixture of **4.7** and **4.8** (152 mg, 0.43 mmol) and KCN (70 mg, 1.08 mmol, 2.5 eq) were taken up in 95% EtOH (3 mL) and refluxed (24 h) until the starting material was no longer visible under TLC. All solvent was removed *in vacuo* and the off-white residue taken up in EtOAc (15 mL), which was subsequently washed with H_2O (3 x 10 mL). The aqueous fractions were pooled and backwashed with CH_2Cl_2 (2 x 5 mL), after which the combined organic fractions were dried ($MgSO_4$) and concentrated *in vacuo* to afford a pale yellow oil (150 mg). Semi-preparative HPLC (10% EtOAc, 90% hexane) was then used to isolate 9α-cyano-15,16-epoxy-7β-hydroxylabda-13(16),14-dien-6-one (**4.1,** 65 mg, 45%) as a very pale yellow solid, 9α-cyano-15,16-epoxy-7β-hydroxylabda-7,13(16),14-trien-6-one (**4.2,** 14 mg, 9%) as fine needle-like white crystals (from hexane/C_6H_6), 6α-hydroxy-15,16-epoxylabda-8,13(16),14-trien-7-one (**4.9**, 2 mg, 1%) as white plates and 6-hydroxy-15,16-epoxylabda-5,8,13(16),14-tetraen-7-one (**4.11,** 3 mg, 2%) as a pale yellow oil.

9α-Cyano-15,16-epoxy-7β-hydroxylabda-13(16),14-dien-6-one (4.1):[100] pale yellow oil; $[\alpha]_D^{25}$ +53 (*c* 0.8, $CHCl_3$), lit.[100] +56; IR (film) ν_{max} 3437, 2928, 2859, 2852, 2221 cm^{-1}; ^1H NMR ($CDCl_3$, 400 MHz) δ 7.36 (1H, t, *J* = 1.6 Hz, H-15), 7.26 (1H, br s, H-16), 6.27 (1H, d, *J* = 0.7,

H-14), 3.96 (1H, dd, *J* = 10.9, 1.9 Hz, H-7), 3.72 (1H, br d, *J* = 3.2, 7-OH), 2.72 (1H, s, H-5), 2.71 (2H, m, H_2-12), 1.94 (1H, m, H-11b), 1.86 (1H, m, H-8), 1.74 (2H, m, H_2-1), 1.61 (2H, m, H_2-2), 1.54 (1H, m, H-11a), 1.42 (3H, d, *J* = 6.4 Hz, H_3-19), 1.38 (1H, m, H-3b), 1.30 (3H, s, H_3-19), 1.29 (1H, m, H-3a), 1.01 (3H, s, H_3-18), 0.88 (3H, s, H_3-20); ^{13}C NMR ($CDCl_3$, 100 MHz) δ 208.9 (s, C-6), 143.1 (d, C-15), 138.8 (d, C-16), 123.5 (s, C-13), 120.2 (s, 9-CN), 110.5 (d, C-14), 77.3 (s, C-7), 59.7 (d, C-5), 53.3 (q, C-9), 47.1 (d, C-8), 47.0 (q, C-10), 41.6 (t, C-3), 35.1 (t, C-1), 32.6 (s, C-4), 32.3 (q, C-18), 31.6 (t, C-11), 24.6 (t, C-12), 22.1 (q, C-19), 18.1 (t, C-2), 15.8 (q, C-20), 14.7 (q, C-17); HRFABMS *m/z* 344.2226 (calcd for $C_{21}H_{30}NO_3$ [$(M + H)^+$], 344.2226).

9α-Cyano-15,16-epoxy-7β-hydroxylabda-7,13(16),14-trien-6-one (4.2): white needles (from hexane/C_6H_6); mp 138-139℃; $[\alpha]_D^{25}$ -44 (*c* 0.7, $CHCl_3$); IR (film) ν_{max} 3397 (br), 2927, 2863, 2351, 2222, 1683 cm^{-1}; ^{1}H and ^{13}C NMR data, see Table 4.2; EIMS m/z (rel. int.) 341 [M^+] (13), 326 (100), 243 (12), 167 (15), 95 (17); HRFABMS m/z 341.1992 (calcd for $C_{21}H_{27}NO_3$ [$(M)^+$], 341.1990).

Crystal data for 4.2: $C_{21}H_{27}NO_3$, *M* = 341.44, monoclinic, space group $P2_1$ (no. 4), *a* = 6.2718 (1) Å, *b* = 14.6696(2) Å, *c* = 9.7782(2) Å, *β* = 103.735(1)°, *V* = 873.92(3) Å^3, *Z* = 2, D_c 1.298 Mg/m^3, *μ*(Mo K_α) = 0.086 mm^{-1}, *F*(000) = 368. A total of 3700 reflections were collected, of which 3410 were observed [$I>2\sigma(I)$]. The structure was solved by direct methods and refined on F^2 using all data, with non-hydrogen atoms treated anisotropically. All H atoms were located but were added in idealised positions in a riding model. The final *R* factors were R_1 = 0.0385 (all data), 0.0334 (observed data), wR_2 = 0.0846 (all data), 0.0816 (observed data) for 231 parameters. Crystallographic data (excluding structure factors) have been deposited at the Cambridge Crystallographic Data Centre (deposition no. 262101).

6α-Hydroxy-15,16-epoxylabda-8,13(16),14-trien-7-one (4.9): white plates; mp 88-89℃, lit.[148] 95-96℃; $[\alpha]_D^{32}$ +48 (*c* 1.0, $CHCl_3$), lit.[148] +51; IR (film) ν_{max} 2434, 2920, 2855, 1663, 1465 cm^{-1}; ^{1}H NMR ($CDCl_3$, 400 MHz), δ 7.37 (1H, t, *J* = 1.7 Hz, H-15), 7.26 (1H, dd, *J* = 1.4, 0.8 Hz, H-16), 6.30 (1H, dd, *J* = 1.7, 0.8 Hz, H-14), 4.39 (1H, d, *J* = 13.1 Hz, H-5), 3.77 (1H, s,

6-OH), 2.54 (2H, m, H_2-12), 2.52 (1H, m, H-11a), 2.44 (1H, m, H-11b), 1.95 (1H, m, H-9), 1.85 (3H, s, H_3-17), 1.69 (1H, d, *J* = 13.1 Hz, H-5), 1.68 (1H, m, H-2a), 1.57 (1H, m, H-2b), 1.46 (1H, m, H-3a), 1.39 (1H, ddd, *J* = 13.4, 12.5, 3.8 Hz, H-1b), 1.27 (1H, m, H-3b), 1.25 (3H, s, H_3-20), 1.17 (6H,s, H_3-18, H_3-19); ^{13}C NMR ($CDCl_3$, 100 MHz) δ 201.7 (s, C-7), 168.9 (s, C-9), 143.1 (d, C-15), 138.7 (d, C-16), 127.4 (s, C-8), 124.2 (s, C-13), 110.5 (d, C-14), 73.3 (d, C-6), 56.7 (d, C-5), 42.8 (t, C-3), 42.5 (s, C-10), 36.7 (t, C-1), 35.8 (q, C-18), 34.0 (s, C-4), 30.6 (t, C-11), 24.0 (t, C-12), 22.0 (q, C-19), 19.4 (q, C-20), 18.2 (t, C-2), 11.6 (q, C-17); HRFABMS *m/z* 317.2117 (calcd for $C_{20}H_{29}O_3$ [(M + H)$^+$], 317.2117).

6-Hydroxy-15,16-epoxylabda-5,8,13(16),14-tetraen-7-one (4.11): pale yellow oil; $[\alpha]_D^{32}$ -38 (*c* 0.7, $CHCl_3$), lit.[100] -41; IR (film) ν_{max} 3367, 2928, 1620, 1605, 1456 cm^{-1}; ^{1}H NMR ($CDCl_3$, 400 MHz) δ 7.38 (1H, t, *J* = 1.7 Hz, H-15), 7.28 (1H, m, H-16), 6.99 (1H, br s, 6-OH), 6.32 (1H, dd, *J* = 1.7, 0.8 Hz, H-14), 2.67 (1H, m, H-11b), 2.56 (1H, m, H_2-12), 2.53 (1H, m, H-11a), 2.05 (1H, m, H-1b), 1.98 (3H, s, H_3-17), 1.89 (1H, m, H-3b), 1.83 (1H, m, H-2b), 1.72 (1H, m, H-2a), 1.42 (1H, m H-3a), 1.38 (3H, s, H_3-18), 1.38 (6H, s, H_3-19, H_3-20); ^{13}C NMR ($CDCl_3$, 100 MHz) δ 181.7 (s, C-7), 165.8 (s, C-9), 143.1 (s, C-6 & d, C-15), 140.5 (s, C-5), 138.7 (d, C-16), 127.4 (s, C-8), 124.4 (s, C-13), 110.5 (d, C-14), 43.9 (s, C-10), 37.3 (t, C-3), 35.7 (s, C-4), 31.5 (t, C-11), 29.4 (t, C-1), 28.1 (q, C-18), 27.9 (q, C-20), 27.6 (q, C-19), 23.8 (t, C-12), 17.2 (t, C-2), 11.6 (q, C-17); HRFABMS *m/z* 315.1960 (calcd for $C_{20}H_{27}O_3$ [(M + H)$^+$], 315.1960).

*7.4.5 Lithium aluminium hydride reduction of **4.1***

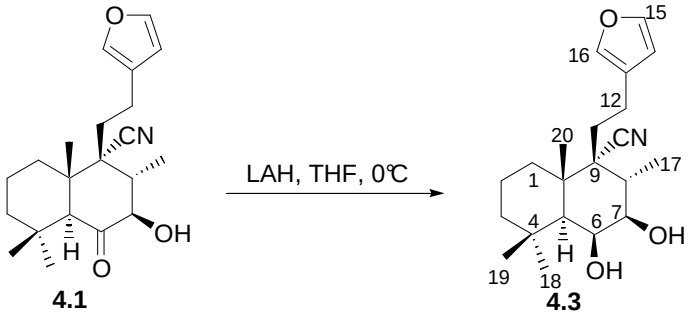

4.1 **4.3**

This method is representative. LAH (4 mg, 0.04 mmol) was dissolved in anhydrous THF (1.5 mL) and stirred (30 min) under an Ar atmosphere at 0℃. The nitrile was dissolved in anhydrous THF (2 mL) and added drop wise *via* cannula to the LAH solution. This mixture was maintained at 0℃ for a further 3 hours while stirring. HCl (1 M, 1 drop) was added, and the solution was neutralised with NaOH (1 M, 1 drop). The THF was removed *in vacuo* and the organic component taken up in EtOAc (5 mL) and washed with H_2O (3 X 2 mL). This organic fraction was dried ($MgSO_4$) and concentrated to afford a yellowish oil (17 mg). Subsequent purification by semi-preparative HPLC in (20% EtOAc, 80% hexane) afforded 9α-cyano-15,16-epoxy-6β,7β-dihydroxylabda-13(16),14-diene (**4.3**) as a colourless oil (13 mg, 98%).

9α-Cyano-15,16-epoxy-6β,7β-dihydroxylabda-13(16),14-diene (4.3): colourless oil; $[\alpha]_D^{19}$ +37 (*c* 1.2, $CHCl_3$); IR (film) ν_{max} 3437, 2938, 3859, 2852, 2221 cm^{-1}; ^1H NMR ($CDCl_3$, 400 MHz), δ 7.35 (1H, t, *J* = 1.6 Hz, H-15), 7.24 (1H, dd, *J* = 1.4, 0.9 Hz, H-16), 6.27 (1H, m, H-14), 4.28 (1H, dd, *J* = 3.2, 1.9 Hz, H-6), 3.52 (1H, dd, *J* = 10.9, 3.5 Hz, H-7), 2.65 (2H, m, H_2-12), 2.11 (1H, m, H-8), 1.95 (1H, ddd, *J* = 14.0, 12.2, 6.5 Hz, H-11b), 1.66 (1H, m, H-2b), 1.60 (2H, m, H_2-1), 1.55 (1H, m, H-2a), 1.53 (1H, m, H-11a), 1.44 (1H, d, *J* = 1.8 Hz, H-5), 1.41 (1H, m, H-3b), 1.28 (1H, m, H-3a), 1.26 (3H, m, H_3-17), 1.25 (6H, s, H_3-19, H_3-20), 1.03 (3H, s, H_3-18); ^{13}C NMR ($CDCl_3$, 100 MHz) δ 143.0 (d, C-15), 138.7 (d, C-16), 124.0 (s, C-13), 121.0 (s, C-21), 110.6 (d, C-14), 74.3 (d, C-7), 69.6 (d, C-6), 54.1 (s, C-9), 51.2 (d, C-5), 43.0 (t, C-3), 41.9 (s, C-10), 38.0 (d, C-8), 37.6 (t, C-1), 34.5 (s, C-4), 33.4 (q, C-18), 31.7 (t, C-11), 24.6 (t, C-12), 24.5 (q, C-19), 18.6 (t, C-2), 17.1 (q, C-17), 13.2 (q, C-20); HRFABMS *m/z* 345.2304 (calcd for $C_{21}H_{31}NO_3$ [M^+], 345.2304).

7.4.6 <u>In planta</u> test methods

The *in planta* assays were performed at Dow AgroSciences (Indianapolis, USA) and methods described here are as supplied by Dr B. Nader. For evaluations in 1 day protectant tests, samples of the compounds were dissolved in acetone at 2000 ppm, then diluted in acetone to 500 and 125 ppm. Samples were then brought to final concentrations of 200, 50 and 12.5

ppm by addition of 9 volumes of milli-Q water containing 110 ppm Triton X-100. Applications were made in 20 mL spray volumes using a turntable sprayer equipped with two Spraying Systems Co. 1/4JAUPM-SS nozzles with 4010055 fluid caps and a spray pressure of 206 kPa.

Inoculation of plants was done by spraying suspensions of 5 x 10^5 - 6 x 10^6 conidia per mL, depending on the pathogen, 1 day after application. Conidial suspensions were prepared with de-ionized water containing 3 drops of Tween-20 per 100 mL of suspension. Inoculated plants were placed in a dew room (99–100% relative humidity, 20℃) overnight to allow infection. The plants were then moved to either a greenhouse or growth chamber at a suitable temperature, daylength and humidity for expression of the disease.

Evaluations of disease control were made 6 days after inoculation in the case of *M. grisea* and 7 days after inoculation in the case of *P. recondita*, by visual estimation of disease severity. Percent disease control was calculated from disease severity ratings by the calculation: %DC = (1- $\%DS_{trt}/\%DS_{untrt}$) x 100, where %DC is percent disease control; $\%DS_{trt}$ is the observed percent disease severity for treated plants; and $\%DS_{untrt}$ is the observed percent disease severity for untreated controls.

7.5 Chapter Five Experimental

*7.5.1 Attempted synthesis of **5.1** and **5.2** via a modification of Wisch's synthetic strategy*

7.5.1.1 $KMnO_4$ oxidation of **5.3**[174;176;190;239;240]

Method A: Oxidation using Me_2CO (distilled over $KMnO_4$) as a solvent. Manool (**5.3**, 540 mg, 1.86 mmol) was dissolved in Me_2CO (30 mL) and finely powdered $KMnO_4$ (1.18 g, 7.44 mmol, 4 eq) was added slowly over 2 hours. The temperature of the the reaction mixture was maintained between 16℃ and 20℃ and stirring conti nued (48 h).The reaction mixture was allowed to settle (24 h) and filtered through Celite (545 coarse) after which the solvent was

removed *in vacuo*. The reaction mixture was taken up in CH_2Cl_2 (15 mL) and washed with a mixture of 3% aqueous oxalic acid (10 mL) and saturated aqueous $Na_2S_2O_3$ (10 mL) to reduce the brown MnO_2 precipitate. The organic fraction was washed with H_2O (2 x 15 mL), dried ($MgSO_4$) and concentrated to afford a yellow oil (360 mg) which was purified using silica flash chromatography (10% EtOAc, 90% hexane) to afford **5.14** (176 mg, 36%) as a colourless oil.

Method B: $KMnO_4$ mediated oxidation of **5.3** using CH_2Cl_2 as a solvent with phenyltriethylammonium chloride (PTEACl) as a phase transfer catalyst

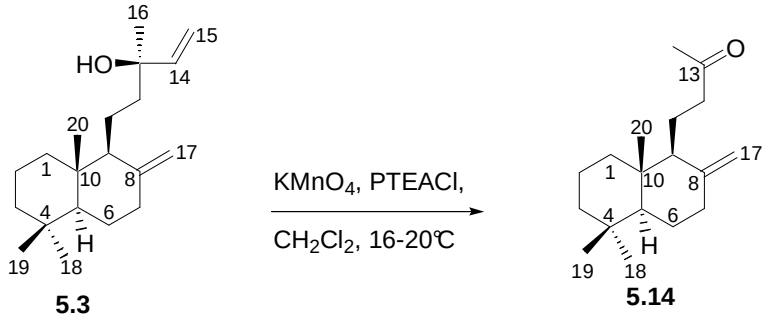

5.3 **5.14**

This method is representative. Manool (**5.3**, 1.00g, 3.46 mmol) and PTEACl (1.84 g, 37.0 mmol, 10.7 eq) were dissolved in CH_2Cl_2 (100 mL) and finely powdered $KMnO_4$ (1.69 g, 10.7 mmol, 3 eq) was added slowly over 2 hours. The temperature of the reaction mixture was maintained between 16℃ and 20℃ and stirring conti nued (48 h).The reaction mixture was allowed to settle (24 h) and filtered through Celite (545 coarse) after which the solvent was removed *in vacuo*. The reaction mixture was taken up in CH_2Cl_2 (15 mL) and washed with a mixture of 1.5% aqueous oxalic acid (30 mL) and saturated aqueous $Na_2S_2O_3$ (15 mL), which reduced the brown precipitate. The organic fraction was washed with H_2O (2 x 15 mL), dried ($MgSO_4$) and concentrated to afford a yellow oil (652 mg) which was purified using silica flash chromatography (10% EtOAc, 90% hexane) to afford 14,15-bisnorlabd-8(17)-en-13-one (**5.14**, 512 mg, 56%) as a colourless oil and manool (**5.3**, 34 mg, 3%).

14,15-Bisnorlabd-8(17)-en-13-one (5.14):[174-176;239;241;242] colourless oil; $[\alpha]_D^{32}$ +32 (*c* 2.9, $CHCl_3$) lit.[242] +35.8; IR (film) ν_{max} 2926, 2834, 1711, 1641, 1455 cm^{-1}; ^1H NMR ($CDCl_3$, 400 MHz) δ 4.82 (1H, br s, H-17b), 4.43 (1H, br s, H-17a), 2.55 (1H, ddd, *J* = 12.7, 9.3, 4.0 Hz, H-12b), 2.37 (1H, ddd, *J* = 12.7, 4.2, 2.5 Hz, H-7b), 2.29 (1H, m, H-12a), 2.08 (3H, s, H_3-16), 1.94 (1H, m, H-7b), 1.84 (1H, m, H-11a), 1.78 (1H, m, H-1b), 1.72 (1H, m, H-6b), 1.55 (2H, m, H-9, H-11b), 1.54 (1H, m, H-2b), 1.50 (1H, m, H-2a), 1.37 (1H, m, H-3b), 1.29 (1H, dddd, *J* = 13.4, 13.4, 13.1, 4.4 Hz, H-6b), 1.17 (1H, ddd, *J* = 13.2, 13.2, 4.2 Hz, H-3b), 1.10 (1H, m, H-1a), 1.09 (1H, dd, *J* = 12.6, 2.5, Hz, H-5), 0.83 (3H, s, H_3-18), 0.80 (3H, s, H_3-19), 0.69 (3H, s, H_3-20); ^{13}C NMR ($CDCl_3$, 100 MHz) δ 209.1 (s, C-13), 148.4 (s, C-8), 106.3 (t, C-17), 56.4 (d, C-9), 55.6 (d, C-5), 42.9 (t, C-12), 42.2 (t, C-3), 39.8 (s, C-10), 39.1 (t, C-7), 33.6 (q, C-18), 33.6 (s, C-4), 29.9 (q, C-16), 24.5 (t, C-6), 21.7 (q, C-19), 19.4 (t, C-2), 17.7 (t, C-11), 14.3 (q, C-20); HRFABMS *m/z* 262.2296 (calcd for $C_{18}H_{30}O$ [M^+], 262.2297).

7.5.1.2 Reduction of methyl ketone **5.14** with LAH

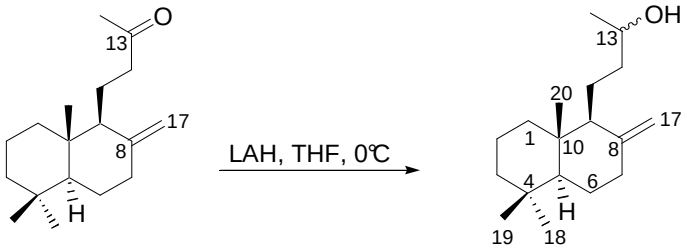

5.14

5.15 13-(*R*)
5.17 13-(*S*)

This method is representative. Methyl ketone (**5.14**, 90 mg, 0.34 mmol) was dissolved in anhydrous THF (2 mL) and added *via* cannula to a 0℃ solution of LAH (26 mg, 0.69 mmol, 2 eq) in anhydrous THF (10 mL). The reaction was allowed to warm naturally to ambient temperature (3 h) before 5% aqueous $NaHCO_3$ (3 drops) was added. The reaction mixture was acidified with 1M HCl (0.5 mL), concentrated to dryness, taken up in EtOAc (5 mL) and washed with H_2O (3 x 5 mL). The organic fraction was dried ($MgSO_4$) and concentrated to afford a colourless oil (92 mg). Semi-preparative HPLC (14% EtOAc, 86% hexane) followed to afford **5.17** 14,15-bisnorlabd-8(17)-en-13*S*-ol (**5.17,** 45 mg, 53%) and 14,15-bisnorlabd-8(17)-en-13*R*-ol (**5.15,** 39 mg, 40%) as colourless oils in 93% combined isolated yield.

14,15-Bisnorlabd-8(17)-en-13*R*-ol (5.15): colourless oil; $[\alpha]_D^{34}$ +28 (*c* 1.0, $CHCl_3$); IR (film) ν_{max} 3353, 2832, 1645, 1462, 1387 cm^{-1}; ^1H NMR ($CDCl_3$, 400 MHz) δ 4.81 (1H, br s, H-17b), 4.48 (1H, br s, H-17a), 3.76 (1H, m, H-13), 2.38 (1H, ddd, *J* = 12.7, 4.1, 2.4 Hz, H-7b), 1.97 (1H, ddd, *J* = 13.6, 12.7, 5.0 Hz, H-7a), 1.77 (1H, m, H-1b), 1.72 (1H, m, H-6b), 1.59 (2H, m, H-2b, H-12b), 1.58 (1H, m, H-9), 1.56 (2H, m, H-2a, H-11b), 1.46 (1H, m, H-11a), 1.38 (1H, m, H-3b), 1.31 (1H, m, H-6b), 1.29 (1H, m, H-2a), 1.26 (1H, m, H-12a), 1.18 (1H, m, H-3a), 1.17 (3H, d, *J* = 6.2 Hz, H_3-16), 1.07 (1H, dd, *J* = 12.7, 2.8 Hz, H-5), 1.02 (1H, ddd, *J* = 13.2, 12.8, 3.6 Hz, H-1a), 0.86 (3H, s, H_3-18), 0.79 (3H, s, H_3-19), 0.67 (3H, s, H_3-20); ^{13}C NMR ($CDCl_3$, 100 MHz) δ 148.8 (s, C-8), 106.2 (t, C-17), 68.9 (d, C-13), 57.0 (d, C-9), 55.6 (d, C-5), 42.2 (t, C-3), 39.8 (s, C-10), 39.1 (t, C-1), 38.6 (t, C-12), 38.4 (t, C-7), 33.62 (q, C-18), 33.57 (s, C-4), 24.5 (t, C-6), 23.5 (q, C-16), 21.7 (q, C-19), 19.8 (t, C-2), 19.4 (t, C-11), 14.4 (q, C-20); HRFABMS *m*/*z* 264.2453 (calcd for $C_{18}H_{32}O$ [M^+], 264.2453).

14,15-Bisnorlabd-8(17)-en-13*S*-ol (5.17): colourless oil; $[\alpha]_D^{34}$ +30 (*c* 1.5, $CHCl_3$); IR (film) ν_{max} 3391, 2923, 1644, 1456, 1410 cm^{-1}; ^1H NMR ($CDCl_3$, 400 MHz) δ 4.81 (1H, br s, H-17b), 4.52 (1H, br s, H-17a), 3.76 (1H, m, H-13), 2.38 (1H, ddd, *J* = 12.6, 4.0, 2.0 Hz, H-7b), 1.95 (1H, ddd, *J* = 13.4, 12.6, 4.8 Hz, H-7a), 1.76 (1H, m, H-1b), 1.70 (1H, m, H-6b), 1.57 (2H, m, H-9, H-12b), 1.56 (1H, m, H-2b), 1.52 (1H, H-2a), 1.50 (H, m, H-11b), 1.46 (1H, H-11a), 1.37 (1H, m, H-3b), 1.30 (1H, m, H-6a), 1.22 (1H, m, H-12a), 1.17 (3H, d, *J* = 6.2 Hz, H_3-16), 1.16 (1H, m, H-3a), 1.08 (1H, dd, *J* = 12.7, 2.6 Hz, H-5), 1.01 (1H, ddd, *J* = 13.5, 12.8, 3.6 Hz, H-1a), 0.86 (3H, s, H_3-18), 0.79 (3H, s, H_3-19), 0.67 (3H, s, H_3-20); ^{13}C NMR ($CDCl_3$, 100 MHz) δ 148.6 (s, C-8), 106.5 (t, C-17), 68.4 (d, C-13), 56.8 (d, C-9), 55.6 (d, C-5), 42.2 (t, C-3), 39.7 (s, C-10), 39.1 (t, C-1), 38.4 (t, C-7), 38.3 (t, C-12), 33.62 (q, C-18), 33.57 (s, C-4), 24.4 (t, C-6), 23.6 (q, C-16), 21.7 (q, C-19), 19.5 (t, C-11), 19.4 (t, C-2), 14.4 (q, C-20); HRFABMS *m*/*z* 264.2454 (calcd for $C_{18}H_{32}O$ [M^+], 264.2453).

7.5.1.3 Preparation of the (*R*)- and (*S*)-MTPA esters of **5.17**

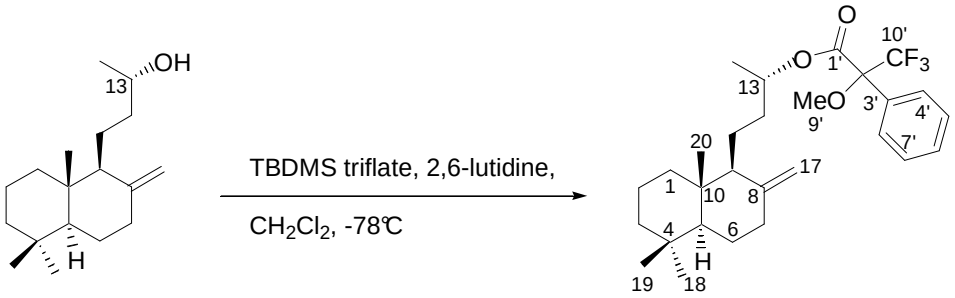

5.17

5.18 (*S*)-MTPA ester
5.19 (*R*)-MTPA ester

This method is representative for the preparation of either the (*R*)- or (*S*)-MTPA esters of **5.17**. *R*-α-methoxy-α-trifluoromethylphenylacetic acid (37 mg), DCC (74 mg) and DMAP (11 mg) were added to a solution of **5.17** in anhydrous CH_2Cl_2 (2 mL). The solution was shaken periodically over period of 1.5 hours at ambient temperature, diluted with a combination of EtOAc (8 mL) and H_2O (1 mL) and filtered. The resulting solution was washed with 1M HCl (1 mL), H_2O (3 mL), saturated aqueous $NaHCO_3$ (2 mL) and once more with H_2O (3 mL) in the order presented. The resulting colourless oil (19 mg) was purified by semi-preparative HPLC (hexane) to afford **5.19** (6 mg). The (*S*)-MTPA ester (**5.18**) of **5.17** was similarly prepared from *S*-α-methoxy-α-trifluoromethylphenylacetic acid.

(*S*)-MTPA ester (5.18): ^{1}H NMR ($CDCl_3$, 600 MHz) δ 7.53 (2H, m, H-4', H-8'), 7.38 (3H, m, H-5', H-6', H-7'), 5.10 (1H, m, H-13), 4.77 (1H, s, H-17b), 4.39 (1H, s, H-17a), 3.53 (3H, s, H_3-9'), 2.35 (1H, ddd, *J* = 12.7, 3.9, 2.4 Hz, H-7b), 1.93 (1H, ddd, *J* = 13.6, 13.0, 4.9 Hz, H-7a), 1.83 (1H, m, H-12b), 1.70 (1H, m, H-6b), 1.67 (1H, m, H-1b), 1.58 (1H, m, H-9), 1.54 (1H, m, H-2b), 1.54 (1H, m, H-2a), 1.38 (2H, m, H-3b, H-12b), 1.37 (1H, m, H-11b), 1.30 (1H, m, H-6a), 1.24 (1H, m, H-11a), 1.24 (1H, d, *J* = 6.2 Hz, H_3-16), 1.16 (1H, ddd, *J* = 13.7, 13.4, 3.8 Hz, H-3a), 1.06 (1H, dd, *J* = 12.6, 2.6 Hz, H-5), 0.98 (1H, ddd, *J* = 13.7, 13.0, 3.8 Hz, H-1a), 0.86 (3H, s, H_3-18), 0.79 (3H, s, H_3-19), 0.63 (3H, s, H_3-20); ^{13}C NMR ($CDCl_3$, 150 MHz) δ 166.3 (s, C-1'), 148.1 (s, C-8), 132.4 (s, C-3'), 129.5 (d, C-5'), 129.5 (d, C-7'), 128.4 (d, C-6'), 127.5 (d, C-4'), 127.5 (d, C-8'), 124.4 (s, C-10'), 122.5 (s, C-2'), 106.5 (t, C-17), 74.7 (d, C-13),

56.6 (d, C-9), 55.5 (d, C-5), 55.5 (q, C-9'), 42.1 (t, C-3), 39.7 (s, C-10), 39.1 (t, C-1), 38.3 (t, C-7), 34.7 (t, C-12), 33.61 (q, C-18), 33.57 (s, C-4), 24.4 (t, C-6), 21.7 (q, C-19), 19.7 (q, C-16), 19.4 (t, C-2), 19.4 (t, C-11), 14.4 (q, C-20).

(*R*)-MTPA ester (5.19): ^{1}H NMR ($CDCl_3$, 600 MHz) δ 7.54 (2H, m, H-4', H-8'), 7.38 (3H, m, H-5', H-6', H-7'), 5.12 (1H, m, H-13), 4.69 (1H, s, H-17b), 4.22 (1H, s, H-17a), 3.57 (3H, d, *J* = 0.7 Hz, H_3-9'), 2.32 (1H, ddd, *J* = 12.7, 4.1, 2.4 Hz, H-7b), 1.90 (1H, ddd, *J* = 13.7, 13.0, 4.9 Hz, H-7a), 1.77 (1H, m, H-12b), 1.68 (1H, m, H-6b), 1.62 (1H, m, H-1b), 1.53 (1H, m, H-3b), 1.48 (1H, d, *J* = 11.2 Hz, H-9), 1.44 (1H, m, H-2a), 1.37 (2H, m, H-3b, H-11b), 1.31 (3H, d, *J* = 5.0 Hz, H_3-16), 1.29 (1H, m, H-12a), 1.26 (1H, m, H-6a), 1.23 (1H, m, H-11a), 1.16 (1H, ddd, *J* = 13.7, 13.4, 4.0 Hz, H-3a), 1.02 (1H, dd, *J* = 12.6, 2.7 Hz, H-5), 0.91 (1H, ddd, *J* = 13.7, 13.0, 3.8 Hz, H-1a), 0.85 (3H, s, H_3-18), 0.78 (3H, s, H_3-19), 0.57 (3H, s, H_3-20); ^{13}C NMR ($CDCl_3$, 150 MHz) δ 166.2 (s, C-1'), 148.0 (s, C-8), 132.7 (s, C-3'), 129.4 (d, C-5'), 129.4 (d, C-7'), 128.3 (d, C-6'), 127.2 (d, C-4'), 127.2 (d, C-8'), 124.2 (s, C-10'), 122.5 (s, C-2'), 106.5 (t, C-17), 74.5 (d, C-13), 56.7 (d, C-9), 55.5 (d, C-5), 55.4 (q, C-9'), 42.1 (t, C-3), 39.6 (s, C-10), 39.0 (t, C-1), 38.3 (t, C-7), 34.9 (t, C-12), 33.60 (q, C-18), 33.55 (s, C-4), 24.4 (t, C-6), 21.7 (q, C-19), 20.1 (q, C-16), 19.4 (t, C-2), 19.1 (t, C-11), 14.4 (q, C-20).

7.5.1.4 TBDMS protection of the 14,15-bisnorlabd-8(17)-en-13-ols, **5.15** and **5.17**

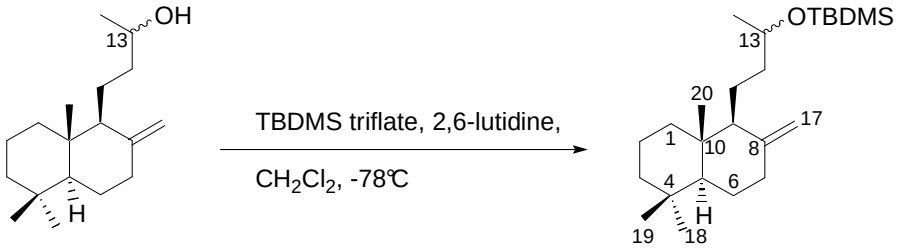

5.15 13-(*R*)
5.17 13-(*S*)

5.8 13-(*R*)
5.9 13-(*S*)

A solution of a mixture of **5.15** and **5.17** (346 mg, 1.31 mmol) in anhydrous CH_2Cl_2 (5 mL) was cooled (-78℃) and 2,6-lutidine (3.01 mmol, 2.4 eq) followed by TBDMS triflate (2.03 mmol, 1.6 eq) were added. The reaction mixture was allowed to warm naturally to ambient

temperature and was stirred for a further 2 hours, after which 50% AcOH (6 mL) was added and the organic and inorganic layers separated. The organic fraction was washed with H_2O (3 x 5 mL), dried ($MgSO_4$) and concentrated to afford a pale brown oil (473 mg). Subsequent purification by silica flash chromatography (5% EtOAc, 95% hexane) afforded a mixture of 13-*tert*-butyldimethylsilanyloxy-14,15-bisnorlabd-8(17)-enes **5.8** and **5.9** (441 mg, 89% combined isolated yield).

13-*tert*-Butyldimethylsilanyloxy-14,15-bisnorlabd-8(17)-enes (5.8 and 5.9): pale brown oil; ^1H and ^{13}C NMR data consistent with literature values;[173]; HRFABMS *m*/*z* 379.3397 (calcd for $C_{24}H_{47}SiO$ [$(M + H)^+$], 379.3396).

7.5.1.5 Reductive ozonolysis of the TMDMS ethers **5.17** and **5.15**[173]

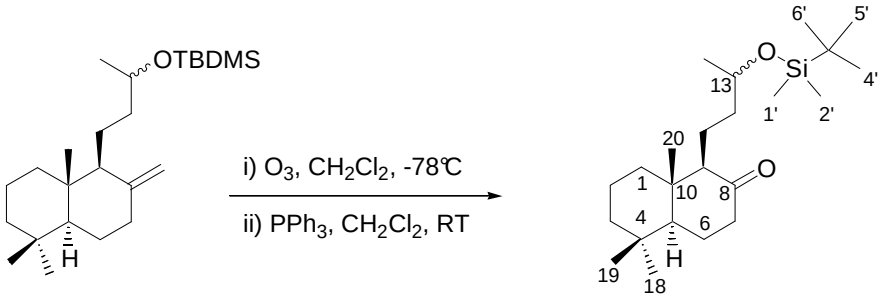

5.8 13-(*R*)
5.9 13-(*S*)

5.10 13-(*R*)
5.11 13-(*S*)

A mixture of **5.17** and **5.15** (208 mg, 0.43 mmol) were dissolved in anhydrous CH_2Cl_2 (20 mL), the solution chilled to -78℃ and O_3 bubbled through for 10 minutes, until the solution had turned blue, indicating that the solution was saturated with O_3. While allowing the reaction mixture to warm to ambient temperature, N_2 was bubbled through the solution to remove any excess O_3. After one hour, triphenylphosphine (450 mg, 3.1 eq) was added and allowed to stir (4 h), after which H_2O_2 (30%, 5 mL) was added slowly (over a period of 30 minutes) to oxidize the remaining triphenylphosphine. The solution was washed with saturated brine (1 x 10 mL) and H_2O (2 x 10 mL), concentrated *in vacuo*, taken up in 15% EtOAc in hexane and passed through a silica plug (5 mL) to remove any remaining triphenylphosphine oxide. The C-13 epimers were separated by semi-preparative HPLC (5% EtOAc, 95% hexane) to afford 13*S*-

tert-butyldimethylsilanyloxy-14,15,17-trisnorlabdan-8-one (**5.10**, 115 mg, 55%) and 13*R*-*tert*-butyldimethylsilanyloxy-14,15,17-trisnorlabdan-8-one (**5.11**, 71 mg, 34%) in 89% overall yield.

13*S*-*tert*-Butyldimethylsilanyloxy-14,15,17-trisnorlabdan-8-one (5.10): colourless oil; $[\alpha]_D^{34}$ -34 (*c* 4.1, $CHCl_3$), lit.[173] -32; IR (film) ν_{max} 2929, 2856, 1713, 1460, 1254 cm^{-1}; ^1H NMR ($CDCl_3$, 400 MHz) δ 3.76 (1H, m, H-13), 2.38 (1H, ddd, *J* = 13.2, 4.9, 2.2 Hz, H-7b), 2.26 (1H, dddd, *J* = 13.4, 13.2, 7.0, 1.0 Hz, H-7a), 2.02 (1H, m, H-6b), 2.01 (1H, m, H-9), 1.74 (1H, m, H-1b), 1.66 (1H, m, H-11b), 1.63 (1H, m, H-6a), 1.49 (2H, m, H_2-2), 1.48 (1H, m, H-12b), 1.46 (1H, m, H-5), 1.43 (1H, m, H-3b), 1.22 (1H, m, H-3a), 1.17 (2H, m, H-3a, H-11a), 1.09 (3H, d, *J* = 6.2 Hz, H_3-16), 1.09 (1H, m, H-1a), 0.94 (3H, s, H_3-19), 0.86 (9H, s, H_3-4', H_3-5', H_3-6'), 0.82 (3H, s, H_3-19), 0.69 (3H, s, H_3-20), 0.03 (3H, s, H_3-1'), 0.02 (3H, s, H_3-2'); ^{13}C NMR ($CDCl_3$, 100 MHz) δ 212.0 (s, C-8), 68.7 (d, C-13), 64.5 (d, C-9), 54.3 (d, C-5), 42.8 (s, C-10), 42.7 (t, C-7), 42.0 (t, C-3), 39.3 (t, C-1), 39.0 (t, C-12), 33.7 (s, C-4), 33.5 (q, C-18), 25.9 (q, C-4', C-5', C-6'), 24.1 (q, C-16), 23.1 (t, C-6), 21.7 (q, C-19), 19.0 (t, C-2), 18.1 (s, C-3'), 17.1 (t, C-11), 14.6 (q, C-20), -4.5 (q, C-1'), -4.7 (q, C-2'); HRFABMS *m*/*z* 380.3111 (calcd for $C_{23}H_{44}SiO_2$ $[M^+]$, 380.3111).

13*R*-*tert*-Butyldimethylsilanyloxy-14,15,17-trisnorlabdan-8-one (5.11): colourless oil; $[\alpha]_D^{34}$ -32 (*c* 3.5, $CHCl_3$), lit.[173] -37; IR (film) ν_{max} 2929, 2856, 1714, 1462, 1255 cm^{-1}; ^1H NMR ($CDCl_3$, 400 MHz) δ 3.74 (1H, m, H-13), 2.38 (1H, ddd, *J* = 13.2, 4.9, 2.2 Hz, H-7b), 2.27 (1H, m, H-7a), 2.04 (1H, m, H-6b), 1.98 (1H, m, H-9), 1.77 (1H, m, H-1b), 1.63 (1H, m, H-6a), 1.57 (1H, m, H-11b), 1.51 (1H, m, H-5), 1.50 (2H, m, H_2-2), 1.46 (1H, m, H-12b), 1.42 (1H, m, H-3b), 1.38 (1H, m, H-11a), 1.22 (1H, m, H-12a), 1.16 (1H, m, H-12a), 1.04 (1H, m, H-1a), 1.08 (3H, d, *J* = 6.1 Hz, H_3-16), 0.94 (3H, s, H_3-18), 0.87 (9H, s, H_3-4', H_3-5', H_3-6') 0.83 (3H, s, H_3-19), 0.70 (3H, s, H_3-20), 0.03 (3H, H_3-1'), 0.02 (3H, s, H_3-2'); ^{13}C NMR ($CDCl_3$, 100 MHz) δ 212.3 (s, C-8), 69.2 (d, C-13), 64.5 (d, C-9), 54.3 (d, C-5), 42.8 (s, C-10), 42.7 (t, C-7), 41.9 (t, C-3), 39.5 (t, C-1), 39.3 (t, C-12), 33.7 (s, C-4), 33.5 (q, C-18), 25.9 (q, C-4', C-5', C-6'), 24.2 (q, C-16), 24.1 (t, C-6), 21.7 (q, C-19), 19.1 (t, C-2), 18.7 (t, C-11), 18.1 (s, C-3'), 14.7 (3H, s, H_3-20), -4.3 (q, C-1'), -4.6 (q, C-2'); HRFABMS *m*/*z* 380.3111 (calcd for $C_{23}H_{44}SiO_2$ $[M^+]$, 380.3111).

7.5.1.6 Nucleophilic addition of MeLi to **5.11** and **5.10**[173]

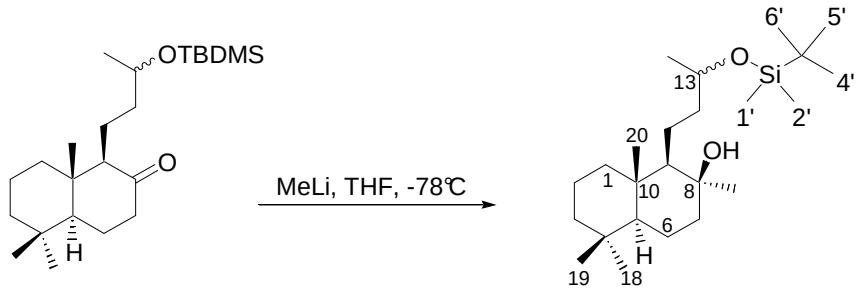

5.10 13-(*R*)
5.11 13-(*S*)

5.20 13-(*R*)
5.21 13-(*S*)

This method is representative of the methylation of both **5.11** and **5.10**. A solution of **5.11** (25 mg, 0.07 mmol) in anhydrous THF (5 mL) was cooled to -78℃ and 1.6 M MeLi solution (0.19 mmol, 2.5 eq) added drop wise . The solution was allowed to reach ambient temperature and left to stir (14 h). Excess MeLi was quenched with an ice cold slurry of saturated aqueous $NaHCO_3$ (2 mL), all THF removed *in vacuo* and the contents of the reaction vessel taken up in Et_2O (5 mL). The Et_2O solution was washed with H_2O (3 x 5 mL), dried ($MgSO_4$) and concentrated to a yellow oil (27 mg), which was subsequently purified by semi-preparative HPLC (10% EtOAc, 90% hexane) to afford 13*R*-*tert*-butyldimethylsilanyloxy-14,15-bisnorlabd-8(17)-en-8β-ol (**5.20**, 20 mg, 82% yield) as a pale yellow oil. 13*S*-*tert*-Butyldimethylsilanyloxy-14,15-bisnorlabd-8(17)-en-8β-ol **(5.21**) was similarly prepared from **5.10** in identical yield.

13*R*-*tert*-Butyldimethylsilanyloxy-14,15-bisnorlabd-8(17)-en-8β-ol (5.20): pale yellow amorphous solid; $[\alpha]_D^{26}$ +8 (*c* 2.2, $CHCl_3$), lit.[173] +15; IR (film) ν_{max} 2926, 2863, 1471, 1372, 1256 cm^{-1}; ^1H NMR ($CDCl_3$, 400 MHz) δ 3.74 (1H, m, H-13), 1.73 (1H, m, H-7b), 1.68 (1H, m, H-12b), 1.60 (1H, m, H-2b), 1.52 (1H, m, H-6b), 1.48 (1H, m, H-6a), 1.49 (1H, m, H-7a), 1.48 (1H, m, H-12b), 1.44 (1H, m, H-12a), 1.42 (1H, m, H-11b), 1.39 (1H, m, H-2a), 1.38 (1H, m, H-3b), 1.28 (1H, m, H-11a), 1.13 (1H, m, H-3a), 1.12 (3H, d, *J* = 6.2 Hz, H_3-16), 1.11 (3H, s, H_3-17), 0.94 (3H, s, H_3-20), 0.88 (9H, s, H_3-4', H_3-5', H_3-6'), 0.87 (1H, m, H-1a), 0.85 (3H, s, H_3-18), 0.85 (1H, m, H-5), 0.81 (3H, s, H_3-19), 0.75 (1H, m, H-9), 0.05 (3H, s, H_3-1') 0.04 (3H, s, H_3-2'); ^{13}C NMR ($CDCl_3$, 100 MHz) δ 73.3 (s, C-8), 69.1 (d, C-13), 59.1 (d, C-9), 56.0 (d, C-5), 43.8 (t, C-12), 42.2 (t, C-7), 42.1 (t, C-3), 39.2 (t, C-1), 39.1 (s, C-10), 33.4 (q, C-18), 33.3

(s, C-4), 30.6 (q, C-17), 25.9 (q, C-4', C-5', C-6'), 23.6 (q, C-16), 21.7 (q, C-19), 21.4 (t, C-11), 18.3 (t, C-2), 18.2 (s, C-3'), 18.1 (d, C-6), 15.0 (q, C-20), -4.4 (q, C-1'), -4.7 (q, C-2'); HRFABMS *m*/*z* 396.3424 (calcd for $C_{24}H_{48}SiO_2$ [M^+], 396.3424).

13*S*-*tert*-Butyldimethylsilanyloxy-14,15-bisnorlabd-8(17)-en-8β-ol (5.21): pale yellow oil; $[\alpha]_D^{26}$ +13 (*c* 1.7, $CHCl_3$), lit.[173] +11; IR (film) ν_{max} 2915, 2856, 1469, 1366, 1252 cm^{-1}; ^1H NMR ($CDCl_3$, 400 MHz) δ 3.74 (1H, m, H-13), 1.73 (1H, m, H-7b), 1.68 (1H, m, H-12b), 1.60 (1H, m, H-2b), 1.52 (1H, m, H-6b), 1.48 (1H, m, H-6a), 1.49 (1H, m, H-7a), 1.43 (1H, m, H-12b), 1.42 (1H, m, H-11b), 1.40 (1H, m, H-12a), 1.39 (1H, m, H-2a), 1.38 (1H, m, H-3b), 1.23 (1H, m, H-11a), 1.13 (1H, m, H-3a), 1.12 (3H, d, *J* = 6.0 Hz, H_3-16), 1.12 (3H, s, H_3-17), 0.94 (3H, s, H_3-20), 0.88 (9H, s, H_3-4', H_3-5', H_3-6'), 0.87 (1H, m, H-1a), 0.85 (3H, s, H_3-18), 0.85 (1H, m, H-5), 0.81 (3H, s, H_3-19), 0.75 (1H, m, H-9), 0.04 (6H, s, H_3-1', H_3-2'); ^{13}C NMR ($CDCl_3$, 100 MHz) δ 73.2 (s, C-8), 69.0 (d, C-13), 59.2 (d, C-9), 56.0 (d, C-5), 43.7 (t, C-12), 42.2 (t, C-7), 42.1 (t, C-3), 39.2 (t, C-1), 38.9 (s, C-10), 33.4 (q, C-18), 33.2 (s, C-4), 30.6 (q, C-17), 25.9 (q, C-4', C-5', C-6'), 23.5 (q, C-16), 21.7 (q, C-19), 21.1 (t, C-11), 18.3 (t, C-2), 18.2 (t, C-6), 18.2 (s, C-3'), 15.1 (q, C-20), -4.5 (q, C-1'), -4.7 (q, C-2'); HRFABMS *m*/*z* 396.3424 (calcd for $C_{24}H_{48}SiO_2$ [M^+], 396.3424).

7.5.1.7 TBAF mediated deprotection of **5.21** and **5.20**[173]

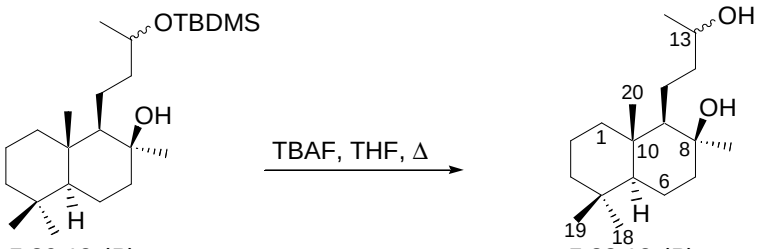

5.20 13-(*R*)
5.21 13-(*S*)

5.22 13-(*R*)
5.23 13-(*S*)

This method is representative for the deprotection of both **5.21** and **5.20**. A solution of **5.20** (42 mg, 0.11 mmol) and TBAF (1 M, 0.66 mmol, 6 eq) in THF (2 mL) was refluxed (4 h). The solution was allowed to cool to ambient temperature and saturated aqueous NH_4Cl (2.5 mL) added. The THF was removed *in vacuo* and the solution taken up in Et_2O (5 mL). The organic

fraction was washed with H_2O (3 x 5 mL), dried ($MgSO_4$) and concentrated to afford a yellow oil (35 mg). Semi-preparative HPLC (50% EtOAc, 50% hexane) followed to afford 14,15-bisnorlabd-8(17)-en-8β,13*R*-diol (**5.22**, 26 mg, 87%) which could be crystallized by slow evaporation from Et_2O. 14,15-bisnorlabd-8(17)-en-8β,13*S*-diol (**5.23**) was similarly prepared from **5.21** in similar yield.

14,15-Bisnorlabd-8(17)-en-8β,13*R*-diol (5.22): pale yellow plates (from ether); mp 95-96℃; $[\alpha]_D^{26}$ +9 (*c* 5.6, $CHCl_3$), lit.[173] +18; IR (film) ν_{max} 3384, 2923, 2856, 1464, 1384 cm^{-1}; ^1H NMR ($CDCl_3$, 400 MHz) δ 3.75 (1H, m, H-13), 1.73 (1H, m, H-7b), 1.69 (1H, m, H-1b), 1.59 (1H, m, H-6b), 1.52 (2H, m, H_2-2), 1.50 (1H, m, H-11b), 1.49 (2H, m, H-3b, H-12b), 1.46 (1H, m, H-7a), 1.44 (1H, m, H-6b), 1.38 (2H, m, H-12a, H-11a), 1.19 (3H, d, *J* = 6.2 Hz, H_3-16), 1.15 (1H, m, H-3a), 1.12 (3H, s, H_3-17), 0.94 (3H, s, H_3-20), 0.86 (1H, m, H-1a), 0.85 (3H, s, H_3-18), 0.82 (1H, m, H-5), 0.81 (3H, s, H_3-19), 0.77 (1H, m, H-9); ^{13}C NMR ($CDCl_3$, 100 MHz) δ 73.2 (s, C-8), 68.6 (d, C-13), 59.1 (d, C-9), 55.9 (d, C-5), 43.2 (t, C-12), 42.2 (t, C-7), 42.0 (t, C-3), 39.2 (t, C-1), 39.0 (s, C-10), 33.4 (q, C-18), 33.2 (s, C-4), 30.6 (q, C-17), 23.4 (q, C-16), 21.6 (q, C-19), 21.3 (t, C-11), 18.3 (t, C-2), 18.1 (t, C-6), 15.1 (q, C-20); HRFABMS *m*/*z* 282.2557 (calcd for $C_{18}H_{34}O_2$ [M^+], 282.2559).

Crystal data for 5.22: $C_{18}H_{34}O_2$, *M* = 282.45, 0.25 x 0.25 x 0.20 mm^3, orthorhombic, space group $P2_12_12_1$ (No. 19), *a* = 8.4923(2), *b* = 9.9407(2), *c* = 20.4323(4) Å, *V* = 1724.88(6) $Å^3$, *Z* = 4, D_c = 1.088 g/cm^3, F_{000} = 632, MoKα radiation, λ = 0.71073 Å, *T* = 113(2)K, $2\theta_{max}$ = 52.7º, 3520 reflections collected, 3520 unique (R_{int} = 0.0000). Final *GooF* = 1.045, *R1* = 0.0433, *wR2* = 0.0999, *R* indices based on 2781 reflections with I >2sigma(I) (refinement on F^2), 195 parameters, 0 restraints. Lp corrections applied, μ = 0.068 mm^{-1}. Absolute structure parameter = -1.8(12).[237] Tables of atmomic co-ordinates and interatomic bond angles and bond lengths have not been deposited with the Cambridge data base and are provided in Appendix II.

14,15-Bisnorlabd-8(17)-en-8β,13*S*-diol (5.23): pale yellow amorphous solid; $[\alpha]_D^{26}$ +16 (*c* 2.4, $CHCl_3$), lit.[173] +8; IR (film) ν_{max} 3321, 2923, 2863, 1462, 1370 cm^{-1}; ^1H NMR ($CDCl_3$, 400 MHz) δ 3.75 (1H, m, H-13), 1.72 (1H, m, H-7b), 1.66 (1H, m, H-1b), 1.58 (1H, m, H-6b), 1.55 (1H, m, H-11b), 1.54 (1H, m, H-12b), 1.49 (3H, m, H_2-2, H-7a), 1.45 (1H, m, H-12a), 1.38 (1H, m, H-3b), 1.26 (1H, m, H-11a), 1.17 (3H, d, *J* = 6.4 Hz, H_3-16), 1.13 (1H, m, H-3b), 1.12 (3H, s, H_3-17), 0.93 (3H, s, H_3-20), 0.87 (1H, m, H-1a), 0.85 (1H, m, H-5), 0.84 (3H, s, H_3-18), 0.80 (3H, s, H_3-19), 0.76 (1H, dd, *J* = 4.4, 2.6 Hz, H-9); ^{13}C NMR ($CDCl_3$, 100 MHz) δ 73.2 (s, C-8), 68.5 (d, C-13), 59.0 (d, C-9), 55.9 (d, C-5), 43.1 (t, C-12), 42.1 (t, C-7), 42.0 (t, C-3), 39.2 (t, C-1), 38.9 (s, C-10), 33.4 (q, C-18), 33.2 (s, C-4), 30.6 (q, C-17), 23.4 (q, C-16), 21.6 (q, C-19), 21.2 (t, C-11), 18.3 (t, C-2), 18.1 (t, C-6), 15.1 (q, C-20); HRFABMS *m*/*z* 282.2560 (calcd for $C_{18}H_{34}O_2$ $[M^+]$, 282.2559).

7.5.1.8 Attempted Swern oxidation[187] of **5.22** and **5.23**

This method is representative. Oxalyl chloride (100 μL, 1.15 mmol, 5.4 eq) was added to anhydrous CH_2Cl_2 (3 mL) at -78℃ and stirred (10 min). Anhydrous DM SO (100 μL, 1.41 mmol, 6.62 eq) was added and after further stirring (10 min), **5.22** (60 mg, 0.21 mmol) in anhydrous CH_2Cl_2 (3 mL) was added *via* cannula and stirring continued (1 h) before adding Et_3N (600 μL, 4.30 mmol, 20 eq) and stirring continued at -78°C (1 h). After allowing the solution to warm to ambient temperature (3 h), saturated aqueous NH_4Cl (4 mL) was added and the reaction mixture stirred (1 h). All solvent was then removed *in vacuo* and the resultant oil taken up in Et_2O (5mL) and washed with H_2O (3 x 5 mL) before drying the organic fraction ($MgSO_4$) to afford a colourless oil (74 mg). Testing the solution with 2,4 DNP hydrazone for a ketone proved negative, TLC and ^1H NMR revealed that although the starting material had been consumed, an inseparable complex mixture of products had formed, which resisted further purification.

7.5.1.9 $KMnO_4$ mediated oxidation of **2.21** using CH_2Cl_2 as a solvent with phenyltriethylammonium chloride (PTEACl) as a phase transfer catalyst

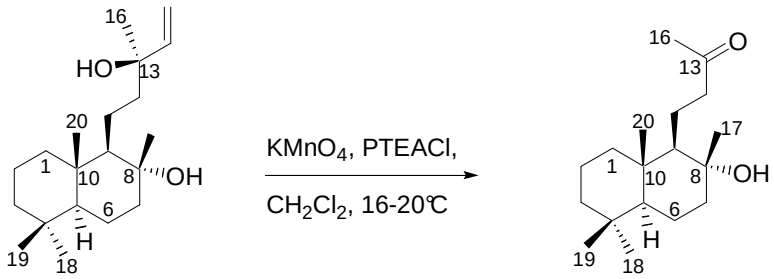

2.21 **5.26**

This method is representative. Sclareol (**2.21**, 1.00g, 3.25 mmol) and PTEACl (1.73 g, 10.7 mmol, 3 eq) were dissolved in CH_2Cl_2 (100 mL) and finely powdered $KMnO_4$ (1.59 g, 10.7 mmol, 3 eq) was added slowly over 2 hours. The temperature of the reaction mixture was maintained between 16℃ and 20℃ and stirring conti nued (48 h).The reaction mixture was allowed to settle (24 h) and filtered through Celite (545 coarse) after which the solvent was removed *in vacuo*. The reaction mixture was taken up in CH_2Cl_2 (15 mL) and washed with a mixture of 1.5% aqueous oxalic acid (30 mL) and saturated aqueous $Na_2S_2O_3$ (15 mL), which reduced the brown precipitate. The organic fraction was washed with H_2O (2 x 15 mL), dried ($MgSO_4$) and concentrated to afford a yellow oil (652 mg) which was purified using silica flash chromatography (20% EtOAc, 80% hexane) to afford 8α-hydroxy-14,15-bisnorlabda-13-one (**5.26**, 455 mg, 53%) as a colourless oil.

8α-hydroxy-14,15-bisnorlabda-13-one (5.26):[190;243] white amorphous solid; $[\alpha]_D^{24}$ +6 (*c* 0.4, $CHCl_3$, lit.[243] +7; IR (film) ν_{max} 3423, 2922, 1713, 1450, 1117 cm^{-1}; ^1H NMR ($CDCl_3$, 400 MHz) δ 2.61 (2H, m, H_2-12), 2.26 (1H, s, 8-OH), 2.11 (3H, s, H_3-16), 1.84 (1H, ddd, *J* = 12.2, 3.4, 3.2 Hz, H-7b), 1.73 (1H, m, H-11b), 1.66 (1H, m, H-2a), 1.62 (1H, m, H-1b), 1.58 (1H, m, H-6b), 1.52 (1H, m, H-11a), 1.42 (1H, m, H-6a), 1.39 (1H, m, H-7a), 1.34 (1H, m, H-3b), 1.25 (1H, m, H-2b), 1.14 (3H, s, H_3-17), 1.12 (1H, m, H-3b), 1.06 (1H, m, H-9), 0.91 (1H, m, H-1a), 0.88 (1H, m, H-5), 0.85 (3H, s, H_3-18), 0.79 (3H, s, H_3-20), 0.77 (3H, s, H_3-19); ^{13}C NMR ($CDCl_3$, 100 MHz) δ 210.4 (s, C-13), 73.7 (s, C-8), 60.7 (d, C-9), 56.1 (d, C-5), 46.2 (t, C-12), 44.5 (t, C-7), 41.9 (t, C-3), 40.1 (t, C-1), 39.3 (s, C-10), 33.3 (q, C-18), 33.2 (s, C-4), 30.0 (q,

C-16), 24.1 (q, C-17), 21.5 (q, C-19), 20.5 (t, C-2), 18.8 (t, C-11), 18.4 (t, C-6), 15.2 (q, C-20); HRFABMS *m/z* 280.2405 (calcd for $C_{18}H_{32}O_2$ [M^+], 280.2402).

7.5.1.10 LAH reduction of methyl ketone **5.26**

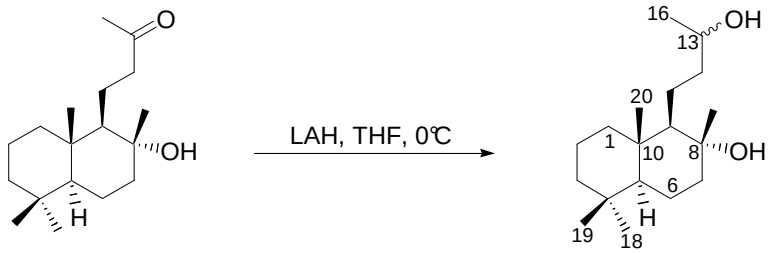

5.26

5.25 13-(*R*)
5.27 13-(*S*)

This method is representative. Methyl ketone (**5.26**, 400 mg, 1.42 mmol) was dissolved in anhydrous THF (5 mL) and added *via* cannula to a 0℃ solution of LAH (116 mg, 2.84 mmol , 2 eq) in anhydrous THF (15 mL). The reaction was allowed to warm naturally to ambient temperature (2 h) before 5% aqueous $NaHCO_3$ (1 mL) was added. The reaction mixture was acidified with 1M HCl (2.0 mL), concentrated to dryness, taken up in EtOAc (5 mL) and washed with H_2O (3 x 5 mL). The organic fraction was dried ($MgSO_4$) and concentrated to afford a colourless oil (425 mg). Semi-preparative HPLC (30% EtOAc, 70% hexane) followed to afford 14,15-bisnorlabda-8α,13*S*-diol (**5.27,** 189 mg, 47%) and 14,15-bisnorlabda-8α,13*R*-diol (**5.25,** 169 mg, 42%) as colourless oils in 89% combined isolated yield.

14,15-Bisnorlabda-8α,13*R*-diol (5.25): colourless oil, $[\alpha]_D^{23}$ -30 (*c* 1.2, $CHCl_3$), lit.[173] -30; IR (film) ν_{max} 3343, 2935, 2870, 1460, 1130 cm^{-1}; ^1H NMR ($CDCl_3$, 400 MHz) δ 3.76 (1H, m, H-13), 1.81 (1H, ddd, *J* = 12.1, 3.6, 3.2 Hz, H-7b), 1.63 (1H, m, H-2b), 1.59 (1H, m, H-1b), 1.57 (1H, m, H-6b), 1.56 (1H, m, H-12b), 1.53 (1H, m, H-11b), 1.45 (1H, m, H-12a), 1.43 (1H, m, H-7a), 1.40 (1H, m, H-6a), 1.34 (1H, m, H-3b) 1.32 (1H, m, H-11b), 1.25 (1H, m, H-2a), 1.22 (1H, m, H-9), 1.14 (3H, d, *J* = 6.2 Hz, H_3-16), 1.13 (3H, s, H_3-17), 1.12 (1H, m, H-3a), 0.94 (1H, m, H-5), 0.94 (1H, ddd, *J* = 12.6, 12.2, 3.5 Hz, H-1a), 0.84 (3H, s, H_3-18), 0.77 (3H, s, H_3-19), 0.76 (3H, s, H_3-20); ^{13}C NMR ($CDCl_3$, 100 MHz) δ 74.6 (s, C-8), 69.7 (d, C-13), 61.5 (d,

C-9), 56.0 (d, C-5), 44.2 (t, C-7), 42.3 (t, C-12), 42.0 (t, C-3), 39.7 (t, C-1), 39.2 (s, C-10), 33.4 (q, C-18), 33.2 (s, C-4), 24.3 (q, C-17), 23.8 (q, C-16), 22.1 (t, C-11), 21.5 (q, C-19), 20.5 (t, C-2), 18.4 (t, C-6), 15.2 (q, C-20); HRFABMS *m*/*z* 282.2551 (calcd for $C_{18}H_{34}O_2$ [M^+], 282.2559).

14,15-Bisnorlabda-8α,13*S*-diol (5.27): white needles (from hexane/EtOAc); mp 94-95℃, lit.[173] 97-99℃; $[\alpha]_D^{23}$ +4 (*c* 0.5, $CHCl_3$), lit.[173] +8; IR (film) ν_{max} 3346, 2932, 2861, 1460, 1132 cm^{-1}; ^{1}H NMR ($CDCl_3$, 400 MHz) δ 3.76 (1H, m, H-13), 1.81 (1H, ddd, *J* = 12.1, 3.6, 3.2 Hz, H-7b), 1.63 (1H, m, H-2b), 1.59 (1H, m, H-1b), 1.57 (1H, m, H-6b), 1.56 (1H, m, H-12b), 1.53 (1H, m, H-11b), 1.45 (1H, m, H-12a), 1.43 (1H, m, H-7a), 1.40 (1H, m, H-6a), 1.34 (1H, m, H-3b) 1.32 (1H, m, H-11b), 1.25 (1H, m, H-2a), 1.22 (1H, m, H-9), 1.14 (3H, d, *J* = 6.2 Hz, H_3-16), 1.13 (3H, s, H_3-17), 1.12 (1H, m, H-3a), 0.94 (1H, m, H-5), 0.94 (1H, ddd, *J* = 12.6, 12.2, 3.5 Hz, H-1a), 0.84 (3H, s, H_3-18), 0.77 (3H, s, H_3-19), 0.76 (3H, s, H_3-20); ^{13}C NMR ($CDCl_3$, 100 MHz) δ 74.4 (s, C-8), 65.4 (d, C-13), 58.4 (d, C-9), 56.2 (d, C-5), 44.2 (t, C-7), 42.0 (t, C-3), 40.8 (t, C-12), 39.8 (t, C-1), 39.2 (s, C-10), 33.4 (q, C-18), 33.2 (s, C-4), 24.6 (q, C-17), 23.2 (q, C-16), 21.5 (q, C-19), 20.5 (t, C-2), 20.0 (t, C-11), 18.4 (t, C-6), 15.2 (q, C-20); HRFABMS *m*/*z* 282.2551 (calcd for $C_{18}H_{34}O_2$ [M^+], 282.2559).

7.5.1.11 Attempted Dess-Martin periodinane oxidation of **5.27**

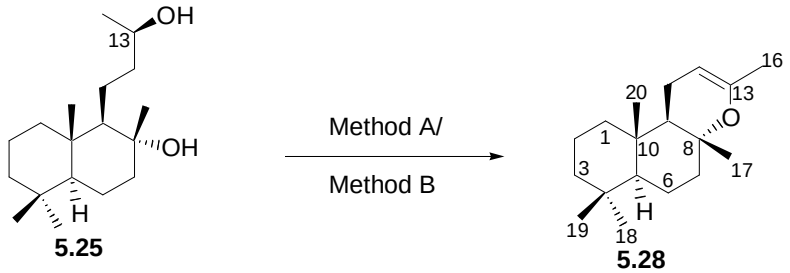

5.25 **5.28**

These methods are representative. The Dess-Martin periodinane (DMP) used in these reactions had previously been prepared in our research group using the method described by Dess and Martin.[188]

Method A: Oxidation in CH_3CN, followed by HWE reaction in THF

Compound **5.25** (60 mg, 0.21 mmol) and DMP (132 mg, 0.31 mmol, 1.5 eq) were dissolved in CH_3CN (10 mL) and stirred at ambient temperature (45 min). The reaction was quenched with aqueous $NaHCO_3$ (5%, 10 mL), all solvent removed *in vacuo* and the residue taken up in Et_2O and washed with H_2O (3 x 5 mL). The Et_2O fraction was dried ($MgSO_4$) and concentrated to afford a yellow oil (31 mg).

The reaction mixture [31 mg, 0.11 mmol (assuming 100% conversion)] was then transferred to a freeze dryer (2 h) and taken up in THF (5 mL) and cooled (0℃). The HWE reagent, triethylphosphonoacetate, (0.22 mmol, 2 eq) was deprotonated with NaH (60%, 4 mg, 0.22 mmol, 2 eq) and added as a THF solution (3 mL) to the reaction mixture, and stirred allowed to warm to ambient temperature while stirring overnight (15 h). Saturated NH_4Cl (1 mL) was added, all solvent removed *in vacuo* and the resultant oil taken up in Et_2O (5 mL), which was washed with H_2O (3 x 5 mL). The organic fraction was dried ($MgSO_4$), concentrated to a yellow oil (124 mg) and subsequently purified by semi-preparative HPLC (33% EtOAc, 67% hexane) to afford 8α,13-epoxy-14,15-bisnorlabda-12-ene (**5.28**, 23 mg, 38%) as an amorphous solid.

Method B: Oxidation and HWE performed in THF

Compound **5.25** (40 mg, 0.14 mmol) and DMP (60 mg, 0.14 mmol, 1 eq) were dissolved in CH_3CN (10 mL) and stirred at ambient temperature (45 minutes), after which the solution was cooled (0℃). The HWE reagent, triethylphosphonoac etate, (0.71 mmol, 5.0 eq) was deprotonated with NaH (60%, 14 mg, 0.71 mmol, 5 eq) and added as a THF solution (3 mL) to the reaction mixture, and stirred allowed to warm to ambient temperature while stirring overnight (15 h). Saturated NH_4Cl (2 mL) was added, all solvent removed *in vacuo* and the resultant oil taken up in Et_2O (5 mL), which was washed with H_2O (3 x 5 mL). The organic fraction was dried ($MgSO_4$), concentrated to a a yellow oil (72 mg), which was subsequently

purified by semi-preparative HPLC (33% EtOAc, 67% hexane) to afford 8α,13-epoxy-14,15-bisnorlabda-12-ene (**5.28**, 18 mg, 45%) as an amorphous solid.

8α,13-Epoxy-14,15-binorlabda-12-ene (5.28):[100;190;195;243] amorphous solid; $[\alpha]_D^{23}$ +5 (*c* 2.3, $CHCl_3$), lit.[100] +3; IR (film) ν_{max} 3440, 2932, 1452, 1382, 1125 cm^{-1}; ^1H NMR ($CDCl_3$, 400 MHz) δ 4.42 (1H, br s, H-12), 1.92 (2H, ddd, *J* = 12.4, 3.8, 3.2 Hz, H_2-7), 1.81 (2H, m, H_2-11), 1.77 (1H, m, H-6b), 1.66 (3H, s, H_3-16), 1.59 (1H, m, H-2b), 1.55 (2H, m, H_2-1), 1.43 (1H, m, H-2a), 1.39 (1H, m, H-9), 1.37 (2H, m, H_2-3), 1.30 (1H, m, H-6a), 1.15 (3H, s, H_3-17), 0.96 (1H, dd, *J* = 12.2, 2.2 Hz, H-5), 0.86 (3H, s, H_3-18), 0.80 (6H, s, H_3-19, H_3-20); ^{13}C NMR ($CDCl_3$, 100 MHz) δ 147.9 (s, C-13), 94.6 (d, C-12), 76.2 (s, C-8), 56.2 (d, C-5), 52.5 (d, C-9), 41.9 (t, C-3), 41.1 (t, C-2), 39.3 (t, C-1), 36.7 (s, C-10), 33.5 (q, C-18), 33.2 (s, C-4), 21.6 (q, C-19), 20.4 (q, C-18), 20.1 (q, C-17), 19.8 (t, c-6), 18.6 (t, C-2), 18.3 (t, C-11), 15.0 (q, C-20); HRFABMS *m/z* 262.2293 (calcd for $C_{18}H_{30}O$ [M^+], 262.2297).

7.5.2 Synthesis of **5.1** and **5.2** *via* a regioselective HWE reaction performed on **5.31**

7.5.2.1 Pyridinium chlorochromate mediated oxidative rearrangement of **5.3**[203;204]

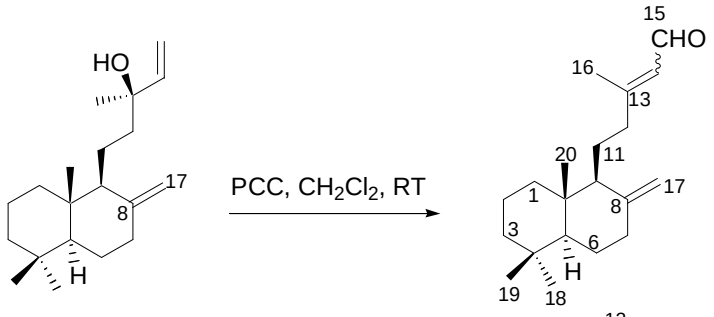

5.3

5.42 Δ^{13} *E*
5.43 Δ^{13} *Z*

A solution of manool (**5.3**, 170 mg, 0.59 mmol) and pyridinium chlorochromate (417 mg, 1.90 mmol, 3.3 eq) in CH_2Cl_2 (8 mL) was stirred (26 h) at room temperature. Et_2O (8 mL) was added, and the formation of an orange precipitate noted. The solution was then filtered through a Celite 545 plug and the filtrate concentrated *in vacuo* to afford a dark brown oil (195 mg). The oil was purified by silica flash chromatography (6% EtOAc, 94% hexane) to

afford an inseparable mixture of (*E*)-labda-8(17)dien-15-al (**5.42**) and (*Z*)-labda-8(17)dien-15-al (**5.43**) in a 2:1 ratio (154 mg, 90% yield) as a pale yellow oil; ^{1}H and ^{13}C NMR data consistent with literature values;[204] HRFABMS *m/z* 289.2531 (calcd for $C_{20}H_{33}O$ [(M + H)$^{+}$], 289.2531.

7.5.2.2 Reductive ozonolysis of **5.42** and **5.43**

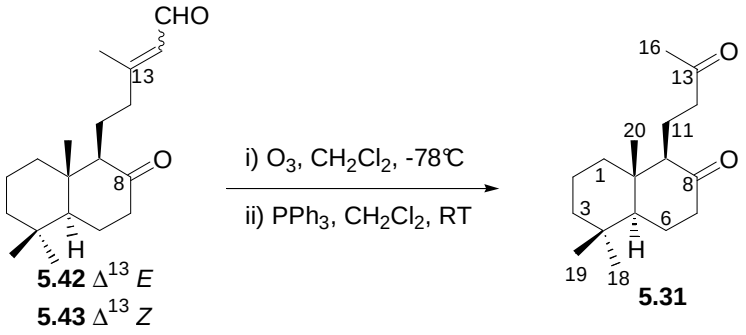

5.42 Δ^{13} *E*
5.43 Δ^{13} *Z*

5.31

The isomeric mixture of **5.42** and **5.43** (100 mg, 0.35 mmol) was dissolved in anhydrous CH_2Cl_2 (5 mL) and cooled (-78℃). A steady stream of O_3 was bubbled through the solution (10 min) until the solution had turned a pale blue colour whereupon N_2 was bubbled through the solution to remove excess O_3. After the addition of triphenylphosphine (548 mg, 2.10 mmol, 6 eq) the solution was stirred at ambient temperature (4 h). The solution was cooled to 0℃, H_2O_2 (30%, 1 mL) added and stirring continued (0.5 h). The solution was then washed with water (3 x 5 mL), the combined organic extracts dried ($MgSO_4$) and concentrated. Subsequent purification of the concentrated organic material by silica flash chromatography (50% EtOAc, 50% hexane) afforded **5.31** (72 mg, 78%).

15,16,17-Trisnorlabdane-8,13-dione (5.31):[174;200;244] colourless oil; $[\alpha]_D^{20}$ -28 (*c* 1.3, $CHCl_3$) lit.[174] -11; IR (film) ν_{max} 2940, 1709, 1698, 1355, 1164 cm^{-1}; ^{1}H NMR ($CDCl_3$, 400 MHz) δ 2.56 (1H, ddd, *J* = 17.4, 8.3, 5.3 Hz, H-12a), 2.38 (1H, ddd, *J* = 13.3, 4.8, 2.0 Hz, H-7b), 2.25 (1H, m, H-7a), 2.17 (1H, m, H-12a), 2.07 (3H, s, H_3-16), 2.04 (m, 1H, H-9), 2.01 (m, 1H, H-6b), 1.79 (1H, m, H-1b), 1.76 (1H, ddd, *J* = 10.7, 5.3, 2.9 Hz, H-11b), 1.61 (1H, m, H-6a), 1.59 (1H, m, H-11a), 1.51 (2H, m, H_2-2), 1.46 (1H, dd, *J* = 12.9, 2.8 Hz, H-5), 1.42 (1H, m, H-3b), 1.21 (2H, m, H-1a, H-3a), 0.93 (3H, s, H_3-18), 0.82 (3H, s, H_3-19), 0.70 (3H, s, H_3-20); ^{13}C NMR

($CDCl_3$, 100 MHz) δ 212.3 (s, C-8), 209.2 (s, C-13), 63.1 (d, C-9), 54.1 (d, C-5), 42.8 (t, C-12), 42.7 (s, C-10), 42.6 (t, C-7), 41.8 (t, C-3), 39.1 (t, C-1), 33.7 (s, C-4), 33.5 (q, C-18), 29.9 (q, C-16), 23.9 (t, C-6), 21.7 (q, C-19), 19.0 (t, C-2), 16.1 (t, C-11), 14.5 (q, C-20); HRFABMS: *m/z* 265.2168 (calcd for $C_{17}H_{28}O_2$ [M^+], 265.2168).

7.5.2.2 Regioselective olefination of **5.31** *via* the HWE reaction

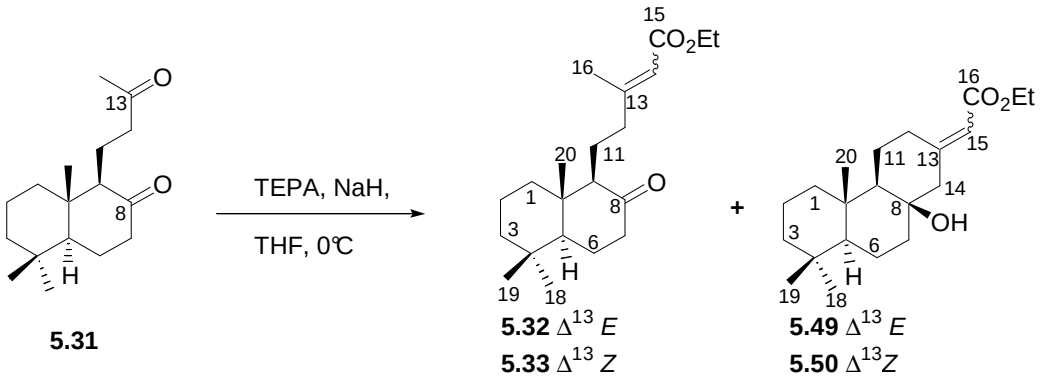

5.31

5.32 Δ^{13} *E*
5.33 Δ^{13} *Z*

5.49 Δ^{13} *E*
5.50 Δ^{13}*Z*

A solution of triethylphosphonoacetate (1660 *μ*L, 3 eq) in anhydrous THF (5 mL) was deprotonated with NaH (140 mg, 2.5 eq) for 30 minutes before addition to a 0℃ solution of **5.31** (737 mg). The solution was warmed to ambient temperature and stirred overnight (16 h), whereupon HCl (1 M, 3 mL) was added and the solution concentrated. The resultant yellow oil was taken up in Et_2O (5 mL) and washed with H_2O (3 x 5 mL). The organic fraction was dried ($MgSO_4$), concentrated and excess triethylphosphonoacetate removed by silica flash chromatography (9% EtOAc, 91% hexane). The mixture of HWE products obtained (927 mg) was further purified by semi-preparative HPLC (6% EtOAc, 94% hexane) to afford ethyl 17-norlabd-13-*E*-en-8-one-15-oate (**5.32**, 409 mg, 55%), ethyl 17-norlabd-13-*E*-en-8-one-15-oate (**5.33**,174 mg, 19%), ethyl 17-norabiet-13(15)-*E*-en-8β-ol-16-oate (**5.49**, 62 mg, 7%) and ethyl 17-norabiet-13(15)-*E*-en-8β-ol-16-oate (**5.50**,18 mg, 2%).

Ethyl 17-norlabd-13-*E*-en-8-one-15-oate (5.32): pale yellow oil; $[\alpha]_D^{34}$ -20 (*c*, 0.5, $CHCl_3$); IR (film) ν_{max} 2948, 1713, 1642, 1218, 1146 cm^{-1}; ^1H and ^{13}C NMR data, see Table 5.1; HRFABMS *m/z* 334.2509 (calcd for $C_{21}H_{34}O_3$ [M^+], 334.2508).

Ethyl 17-norlabd-13-*Z*-en-8-one-15-oate (5.33): pale yellow oil; $[\alpha]_D^{25}$ -57 (*c*, 0.9, $CHCl_3$); IR (film) ν_{max} 2945, 1712, 1646, 1244, 1168 cm^{-1}; ^1H NMR (400 MHz, $CDCl_3$) δ 5.60 (1H, br s, H-14), 4.11 (2H, dd, *J* = 13.2, 6.4 Hz, -OC*H*$_2$CH$_3$), 2.85 (1H, m, H-12b), 2.34 (2H, m, H$_2$-7), 2.13 (1H, m, H-9), 2.11 (1H, m, H-12a), 2.03 (1H, m, H-6b), 1.90 (1H, m, H-11b), 1.89 (3H, s, H$_3$-16), 1.73 (1H, m, H-1b), 1.63 (2H, m, H$_2$-6), 1.52 (2H, m, H$_2$-2), 1.48 (1H, m, H-5), 1.43 (1H, m, H-3), 1.35 (1H, m, H-11a), 1.23 (1H, m, H-3a), 1.25 (3H, t, *J* = 6.6 Hz, -OCH$_2$C*H$_3$*), 1.19 (1H, m, H-1a), 0.95 (3H, s, H$_3$-18), 0.83 (3H, s, H$_3$-19), 0.69 (3H, s, H$_3$-20); ^{13}C NMR (100 MHz, $CDCl_3$) δ 212.0 (s, C-8), 166.4 (s, C-15), 160.5 (s, C-13), 116.3 (d, C-14), 63.6 (d, C-9), 59.5 (t, -O*C*H$_2$CH$_3$), 54.2 (d, C-5), 42.7 (s, C-10), 42.6 (t, C-7), 41.9 (t, C-3), 39.1 (t, C-1), 33.6 (s, C-4), 33.5 (q, C-18), 32.6 (t, C-12), 25.0 (q, C-16), 24.1 (t, C-6), 21.7 (q, C-19), 20.0 (t, C-11), 19.0 (t, C-2), 14.7 (q, C-20), 14.4 (q, -OCH$_2$*C*H$_3$); HRFABMS *m*/*z* 334.2509 (calcd for $C_{21}H_{34}O_3$ [M^+], 334.2508).

Ethyl 17-norabiet-13(15)-*E*-en-8β-ol-16-oate (5.49): white plates (from Et_2O); mp 110-111℃; $[\alpha]_D^{34}$ -68.1 (*c* 1.8, $CHCl_3$); IR (film) ν_{max} 2942, 1720, 1634, 1156, 1046 cm^{-1}; ^1H and ^{13}C NMR data, see Table 6.1; LREIMS m/z (rel int) 334 [M^+] (30), 319 (100), 273 (50), 207 (53), 149 (35); HRFABMS *m*/*z* 334.2509 (calcd for $C_{21}H_{34}O_3$ [M^+], 334.2508).

Crystal data for 5.49: $C_{21}H_{34}O_3$, *M* = 334.48, orthorhombic, space group $P2_12_12_1$ (no. 19), *a* = 7.3750(2) Å, *b* = 9.7769(3) Å, *c* = 27.077(1) Å, *V* = 1952.4(1) $Å^3$, *Z* = 4, D_c = 1.138 Mg/m^3, *μ*(MoKα) = 0.074 mm^{-1}, *F*(000) = 736. A total of 4302 reflections were collected of which 2405 were observed [$I > 2\sigma(I)$]. The structure was solved by direct methods and refined on F^2 using all data, with non-hydrogen atoms treated anisotropically. All H atoms were located and then added in idealised positions in a riding model. The final *R* factors were R_1 = 0.1455 (all data), 0.0510 (observed data), wR_2 = 0.0917 (all data), 0.0742 (observed data) for 222 parameters. Crystallographic data (excluding structure factors) have been deposited at the Cambridge Crystallographic Data Centre (deposition no. 620303).

Ethyl 17-norabiet-13(15)-*Z*-en-8β-ol-16-oate (5.50): yellow oil; $[\alpha]_D^{34}$ +66 (*c* 0.8, $CHCl_3$); IR (film) ν_{max} 2941, 1695, 1652, 1165, 1037 cm^{-1}; ^1H NMR ($CDCl_3$, 400 MHz) δ 5.75 (1H, t, *J* = 1.5 Hz, H-15), 4.12 (2H, dq, *J* = 7.1, 1.0 Hz, -OC*H*$_2$CH$_3$), 3.66 (1H, dd, *J* = 13.5, 0.9 Hz, H-14b), 2.34 (1H, m, H-12b), 2.11 (1H, dt, *J* = 12.8, 4.3 Hz, H-12a), 1.86 (1H, dd, *J* = 13.5, 0.9 Hz, H-14a), 1.78 (1H, m, H-11b), 1.77 (1H, m, H-7a), 1.67 (1H, m, H-1b), 1.62 (2H, m, H-2b, H-11a), 1.55 (1H, m, H-6b), 1.52 (1H, m, H-7a), 1.40 (1H, m, H-2a), 1.39 (1H, m, H-3b), 1.37 (1H, m, H-6a), 1.25 (3H, t, *J* = 7.1 Hz, -OCH$_2$C*H*$_3$), 1.16 (1H, m, H-9) 1.15 (1H, m, H-3a), 0.94 (3H, s, H$_3$-20), 0.88 (1H, m, H-5), 0.87 (3H, s, H$_3$-18), 0.86 (1H, m, H-1a), 0.84 (3H, s, H$_3$-19) ; ^{13}C NMR ($CDCl_3$, 100 MHz) δ 167.2 (s, C-16), 160.0 (s, C-13), 115.6 (d, C-15), 74.3 (s, C-8), 59.7 (t, -O*C*H$_2$CH$_3$), 56.7 (d, C-9), 56.4 (d, C-5), 45.3 (t, C-14), 42.4 (t, C-7), 42.1 (t, C-3), 39.7 (t, C-1), 37.9 (t, C-12), 37.5 (s, C-10), 33.7 (q, C-18), 33.3 (s, C-4), 23.5 (t, C-11), 21.7 (q, C-19), 18.5 (t, C-2), 18.3 (t, C-6), 15.3 (q, C-20), 14.3 (q, -OCH$_2$*C*H$_3$); LREIMS m/z (rel int) 334 [M^+] (35), 319 (100), 273 (36), 255 (27), 207 (33); HRFABMS m/z 335.2582 (calcd for $C_{21}H_{35}O_3$ [$(M + H)^+$], 335.2588).

7.5.2.4 Chemoselective alkylation of **5.32** and **5.33**

Method A: Attempted chemoselective alkylation using $MeTiCl_3$[196]

Anhydrous conditions. An ether solution of $TiCl_4$ (1 M, 60 μL, 0.06 mmol, 1 eq) was added to ether (2 mL) at -78℃, followed by drop wise addition of MeLi (1.6 M, 40 μL, 0.06 mmol, 1 eq) with vigorous stirring. The solution was allowed to warm to -50℃ and changed to a deep purple colour, whereupon it was slowly added *via* cannula to a cooled solution (-50℃) of **5.32** (19 mg, 0.06 mmol) in ether (1 mL) and allowed to stir (8 h, temperature gradually allowed to warm to -30℃ over this time). The reaction was quenched with H_2O (1 mL), then washed with H_2O (3 x 5 mL), dried ($MgSO_4$) and concentrated to a green oil (16 mg). Analysis of the ^1H spectrum of the reaction mixture revealed only unreacted **5.32**.

Method B: Chemoselective alkylation of **5.32** and **5.33** using MeMgCl

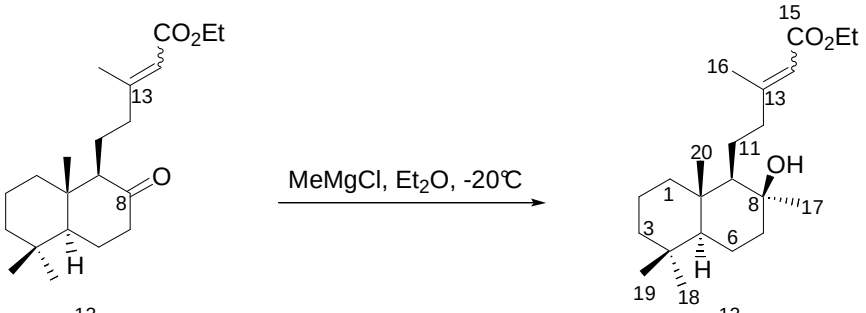

5.32 Δ^{13} *E*
5.33 Δ^{13} *Z*

5.34 Δ^{13} *E*
5.35 Δ^{13} *Z*

This method is representative of the alkylation of **5.32**. A solution of **5.32** (76 mg, 0.23 mmol) in anhydrous Et_2O (5 mL) was cooled to -20℃. An ether solution of MeMgCl (3 M, 100 *µ*L, 1.3 eq) was slowly added drop wise with vigorous stirring. The solution was maintained at -20℃ (1 h), warmed to 0℃ (3 h) and excess MeMgCl quenched through the addition of 3 drops of H_2O. The reaction mixture was further acidified with HCl (1 M, 2 mL) and stirred until the solution had become clear. The Et_2O solution was washed with H_2O (3 x 5 mL), dried ($MgSO_4$) and concentrated *in vacuo* to afford a pale yellow oil. Subsequent purification of this oil *via* semi-preparative HPLC (14% EtOAc, 86% hexane) afforded ethyl labd-13*E*-en-8β-ol-15-oate (**5.34**, 64 mg, 81%). In the same manner, ethyl labd-13*Z*-en-8β-ol-15-oate, **5.35** (81%), was obtained from **5.33.** The reaction was also attempted in the same manner using either MeLi or MeMgBr as the alkylating agent to afford **5.34** in lower yield (50% and 71% respectively).

Ethyl labd-13*E*-en-8β-ol-15-oate (**5.34**)**:** pale yellow oil; $[\alpha]_D^{34}$ +25 (*c* 2.2, $CHCl_3$); IR (film) ν_{max} 3498, 2937, 1712, 1454, 1163 cm^{-1}; ^1H NMR ($CDCl_3$, 400 MHz) δ 5.67 (1H, dd, *J* = 2.3, 1.1 Hz, H-14), 4.14 (2H, q, *J* = 7.1 Hz, -OC*H*$_2$$CH_3$), 2.15 (1H, m, H-12b), 2.14 (1H, m, H-12a), 2.12 (3H, d, *J* = 1.3 Hz, H_3-16), 1.75 (1H, m, H-7b), 1.66 (1H, m, H-1b), 1.57 (1H, m, H-11b), 1.56 (1H, m, H-2b), 1.50 (1H, m, H-6b), 1.49 (1H, m, H-7a), 1.48 (1H, m, H-6a), 1.41 (2H, m, H-2a and H-11a), 1.36 (1H, m, H-3b), 1.26 (3H, t, *J* = 7.1 Hz, -OCH$_2$C*H*$_3$), 1.13 (3H, s, H-17), 1.12 (1H, m, H-3a), 0.94 (3H, s, H_3-20), 0.87 (1H, m, H-1a), 0.86 (3H, s, H_3-18), 0.85 (1H, m, H-9), 0.81 (3H, s, H_3-19), 0.79 (1H, dd, *J* = 4.4, 2.7 Hz, H-5); ^{13}C NMR ($CDCl_3$,

100 MHz) δ 166.9 (s, C-15), 160.2 (s, C-13), 115.3 (d, C-14), 73.1 (s, C-8), 59.5 (t, -O*C*$H_2$$CH_3$), 58.8 (d, C-9), 55.9 (d, C-5), 44.6 (t, C-12), 42.3 (t, C-7), 42.0 (t, C-3), 39.2 (t, C-1), 39.0 (s, C-10), 33.4 (q, C-18), 33.2 (s, C-4), 30.6 (q, C-17), 23.6 (t, C-11), 21.6 (q, C-19), 19.0 (q, C-16), 18.3 (t, C-2), 18.1 (t, C-6), 15.1 (q, C-20), 14.3 (q, -OCH$_2$*C*H$_3$); HRFABMS *m/z* 351.2895 (calcd for $C_{22}H_{39}O_3$ [(M + H)$^+$], 351.2899).

Ethyl labd-13*Z*-en-8β-ol-15-oate (**5.35):** pale yellow oil; $[\alpha]_D^{34}$ +15 (*c* 0.7, $CHCl_3$); IR (film) ν_{max} 3461, 2923, 1709, 1451, 1159 cm^{-1}; ^{1}H NMR ($CDCl_3$, 400 MHz) δ 5.60 (1H, d, *J* = 1.3 Hz, H-14), 4.12 (2H, q, *J* = 7.1 Hz, -OC*H*$_2$CH$_3$), 2.75 (1H, ddd, *J* = 12.4, 6.2, 2.7 Hz), 2.65 (1H, ddd, *J* = 12.4, 5.8, 5.3 Hz, H-12a), 1.90 (3H, d, *J* = 2.8 Hz, H$_3$-16), 1.75 (2H, m, H-1b and H-7b), 1.60 (1H, m, H-2b), 1.51 (2H, m, H-6b, H-11b), 1.49 (2H, m, H-6a, H-7a), 1.41 (1H, m, H-11a), 1.37 (1H, m, H-3b), 1.25 (3H, t, *J* = 7.1 Hz, -OCH$_2$C*H*$_3$), 1.24 (3H, s, H$_3$-17), 1.14 (1H, ddd, *J* = 13.9, 6.6, 4.2 Hz, H-3a), 0.94 (3H, s, H$_3$-20), 0.94 (1H, ddd, *J* = 14.0, 6.8, 4.0 Hz, H-1a), 0.86 (3H, s, H$_3$-18), 0.85 (1H, m, H-9), 0.84 (1H, m, H-5), 0.82 (3H, s, H$_3$-19); ^{13}C NMR ($CDCl_3$, 100 MHz) δ 166.2 (s, C-15), 159.9 (s, C-13), 115.9 (s, C-14), 59.4 (d, C-9), 59.3 (t, -O*C*H$_2$CH$_3$), 55.9 (d, C-5), 42.4 (t, C-7), 42.0 (t, C-3), 39.1 (t, C-1), 39.0 (s, C-10), 36.7 (t, C-12), 33.4, (q, C-18), 33.3 (s, C-10), 30.6 (q, C-17), 25.1 (q, C-16), 23.8 (t, C-11), 21.7(q, C-19), 18.3 (t, C-6), 18.2 (t, C-2), 15.1 (q, C-20), 14.4 (q, -OCH$_2$*C*H$_3$); HRFABMS *m/z* 351.2895 (calcd for $C_{22}H_{39}O_3$ [(M + H)$^+$], 351.2899).

7.5.2.5 Reduction of **5.34** and **5.35**

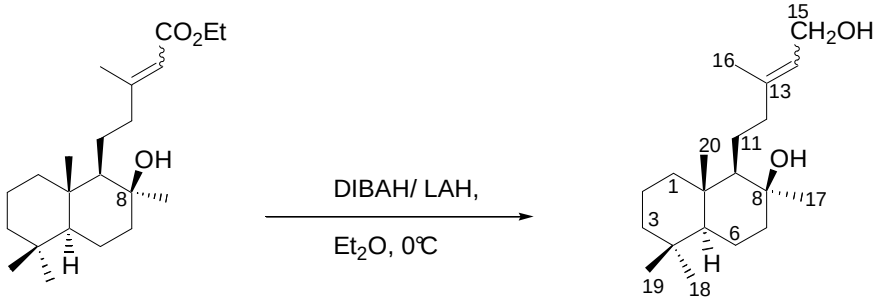

5.34 Δ^{13} *E*
5.35 Δ^{13} *Z*

5.4 Δ^{13} *E*
5.5 Δ^{13} *Z*

Method A: Reduction of **5.34** using DIBAH

Compound **5.34** (101 mg, 0.29 mmol) was dissolved in anhydrous Et_2O (10 mL) and cooled to 0℃. DIBAH (580 μL, 0.58 mmol, 2 eq) was added and stirring continued (4 h) after which the solution was warmed to ambient temperature. Saturated aq. NH_4Cl (2 mL) was added slowly and the ether solution washed with H_2O (3 x 2 mL). The organic fraction was then dried ($MgSO_4$) and concentrated to afford a white amorphous powder which was further purified by semi-preparative HPLC (50% EtOAc, 50% hexane) to afford labd-13*E*-ene-8β,15-diol (**5.4**, 47 mg, 54%) as a white amorphous powder. Similar yields (53%) were obtained for the reduction of **5.35** to labd-13*E*-ene-8β,15-diol, **5.5**. No improvement in yield was obtained by performing the reaction at -20℃ or in THF.

Method B: Reduction of **5.34** and **5.35** using LAH

This method is representative. Compound **5.35** (42 mg, 0.12 mmol) was dissolved in anhydrous Et_2O (2 mL) and cooled to 0℃. LAH (14 mg, 0.36 mmol, 3 eq) was added and stirring continued (0.5 h) after which the solution was warmed to ambient temperature over a period of 2 hours. HCl (1 M, 3 mL) was added slowly and the ether solution washed with H_2O (3 x 2 mL). The organic fraction was then dried ($MgSO_4$) and concentrated to afford a white amorphous powder which was further purified by semi-preparative HPLC (50% EtOAc, 50% Hexane) to afford labd-13*E*-ene-8β,15-diol **5.4** (24 mg, 66%). Similar yields (64%) were obtained for the reduction of **5.35** to labd-13*E*-ene-8β,15-diol, **5.5**. No improvement in yield was obtained by performing the reaction at -20℃ or in THF.

Labd-13*E*-ene-8β,15-diol (5.4): white amorphous powder; $[\alpha]_D^{34}$ +21 (*c* 1.5, $CHCl_3$), lit.[171] +32; IR (film) ν_{max} 3420, 2921, 1189, 912, 758 cm^{-1}; ^1H NMR ($CDCl_3$, 600 MHz) δ 5.41 (1H, dt, *J* = 6.9, 1.2 Hz, H-14), 4.14 (1H, d, *J* = 6.9 Hz, H_2-15), 2.05 (1H, m, H-12b), 2.02 (1H, m, H-12a), 1.77 (1H, m, H-7b), 1.69 (3H, s, H_3-16), 1.67 (1H, m, H-1b), 1.59 (1H, dt, *J* = 13.5, 3.4 Hz, H-2b), 1.54 (1H, m, H-6b), 1.52 (2H, m, H-6a, H-11b), 1.51 (1H, m, H-7a), 1.42 (1H, m, H-2a), 1.40 (1H, m, H-11a), 1.38 (1H, m, H-3b), 1.14 (1H, m, H-3a), 1.13 (3H, s, H_3-17), 0.94 (3H, s, H_3-20), 0.86 (3H, s, H_3-18), 0.88 (1H, m, H-1a), 0.85 (1H, m, H-5), 0.81 (3H, s,

H_3-19), 0.79 (1H, dd, *J* = 4.3, 2.7 Hz, H-9); ^{13}C NMR ($CDCl_3$, 150 MHz) δ 140.4 (s, C-13), 123.1 (d, C-14), 73.2 (s, C-8), 59.4 (t, C-15), 58.8 (d, C-9), 55.9 (d, C-5), 43.3 (t, C-12), 42.2 (t, C-7), 42.0 (t, C-3), 39.1 (t, C-1), 38.9 (s, C-10), 33.4 (q, C-18), 33.2 (s, C-4), 30.6 (q, C-17), 23.9 (t, C-6), 21.6 (q, C-19), 18.3 (t, C-6), 18.2 (t, C-2), 16.4 (q, C-2), 15.1 (q, C-20); HRFABMS *m/z* 308.2715 (calcd for $C_{20}H_{36}O_2$ [M^+], 308.2715).

Labd-13*Z*-ene-8β,15-diol (5.5): white amorphous powder; $[\alpha]_D^{34}$ +24 (*c* 1.0, $CHCl_3$); IR (film) ν_{max} 3395, 2930, 1182, 909, 758 cm^{-1}; ^{1}H NMR ($CDCl_3$, 600 MHz,) δ 5.37 (1H, t, *J* = 7.1 Hz, H-14), 4.13 (2H, d, *J* = 6.8 Hz, H_2-15), 2.08 (1H, m, H-12b), 2.05 (1H, m, H-12a), 1.77 (3H, d, *J* = 0.9 Hz, H_3-16), 1.76 (1H, m, H-7b), 1.69 (1H, ddd, *J* = 12.3, 4.3, 3.0 Hz, H-1b), 1.60 (1H, dt, *J* = 13.4, 3.1 Hz, H-2b), 1.52 (1H, m, H-6b), 1.50 (1H, m, H-6a), 1.48 (1H, m, H-7a), 1.45 (1H, m, H-11b), 1.41 (1H, m, H-2a), 1.39 (1H, m, H-3b), 1.31 (1H, m, H-11a), 1.17 (3H, s, H_3-17), 1.14 (1H, m, H-3a), 0.93 (3H, s, H_3-20), 0.89 (1H, m, H-1a), 0.86 (3H, s, H_3-18), 0.84 (1H, m, H-5), 0.81 (3H, s, H_3-19), 0.79 (1H, dd, *J* = 2.7, 1.6 Hz, H-9); ^{13}C NMR ($CDCl_3$, 150 MHz) δ 140.9 (s, C-13), 123.6 (d, C-14), 73.1 (s, C-8), 59.32 (d, C-9), 59.28 (t, C-15), 55.9 (d, C-5), 42.2 (t, C-7), 42.0 (t, C-3), 39.1 (t, C-1), 38.9 (s, C-10), 36.0 (t, C-12), 33.4 (q, C-18), 33.3 (s, C-4), 30.6 (q, C-17), 24.5 (t, C-11), 23.6 (q, C-16), 21.6 (q, C-19), 18.3 (t, C-6), 18.2 (t, C-2), 15.1 (q, C-20); HRFABMS *m/z* 308.2716 (calcd for $C_{20}H_{36}O_2$ [M^+], 308.2715).

7.5.2.6 MnO_2 oxidation of **5.4** and **5.5**

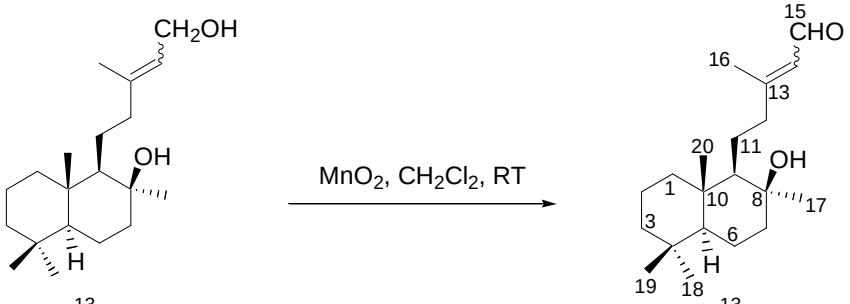

5.4 Δ^{13} *E*
5.5 Δ^{13} *Z*

5.1 Δ^{13} *E*
5.2 Δ^{13} Z

This method is representative. The allylic alcohol **5.4** (41 mg, 0.14 mmol) was dissolved in

anhydrous CH_2Cl_2 (2 mL) and finely powdered activated MnO_2 (87 mg, 1.36 mmol, 10 eq) added. The solution was stirred at ambient temperature overnight (16 h) and filtered through Celite 545 to give labd-13*E*-ene-8β-ol-15-al (**5.1**, 37 mg, 90%) as a white amorphous powder (>95% purity from NMR). Labd-13*Z*-ene-8β-ol-15-al (**5.2**) was obtained in similar yield (91%) and purity *via* the oxidation of **5.5**.

Labd-13*E*-ene-8β-ol-15-al (5.1):[171] white amorphous powder $[\alpha]_D^{34}$ +26 (*c* 1.4, C_6H_6); IR (film) ν_{max} 3481, 2921, 1668, 1454, 1382 cm^{-1}; ^1H and ^{13}C NMR data, see Table 5.2; HRFABMS *m/z* 306.2559 (calcd for $C_{20}H_{34}O_2$ [M^+], 306.2559).

Labd-13*Z*-ene-8β-ol-15-al (5.2):[171] pale yellow oil $[\alpha]_D^{34}$ +24 (*c* 0.9, C_6H_6); IR (film) ν_{max} 3410, 2915, 1661, 1447, 1381 cm^{-1}; ^1H NMR (C_6D_6, 600 MHz) δ 10.08 (1H, d, *J* = 7.9 Hz, H-15), 5.81 (1H, d, *J* = 7.9 Hz, H-14), 2.19 (1H, ddd, *J* = 10.9, 6.0, 5.8 Hz, H-12b), 2.17 (1H, ddd, *J* = 10.9, 6.2, 5.8 Hz, H-12a), 1.52 (1H, m, H-1b), 1.49 (3H, d, *J* = 1.3 Hz, H_3-16), 1.48 (1H, m, H-2b), 1.47 (1H, m, H-7b), 1.46 (1H, m, H-11b), 1.36 (1H, m, H-3b), 1.35 (1H, m, H-6b), 1.32 (1H, m, H-6a), 1.25 (1H, m, H-11a), 1.20 (1H, m, H-2a), 1.17 (1H, m, H-7a), 1.10 (1H, ddd, *J* = 13.5, 6.6, 4.0 Hz, H-3a), 0.93 (3H, s, H_3-20), 0.89 (3H, s, H_3-18), 0.88 (3H, s, H_3-17), 0.83 (3H, s, H_3-19), 0.68 (1H, ddd, *J* = 13.2, 6.4, 3.4 Hz, H-1a), 0.63 (1H, dd, *J* = 12.1, 2.3 Hz, H-5), 0.43 (1H, dd, *J* = 4.4, 2.6 Hz, H-9); ^{13}C NMR (C_6D_6, 150 MHz) δ 189.2 (d, C-15), 162.9 (s, C-13), 128.3 (d, C-14), 72.3 (s, C-8), 59.3 (d, C-9), 55.9 (d, C-5), 42.6 (t, C-3), 42.3 (t, C-7), 39.4 (t, C-1), 39.2 (s, C-10), 36.3 (t, C-12), 33.6 (q, C-18), 33.4 (s, C-4), 30.9 (q, C-17), 25.1 (t, C-11), 24.5 (q, C-16), 21.9 (q, C-19), 18.60 (t, C-6), 18.57 (t, C-2), 15.3 (q, C-20); HRFABMS *m/z* 306.2559 (calcd for $C_{20}H_{34}O_2$ [M^+], 306.2559).

7.5.3 Activity of selected diterpenes from Chapter Five against oesophageal cancer

See section 7.3.3.

7.6 Chapter Six Experimental

7.6.1 Semi-synthesis of potential anti-malarial compounds

7.6.1.1 NaH mediated intramolecular aldol condensation of **5.31**

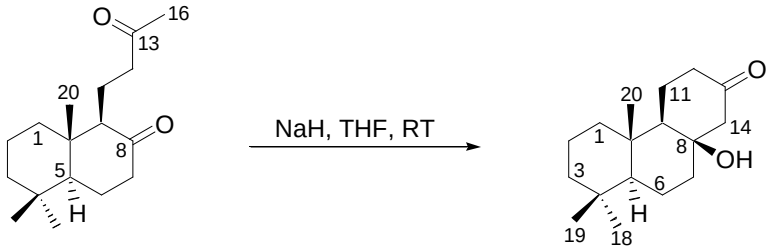

5.31 **5.51**

This method is representative. NaH (60%, 18 mg, 1 eq) was added to a solution of **5.31** (241 mg, 0.91 mmol) in anhydrous THF (60 mL) and the resulting mixture stirred under Ar at ambient temperature (6 h). The yellow solution was concentrated to dryness, taken up in Et_2O (5 mL), and washed with H_2O acidified with a few drops of 1 M HCl (3 x 5 mL). The organic fraction was concentrated *in vacuo* to afford 8-hydroxy-13-podocarpanone (**5.51**) as a pale yellow amorphous solid (228 mg, 95%).

8-Hydroxy-13-podocarpanone (5.51):[202] pale yellow amorphous solid; $[\alpha]_D^{28}$ +12 (*c* 2.2, $CHCl_3$); ^{13}C NMR ($CDCl_3$, 100 MHz) δ 210.7 (s, C-13), 75.5 (s, C-8), 57.3 (t, C-14), 56.1 (d, C-9), 55.3 (d, C-5), 42.2 (t, C-3), 42.0 (t, C-7), 41.4 (t, C-12), 39.8 (t, C-1), 37.5 (s, C-10), 33.6 (q, C-18), 33.2 (s, C-4), 21.8 (q, C-19), 21.4 (t, C-11), 18.4 (t, C-2), 17.9 (t, C-6), 15.3 (q, C-20).

7.6.1.2 Alkenylation of **5.31**[202]

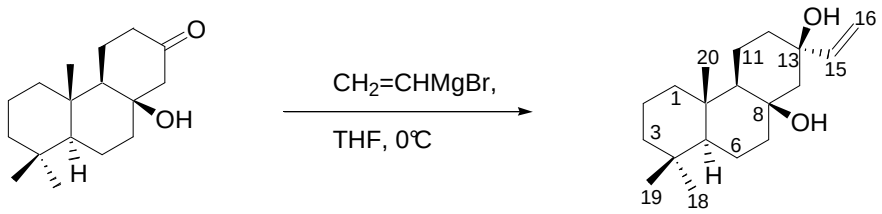

5.51 **6.7**

A THF solution of vinyl magnesium bromide (0.92 mmol, 1.5 eq) was added to a cooled (0℃) solution of **5.51** (162 mg, 0.61 mol) in anhydrous THF under an Ar atmosphere. The solution was gradually warmed to ambient temperature and stirred (1.5 h). Et_2O (10 mL) and a saturated aqueous solution of NH_4Cl (6 mL) were added, and the resulting mixture was stirred (10 min), after which the organic and aqueous phases were separated and the aqueous fraction was extracted with Et_2O (3 x 5 mL). The organic fractions were pooled, dried ($MgSO_4$), and concentrated to afford a yellow oil (362 mg). This oil was subsequently purified by semi-preparative HPLC (75% EtOAc, 25% hexane) to afford 17-norisopimar-15-ene-8β,13β-diol (**6.7**, 48 mg, 27%) which yielded white plates (from hexane).

17-Norisopimar-15-ene-8β,13β-diol (6.7):[202] white plates (from hexane); mp 157.5-159.5℃ lit.[202] 154-155℃; $[\alpha]_D^{28}$ -6 (*c* 2.6, $CHCl_3$); IR (film) ν_{max} 3299, 2945, 1436, 1196, 761 cm^{-1}; ^1H NMR (C_6D_6, 600 MHz) δ 5.71 (1H, dd, *J* = 17.3, 10.7 Hz, H-15), 5.25 (1H, d, *J* = 13.7 Hz, H-16b), 4.96 (1H, d, *J* = 10.7 Hz, H-16a), 1.76 (1H, ddd, *J* = 13.4, 12.8, 3.2 Hz, H-11b), 1.63 (1H, m, H-7b), 1.60 (3H, m, H-1b, H-2b, H-12b), 1.59 (1H, m, H-6b), 1.52 (1H, dd, *J* = 14.0, 2.6 Hz, H-14b), 1.39 (1H, m, H-3b), 1.40 (1H, m, H-6a), 1.37 (2H, m, H-2a, H-11a), 1.21 (1H, m, H-12a), 1.16 (1H, dd, *J* = 13.3, 3.9 Hz, H-3a), 1.13 (3H, s, H_3-20), 1.11 (1H, d, *J* = 14.0 Hz, H-14a), 1.04 (1H, ddd, *J* = 13.4, 12.9, 4.0 Hz, H-7a), 0.90 (3H, s, H_3-18), 0.89 (3H, s, H_3-19), 0.71 (2H, m, H-1a, H-5), 0.56 (1H, d, *J* = 12.6, 2.8 Hz, H-9); ^{13}C NMR (150 MHz, C_6D_6) δ 146.2 (d, C-15), 111.3 (t, C-16), 73.4 (s, C-13), 72.4 (s, C-8), 56.5 (d, C-5), 56.1 (d, C-9), 49.7 (t, C-14), 42.5 (t, C-3), 42.4 (t, C-7), 39.8 (t, C-1), 37.6 (s, C-10), 38.6 (t, C-12), 33.9 (q, C-18), 33.5 (s, C-4), 22.0 (q, C-19), 18.9 (t, C-2), 18.2 (t, C-6), 16.6 (t, C-11), 15.7 (q, C-20); LREIMS m/z (rel int) 293 $[(M + H)^+]$ (1), 274 (72), 259 (100), 149 (39), 136 (45); HRFABMS m/z 293.2481 (calcd for $C_{19}H_{33}O_2$ $[(M + H)^+]$, 293.2480).

7.6.1.3 HWE reaction on **5.51**

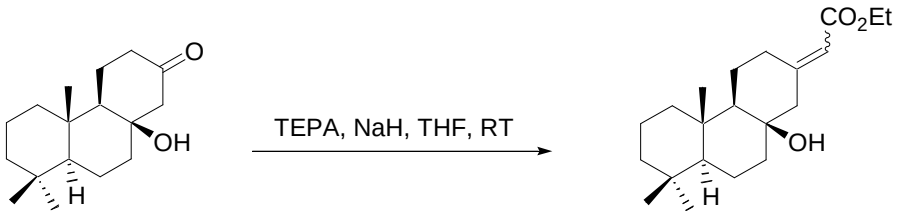

5.51

5.49 Δ^{13} *E*
5.50 Δ^{13}*Z*

This method is representative. Triethylphosphonoacetate (380 μL, 1.90 mmol, 2.5 eq) was added to an anhydrous solution of NaH (60%, 38 mg, 1.90 mmol, 2.5 eq) in THF (15 mL), and the mixture was stirred under an Ar atmosphere (0.5 h). A solution of **5.31** (264 mg, 0.76 mmol) in anhydrous THF (10 mL) was added *via* cannula and the reaction mixture stirred at ambient temperature (10 h), after which HCl (1 M, 3 drops) was added and the mixture concentrated *in vacuo*. The resulting oil was taken up in Et_2O (5 mL) and washed with H_2O (3 x 5 mL). The combined organic fractions were dried ($MgSO_4$) and concentrated *in vacuo* to afford a yellow oil, which was subsequently purified on silica (20% EtOAc, 80% hexane) to afford a mixture of the E/Z isomers **5.49** and **5.50**. This mixture was further purified using semi-preparative HPLC (10% EtOAc, 90% hexane) to afford ethyl 17-norabiet-13(15)-*E*-en-8β-ol-16-oate (**5.49**, 105 mg, 41%) and ethyl 17-norabiet-13(15)-*Z*-en-8β-ol-16-oate (**5.50**, 76 mg, 29%). The one-pot reaction cyclization-HWE reaction referred to in Chapter Six was simply a combination of the methods described in Section 7.6.1.1 and here. On one isolated occasion the minor product 17-norpimaran-13α-ethoxy-8,16-olactone, **6.6**, was isolated in 10% yield from the one-pot cyclization-HWE reaction.

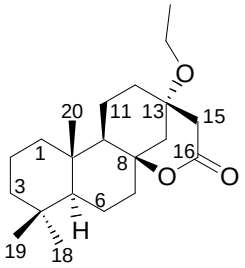

6.6

17-Norpimaran-13α-ethoxy-8,16-olactone (6.6): white needles (from hexane); mp 143-144℃; $[\alpha]_D^{25}$ +12 (*c* 0.7, $CHCl_3$); IR (film) ν_{max} 2922, 2952, 1716, 1086, 986 cm^{-1}; ^1H and ^{13}C data, see Table 6.2; LREIMS m/z (rel int) 334 [M^+] (18), 319 (35), 288 (100), 276 (70), 228 (31); HRFABMS m/z 334.2509 (calcd for $C_{21}H_{34}O_3$ [M^+], 334.2508).

Crystal data for 6.6: $C_{21}H_{34}O_3$, *M* = 334.48, monoclinic, space group $P2_1$ (no. 4), *a* = 6.9880(1) Å, *b* = 22.0165(4) Å, *c* = 12.6710(3) Å, *β* = 101.345(1)°, *V* = 1911.36(6) $Å^3$, *Z* = 4, D_c = 1.162 Mg/m^3, $\mu(MoK_\alpha)$ = 0.075 mm^{-1}, *F*(000) = 736. A total of 8635 reflections were collected of which 5846 were observed [$I > 2\sigma(I)$]. The structure was solved by direct methods and refined on F^2 using all data, with non-hydrogen atoms treated anisotropically. All H atoms were located and then added in idealised positions in a riding model. The final *R* factors were R_1 = 0.0828 (all data), 0.0387 (observed data), wR_2 = 0.0782 (all data), 0.0692 (observed data) for 441 parameters. Crystallographic data (excluding structure factors) have been deposited at the Cambridge Crystallographic Data Centre (deposition no. 620304).

7.6.1.4 Reduction of **5.49** and **5.50** with LAH

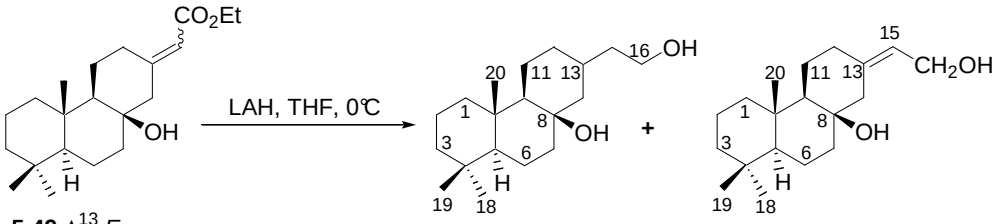

5.49 Δ^{13} *E*
5.50 Δ^{13}*Z*

6.8 **6.9**

A solution of either the ethyl ester **5.49** (90, 0.27 mmol) or the ethyl ester **5.50** (59 mg, 0.18 mmol) in anhydrous THF (5 mL) was added to a cooled (0℃) solution of LAH (2.2 eq) in THF (5 mL). The solution was stirred (2.5 h) while gradually warming to ambient temperature. The remaining LAH was quenched with H_2O (2 mL), concentrated *in vacuo*, and taken up in Et_2O (5 mL), which was washed with H_2O (3 x 5 mL). The combined organic partition fractions were dried ($MgSO_4$) and concentrated under reduced pressure to afford a yellow oil. The oil was purified by normal-phase HPLC (100% EtOAc). The reduction of the *Z* isomer **5.50** yielded 17-norisopimarane-8β,16-diol (**6.8**, 8 mg, 15%) and 17-norabiet-13(15)-ene-8β,16-diol (**6.9**,

24 mg, 46%). The reduction of the *E* isomer **5.49** yielded exclusively **6.8** (35 mg, 43%).

17-Norisopimarane-8β,16-diol (6.8): yellow oil, $[\alpha]_D^{34}$ -10 (*c* 3.5, $CHCl_3$); IR (film) ν_{max} 3361, 2921, 1451, 1060, 735 cm^{-1}; ^1H NMR (C_6D_6, 600 MHz) δ 3.43 (2H, t, *J* = 6.6 Hz, H_2-16), 1.72 (1H, m, H-12b), 1.70 (1H, m, H-13), 1.60 (1H, m, H-2b), 1.59 (2H, m, H-1b, H-2a), 1.51 (1H, ddd, *J* = 13.5, 3.9, 2.8 Hz, H-7b), 1.44 (1H, m, H-11b), 1.43 (1H, m, H-6a), 1.42 (1H, m, H-11a), 1.39 (1H, m, H-3b), 1.36 (1H, m, H-6b), 1.33 (1H, m, H-14b), 1.27 (1H, m, H-15b), 1.25 (H-15a), 1.17 (1H, m, H-7a), 1.14 (1H, m, H-3a), 1.05 (3H, s, H_3-20), 0.90 (3H, s, H_3-18), 0.89 (3H, s, H_3-19), 0.72 (1H, m, H-5), 0.71 (1H, m, H-12a), 0.70 (1H, m, H-14a), 0.69 (1H, m, H-1a), 0.62 (1H, dd, *J* = 12.4, 3.3 Hz, H-9) ; ^{13}C NMR ($CDCl_3$, 150 MHz) δ 71.3 (s, C-8), 60.3 (t, C-16), 56.7 (d, C-9), 56.5 (d, C-5), 49.3 (t, C-14), 42.8 (t, C-7), 42.5 (t, C-3), 40.4 (t, C-15), 39.7 (t, C-1), 37.5 (s, C-10), 33.88 (t, C-12), 33.85 (q, C-18), 33.5 (s, C-4), 29.4 (d, C-13), 22.0 (q, C-19), 20.7 (t, C-6), 18.9 (t, C-2), 18.5 (t, C-11), 15.8 (q, C-20) ; LREIMS m/z (rel int) 294 [M^+] (1), 279 (100), 261 (85), 243 (21), 179 (16); HRFABMS m/z 295.2637(calcd for $C_{19}H_{35}O_2$ [$(M + H)^+$], 295.2636).

17-Norabiet-13(15)-ene-8β,16-diol (6.9): yellow oil; $[\alpha]_D^{34}$ -11 (*c* 1.4, $CHCl_3$); IR (film) ν_{max} 3446, 2945, 1709, 1386, 757 cm^{-1}; ^1H NMR ($CDCl_3$, 400 MHz) δ 5.65 (1H, dd, *J* = 8.1, 6.8 Hz, H-15), 4.12 (1H, dd, *J* = 11.6, 6.8 Hz, H-16b), 3.92 (1H, dd, *J* = 11.6, 8.1 Hz, H-16a), 2.49 (1H, dd, *J* = 13.2, 2.1 Hz, H-14b), 2.27 (1H, m, H-12b), 1.97 (1H, dt, *J* = 12.8, 4.5 Hz, H-12a), 1.79 (1H, m, H-7b), 1.77 (1H, m, H-14a), 1.72 (1H, m, H-11b), 1.64 (1H, m, H-1b), 1.58 (1H, m, H-2b), 1.54 (1H, m, H-6b), 1.45 (1H, m, H-7a), 1.40 (2H, m, H-3b, H-6a), 1.38 (1H, m, H-11a), 1.37 (1H, m, H-2a), 1.12 (1H, m, H-3a), 1.10 (1H, m, H-9), 0.94 (3H, s, H_3-20), 0.90 (1H, m, H-5), 0.87 (3H, s, H_3-18), 0.85 (1H, m, H-1a), 0.84 (3H, s, H_3-19); ^{13}C NMR ($CDCl_3$, 100 MHz) δ 142.1 (s, C-13), 123.5 (d, C-15), 73.0 (s, C-8), 57.5 (t, C-16), 56.7 (d, C-9), 56.4 (d, C-5), 44.4 (t, C-14), 42.1 (t, C-3), 41.3 (t, C-7), 39.5 (t, C-1), 37.4 (s, C-10), 36.7 (t, C-12), 33.6 (q, C-18), 33.3 (s, C-4), 23.1 (t, C-11), 21.7 (q, C-19), 18.4 (t, C-6), 18.3 (t, C-2), 15.4 (q, C-20) ; LREIMS m/z (rel int) 292 [M^+] (2), 259 (86), 179 (92), 149 (100), 91 (93); HRFABMS m/z 293.2480 (calcd for $C_{19}H_{33}O_2$ [$(M + H)^+$], 293.2481).

7.6.2 Malaria Parasite Viability, Haemolysis, and Erythrocyte Shape Assays

Details as provided by Dr H. Hoppe of the Division of Pharmacology, Faculty of Health Sciences, University of Cape Town. *P. falciparum* (3D7 strain) was cultured under an atmosphere of 3% CO_2, 4%O_2, and 93% N_2 in RPMI-1640 medium supplemented with 50 mM glucose, 0.65 mM hypoxanthine, 25 mM HEPES, 0.2% (w/v) $NaHCO_3$, 0.048 $mgmL^{-1}$ gentamicin, 0.5% (w/v) Albumax II, and 2-4% (v/v) human O^+ erythrocytes. Parasite-infected erythrocytes from culture were mixed with fresh culture medium and erythrocytes to yield a 2% parasitemia and 2% haematocrit suspension and distributed in microtiter plates at 100 μL/well. Serial dilutions of each compound were prepared in a duplicate plate and transferred to the parasite plate at 100 μL/well. The plates were incubated at 37℃ for 48 h, and parasite viability in each well was determined by measuring parasite lactate dehydrogenase activity.[245] Parasite viabilities were determined relative to solvent controls (wells containing 0.5% DMSO). To assess haemolytic activity, duplicate plates containing normal, uninfected erythrocytes at 2% haematocrit were also incubated for 48 h with the various compound dilutions. The intact erythrocytes were sedimented in the microtiter plate wells by centrifugation at 200*g* for 3 min, and released haemoglobin in the supernatants was measured by removing aliquots and measuring absorbance at 405 nm. Wells treated with 0.2% saponin (from Quillaja bark supplied by Sigma-Aldrich, Steinheim, Germany) were used as 100% haemolysis controls. Erythrocyte shape changes after 48 h incubation with the various test compounds were assessed by removing aliquots from treated wells and preparing Giemsa-stained thin blood smears for light microscopy. In addition, aliquots were wet-mounted under glass coverslips and viewed directly by phase-contrast microscopy. To assess the effects of the compounds on erythrocyte shape at subhaemolytic concentrations, 2% haematocrit suspensions of fresh erythrocytes were incubated with parasite culture medium alone (control) or with medium containing 100, 50, or 25 μgmL^{-1} of the various compounds for 48 h. After incubation, the erythrocyte suspensions were mounted directly under coverslips on microscope slides and immediately viewed with a Nikon Eclipse E600 light microscope using a 100 x Apochromat oil-immersion objective and phase contrast optics. Images were captured with a Media Cybernetics CoolSNAP-Pro monochrome cooled charge-coupled device camera. Discocytes, echinocytes, stomatocytes, and knizocytes in the samples were defined according to Lim *et al*.[246]

References

1. Darias, J.; Cueto, M.T.; Diaz-Marrero, A. R. In *Molluscs*; Springer: Berlin, 2006; pp 105-131.
2. Davies-Coleman, M. In *Molluscs*; Springer: Berlin, 2006; pp 133-157.
3. Kay, E. A.; Wells, F. E.; Ponder, W. F. In *Mollusca: The Southern Synthesis. Fauna of Australia. Vol. 5.*; Beesly, P. L.; Ross, G. J. B.; Wells, A., Eds.; CSIRO Publishing: Melbourne, 1998; pp 565-604.
4. Gavagnin, M.; Fontana, A. *Curr. Org. Chem* **2000**, *4*, 1201-1248.
5. Cimino, G.; Ghiselin, M. T. *Chemoecology* **1998**, *8*, 51-60.
6. Faulkner, D. J.; Ghiselin, M. T. *Mar. Ecol. Prog. Ser.* **1983**, *13*, 295-301.
7. Faulkner, D. J. In *Biomedical importance of marine organisms*; Fautin, D. G., Ed.; Mem. Calif. Acad. Sci: 1988; pp 29-36.
8. Iken, K.; Avila, C.; Fontana, A.; Gavagnin, M. *Mar. Biol.* **2002**, *141*, 101-109.
9. Gavagnin, M.; Fontana, A.; Ciavatta, M. L.; Cimino, G. *Ital. J. Zool.* **2000**, *67*, 101-109.
10. Gray, C. A.; Davies-Coleman, M. T.; McQuaid, C. *Nat. Prod. Lett.* **1998**, *12*, 47-53.
11. Manker, D. C.; Faulkner, D. J. *J. Chem. Ecol.* **1995**, *22*, 23-35.
12. Paul, V. J.; Van Alstyne, K. L. *J. Exp. Mar. Biol. Ecol.* **1988**, *119*, 15-29.
13. Estrada, D. M.; Ravelo, J. L.; Ruiz-Pérez, C.; Martin, J. D.; Solans, X. *Tetrahedron Lett.* **1989**, *30*, 6219-6220.
14. Gavagnin, M.; Spinella, A.; Crispino, A.; de Almeida Epifiano, R.; Marin, A.; Cimino, G. *Gazz. Chim. Ital.* **1993**, *123*, 205-208.
15. Finer, J.; Clardy, J.; Fenical, W.; Minale, L.; Riccio, R.; Battaile, J.; Kirkup, M.; Moore, R. E. *J. Org. Chem.* **1979**, *44*, 2044-2047.

16. Coll, J. C.; Bowden, B. F.; Tapiolas, D. M.; Willis, R. H.; Djura, P.; Streamer, M.; Trott, L. *Tetrahedron* **1985**, *41*, 1085-1092.

17. Davies-Coleman, M. T.; Faulkner, D. J. *Tetrahedron* **1991**, *47*, 9743-9750.

18. Ojika, M.; Kigoshi, H.; Yoshikawa, K.; Nayakama, Y.; Yamada, K. *Bull. Chem. Soc. Jpn.* **1992**, *65*, 2300-2302.

19. Guerriero, A.; D'Ambrosio, M.; Pietra, F. *Helv. Chim. Acta* **1987**, *70*, 984-991.

20. Ojika, M.; Yoshida, Y.; Okumura, M.; Ieda, S.; Yamada, K. *J. Nat. Prod.* **1990**, *53*, 1619-1622.

21. Schmitz, F. J.; Hollenbeak, K. H.; Carter, D. C.; Hossain, M. B.; Van der Helm, D. *J. Org. Chem.* **1979**, *44*, 2445-2447.

22. Ireland, C.; Faulkner, D. J. *J.Org.Chem.* **1977**, *42*, 3157-3162.

23. Danise, B.; Minale, L.; Riccio, R.; Amico, V.; Oriente, G.; Piattelli, M.; Tringali, C.; Fattorusso, E.; Magno, S.; Mayol, L. *Experentia* **1977**, *33*, 413-415.

24. Midland, S. L.; Wing, R. M.; Sims, J. J. *J. Org. Chem.* **1983**, *48*, 1906-1909.

25. Pika, J.; John Faulkner, D. *Tetrahedron* **1995**, *51*, 8189-8198.

26. Dumdei, E. J.; Kubanek, J.; Coleman, J. E.; Pika, J.; Andersen, R. J.; Steiner, J. R.; Clardy, J. *Can. J. Chem.* **1997**, *75*, 773-789.

27. Pettit, G. R.; Herald, C. L.; Einck, J. J.; Vanell, L. D.; Brown, P.; Gust, D. *J. Org. Chem.* **1978**, *43*, 4685-4686.

28. Schmitz, F. J.; Gopichand, Y.; Michaud, D. P.; Prasad, R. S.; Remaley, S.; Hossain, M. B.; Rahman, A.; Sengupta, P. K.; van der Helm, D. *Pure Appl. Chem.* **1981**, *53*, 853-865.

29. Dumdei, E. J.; De Silva, E. D.; Andersen, R. J. *J. Am. Chem. Soc.* **1989**, *111*, 2712-2713.

30. Schmitz, F. J.; Michaud, D. P.; Schmidt, P. G. *J. Am. Chem. Soc.* **1982**, *104*, 6415-6423.

31. Keyzers, R. A.; Northcote, P. T.; Davies-Coleman, M. T. *Nat. Prod. Rep 23* **2006**, 321-334.

32. Rudi, A.; Benayahu, Y.; Kashman, Y. *J. Nat. Prod.* **2005**, *68*, 280-281.

33. Wessels, M.; Konig, G. M.; Wright, A. D. *J. Nat. Prod.* **2000**, *63*, 920-928.

34. Fernandez, J. J.; Souto, M. L.; Gil, L. V.; Norte, M. *Tetrahedron* **2005**, *61*, 8910-8915.

35. Findlay, J. A.; Li, G. *Can. J. Chem.* **2002**, *80*, 1697-1707.

36. Caccamese, S.; Toscano, R. M.; Cerrini, S.; Gavuzzo, E. *Tetrahedron Lett.* **1982**, *23*, 3415-3418.

37. Fu, X.; Palomar, A. J.; Hong, E. P.; Schmitz, F. J.; Valeriote, F. A. *J. Nat. Prod.* **2004**, *67*, 1415-1418.

38. Toupet, L.; Biard, J. F.; Verbist, J. F. *J. Nat. Prod.* **1996**, *59*, 1203-1204.

39. Biard, J. F.; Malochet-Grivois, C.; Roussakis, C.; Cotelle, P.; Henichart, J. P.; Verbist, J. F. *Nat. Prod. Lett.* **1994**, *4*, 43-50.

40. Malochet-Grivois, C.; Cotelle, P.; Biard, J. F.; Henichart, J. P.; Debitus, C.; Roussakis, C.; Verbist, J. F. *Tetrahedron Lett.* **1991**, *32*, 6701-6702.

41. Uddin, M. J.; Kokubo, S.; Ueda, K.; Suenaga, K.; Uemura, D. *J. Nat. Prod.* **2001**, *64*, 1169-1173.

42. Uddin, M. J.; Kokubo, S.; Ueda, K.; Suenaga, K.; Uemura, D. *Chem. Lett.* **2002**, *10*, 1028-1029.

43. Uddin, M. J.; Kokubo, S.; Suenaga, K.; Ueda, K.; Uemura, D. *Heterocycles* **2001**, *54*, 1039-1047.

44. Cimino, G.; Gavagnin, M. *Curr. Org. Chem* **1999**, *3*, 327-372.

45. Somerville, M. J.; Mollo, E.; Cimino, G.; Rungprom, W.; Garson, M. J. *J. Nat. Prod.* **2006**, *69*, 1086-1088.

46. Sakamoto, T.; Kanematsu, K. *Tetrahedron* **1995**, *51*, 5771-5780.

47. Gavagnin, M.; Carbone, M.; Mollo, E.; Cimino, G. *Tetrahedron* **2003**, *59*, 5579-5583.

48. Cimino, G.; Crispino, A.; Gavagnin, M.; Zubia, E.; Trivellone, E. *J. Nat. Prod.* **1993**, *56*, 1642-1646.

49. Manzo, E.; Ciavatta, M. L.; Gavagnin, M.; Mollo, E.; Guo, Y.-W.; Cimino, G. *J. Nat. Prod.* **2004**, *67*, 1701-1704.

50. Ciavatta, M. L.; Fontana, A.; Puliti, R.; Scognamiglio, G.; Cimino, G. *Tetrahedron* **1999**, *55*, 12629-12636.

51. Wratten, S. J.; Faulkner, D. J.; Hirotsu, K.; Clardy, J. *Tetrahedron Lett.* **1978**, *19*, 4345-4348.

52. Fusetani, N.; Yasumuro, K.; Kawai, H.; Natori, T.; Brinen, L.; Clardy, J. *Tetrahedron Lett.* **1990**, *31*, 3599-3602.

53. Hirota, H.; Tomono, Y.; Fusetani, N. *Tetrahedron* **1996**, *52*, 2359-2368.

54. Shimomura, M.; Miyaoka, H.; Yamada, Y. *Tetrahedron Lett.* **1999**, *40*, 8015-8017.

55. Patra, A.; Chang, C. W. J.; Scheuer, P. J.; Van Duyne, G. D.; Matsumoto, G. K.; Clardy, J. *J. Am. Chem. Soc.* **1984**, *106*, 7981-7983.

56. Chang, C. W. J.; Patra, A.; Baker, J. A.; Scheuer, P. J. *J. Am. Chem. Soc.* **1987**, *109*, 6119-6123.

57. Chang, C. W. J.; Patra, A.; Roll, D. M.; Scheuer, P. J.; Matsumoto, G. K.; Clardy, J. *J. Am. Chem. Soc.* **1984**, *106*, 4644-4646.

58. Zhang, W.; Gavagnin, M.; Guo, Y. W.; Mollo, E.; Ghiselin, M. T.; Cimino, G. *Tetrahedron* **2007**, *63*, 4725-4729.

59. Fattorusso, E.; Romano, A.; Taglialatela-Scafati, O.; Bavestrello, G.; Bonelli, P.; Calcinai, B. *Tetrahedron Lett.* **2006**, *47*, 2197-2200.

60. De Miranda, D. S.; Brendolan, G.; Imamura, P. M.; González Sierra, M.; Marsaioli, A. J.; Rúveda, E. A. *J. Org. Chem* **1981**, *46*, 4851-4858.

61. Imamura, P. M.; Ruveda, E. A. *J. Org. Chem.* **1980**, *45*, 510-515.

62. Yamamura, S.; Terada, Y. *Tetrahedron Lett.* **1977**, *18*, 2171-2172.

63. Nishizawa, M.; Takenaka, H.; Hirotsu, K.; Higuchi, T.; Hayashi, Y. *J. Am. Chem. Soc.* **1984**, *106*, 4290-4291.

64. Nishizawa, M.; Takenaka, H.; Hayashi, Y. *J. Org. Chem.* **1986**, *51*, 806-813.

65. Gustafson, K.; Andersen, R. J.; Chen, M. H. M.; Clardy, J.; Hochlowski, J. E. *Tetrahedron Lett.* **1984**, *25*, 11-14.

66. Gustafson, K.; Andersen, R. J. *Tetrahedron* **1985**, *41*, 1101-1108.

67. Cimino, G.; De Rosa, D.; De Stefano, S.; Minale, L. *Tetrahedron* **1974**, *30*, 645-649.

68. Zubia, E.; Gavagnin, M.; Crispino, A.; Martinez, E.; Ortea, J.; Cimino, G. *Experientia* **1993**, *49*, 268-271.

69. Gavagnin, M.; Ungur, N.; Castelluccio, F.; Muniain, C.; Cimino, G. *J. Nat. Prod.* **1999**, *62*, 269-274.

70. Gavagnin, M.; Ungur, N.; Castelluccio, F.; Cimino, G. *Tetrahedron* **1997**, *53*, 1491-1504.

71. Ungur, N.; Gavagnin, M.; Mollo, E.; Cimino, G. *Tetrahedron: Asymmetry* **1999**, *10*, 1635-1636.

72. Cimino, G.; Gavagnin, M.; Sodano, G.; Puliti, R.; Mattia, C. A.; Mazzarella, L. *Tetrahedron* **1988**, *44*, 2301-2310.

73. Gavagnin, M.; De Napoli, A.; Castelluccio, F.; Cimino, G. *Tetrahedron Lett.* **1999**, *40*, 8471-8475.

74. Cimino, G.; Morrone, R.; Sodano, G. *Tetrahedron Lett.* **1982**, *23*, 4139-4142.

75. Nakano, T.; Hernandez, M. I.; Martin, A. *J. Chem. Res.* **1984**, *S*, 262-263.

76. Puliti, R.; Mattia, C. A. *Acta Cryst.* **1999**, *C*, 2160-2163.

77. Zubia, E.; Gavagnin, M.; Scognamiglio, G.; Cimino, G.; Giusto, G. B. *J. Nat. Prod.* **1994**, *57*, 725-731.

78. Eliel, L. E.; Wilen, S. H.; Mander, L. N. *Stereochemistry of Organic Compounds*; John Wiley and Sons Inc.: New York, 1994; 991 pp.

79. Harada, N.; Nakanishi, K. *Circular Dichroic Spectroscopy. Exciton coupling in Organic Stereochemistry.*; Oxford University Press: Oxford, 1983; pp 1-9.

80. Hyosu, M.; Kimura, J. *J. Nat. Prod.* **2000**, *63*, 422-423.

81. Herz, W.; Prasad, J. S. *J. Org. Chem.* **1984**, *49*, 326-333.

82. Vlad, P. F.; Ungur, N. D.; Barba, A. N.; Tamarova, A. E.; Gatilov, Y. V.; Korchagina, D. V. *Zh. Org. Khim.* **1986**, *22*, 2519-2533.

83. Ungur, N.; Gavagnin, M.; Fontana, A.; Cimino, G. *Tetrahedron* **2000**, *56*, 2503-2512.

84. Azevedo, D. A.; Neto, F. R. A.; Simoneit, B. R. T. *Org. Geochem.* **1998**, *28*, 289-295.

85. Bowden, S. A.; Farrimond, P.; Snape, C. E.; Love, G. D. *Org. Geochem.* **2006**, *37*, 369-383.

86. Jincai, T.; Xianbin, W.; Jianfa, C. *Org. Geochem.* **1999**, *30*, 1429-1435.

87. Fontana, A.; Ungur, N.; Gavagnin, M.; Salierno, C.; Cimino, G. *Tetrahedron Lett.* **1997**, *38*, 4145-4148.

88. Cimino, G.; Ciavatta, M. L.; Fontana, A.; Gavagnin, M. *Bioactive Compounds from Natural Sources*; Tringali, C., Ed.; Taylor and Francis: London, 2001; pp 577-637.

89. Cimino, G.; Fontana, A.; Cutignano, A.; Gavagnin, M. *Phytochemistry Reviews* **2004**, *3*, 285-307.

90. Graziani, E. I.; Andersen, R. J.; Krug, P. J.; John Faulkner, D. *Tetrahedron* **1996**, *52*, 6869-6878.

91. de Petrocellis, L.; Di Marzo, V.; Arca, B.; Gavagnin, M.; Minei, J.; Cimino, G. *Comp. Biochem. Physiol.* **1991**, *100C*, 603-607.

92. Keyzers, R. A. PhD Thesis, Victoria University of Wellington, 2003.

93. West, C.; Lesellier, E. *J. Chromatogr. A* **2006**, *1110*, 200-213.

94. Claridge, T. W. *High Resolution NMR Techniques in Organic Chemistry*; Pergamon: Oxford, 1999; Vol. 19; 317 pp.

95. Diaz-Marrero, A. R.; Dorta, E.; Cueto, M.; Rovirosa, J.; San Martin, A.; Loyola, A.; Darias, J. *Tetrahedron* **2003**, *59*, 4805-4809.

96. Diaz-Marrero, A. R.; Dorta, E.; Cueto, M.; Rovirosa, J.; San Martin, A.; Loyola, A.; Darias, J. *ARKIVOC* **2003**, *X*, 107-117.

97. San Martin, A.; Quezada, E.; Soto, P.; Palacios, Y.; Rovirosa, J. *Can. J. Chem* **1996**, *74*, 2471-2475.

98. Walsby, J. R.; Morton, J. E.; Croxall, J. P. *J. Zool. Lond.* **1973**, *171*, 257-283.

99. Manker, D. C.; Faulkner, D. J. *Tetrahedron* **1987**, *43*, 3677-3680.

100. Gray, C. A. PhD Thesis, Rhodes University, 2002.

101. Rice, S. H. *J. Exp. Mar. Biol. Ecol* **1985**, *93*, 83-89.

102. Gao, W. g.; Sakaguchi, K.; Isoe, S.; Ohfune, Y. *Tetrahedron Lett.* **1996**, *37*, 7071-7074.

103. Pathak, A.; Aslaoui, J.; Morin, C. *J.Org.Chem.* **2005**, *70*, 4184-4187.

104. Rovirosa, J.; Quezada, E.; San Martin, A. *Bol.Soc.Chil.Quim* **1992**, *37*, 143-145.

105. Blumenthal, F.; Polborn, K.; Steffan, B. *Tetrahedron* **2002**, *58*, 8433-8437.

106. Yamashita, M.; Shimizu, T.; Kawasaki, I.; Ohta, S. *Tetrahedron: Asymmetry* **2004**, *15*, 2315-2317.

107. Aiello, A.; Esposito, G.; Fattorusso, E.; Iuvone, T.; Luciano, P.; Menna, M. *Steroids* **2003**, *68*, 719-723.

108. Aknin, M.; Constantino, V.; Mangoni, A.; Fattorusso, E.; Gaydou, E. M. *Steroids* **1998**, *63*, 575-578.

109. Bonini, C.; Cooper, C. B.; Kazlauskas, R.; Wells, R. J.; Djerassi, C. *J. Org. Chem.* **1983**, *48*, 2108-2111.

110. Morris, L. A.; Christie, E. M.; Jaspars, M.; van Ofwegen, L. P. *J. Nat. Prod.* **1998**, *61*, 538-541.

111. Kazlauskas, R.; Murphy, P. T.; Ravi, B. N.; Sanders, R. L.; Wells, R. J. *Aust. J. Chem* **1982**, *35*, 69-75.

112. Koljak, R.; Lopp, A.; Pehk, T.; Varvas, K.; Muurisepp, A. M.; Jarving, I.; Samel, N. *Tetrahedron* **1998**, *54*, 179-186.

113. Naz, S.; Kerr, R. G.; Narayanan, R. *Tetrahedron Lett.* **2000**, *41*, 6035-6040.

114. Anta, C.; Gonzalez, N.; Rodriguez, J.; Jimenez, C. *J. Nat. Prod.* **2002**, *65*, 1357-1359.

115. Su, J. H.; Tseng, Y. J.; Huang, H. H.; Ahmed, A. F.; Lu, C. K.; Wu, Y. C.; Sheu, J. H. *J. Nat. Prod.* **2006**, *69*, 850-852.

116. Duh, C. Y.; Li, C. H.; Wang, S. K.; Dai, C. F. *J. Nat. Prod.* **2006**, *69*, 1188-1192.

117. Dopeso, J.; Quinoa, E.; Riguera, R.; Debitus, C.; Bergquist, P. R. *Tetrahedron* **1994**, *50*, 3813-3828.

118. Lu, Q.; Faulkner, D. J. *J. Nat. Prod.* **1997**, *60*, 195-198.

119. Reddy, M. V. R.; Harper, M. K.; Faulkner, D. J. *J. Nat. Prod.* **1997**, *60*, 41-43.

120. Rueda, A.; Zubia, E.; Ortega, M. J.; Carballo, J. L.; Salva, J. *J. Nat. Prod.* **1998**, *61*, 258-261.

121. van Altena, I. A.; Butler, A. J.; Dunne, S. J. *J. Nat. Prod.* **1999**, *62*, 1154-1157.

122. Goetz, G. H.; Harrigan, G. G.; Likos, J. *J. Nat. Prod.* **2001**, *64*, 1486-1488.

123. Ohtani, I.; Kusumi, T.; Kashman, Y.; Kakisawa, H. *J. Am. Chem. Soc.* **1991**, *113*, 4092-4096.

124. Ishihara, K.; Kurihara, H.; Yamamoto, H. *J. Org. Chem.* **1993**, *58*, 3791-3793.

125. Dale, J. A.; Mosher, H. S. *J. Am. Chem. Soc.* **1973**, *95*, 512-519.

126. Gunatilaka, A. A. L.; Gopichand, Y.; Schmitz, F. J.; Djerassi, C. *J. Org. Chem.* **1981**, *46*, 3860-3866.

127. Sera, Y.; Adachi, K.; Shizuri, Y. *J. Nat. Prod.* **1999**, *62*, 152-154.

128. Jiménez, C.; Quinoa, E.; Castedo, L.; Riguera, R. *J. Nat. Prod.* **1986**, *49*, 905-909.

129. Pickens, A.; Orringer, M. B. *Ann. Thorac. Surg.* **2003**, *76*, S1367-S1369.

130. Voutalainen, M. E.; Juhola, M. T. *Dis. Esophagus* **2005**, *18*, 221-225.

131. Day, N. E. *Cancer Res.* **1975**, *35*, 3304-3307.

132. Devesa, S. S.; Blot, W. J.; Fraumeni, J. F. *Cancer* **1998**, *83*, 2049-2053.

133. Whibley, C. E.; Keyzers, R. A.; Soper, A. G.; Davies-Coleman, M. T.; Samaai, T.; Hendicks, D. T. In *Natural Products and Molecular Therapy: First International Conference,* vol 1056 of the *Annals of the New York Academy of Sciences*; Kotwal, J.G.; Lahiri, D.K. Eds; 2005; pp 233-252.

134. Bohr, U. R. M.; Segal, I.; Primus, A.; Wex, T.; Hassan, H.; Ally, R.; Malfertheiner, P. *Helicobacter* **2003**, *8*, 608-612.

135. Whibley, C. E. PhD Thesis, University of Cape Town, 2006.

136. Matsha, T.; Brink, L.; van Rensburg, S.; Hon, D.; Lombard, C.; Erasmus, R. *Nutr. Cancer* **2006**, *56*, 67-73.

137. Law, S.; Wong, J. *J. Gastroen. Hepatol.* **2002**, *17*, 374-381.

138. Vistica, D. T.; Skehan, P.; Scudiero, D.; Monks, A.; Pittman, A.; Boyd, M. R. *Cancer Res.* **1991**, *51*, 2515-2520.

139. Dekker, T. G.; Fourie, T. G.; Matthee, E.; Snyckers, F. O.; van der Schyft, C. J.; Boeyens, J. C. A.; Denner, L. *S. Afr. J. Chem.* **1988**, *41*, 33-35.

140. Gray, C. A.; Davies-Coleman, M. T.; Rivett, D. E. A. *Tetrahedron* **2003**, *59*, 165-173.

141. Davies-Coleman, M. T.; Rivett, D. E. A. *S. Afr. J. Chem.* **1990**, *43*, 117-119.

142. Garcia-Alvarez, M. C.; Pérez-Sirvent, L.; Rodríguez, B.; Savona, G. *An. Quim.* **1981**, *77*, 316-319.

143. Dominguez, G.; Marco, J. L.; Hueso-Rodríguez, J. A.; Rodriguez, B. *An. Quim.* **1988**, *84*, 211-214.

144. Hueso-Rodríguez, J. A.; Dominguez, G.; Rodriguez, B. *An. Quim.* **1988**, *84*, 215-218.

145. Mori, K.; Tominaga, M.; Takigawa, T.; Matsui, M. *Synthesis* **1973**, 790-791.

146. Garelik, G. *Science* **2002**, *298*, 1702-1704.

147. Mangoni, L.; Bellardini, M. *Gazz. Chim. Ital.* **1963**, *93*, 465-475.

148. Gray, C. A.; Rivett, D. E. A.; Davies-Coleman, M. T. *Phytochemistry* **2003**, *63*, 409-413.

149. Reeve, W.; Doherty, R. M. *J. Org. Chem.* **1975**, *40*, 1662-1664.

150. Demir, A. S.; Reis, O.; Cigdem Igdir, A. *Tetrahedron* **2004**, *60*, 3427-3432.

151. Tanyeli, C.; Ozdemirhan, D. *Tetrahedron Lett.* **2003**, *44*, 7311-7313.

152. Bush, J. B.; Finkbeiner, H. *J. Am. Chem. Soc.* **1968**, *90*, 5903-5905.

153. Williams, G. J.; Hunter, N. R. *Can. J. Chem.* **1976**, *54*, 3830-3832.

154. Snider, B. B.; Kiselgof, E. Y. *Tetrahedron* **1996**, *52*, 6073-6084.

155. Jones, M. *Organic Chemistry*; W.W. Norton & Company, Inc.: New York, 1997; pp 1246-1248.

156. Byun, H.-G.; Huiping, Z.; Mochizuki, M.; Adachi, K.; Shizuri, Y.; Lee, W.-J.; Kim, S.-K. *J. Antibiot.* **2003**, *56*, 102-106.

157. Ou, S. H. *Rice Diseases*; CAB: Surrey, UK, 1985; 110 pp.

158. Hamer, J. E.; Talbot, N. J. *Curr. Opin. Microbiol.* **1998**, *1*, 693-697.

159. Talbot, N. J. *Ann. Rev. Microbiol.* **2003**, *57*, 177-202.

160. Geagea, L.; Huber, L.; Sache, I.; Flura, D.; McCartney, H. A.; Fitt, B. D. L. *Agr.Forest Meteorol.* **2000**, *101*, 53-66.

161. Rossing, W. A. H.; Daamen, R. A.; Hendrix, E. M. T. *Crop Prot.* **1994**, *13*, 25-34.

162. Kim, H. T.; Min, J. Y.; Choi, G. J.; Kim, J.-C.; Kim, B. S.; Chung, Y. R.; Kim, B. T.; Kim, Y. S.; Yamaguchi, I.; Cho, K. Y. *J. Pestic. Sci* **2002**, *27*, 229-234.

163. Ra, C. S.; Jung, B. Y.; Park, G. *Heterocycles* **2004**, *62*, 793-802.

164. Hewitt, G. *Pesticide Outlook* **2000**, *11*, 28-32.

165. Ming, Y.; Zhao, L.; Zhang, H.; Shi, Y.; Li, Y. *Chromatographia* **2006**, *64*, 273-280.

166. Lamb, D. C.; Kelly, D. E.; Manning, N. J.; Hollomon, D. W.; Kelly, S. L. *FEMS Microbiol. Lett.* **1998**, *169*, 369-373.

167. Jordan, D. B.; Lessen, T. A.; Wawrzak, Z.; Bisaha, J. J.; Gehret, T. C.; Hansen, S. L.; Schwartz, R. S.; Basarab, G. S. *Bioorg. Med. Chem. Lett.* **1999**, *9*, 1607-1612.

168. Basarab, G. S.; Jordan, D. B.; Gehret, T. C.; Schwartz, R. S.; Wawrzak, Z. *Bioorg. Med. Chem. Lett.* **1999**, *9*, 1613-1618.

169. Manabe, A.; Maeda, K.; Enomoto, M.; Takano, H.; Katoh, T.; Yamada, Y.; Oguri, Y. *J. Pestic. Sci* **2002**, *27*, 257-266.

170. Kurahashi, Y. *Pesticide Outlook* **2001**, *12*, 32-35.

171. Ciavatta, M. L.; Villani, G.; Trivellone, E.; Cimino, G. *Tetrahedron Lett.* **1995**, *36*, 8673-8676.

172. Proksch, P.; Edrada-Ebel, R.; Ebel, R. *Mar. Drugs* **2003**, *1*, 5-17.

173. Wisch, G. A. MSc Thesis, Rhodes University, 2002.

174. Do Khac Manh, D.; Fetizon, M.; Flament, J. P. *Tetrahedron* **1975**, *31*, 1897-1902.

175. Zambrano, J. L.; Rosales, V.; Nakano, T. *Tetrahedron Lett.* **2003**, *44*, 1859-1862.

176. Bolster, M. G.; Lagnel, B. M. F.; Jansen, B. J. M.; Morin, C.; de Groot, A. *Tetrahedron* **2001**, *57*, 8369-8379.

177. do Céu Costa; Tavares, R.; Motherwell, W. B.; Marcelo Curto, M. J. *Tetrahedron Lett.* **1994**, *35*, 8839-8842.

178. Grant, P. K.; Weavers, R. T. *Tetrahedron* **1974**, *30*, 2385-2395.

179. Ohloff, G.; Vial, C.; Demole, E.; Enggist, P.; Giersch, W.; Jégou, E.; Caruso, A. J.; Polonsky, J.; Lederer, E. *Helv. Chim. Acta* **1986**, *69*, 163-173.

180. Macdonald, T. L.; Still, W. C. *J. Am. Chem. Soc.* **1975**, *97*, 5280-5281.

181. Maruoka, K.; Itoh, T.; Yamamoto, H. *J. Am. Chem. Soc.* **1985**, *107*, 4573-4576.

182. Hugel, G.; Oehlschlager, A. C.; Ourisson, G. *Tetrahedron* **1966**, *22*, 203-216.

183. San Feliciano, A.; Medarde, M.; Lopez, J. L.; del Corral, M.; Puebla, P.; Barrero, A. F. *Phytochemistry* **1988**, *27*, 2241-2248.

184. Buckwalter, B. L.; Burfitt, I. R.; Nagel, A. A.; Wenkert, E.; Näf, F. *Helv. Chim. Acta* **1975**, *58*, 1567-1573.

185. Schmidt, T. J.; Passreiter, C. M.; Wendisch, D.; Willuhn, G. *Phytochemistry* **1995**, *40*, 1213-1218.

186. Munro, O. Q.; du Toit, K.; Drewes, S. E.; Crouch, N. R.; Mullholland, D. A. *New J. Chem.* **2006**, *30*, 197-207.

187. Mancuso, A. J.; Swern, D. *Synthesis* **1981**, 165-185.

188. Dess, D. B.; Martin, J. C. *J. Am. Chem. Soc.* **1991**, *113*, 7277-7287.

189. Zhdankin, V. V. *Curr. Org. Synth* **2005**, *2*, 121-145.

190. Bigley, D. B.; Rogers, N. A. J.; Barltrop, J. A. *J. Chem. Soc.* **1960**, *4*, 4613-4627.

191. Ruzicka, L.; Seidel, C. F.; Engel, L. L. *Helv. Chim. Acta* **1942**, *25*, 621-630.

192. Popa, D. P.; Pasechnik, G. S. *Zh. Obshch. Khim.* **1969**, *39*, 2374-2375.

193. Leite, M. A.; Sarragiotto, M. H.; Imamura, P. M.; Marsaioli, A. J. *J. Org. Chem.* **1986**, *51*, 5409-5410.

194. Gray, C. A.; Davies-Coleman, M. T.; Caira, M. R.; Nathanson, C. A.; Wisch, G. A. *J. Chem. Research (S)* **2003**, 405-407.

195. Gansaüer, A.; Worgull, D.; Justicia, J. *Synthesis* **2006**, *13*, 2151-2154.

196. Reetz, M. T.; Kyung, S. H.; Hüllmann, M. *Tetrahedron* **1986**, *42*, 2931-2935.

197. Sun, J.; Dong, Y.; Cao, L.; Wang, X.; Wang, S.; Hu, Y. *J. Org. Chem.* **2004**, *69*, 8932-8934.

198. Li, T.-S.; Zhang, Z.-H.; Fu, C.-G. *Tetrahedron Lett.* **1997**, *38*, 3285-3288.

199. Wenkert, E.; Mahajan, J. R.; Nussim, M.; Schenker, F. *Can. J. Chem.* **1966**, *44*, 2575-2579.

200. Sarragiotto, M. H.; Gower, A. E.; Marsaioli, A. J. *J. Chem. Soc., Perkin Trans.1* **1989**, *48*, 559-562.

201. Roldan, E. A. M.; Santiago, J. L. R.; Chahboun, R. *J. Nat. Prod.* **2006**, *69*, 563-566.

202. Buckwalter, B. L.; Burfitt, I. R.; Felkin, H.; Joly-Goudket, M.; Naemura, K.; Salomon, M. F.; Wenkert, E.; Wovkulich, P. M. *J. Am. Chem. Soc.* **1978**, *100*, 6445-6450.

203. Sundararaman, P.; Herz, W. *J. Org. Chem.* **1977**, *42*, 813-819.

204. Ravn, M. M.; Coates, R. M.; Flory, J. E.; Peters, R. J.; Croteau, R. *Org. Lett.* **2000**, *2*, 573-576.

205. Boutagy, J.; Thomas, R. *Chem. Rev.* **1974**, *74*, 87-99.

206. Maryanoff, B. E.; Reitz, A. B. *Chem. Rev.* **1989**, *89*, 863-927.

207. Kelly, S. E. *Alkene Synthesis. Comparative Organic Synthesis*; Pergamon: Oxford, 1991; Vol. 1; pp 761-773.

208. Touchard, F. P. *Tetrahedron Lett.* **2004**, *45*, 5519-5523.

209. Duthaler, R. O.; Bienewald, F.; Hafner, A. In *Transition Metals for Organic Synthesis, Vol. 1*; 2nd ed.; Beller, M.; Bolm, C., Eds.; Wiley-VCH Verlag GmbH & Co. KGaA: Weinheim, 2004; pp 491-517.

210. Giang, P. M.; Son, P. T.; Matsunami, K.; Otsuka, H. *Chem. Pharm. Bull.* **2005**, *53*, 938-941.

211. Carman, R. M. *Aust. J. Chem* **1973**, *26*, 879-881.

212. Hofmann, J. J.; Jolad, S. D.; Timmermann, B. N.; Bates, R. B.; Camou, F. A.; Siahaan, T. *Phytochemistry* **1987**, *26*, 2861-2863.

213. Asili, J.; Lambert, M.; Ziegler, H. L.; Stærk, D.; Sairafianpour, M.; Witt, M.; Asghari, G.; Ibrahimi, I. S.; Jaroszewski, J. W. *J. Nat. Prod.* **2004**, *67*, 631-637.

214. Ziegler, H. L.; Jensen, T. H.; Christensen, J.; Stærk, D.; Hägerstrand, H.; Sittie, A. A.; Olsen, C. E.; Staalsø, T.; Ekpe, P.; Jaroszewski, J. W. *Planta Med.* **2002**, 547-549.

215. Sachs, J.; Malaney, P. *Nature* **2002**, *415*, 680-685.

216. Snow, R. W.; Trape, J. F.; Marsh, K. *Trends Parasitol.* **2001**, *17*, 593-597.

217. Snow, R. W.; Guerra, C. A.; Noor, A. M.; Myint, H. Y.; Hay, S. I. *Nature* **2005**, *434*, 214-217.

218. Breman, J. G. *Am. J. Trop. Med. Hyg.* **2001**, *64*, 1-11.

219. Winstanley, P. A. *Parasitology Today* **2000**, *16*, 146-153.

220. Ridley, R. G. *Nature* **2002**, *415*, 686-693.

221. Macreadie, I.; Ginsburg, H.; Sirawaraporn, W.; Tilley, L. *Parasitology Today* **2000**, *16*, 438-444.

222. Hyde, J. E. *Trends Parasitol.* **2005**, *21*, 494-498.

223. Rosenthal, P. J. *J. Exp. Biol.* **2003**, *206*, 3735-3744.

224. Tagboto, S.; Townson, S. In *Advances in Parasitology*; Volume 50 ed.; Academic Press: 2001; pp 199-295.

225. Sams-Dodd, F. *Drug Disc.Today* **2005**, *10*, 139-147.

226. Manitto, P. *Biosynthesis of Natural Products*; Ellis Horwood Ltd.: Chichester, 1981; Vol. 1; pp 761-773.

227. Claridge, T. W. *High Resolution NMR Techniques in Organic Chemistry*; Pergamon: Oxford, 1999; Vol. 19; pp 242-247.

228. Clayden, J.; Greeves, N.; Warren, S. Wothers, P. *Organic Chemistry*; Oxford University Press: Oxford.

229. Ziegler, H. L.; Stærk, D.; Christensen, J.; Olsen, C. E.; Sittie, A. A.; Jaroszewski, J. W. *J. Nat. Prod.* **2002**, *65*, 1764-1768.

230. Ziegler, H. L.; Franzyk, H.; Sairafianpour, M.; Tabatabai, M.; Tehrani, M. D.; Bagherzadeh, K.; Hagerstrand, H.; Stærk, D.; Jaroszewski, J. W. *Bioorg. Med. Chem.* **2004**, *12*, 119-127.

231. Mills, J. P.; Diez-Silva, M.; Quinn, D. J.; Dao, M.; Lang, M. J.; Tan, K. S. W.; Lim, C. T.; Milon, G.; David, P. H.; Mercereau-Puijalon, O.; Bonnefoy, S.; Suresh, S. *PNAS* **2007**, *104*, 9213-9217.

232. Glenister, F. K.; Coppel, R. L.; Cowman, A. F.; Mohandas, N.; Cooke, B. M. *Blood* **2002**, *99*, 1060-1063.

233. Nash, G. B.; O'Brien, E.; Gordon-Smith, E. C.; Dormandy, J. A. *Blood* **1989**, *74*, 855-861.

234. Perrin, D. D.; Armarego, W. L. F. *Purification of Laboratory Chemicals (3rd edition)*; Pergamon Press: Oxford, 1988.

235. Rappé, A. K.; Casewit, C. J.; Colwell, K. S.; Goddard, W. A.; Skiff, W. M. *J. Am. Chem. Soc.* **1992**, *114*, 10024-10035.

236. Rappé, A. K.; Goddard, W. A. *J. Phys. Chem.* **1991**, *95*, 3358-3363.

237. Flack, H. D. *Acta Cryst.* **1983**, *A39*, 876-881.

238. Veale, R. B.; Thornley, A. L. *S. Afr. J. Sci.* **1989**, *85*, 375-379.

239. Bolster, M. G.; Jansen, B. J. M.; de Groot, A. *Tetrahedron* **2001**, *57*, 5663-5679.

240. Nunes, F. M. N.; Imamura, P. M. *J. Braz. Chem. Soc.* **1996**, *7*, 181-186.

241. Dawson, R. M.; Godfrey, I. M.; Hogg, R. W. *Aust. J. Chem* **1989**, *42*, 561-579.

242. Toshima, H.; Oikawa, H.; Toyomasu, T.; Sassa, T. *Tetrahedron* **2000**, *56*, 8443-8450.

243. Barrero, A. F.; Alvarez-Manzaneda, E. J.; Altarejos, J.; Salido, S.; Ramos, J. M. *Tetrahedron* **1993**, *49*, 10405-10412.

244. Bastard, J.; Duc, D. K.; Fetizon, M.; Francis, M. J.; Grant, P. K.; Weavers, R. T.; Kaneko, C.; Baddeley, G. V.; Bernassau, J. M.; Burfitt, I. R.; Wovkulich, P. M.; Wenkert, E. *J. Nat. Prod.* **1984**, *47*, 592-599.

245. Makler, M. T.; Hinrichs, D. J. *Am. J. Trop. Med. Hyg.* **1993**, *48*, 205-210.

246. Lim, G. H. W.; Wortis, M.; Mukhopadhyay, R. *Proc. Natl. Acad. Sci. U.S.A.* **2002**, *99*, 16766-16769.

Appendix I X-ray crystallographic data for 3.33

Table 1 - Crystal Data and Details of the Structure Determination

Crystal Data			
Formula			C36 H50 O10
Formula Weight			642.76
Crystal System			Monoclinic
Space group		P21	(No. 4)
a, b, c [Angstrom]	10.4893(2)	7.7835(2)	21.1003(5)
alpha, beta, gamma [deg]	90	93.5180(10)	90
V [Ang**3]			1719.46(7)
Z			2
D(calc) [g/cm**3]			1.242
Mu(MoKa) [/mm]			0.090
F(000)			692
Crystal Size [mm]		0.09 x 0.12 x 0.12	

Data Collection			
Temperature (K)			113
Radiation [Angstrom]		MoKa	0.71073
Theta Min-Max [Deg]			3.3, 25.7
Dataset		-12: 12 ; -9: 9 ; -25: 25	
Tot., Uniq. Data, R(int)		6480, 6480, 0.000	
Observed data [I > 2.0 sigma(I)]			5199

Refinement			
Nref, Npar			6480, 429
R, wR2, S		0.0606, 0.1606, 1.04	
w = 1/[\s^2^(Fo^2^)+(0.0759P)^2^+1.0114P] where P=(Fo^2^+2Fc^2^)/3			
Max. and Av. Shift/Error			0.00, 0.00
Flack x			0.1(13)
Min. and Max. Resd. Dens. [e/Ang^3]			-0.40, 0.69

Table S2 - Final Coordinates and Equivalent Isotropic Displacement Parameters of the non-Hydrogen atoms

Atom	x	y	z	U(eq) [Ang^2]
O21	0.29576(18)	0.3315(2)	0.41881(10)	0.0340(6)
O23	0.2071(2)	0.5234(3)	0.48244(11)	0.0428(7)
O25	0.80342(18)	0.7270(3)	0.34918(10)	0.0375(7)
O27	0.9860(2)	0.5787(3)	0.34612(13)	0.0578(9)
O29	0.6715(2)	0.5547(3)	0.20077(10)	0.0455(8)
O31	0.8231(4)	0.6515(5)	0.14112(18)	0.1052(17)
*O33A	0.1134(6)	1.3843(8)	0.2036(3)	0.0384(19)
*O35A	-0.0061(4)	1.2262(7)	0.1334(2)	0.0578(17)
O37	0.2057(4)	1.6011(4)	0.11305(14)	0.0779(13)
O46	0.3489(5)	1.7526(5)	0.0637(4)	0.154(3)
C1	0.3945(3)	0.5695(4)	0.36634(14)	0.0311(6)
C2	0.4131(3)	0.4318(4)	0.41718(14)	0.0319(9)
C3	0.5142(3)	0.3020(4)	0.40160(16)	0.0352(9)
C4	0.6445(3)	0.3822(4)	0.38936(14)	0.0343(9)
C5	0.6191(3)	0.5272(4)	0.33962(14)	0.0313(9)
C6	0.7354(3)	0.6008(4)	0.30913(15)	0.0364(9)
C7	0.6951(3)	0.6902(4)	0.24827(15)	0.0389(10)
C8	0.5753(3)	0.7974(4)	0.25000(15)	0.0400(10)
C9	0.4969(3)	0.7882(4)	0.29829(14)	0.0343(9)
C10	0.5196(3)	0.6675(4)	0.35500(14)	0.0294(8)
C11	0.3804(3)	0.9064(4)	0.29799(15)	0.0378(9)
C12	0.2663(3)	0.8405(4)	0.25645(16)	0.0427(10)
C13	0.1556(3)	0.9644(5)	0.24535(16)	0.0422(11)
C14	0.1583(4)	1.1247(5)	0.26660(17)	0.0508(11)
C15	0.0549(4)	1.2581(6)	0.2531(2)	0.0655(11)
C16	0.0452(3)	0.8859(5)	0.2080(2)	0.0576(13)

Table 2 - Final Coordinates and Equivalent Isotropic Displacement Parameters of the non-Hydrogen atoms(continued)

Atom	x	y	z	U(eq) [Ang^2]
C17	0.5551(4)	0.9170(5)	0.19385(17)	0.0529(12)
C18	0.7166(3)	0.4350(4)	0.45172(15)	0.0402(7)
C19	0.7238(3)	0.2392(4)	0.35989(17)	0.0427(10)
C20	0.5571(3)	0.7812(4)	0.41338(14)	0.0335(7)
C22	0.1998(3)	0.3939(4)	0.45130(14)	0.0333(9)
C24	0.0873(3)	0.2776(4)	0.44456(16)	0.0391(10)
C26	0.9301(3)	0.7050(4)	0.36070(14)	0.0348(9)
C28	0.9918(3)	0.8557(5)	0.39353(16)	0.0417(10)
C30	0.7465(3)	0.5448(5)	0.15202(16)	0.0445(10)
C32	0.7194(4)	0.3892(6)	0.1124(2)	0.0654(14)
*C34A	0.0700(6)	1.3362(9)	0.1460(4)	0.043(2)
C36	0.1470(4)	1.4358(6)	0.1001(2)	0.0673(16)
C38	0.2876(4)	1.6232(6)	0.0663(2)	0.0661(14)
C39	0.2806(4)	1.4699(5)	0.02612(18)	0.0531(12)
C40	0.1477(5)	1.4860(9)	-0.0079(2)	0.097(2)
C41	0.0569(4)	1.4631(8)	0.0447(3)	0.099(2)
C42	0.2598(3)	1.3324(5)	0.07550(17)	0.0466(11)
C43	0.3694(5)	1.3081(9)	0.1247(2)	0.092(2)
C44	0.2234(6)	1.1555(7)	0.0498(4)	0.117(3)
C45	0.3912(6)	1.4499(10)	-0.0155(3)	0.110(2)
*C34B	0.1445(14)	1.4101(15)	0.1779(6)	0.043(4)
*O33B	0.0444(7)	1.3068(10)	0.1845(4)	0.041(2)
*O35B	0.2097(8)	1.4602(8)	0.2247(3)	0.065(3)

U(eq) = 1/3 of the trace of the orthogonalized U Tensor

Starred Atom sites have a S.O.F less than 1.0

Table 3 - Hydrogen Atom Positions and Isotropic Displacement Parameters

Atom	x	y	z	U(iso) [Ang^2]
H1A	0.32930	0.65250	0.37920	0.0370
H1B	0.36200	0.51530	0.32610	0.0370
H2	0.43480	0.48540	0.45950	0.0380
H3A	0.48340	0.23660	0.36340	0.0420
H9	0.79490	0.50490	0.29990	0.0440
H11A	0.35460	0.91960	0.34210	0.0450
H11B	0.40470	1.02140	0.28260	0.0450
H12A	0.29680	0.80760	0.21470	0.0510
H12B	0.23400	0.73500	0.27620	0.0510
H14	0.23120	1.15890	0.29250	0.0610
H16A	0.07060	0.85730	0.16530	0.0870
H16B	0.01840	0.78120	0.22920	0.0870
H16C	-0.02590	0.96770	0.20480	0.0870
H17A	0.62400	0.90070	0.16500	0.0800
H17B	0.55560	1.03620	0.20880	0.0800
H17C	0.47280	0.89170	0.17130	0.0800
H3B	0.52580	0.21970	0.43720	0.0420
H5	0.57430	0.46420	0.30340	0.0370
H7	0.76670	0.76460	0.23530	0.0470
H19A	0.72490	0.13740	0.38720	0.0640
H19B	0.81140	0.27980	0.35600	0.0640
H19C	0.68550	0.20970	0.31780	0.0640
H20A	0.64270	0.82880	0.40910	0.0500
H20B	0.55690	0.71160	0.45210	0.0500
H20C	0.49550	0.87530	0.41590	0.0500
H24A	0.01350	0.33370	0.46200	0.0590

Table 3 - Hydrogen Atom Positions and Isotropic Displacement Parameters (continued)

Atom	x	y	z	U(iso) [Ang^2]
H24B	0.10640	0.17060	0.46770	0.0590
H24C	0.06800	0.25180	0.39950	0.0590
H28A	1.06550	0.81690	0.42060	0.0630
H28B	0.93020	0.91230	0.41970	0.0630
H28C	1.02030	0.93700	0.36190	0.0630
H32A	0.72200	0.41930	0.06740	0.0980
H32B	0.63450	0.34480	0.12050	0.0980
H32C	0.78380	0.30110	0.12330	0.0980
H40A	0.13630	1.60010	-0.02820	0.1170
H40B	0.13400	1.39580	-0.04070	0.1170
H41A	0.00410	1.56690	0.04990	0.1190
H41B	0.00050	1.36240	0.03690	0.1190
H43A	0.44580	1.27220	0.10370	0.1390
H43B	0.34680	1.21960	0.15510	0.1390
H43C	0.38650	1.41660	0.14720	0.1390
H44A	0.29530	1.10650	0.02840	0.1760
H44B	0.14910	1.16550	0.01960	0.1760
H44C	0.20240	1.08050	0.08500	0.1760
H45A	0.40580	1.55870	-0.03730	0.1650
H45B	0.37170	1.35970	-0.04700	0.1650
H45C	0.46800	1.41840	0.01070	0.1650
H18A	0.66070	0.50530	0.47680	0.0600
H18B	0.79250	0.50160	0.44240	0.0600
H18C	0.74260	0.33190	0.47580	0.0600

The Temperature Factor has the Form of Exp(-T) Where
T = 8*(Pi**2)*U*(Sin(Theta)/Lambda)**2 for Isotropic Atoms

Table 4 - (An)isotropic Displacement Parameters

Atom	U(1,1) or U	U(2,2)	U(3,3)	U(2,3)	U(1,3)	U(1,2)
O21	0.0311(10)	0.0251(11)	0.0466(12)	-0.0018(9)	0.0082(9)	-0.0065(9)
O23	0.0428(12)	0.0376(13)	0.0493(13)	-0.0077(11)	0.0125(10)	-0.0047(10)
O25	0.0297(10)	0.0330(11)	0.0507(13)	-0.0093(10)	0.0087(9)	-0.0088(9)
O27	0.0435(13)	0.0475(16)	0.0812(18)	-0.0172(14)	-0.0059(12)	0.0076(12)
O29	0.0421(12)	0.0513(14)	0.0451(13)	-0.0138(11)	0.0182(10)	-0.0128(11)
O31	0.113(3)	0.108(3)	0.103(3)	-0.051(2)	0.075(2)	-0.060(2)
O33A	0.046(3)	0.031(3)	0.039(4)	0.002(3)	0.010(3)	0.004(2)
O35A	0.053(3)	0.065(3)	0.055(3)	0.015(2)	0.000(2)	-0.010(3)
O37	0.119(3)	0.0568(19)	0.0590(17)	-0.0058(15)	0.0134(18)	0.0224(19)
O46	0.115(3)	0.062(3)	0.284(7)	0.022(4)	0.008(4)	-0.037(3)
C2	0.0320(15)	0.0262(16)	0.0382(16)	-0.0005(13)	0.0071(13)	-0.0056(12)
C3	0.0377(16)	0.0211(14)	0.0470(17)	-0.0007(13)	0.0046(13)	-0.0045(13)
C4	0.0335(14)	0.0257(15)	0.0442(17)	-0.0010(14)	0.0057(13)	-0.0005(13)
C5	0.0335(15)	0.0229(14)	0.0377(16)	-0.0014(13)	0.0050(12)	-0.0053(12)
C6	0.0351(15)	0.0283(15)	0.0463(18)	-0.0058(14)	0.0065(13)	-0.0043(13)
C7	0.0425(17)	0.0367(18)	0.0387(17)	-0.0041(14)	0.0116(14)	-0.0084(14)
C8	0.0458(18)	0.0307(17)	0.0440(18)	0.0017(14)	0.0064(14)	-0.0052(14)
C9	0.0395(16)	0.0255(15)	0.0378(16)	-0.0015(13)	0.0018(13)	-0.0019(13)
C10	0.0308(14)	0.0204(14)	0.0377(16)	-0.0012(12)	0.0072(12)	-0.0014(11)
C11	0.0487(18)	0.0251(15)	0.0396(16)	0.0040(14)	0.0034(14)	0.0039(14)
C12	0.0428(17)	0.0321(17)	0.0533(19)	0.0043(16)	0.0033(15)	0.0048(15)
C13	0.0421(18)	0.0426(19)	0.0433(18)	0.0119(15)	0.0129(14)	0.0080(15)
C14	0.070(2)	0.046(2)	0.0377(18)	0.0067(16)	0.0142(17)	0.0241(19)
C16	0.0376(17)	0.050(2)	0.085(3)	0.016(2)	0.0022(18)	-0.0001(17)
C17	0.067(2)	0.046(2)	0.047(2)	0.0121(17)	0.0131(17)	-0.0004(19)
C19	0.0375(16)	0.0262(16)	0.065(2)	-0.0012(16)	0.0084(15)	0.0026(14)

Table 4 - (An)isotropic Displacement Parameters (continued)

Atom	U(1,1) or U	U(2,2)	U(3,3)	U(2,3)	U(1,3)	U(1,2)
C22	0.0356(16)	0.0290(16)	0.0360(16)	0.0033(14)	0.0068(12)	0.0014(13)
C24	0.0329(15)	0.0381(18)	0.0469(18)	0.0013(15)	0.0073(13)	-0.0029(13)
C26	0.0359(16)	0.0314(17)	0.0378(16)	0.0040(14)	0.0070(13)	-0.0011(14)
C28	0.0392(16)	0.0410(18)	0.0458(18)	-0.0056(15)	0.0095(14)	-0.0102(15)
C30	0.0325(16)	0.058(2)	0.0438(18)	-0.0078(17)	0.0088(14)	-0.0024(17)
C32	0.051(2)	0.081(3)	0.066(2)	-0.028(2)	0.0176(18)	-0.005(2)
C34A	0.030(3)	0.041(4)	0.058(5)	0.000(4)	0.004(4)	0.007(3)
C36	0.069(3)	0.051(2)	0.086(3)	0.033(2)	0.039(2)	0.025(2)
C38	0.060(2)	0.048(2)	0.090(3)	0.009(2)	0.003(2)	-0.009(2)
C39	0.056(2)	0.059(2)	0.046(2)	0.0082(18)	0.0173(17)	0.0121(19)
C40	0.100(4)	0.118(5)	0.070(3)	-0.009(3)	-0.029(3)	0.045(4)
C41	0.039(2)	0.075(3)	0.183(6)	0.031(4)	-0.004(3)	0.004(2)
C42	0.0422(18)	0.047(2)	0.052(2)	0.0043(17)	0.0144(15)	0.0057(16)
C43	0.078(3)	0.117(5)	0.081(3)	0.028(3)	-0.001(3)	0.049(3)
C44	0.107(5)	0.047(3)	0.197(7)	-0.008(4)	0.005(5)	0.018(3)
C34B	0.067(9)	0.029(5)	0.035(7)	0.011(5)	0.013(6)	0.011(6)
O33B	0.047(4)	0.050(4)	0.026(4)	0.008(3)	0.014(3)	0.016(4)
O35B	0.110(6)	0.036(3)	0.048(4)	-0.001(3)	-0.010(4)	-0.028(4)

The Temperature Factor has the Form of Exp(-T) Where
T = 8*(Pi**2)*U*(Sin(Theta)/Lambda)**2 for Isotropic Atoms
T = 2*(Pi**2)*Sumij(h(i)*h(j)*U(i,j)*Astar(i)*Astar(j)), for Anisotropic Atoms. Astar(i) are Reciprocal Axial Lengths and h(i) are the Reflection Indices.

Table 5 - Bond Distances (Angstrom)

O21	-C2	1.460(4)	C7	-C8	1.511(4)
O21	-C22	1.343(4)	C8	-C9	1.350(4)
O23	-C22	1.203(4)	C8	-C17	1.511(5)
O25	-C6	1.454(4)	C9	-C11	1.529(4)
O25	-C26	1.347(4)	C9	-C10	1.529(4)
O27	-C26	1.195(4)	C10	-C20	1.548(4)
O29	-C7	1.466(4)	C11	-C12	1.528(5)
O29	-C30	1.335(4)	C12	-C13	1.517(5)
O31	-C30	1.188(5)	C13	-C14	1.326(5)
O33A	-C15	1.585(8)	C13	-C16	1.491(5)
O33A	-C34A	1.325(10)	C14	-C15	1.516(6)
O33B	-C15	1.494(9)	C22	-C24	1.487(4)
O33B	-C34B	1.337(16)	C26	-C28	1.490(5)
O35A	-C34A	1.190(8)	C30	-C32	1.489(6)
O35B	-C34B	1.230(15)	C34A	-C36	1.512(9)
O37	-C38	1.358(6)	C34B	-C36	1.656(13)
O37	-C36	1.445(6)	C36	-C41	1.473(7)
O46	-C38	1.198(6)	C36	-C42	1.547(6)
C1	-C2	1.521(4)	C38	-C39	1.463(6)
C1	-C10	1.549(4)	C39	-C40	1.534(7)
C2	-C3	1.515(4)	C39	-C42	1.519(5)
C3	-C4	1.539(4)	C39	-C45	1.505(8)
C4	-C18	1.533(4)	C40	-C41	1.517(7)
C4	-C19	1.543(4)	C42	-C43	1.513(6)
C4	-C5	1.553(4)	C42	-C44	1.520(7)
C5	-C10	1.558(4)	C1	-H1A	0.9900
C5	-C6	1.525(4)	C1	-H1B	0.9900
C6	-C7	1.499(4)	C2	-H2	1.0000

Table S5 - Bond Distances (Angstrom) (continued)

C3	-H3A	0.9900	C20	-H20C	0.9800
C3	-H3B	0.9900	C24	-H24A	0.9800
C5	-H5	1.0000	C24	-H24B	0.9800
C6	-H9	1.0000	C24	-H24C	0.9800
C7	-H7	1.0000	C28	-H28A	0.9800
C11	-H11A	0.9900	C28	-H28B	0.9800
C11	-H11B	0.9900	C28	-H28C	0.9800
C12	-H12A	0.9900	C32	-H32A	0.9800
C12	-H12B	0.9900	C32	-H32B	0.9800
C14	-H14	0.9500	C32	-H32C	0.9800
C16	-H16A	0.9800	C40	-H40A	0.9900
C16	-H16B	0.9800	C40	-H40B	0.9900
C16	-H16C	0.9800	C41	-H41A	0.9900
C17	-H17A	0.9800	C41	-H41B	0.9900
C17	-H17B	0.9800	C43	-H43A	0.9800
C17	-H17C	0.9800	C43	-H43B	0.9800
C18	-H18A	0.9800	C43	-H43C	0.9800
C18	-H18B	0.9800	C44	-H44A	0.9800
C18	-H18C	0.9800	C44	-H44B	0.9800
C19	-H19A	0.9800	C44	-H44C	0.9800
C19	-H19B	0.9800	C45	-H45A	0.9800
C19	-H19C	0.9800	C45	-H45B	0.9800
C20	-H20A	0.9800	C45	-H45C	0.9800
C20	-H20B	0.9800			

Table 6 - Bond Angles (Degrees)

C2	-O21	-C22	118.6(2)	C9	-C8	-C17	124.2(3)
C6	-O25	-C26	117.6(2)	C8	-C9	-C10	123.4(3)
C7	-O29	-C30	119.1(3)	C8	-C9	-C11	119.3(3)
C15	-O33A	-C34A	107.7(5)	C10	-C9	-C11	117.3(3)
C15	-O33B	-C34B	104.0(8)	C1	-C10	-C9	109.3(2)
C36	-O37	-C38	104.9(3)	C1	-C10	-C20	109.6(2)
C2	-C1	-C10	112.5(3)	C1	-C10	-C5	105.8(2)
O21	-C2	-C3	104.5(2)	C5	-C10	-C20	115.2(3)
C1	-C2	-C3	112.2(3)	C9	-C10	-C20	106.9(2)
O21	-C2	-C1	108.8(2)	C5	-C10	-C9	110.0(2)
C2	-C3	-C4	114.0(3)	C9	-C11	-C12	113.5(3)
C3	-C4	-C18	111.2(3)	C11	-C12	-C13	116.1(3)
C3	-C4	-C19	106.3(2)	C12	-C13	-C16	112.6(3)
C3	-C4	-C5	106.9(2)	C14	-C13	-C16	124.4(3)
C5	-C4	-C19	109.0(2)	C12	-C13	-C14	123.1(3)
C18	-C4	-C19	106.8(3)	C13	-C14	-C15	125.5(4)
C5	-C4	-C18	116.1(3)	O33A	-C15	-C14	104.3(4)
C4	-C5	-C6	116.7(3)	O33B	-C15	-C14	111.4(4)
C6	-C5	-C10	112.8(3)	O21	-C22	-C24	110.3(3)
C4	-C5	-C10	117.3(2)	O23	-C22	-C24	125.9(3)
O25	-C6	-C5	112.7(2)	O21	-C22	-O23	123.9(3)
C5	-C6	-C7	110.2(3)	O25	-C26	-O27	123.5(3)
O25	-C6	-C7	106.7(2)	O27	-C26	-C28	124.2(3)
O29	-C7	-C8	108.0(2)	O25	-C26	-C28	112.3(3)
C6	-C7	-C8	115.3(3)	O29	-C30	-O31	123.1(4)
O29	-C7	-C6	106.2(2)	O31	-C30	-C32	124.6(4)
C7	-C8	-C9	122.4(3)	O29	-C30	-C32	112.2(3)
C7	-C8	-C17	113.5(3)	O33A	-C34A	-C36	106.0(5)

Table 6 - Bond Angles (Degrees) (continued)

O35A	-C34A	-C36	127.1(7)	C36	-C42	-C39	90.5(3)
O33A	-C34A	-O35A	126.6(7)	C36	-C42	-C43	113.6(3)
O33B	-C34B	-O35B	120.6(11)	C36	-C42	-C44	114.2(4)
O33B	-C34B	-C36	103.7(9)	C2	-C1	-H1A	109.00
O35B	-C34B	-C36	135.7(11)	C2	-C1	-H1B	109.00
O37	-C36	-C41	105.5(4)	C10	-C1	-H1A	109.00
O37	-C36	-C42	101.6(3)	C10	-C1	-H1B	109.00
O37	-C36	-C34B	87.3(5)	H1A	-C1	-H1B	108.00
O37	-C36	-C34A	125.0(4)	O21	-C2	-H2	110.00
C34B	-C36	-C42	109.2(6)	C1	-C2	-H2	110.00
C34A	-C36	-C42	113.4(4)	C3	-C2	-H2	110.00
C41	-C36	-C42	106.0(4)	C2	-C3	-H3A	109.00
C34A	-C36	-C41	103.9(4)	C2	-C3	-H3B	109.00
C34B	-C36	-C41	139.1(6)	C4	-C3	-H3A	109.00
O37	-C38	-O46	120.3(5)	C4	-C3	-H3B	109.00
O37	-C38	-C39	107.8(4)	H3A	-C3	-H3B	108.00
O46	-C38	-C39	131.9(5)	C4	-C5	-H5	102.00
C40	-C39	-C42	102.4(3)	C6	-C5	-H5	102.00
C42	-C39	-C45	118.4(4)	C10	-C5	-H5	102.00
C38	-C39	-C42	100.5(3)	O25	-C6	-H9	109.00
C40	-C39	-C45	116.5(4)	C5	-C6	-H9	109.00
C38	-C39	-C40	102.5(4)	C7	-C6	-H9	109.00
C38	-C39	-C45	114.2(4)	O29	-C7	-H7	109.00
C39	-C40	-C41	104.0(4)	C6	-C7	-H7	109.00
C36	-C41	-C40	101.3(4)	C8	-C7	-H7	109.00
C39	-C42	-C44	115.9(4)	C9	-C11	-H11A	109.00
C43	-C42	-C44	107.2(4)	C9	-C11	-H11B	109.00
C39	-C42	-C43	115.1(4)	C12	-C11	-H11A	109.00

Table 6 - Bond Angles (Degrees) (continued)

C12	-C11	-H11B	109.00	C4	-C19	-H19B	109.00
H11A	-C11	-H11B	108.00	C4	-C19	-H19C	109.00
C11	-C12	-H12A	108.00	H19A	-C19	-H19B	109.00
C11	-C12	-H12B	108.00	H19A	-C19	-H19C	109.00
C13	-C12	-H12A	108.00	H19B	-C19	-H19C	110.00
C13	-C12	-H12B	108.00	C10	-C20	-H20A	109.00
H12A	-C12	-H12B	107.00	C10	-C20	-H20B	110.00
C13	-C14	-H14	117.00	C10	-C20	-H20C	110.00
C15	-C14	-H14	117.00	H20A	-C20	-H20B	110.00
C13	-C16	-H16A	109.00	H20A	-C20	-H20C	109.00
C13	-C16	-H16B	110.00	H20B	-C20	-H20C	109.00
C13	-C16	-H16C	109.00	C22	-C24	-H24A	109.00
H16A	-C16	-H16B	109.00	C22	-C24	-H24B	109.00
H16A	-C16	-H16C	109.00	C22	-C24	-H24C	109.00
H16B	-C16	-H16C	109.00	H24A	-C24	-H24B	109.00
C8	-C17	-H17A	109.00	H24A	-C24	-H24C	110.00
C8	-C17	-H17B	109.00	H24B	-C24	-H24C	109.00
C8	-C17	-H17C	110.00	C26	-C28	-H28A	109.00
H17A	-C17	-H17B	109.00	C26	-C28	-H28B	109.00
H17A	-C17	-H17C	109.00	C26	-C28	-H28C	110.00
H17B	-C17	-H17C	109.00	H28A	-C28	-H28B	110.00
C4	-C18	-H18A	109.00	H28A	-C28	-H28C	109.00
C4	-C18	-H18B	109.00	H28B	-C28	-H28C	109.00
C4	-C18	-H18C	109.00	C30	-C32	-H32A	110.00
H18A	-C18	-H18B	109.00	C30	-C32	-H32B	109.00
H18A	-C18	-H18C	110.00	C30	-C32	-H32C	109.00
H18B	-C18	-H18C	109.00	H32A	-C32	-H32B	109.00
C4	-C19	-H19A	109.00	H32A	-C32	-H32C	110.00

Table 6 - Bond Angles (Degrees) (continued)

H32B	-C32	-H32C	109.00	H43A	-C43	-H43C	110.00
C39	-C40	-H40A	111.00	H43B	-C43	-H43C	109.00
C39	-C40	-H40B	111.00	C42	-C44	-H44A	109.00
C41	-C40	-H40A	111.00	C42	-C44	-H44B	109.00
C41	-C40	-H40B	111.00	C42	-C44	-H44C	109.00
H40A	-C40	-H40B	109.00	H44A	-C44	-H44B	110.00
C36	-C41	-H41A	111.00	H44A	-C44	-H44C	109.00
C36	-C41	-H41B	111.00	H44B	-C44	-H44C	109.00
C40	-C41	-H41A	111.00	C39	-C45	-H45A	109.00
C40	-C41	-H41B	112.00	C39	-C45	-H45B	109.00
H41A	-C41	-H41B	109.00	C39	-C45	-H45C	109.00
C42	-C43	-H43A	109.00	H45A	-C45	-H45B	109.00
C42	-C43	-H43B	109.00	H45A	-C45	-H45C	110.00
C42	-C43	-H43C	109.00	H45B	-C45	-H45C	109.00
H43A	-C43	-H43B	109.00				

Table 7 - Torsion Angles (Degrees)

C2	-O21	-C22	-C24	177.3(2)
C2	-O21	-C22	-O23	-4.5(4)
C22	-O21	-C2	-C1	-82.0(3)
C22	-O21	-C2	-C3	158.0(2)
C6	-O25	-C26	-O27	-9.0(4)
C26	-O25	-C6	-C7	-111.0(3)
C6	-O25	-C26	-C28	171.1(3)
C26	-O25	-C6	-C5	128.0(3)
C30	-O29	-C7	-C6	-114.6(3)
C7	-O29	-C30	-O31	-8.5(5)
C30	-O29	-C7	-C8	121.2(3)
C7	-O29	-C30	-C32	173.5(3)
C15	-O33A	-C34A	-O35A	4.9(9)
C34A	-O33A	-C15	-C14	96.6(5)
C15	-O33A	-C34A	-C36	-169.2(4)
C38	-O37	-C36	-C41	-73.8(4)
C38	-O37	-C36	-C42	36.6(4)
C36	-O37	-C38	-C39	-1.3(4)
C36	-O37	-C38	-O46	178.4(5)
C38	-O37	-C36	-C34A	166.3(5)
C2	-C1	-C10	-C9	173.4(2)
C2	-C1	-C10	-C5	55.0(3)
C10	-C1	-C2	-C3	-57.4(3)
C10	-C1	-C2	-O21	-172.6(2)
C2	-C1	-C10	-C20	-69.7(3)
C1	-C2	-C3	-C4	55.3(4)
O21	-C2	-C3	-C4	173.0(2)
C2	-C3	-C4	-C5	-51.1(3)

Table 7 - Torsion Angles (Degrees) (continued)

C2	-C3	-C4	-C18	76.6(3)
C2	-C3	-C4	-C19	-167.4(3)
C19	-C4	-C5	-C6	-52.8(3)
C18	-C4	-C5	-C10	-70.5(4)
C3	-C4	-C5	-C10	54.3(3)
C18	-C4	-C5	-C6	67.9(4)
C19	-C4	-C5	-C10	168.8(3)
C3	-C4	-C5	-C6	-167.4(3)
C4	-C5	-C6	-C7	160.3(3)
C4	-C5	-C6	-O25	-80.7(3)
C4	-C5	-C10	-C9	-174.2(3)
C4	-C5	-C10	-C1	-56.3(3)
C10	-C5	-C6	-C7	-59.6(3)
C6	-C5	-C10	-C20	-75.1(3)
C6	-C5	-C10	-C9	45.8(3)
C10	-C5	-C6	-O25	59.4(3)
C4	-C5	-C10	-C20	64.9(4)
C6	-C5	-C10	-C1	163.8(2)
O25	-C6	-C7	-C8	-81.3(3)
O25	-C6	-C7	-O29	159.2(2)
C5	-C6	-C7	-O29	-78.2(3)
C5	-C6	-C7	-C8	41.3(4)
C6	-C7	-C8	-C17	166.5(3)
O29	-C7	-C8	-C17	-75.1(3)
C6	-C7	-C8	-C9	-12.0(4)
O29	-C7	-C8	-C9	106.5(3)
C7	-C8	-C9	-C10	-1.1(5)
C7	-C8	-C9	-C11	177.4(3)

Table 7 - Torsion Angles (Degrees) (continued)

C17	-C8	-C9	-C10	-179.4(3)
C17	-C8	-C9	-C11	-0.9(5)
C11	-C9	-C10	-C1	50.0(3)
C11	-C9	-C10	-C5	165.7(3)
C8	-C9	-C10	-C5	-15.8(4)
C8	-C9	-C10	-C20	110.0(3)
C8	-C9	-C11	-C12	81.6(4)
C10	-C9	-C11	-C12	-99.8(3)
C11	-C9	-C10	-C20	-68.6(3)
C8	-C9	-C10	-C1	-131.5(3)
C9	-C11	-C12	-C13	-170.4(3)
C11	-C12	-C13	-C16	-176.2(3)
C11	-C12	-C13	-C14	4.0(5)
C12	-C13	-C14	-C15	175.4(3)
C16	-C13	-C14	-C15	-4.4(6)
C13	-C14	-C15	-O33A	-106.1(5)
O33A	-C34A	-C36	-C42	97.7(6)
O35A	-C34A	-C36	-O37	158.9(6)
O35A	-C34A	-C36	-C41	38.3(8)
O35A	-C34A	-C36	-C42	-76.3(8)
O33A	-C34A	-C36	-C41	-147.7(5)
O33A	-C34A	-C36	-O37	-27.1(7)
C34A	-C36	-C41	-C40	-155.4(5)
O37	-C36	-C41	-C40	71.6(5)
O37	-C36	-C42	-C43	63.9(4)
C42	-C36	-C41	-C40	-35.6(5)
O37	-C36	-C42	-C39	-53.9(3)
C34A	-C36	-C42	-C43	-72.8(6)

Table 7 - Torsion Angles (Degrees) (continued)

C34A	-C36	-C42	-C44	50.6(6)
C41	-C36	-C42	-C39	56.1(4)
C41	-C36	-C42	-C43	173.9(4)
C41	-C36	-C42	-C44	-62.8(5)
O37	-C36	-C42	-C44	-172.8(4)
C34A	-C36	-C42	-C39	169.5(4)
O37	-C38	-C39	-C40	70.3(4)
O37	-C38	-C39	-C42	-35.0(4)
O37	-C38	-C39	-C45	-162.8(4)
O46	-C38	-C39	-C40	-109.3(6)
O46	-C38	-C39	-C42	145.4(6)
O46	-C38	-C39	-C45	17.6(8)
C38	-C39	-C40	-C41	-67.1(5)
C42	-C39	-C40	-C41	36.7(5)
C45	-C39	-C40	-C41	167.5(5)
C38	-C39	-C42	-C36	51.8(3)
C38	-C39	-C42	-C43	-64.6(4)
C38	-C39	-C42	-C44	169.2(4)
C40	-C39	-C42	-C36	-53.6(4)
C40	-C39	-C42	-C43	-170.1(4)
C40	-C39	-C42	-C44	63.8(5)
C45	-C39	-C42	-C36	176.8(4)
C45	-C39	-C42	-C43	60.3(5)
C45	-C39	-C42	-C44	-65.8(5)
C39	-C40	-C41	-C36	-0.6(6)

Table 8 - Contact Distances(Angstrom)

O23	.C1	3.253(4)	O25	.H18B	2.6400
O25	.C20	3.020(4)	O27	.H9	2.2500
O25	.C9	3.361(4)	O27	.H24C_d	2.8900
O25	.C18	3.304(4)	O29	.H17A	2.8300
O27	.C22_d	3.378(4)	O29	.H5	2.5500
O27	.C15_c	3.283(5)	O31	.H40B_e	2.9000
O27	.C24_d	3.266(4)	O31	.H41A_c	2.8600
O31	.C16_d	3.216(5)	O31	.H16B_d	2.8600
O33A	.O37	2.768(7)	O31	.H17A	2.9200
O33A	.C43	3.299(8)	O31	.H7	2.2800
O33B	.C16	3.313(9)	O33B	.H16C	2.7800
O35A	.C44	3.119(8)	O35A	.H32C_f	2.2800
O35A	.C14	3.302(6)	O35A	.H41B	2.3000
O35A	.C16	3.111(6)	O35A	.H44C	2.7200
O35A	.C32_f	3.153(6)	O35A	.H40A_g	2.7200
O35B	.C12_h	3.085(7)	O35A	.H16C	2.5300
O35B	.O37	2.597(7)	O35B	.H43C	2.5700
O35B	.C43	3.016(9)	O35B	.H14	2.7500
O35B	.C14	2.820(7)	O35B	.H1B_h	2.6300
O37	.O35B	2.597(7)	O35B	.H12B_h	2.4100
O37	.O33A	2.768(7)	O35B	.H12A_h	2.8700
O46	.C44_h	3.407(7)	O35B	.H43B	2.8300
O46	.C45_i	3.341(9)	O37	.H12A_h	2.8000
O23	.H1A	2.7800	O37	.H43C	2.4500
O23	.H2	2.4800	O37	.H16A_h	2.7200
O23	.H18C_a	2.6000	O46	.H17C_h	2.7700
O23	.H28B_b	2.7300	O46	.H44A_h	2.9000
O25	.H20A	2.3100	O46	.H45C_i	2.8600

Table 8 - Contact Distances(Angstrom) (continued)

O46	.H45A	2.7100	C1	.H11A	2.8000
C1	.C12	3.354(4)	C1	.H12B	2.7800
C1	.O23	3.253(4)	C2	.H20B	2.7200
C9	.O25	3.361(4)	C2	.H18A	2.8700
C12	.C17	3.430(5)	C2	.H5	3.0300
C12	.O35B_j	3.085(7)	C4	.H20B	3.0500
C12	.C1	3.354(4)	C6	.H19C	3.1000
C14	.O35B	2.820(7)	C6	.H19B	2.7900
C14	.O35A	3.302(6)	C6	.H18B	2.9400
C15	.O27_f	3.283(5)	C6	.H20A	2.9700
C16	.O35A	3.111(6)	C8	.H5	2.8300
C16	.O33B	3.313(9)	C8	.H12A	2.9700
C16	.O31_k	3.216(5)	C11	.H1A	2.6900
C17	.C12	3.430(5)	C11	.H17B	2.8900
C18	.O25	3.304(4)	C11	.H3A_h	3.0800
C18	.C20	3.248(4)	C11	.H20C	2.7100
C20	.O25	3.020(4)	C11	.H14	2.5100
C20	.C18	3.248(4)	C11	.H17C	2.9000
C22	.O27_k	3.378(4)	C12	.H17C	2.9300
C24	.O27_k	3.266(4)	C12	.H1B	3.0600
C24	.C28_l	3.580(5)	C12	.H1A	3.0100
C28	.C24_m	3.580(5)	C13	.H28C_k	2.9200
C32	.O35A_c	3.153(6)	C14	.H28C_k	2.9400
C43	.O33A	3.299(8)	C14	.H11A	2.9900
C43	.O35B	3.016(9)	C14	.H11B	2.7100
C44	.O35A	3.119(8)	C15	.H24C_h	3.0800
C44	.O46_j	3.407(7)	C15	.H16C	2.6000
C45	.O46_e	3.341(9)	C17	.H12A	2.9000

Table 8 - Contact Distances(Angstrom) (continued)

C17	.H11B	2.6500	C44	.H40B	2.7900
C18	.H24B_a	3.0500	C44	.H45B	3.0800
C18	.H20B	2.7300	C44	.H41B	2.8400
C18	.H2	3.0000	C45	.H44A	3.0200
C19	.H9	2.5600	C45	.H43A	2.9000
C20	.H2	2.8400	H1A	.H11A	2.2400
C20	.H18A	2.7200	H1A	.O23	2.7800
C20	.H11A	2.7500	H1A	.C11	2.6900
C22	.H1A	2.9100	H1A	.C12	3.0100
C24	.H28B_b	3.0700	H1A	.C22	2.9100
C26	.H16B_d	3.0400	H1A	.H12B	2.4200
C26	.H18B	2.8000	H1A	.H20C	2.5500
C26	.H7	3.1000	H1B	.C12	3.0600
C28	.H24A_a	3.0600	H1B	.O35B_j	2.6300
C30	.H17A	3.0700	H1B	.H5	2.3400
C32	.H43A_j	3.0100	H1B	.H12B	2.3800
C34A	.H44C	2.7900	H2	.C18	3.0000
C34A	.H32C_f	3.0200	H2	.O23	2.4800
C34A	.H43B	3.0400	H2	.H18A	2.3800
C34B	.H43B	2.6600	H2	.H20B	2.1900
C34B	.H43C	2.6600	H2	.C20	2.8400
C38	.H41A	3.0000	H3A	.H11B_j	2.4900
C38	.H43C	2.5200	H3A	.H19C	2.3900
C40	.H44B	2.5600	H3A	.C11_j	3.0800
C41	.H44B_n	2.9400	H3A	.H5	2.4100
C41	.H44B	2.5800	H3B	.H19A	2.4800
C43	.H32B_h	2.8000	H3B	.H20B_b	2.5400
C43	.H45C	2.8100	H3B	.H18C	2.5200

Table 8 - Contact Distances(Angstrom) (continued)

H5	.H3A	2.4100	H12A	.O35B_j	2.8700
H5	.H19C	2.3100	H12B	.O35B_j	2.4100
H5	.O29	2.5500	H12B	.C1	2.7800
H5	.C2	3.0300	H12B	.H1A	2.4200
H5	.C8	2.8300	H12B	.H16B	2.4400
H5	.H1B	2.3400	H12B	.H1B	2.3800
H7	.H17A	2.3000	H14	.O35B	2.7500
H7	.O31	2.2800	H14	.C11	2.5100
H7	.C26	3.1000	H14	.H11B	2.1300
H9	.H19B	2.1200	H14	.H11A	2.4600
H9	.O27	2.2500	H16A	.O37_j	2.7200
H9	.C19	2.5600	H16A	.H12A	2.5600
H11A	.C1	2.8000	H16B	.C26_k	3.0400
H11A	.H1A	2.2400	H16B	.O31_k	2.8600
H11A	.C14	2.9900	H16B	.H12B	2.4400
H11A	.C20	2.7500	H16C	.O33B	2.7800
H11A	.H14	2.4600	H16C	.O35A	2.5300
H11A	.H20C	2.1100	H16C	.C15	2.6000
H11B	.H3A_h	2.4900	H17A	.C30	3.0700
H11B	.C14	2.7100	H17A	.O29	2.8300
H11B	.C17	2.6500	H17A	.O31	2.9200
H11B	.H14	2.1300	H17A	.H7	2.3000
H11B	.H17B	2.2900	H17A	.H45B_e	2.5100
H12A	.C8	2.9700	H17B	.H11B	2.2900
H12A	.H17C	2.2100	H17B	.C11	2.8900
H12A	.C17	2.9000	H17C	.O46_j	2.7700
H12A	.H16A	2.5600	H17C	.C12	2.9300
H12A	.O37_j	2.8000	H17C	.H12A	2.2100

Table 8 - Contact Distances(Angstrom) (continued)

H17C	.C11	2.9000	H20B	.H18A	1.9900
H18A	.H2	2.3800	H20C	.C11	2.7100
H18A	.H20B	1.9900	H20C	.H1A	2.5500
H18A	.C2	2.8700	H20C	.H11A	2.1100
H18A	.C20	2.7200	H24A	.C28_b	3.0600
H18B	.C6	2.9400	H24B	.H18B_b	2.4900
H18B	.C26	2.8000	H24B	.C18_b	3.0500
H18B	.O25	2.6400	H24C	.O27_k	2.8900
H18B	.H24B_a	2.4900	H24C	.C15_j	3.0800
H18B	.H19B	2.5300	H28B	.O23_a	2.7300
H18C	.H19A	2.4000	H28B	.C24_a	3.0700
H18C	.O23_b	2.6000	H28C	.C14_d	2.9400
H18C	.H3B	2.5200	H28C	.C13_d	2.9200
H19A	.H3B	2.4800	H32A	.H44A_e	2.4900
H19A	.H18C	2.4000	H32B	.H43A_j	2.0700
H19B	.H9	2.1200	H32B	.C43_j	2.8000
H19B	.C6	2.7900	H32C	.C34A_c	3.0200
H19B	.H18B	2.5300	H32C	.O35A_c	2.2800
H19C	.H5	2.3100	H40A	.O35A_n	2.7200
H19C	.C6	3.1000	H40A	.H41B_n	2.5000
H19C	.H3A	2.3900	H40B	.C44	2.7900
H20A	.O25	2.3100	H40B	.O31_i	2.9000
H20A	.C6	2.9700	H40B	.H44B	2.2000
H20B	.H3B_a	2.5400	H40B	.H45B	2.5200
H20B	.C2	2.7200	H41A	.O31_f	2.8600
H20B	.C4	3.0500	H41A	.C38	3.0000
H20B	.C18	2.7300	H41A	.H44B_n	2.2400
H20B	.H2	2.1900	H41B	.O35A	2.3000

Table 8 - Contact Distances(Angstrom) (continued)

H41B	.H40A_g	2.5000	H44A	.O46_j	2.9000
H41B	.C44	2.8400	H44A	.C45	3.0200
H41B	.H44B	2.2300	H44B	.C40	2.5600
H43A	.C45	2.9000	H44B	.H41B	2.2300
H43A	.C32_h	3.0100	H44B	.C41	2.5800
H43A	.H44A	2.5200	H44B	.H40B	2.2000
H43A	.H45C	2.2900	H44B	.C41_g	2.9400
H43A	.H32B_h	2.0700	H44B	.H41A_g	2.2400
H43B	.O35B	2.8300	H44C	.C34A	2.7900
H43B	.C34B	2.6600	H44C	.O35A	2.7200
H43B	.C34A	3.0400	H44C	.H43B	2.3200
H43B	.H44C	2.3200	H45A	.O46	2.7100
H43C	.C38	2.5200	H45B	.C44	3.0800
H43C	.O35B	2.5700	H45B	.H40B	2.5200
H43C	.O37	2.4500	H45B	.H17A_i	2.5100
H43C	.C34B	2.6600	H45C	.O46_e	2.8600
H44A	.H32A_i	2.4900	H45C	.C43	2.8100
H44A	.H43A	2.5200	H45C	.H43A	2.2900

Table 9 - Hydrogen Bonds (Angstrom, Deg)

C5 -- H5 .. O29	1.0000	2.5500	3.021(4)	109.00	.
C7 -- H7 .. O31	1.0000	2.2800	2.716(5)	105.00	.
C6 -- H9 .. O27	1.0000	2.2500	2.701(4)	106.00	.
C16 -- H16C .. O35A	0.9800	2.5300	3.111(6)	118.00	.
C20 -- H20A .. O25	0.9800	2.3100	3.020(4)	129.00	.
C32 -- H32C .. O35A	0.9800	2.2800	3.153(6)	148.00	1_645
C41 -- H41B .. O35A	0.9900	2.3000	2.737(8)	106.00	.
C43 -- H43C .. O37	0.9800	2.4500	2.856(7)	104.00	.

Translation of Symmetry Code to Equiv.Pos

a =[2656.00] = 1-x,1/2+y,1-z
b =[2646.00] = 1-x,-1/2+y,1-z
c =[1645.00] = 1+x,-1+y,z
d =[1655.00] = 1+x,y,z
e =[2645.00] = 1-x,-1/2+y,-z
f =[1465.00] = -1+x,1+y,z
g =[2545.00] = -x,-1/2+y,-z
h =[1565.00] = x,1+y,z
i =[2655.00] = 1-x,1/2+y,-z
j =[1545.00] = x,-1+y,z
k =[1455.00] = -1+x,y,z
l =[1445.00] = -1+x,-1+y,z
m =[1665.00] = 1+x,1+y,z
n =[2555.00] = -x,1/2+y,-z

Appendix II X-ray crystallographic data for 5.22

Table 1 - Crystal Data and Details of the Structure Determination

Crystal Data			
Formula			C18 H34 O2
Formula Weight			282.45
Crystal System			Orthorhombic
Space group		P212121	(No. 19)
a, b, c [Angstrom]	8.4923(2)	9.9407(2)	20.4323(4)
V [Ang**3]			1724.88(6)
Z			4
D(obs), D(calc) [g/cm**3]			1.040, 1.088
Mu(MoKa) [/mm]			0.068
F(000)			632
Crystal Size [mm]		0.20 x	0.25 x 0.25
Data Collection			
Temperature (K)			113
Radiation [Angstrom]		MoKa	0.71073
Theta Min-Max [Deg]			3.6, 26.4
Dataset		-10: 10 ; -12: 12 ; -25: 25	
Tot., Uniq. Data, R(int)		3520,	3520, 0.000
Observed data [I > 2.0 sigma(I)]			2781
Refinement			
Nref, Npar			3520, 195
R, wR2, S		0.0433,	0.1079, 1.04
w = 1/[\s^2^(Fo^2^)+(0.0593P)^2^+0.0176P] where P=(Fo^2^+2Fc^2^)/3			
Max. and Av. Shift/Error			0.00, 0.00
Flack x			-1.8(12)
Min. and Max. Resd. Dens. [e/Ang^3]			-0.16, 0.27

Table 2 - Final Coordinates and Equivalent Isotropic Displacement Parameters of the non-Hydrogen atoms

Atom	x	y	z	U(eq) [Ang^2]
O19	0.10047(15)	0.63548(12)	0.45984(6)	0.0231(4)
O20	0.77002(14)	0.62257(14)	0.51153(6)	0.0244(4)
C1	0.4932(2)	0.52461(19)	0.31901(9)	0.0228(5)
C2	0.5107(2)	0.5458(2)	0.24519(9)	0.0278(6)
C3	0.3933(2)	0.4589(2)	0.20790(9)	0.0271(6)
C4	0.2208(2)	0.48060(19)	0.22757(9)	0.0249(6)
C5	0.2076(2)	0.46864(18)	0.30371(8)	0.0217(5)
C6	0.0404(2)	0.48409(19)	0.33077(9)	0.0226(5)
C7	0.0324(2)	0.43120(19)	0.40078(9)	0.0234(5)
C8	0.1510(2)	0.49825(17)	0.44706(8)	0.0202(5)
C9	0.3173(2)	0.50119(17)	0.41686(8)	0.0193(5)
C10	0.3264(2)	0.55369(17)	0.34482(8)	0.0189(5)
C11	0.4383(2)	0.56784(18)	0.46345(8)	0.0196(5)
C12	0.5500(2)	0.46940(17)	0.49627(9)	0.0215(5)
C13	0.6600(2)	0.53617(17)	0.54550(8)	0.0208(5)
C14	0.7498(2)	0.4356(2)	0.58636(9)	0.0273(6)
C15	0.1525(2)	0.4233(2)	0.51246(9)	0.0272(6)
C16	0.2956(2)	0.70576(17)	0.34160(9)	0.0225(6)
C17	0.1568(2)	0.6132(2)	0.19946(9)	0.0326(7)
C18	0.1262(2)	0.3649(2)	0.19635(10)	0.0343(7)

U(eq) = 1/3 of the trace of the orthogonalized U Tensor

Table 3 - Hydrogen Atom Positions and Isotropic Displacement Parameters

Atom	x	y	z	U(iso) [Ang^2]
H1A	0.56880	0.58390	0.34200	0.0270
H1B	0.52110	0.43040	0.32960	0.0270
H2A	0.49260	0.64170	0.23450	0.0330
H2B	0.61910	0.52220	0.23160	0.0330
H3A	0.42050	0.36320	0.21500	0.0320
H3B	0.40430	0.47780	0.16050	0.0320
H5	0.23640	0.37310	0.31330	0.0260
H6A	0.00960	0.58010	0.33000	0.0270
H6B	-0.03440	0.43350	0.30290	0.0270
H7A	0.05210	0.33300	0.40030	0.0280
H7B	-0.07520	0.44580	0.41800	0.0280
H9	0.35010	0.40470	0.41430	0.0230
H11A	0.50100	0.63390	0.43820	0.0240
H11B	0.38040	0.61780	0.49780	0.0240
H12A	0.61390	0.42420	0.46220	0.0260
H12B	0.48750	0.39950	0.51900	0.0260
H13	0.59520	0.59310	0.57550	0.0250
H13A	0.14830	0.36130	0.14930	0.0510
H13B	0.01340	0.38040	0.20320	0.0510
H13C	0.15660	0.27950	0.21670	0.0510
H14A	0.80460	0.37220	0.55750	0.0410
H14B	0.82690	0.48300	0.61360	0.0410
H14C	0.67630	0.38640	0.61450	0.0410
H15A	0.21870	0.47210	0.54380	0.0410
H15B	0.19480	0.33250	0.50600	0.0410
H15C	0.04490	0.41720	0.52950	0.0410

Table 3 - Hydrogen Atom Positions and Isotropic Displacement Parameters (continued)

Atom	x	y	z	U(iso) [Ang^2]
H16A	0.35830	0.75140	0.37520	0.0340
H16B	0.18350	0.72320	0.34930	0.0340
H16C	0.32520	0.73960	0.29830	0.0340
H17A	0.14960	0.60620	0.15170	0.0490
H17B	0.22800	0.68700	0.21110	0.0490
H17C	0.05210	0.63090	0.21760	0.0490
H19	0.006(3)	0.627(2)	0.4788(11)	0.037(6)
H20	0.724(3)	0.700(3)	0.5108(13)	0.058(8)

The Temperature Factor has the Form of Exp(-T) Where
T = 8*(Pi**2)*U*(Sin(Theta)/Lambda)**2 for Isotropic Atoms

Table S4 - (An)isotropic Displacement Parameters

Atom	U(1,1) or U	U(2,2)	U(3,3)	U(2,3)	U(1,3)	U(1,2)
O19	0.0225(7)	0.0207(7)	0.0261(7)	-0.0042(6)	0.0028(6)	0.0002(6)
O20	0.0210(7)	0.0229(7)	0.0292(7)	-0.0005(6)	0.0022(5)	-0.0006(6)
C1	0.0206(9)	0.0247(9)	0.0232(9)	-0.0023(8)	-0.0010(7)	-0.0006(8)
C2	0.0223(10)	0.0351(11)	0.0259(10)	-0.0030(9)	0.0055(8)	-0.0019(8)
C3	0.0282(11)	0.0347(12)	0.0183(9)	0.0000(8)	0.0039(7)	0.0029(9)
C4	0.0258(10)	0.0294(10)	0.0196(9)	-0.0022(8)	-0.0010(7)	0.0025(8)
C5	0.0207(9)	0.0214(10)	0.0229(9)	-0.0008(8)	-0.0011(7)	0.0009(8)
C6	0.0179(9)	0.0257(10)	0.0243(9)	-0.0018(8)	-0.0026(7)	-0.0005(8)
C7	0.0210(9)	0.0232(9)	0.0259(9)	-0.0034(8)	0.0018(8)	-0.0020(8)
C8	0.0239(9)	0.0133(8)	0.0234(9)	-0.0023(7)	-0.0002(7)	-0.0001(8)
C9	0.0188(9)	0.0172(9)	0.0218(9)	-0.0023(8)	0.0007(7)	0.0011(8)
C10	0.0181(9)	0.0187(9)	0.0198(9)	-0.0012(8)	0.0004(7)	0.0001(8)
C11	0.0217(9)	0.0188(9)	0.0184(9)	-0.0005(8)	-0.0005(7)	0.0002(8)
C12	0.0235(10)	0.0194(9)	0.0215(9)	-0.0012(8)	-0.0016(7)	0.0003(8)
C13	0.0192(9)	0.0235(10)	0.0198(9)	-0.0001(8)	0.0001(7)	-0.0022(8)
C14	0.0244(10)	0.0300(10)	0.0275(10)	0.0021(9)	-0.0059(8)	-0.0032(8)
C15	0.0291(11)	0.0297(10)	0.0228(10)	0.0005(8)	0.0015(8)	-0.0013(9)
C16	0.0235(10)	0.0241(10)	0.0199(9)	-0.0001(8)	0.0008(8)	-0.0017(8)
C17	0.0336(11)	0.0443(13)	0.0198(10)	0.0008(9)	-0.0013(8)	0.0081(10)
C18	0.0365(12)	0.0395(12)	0.0268(11)	-0.0105(10)	-0.0032(9)	-0.0045(10)

The Temperature Factor has the Form of Exp(-T) Where
T = 8*(Pi**2)*U*(Sin(Theta)/Lambda)**2 for Isotropic Atoms
T = 2*(Pi**2)*Sumij(h(i)*h(j)*U(i,j)*Astar(i)*Astar(j)), for Anisotropic Atoms. Astar(i) are Reciprocal Axial Lengths and h(i) are the Reflection Indices.

Table 5 - Bond Distances (Angstrom)

O19	-C8	1.454(2)	C3	-H3B	0.9900
O20	-C13	1.447(2)	C5	-H5	1.0000
O19	-H19	0.90(2)	C6	-H6A	0.9900
O20	-H20	0.86(3)	C6	-H6B	0.9900
C1	-C2	1.530(3)	C7	-H7A	0.9900
C1	-C10	1.539(2)	C7	-H7B	0.9900
C2	-C3	1.523(3)	C9	-H9	1.0000
C3	-C4	1.534(2)	C11	-H11A	0.9900
C4	-C18	1.541(3)	C11	-H11B	0.9900
C4	-C17	1.537(3)	C12	-H12A	0.9900
C4	-C5	1.564(2)	C12	-H12B	0.9900
C5	-C10	1.562(2)	C13	-H13	1.0000
C5	-C6	1.532(2)	C14	-H14A	0.9800
C6	-C7	1.526(3)	C14	-H14B	0.9800
C7	-C8	1.534(2)	C14	-H14C	0.9800
C8	-C9	1.542(2)	C15	-H15A	0.9800
C8	-C15	1.530(2)	C15	-H15B	0.9800
C9	-C11	1.550(2)	C15	-H15C	0.9800
C9	-C10	1.564(2)	C16	-H16A	0.9800
C10	-C16	1.536(2)	C16	-H16B	0.9800
C11	-C12	1.519(2)	C16	-H16C	0.9800
C12	-C13	1.525(2)	C17	-H17A	0.9800
C13	-C14	1.509(3)	C17	-H17B	0.9800
C1	-H1A	0.9900	C17	-H17C	0.9800
C1	-H1B	0.9900	C18	-H13A	0.9800
C2	-H2A	0.9900	C18	-H13B	0.9800
C2	-H2B	0.9900	C18	-H13C	0.9800
C3	-H3A	0.9900			

Table 6 - Bond Angles (Degrees)

C8	-O19	-H19	104.7(13)	C1	-C10	-C16	109.09(14)
C13	-O20	-H20	104.2(18)	C9	-C10	-C16	111.13(14)
C2	-C1	-C10	113.66(14)	C5	-C10	-C16	113.57(14)
C1	-C2	-C3	110.57(15)	C9	-C11	-C12	114.20(14)
C2	-C3	-C4	114.46(15)	C11	-C12	-C13	113.17(14)
C3	-C4	-C18	106.52(15)	C12	-C13	-C14	112.71(14)
C5	-C4	-C17	114.30(15)	O20	-C13	-C12	109.73(13)
C5	-C4	-C18	108.52(15)	O20	-C13	-C14	109.41(14)
C17	-C4	-C18	107.52(14)	C2	-C1	-H1A	109.00
C3	-C4	-C5	108.56(14)	C2	-C1	-H1B	109.00
C3	-C4	-C17	111.12(15)	C10	-C1	-H1A	109.00
C6	-C5	-C10	110.52(14)	C10	-C1	-H1B	109.00
C4	-C5	-C6	114.70(14)	H1A	-C1	-H1B	108.00
C4	-C5	-C10	116.59(14)	C1	-C2	-H2A	110.00
C5	-C6	-C7	110.20(14)	C1	-C2	-H2B	110.00
C6	-C7	-C8	113.52(15)	C3	-C2	-H2A	110.00
O19	-C8	-C9	108.94(13)	C3	-C2	-H2B	110.00
O19	-C8	-C7	108.95(14)	H2A	-C2	-H2B	108.00
C7	-C8	-C15	109.41(14)	C2	-C3	-H3A	109.00
O19	-C8	-C15	107.61(13)	C2	-C3	-H3B	109.00
C7	-C8	-C9	111.29(14)	C4	-C3	-H3A	109.00
C9	-C8	-C15	110.56(14)	C4	-C3	-H3B	109.00
C10	-C9	-C11	113.76(14)	H3A	-C3	-H3B	108.00
C8	-C9	-C11	111.70(13)	C4	-C5	-H5	104.00
C8	-C9	-C10	115.37(14)	C6	-C5	-H5	105.00
C1	-C10	-C5	107.98(14)	C10	-C5	-H5	105.00
C5	-C10	-C9	107.08(13)	C5	-C6	-H6A	110.00
C1	-C10	-C9	107.78(14)	C5	-C6	-H6B	110.00

Table 6 - Bond Angles (Degrees) (continued)

C7	-C6	-H6A	110.00	H14A	-C14	-H14B	109.00
C7	-C6	-H6B	110.00	H14A	-C14	-H14C	110.00
H6A	-C6	-H6B	108.00	H14B	-C14	-H14C	109.00
C6	-C7	-H7A	109.00	C8	-C15	-H15A	110.00
C6	-C7	-H7B	109.00	C8	-C15	-H15B	109.00
C8	-C7	-H7A	109.00	C8	-C15	-H15C	109.00
C8	-C7	-H7B	109.00	H15A	-C15	-H15B	109.00
H7A	-C7	-H7B	108.00	H15A	-C15	-H15C	109.00
C8	-C9	-H9	105.00	H15B	-C15	-H15C	109.00
C10	-C9	-H9	105.00	C10	-C16	-H16A	109.00
C11	-C9	-H9	105.00	C10	-C16	-H16B	109.00
C9	-C11	-H11A	109.00	C10	-C16	-H16C	109.00
C9	-C11	-H11B	109.00	H16A	-C16	-H16B	109.00
C12	-C11	-H11A	109.00	H16A	-C16	-H16C	110.00
C12	-C11	-H11B	109.00	H16B	-C16	-H16C	109.00
H11A	-C11	-H11B	108.00	C4	-C17	-H17A	109.00
C11	-C12	-H12A	109.00	C4	-C17	-H17B	109.00
C11	-C12	-H12B	109.00	C4	-C17	-H17C	109.00
C13	-C12	-H12A	109.00	H17A	-C17	-H17B	109.00
C13	-C12	-H12B	109.00	H17A	-C17	-H17C	109.00
H12A	-C12	-H12B	108.00	H17B	-C17	-H17C	110.00
O20	-C13	-H13	108.00	C4	-C18	-H13A	109.00
C12	-C13	-H13	108.00	C4	-C18	-H13B	109.00
C14	-C13	-H13	108.00	C4	-C18	-H13C	109.00
C13	-C14	-H14A	109.00	H13A	-C18	-H13B	109.00
C13	-C14	-H14B	109.00	H13A	-C18	-H13C	110.00
C13	-C14	-H14C	109.00	H13B	-C18	-H13C	109.00

Table 7 - Torsion Angles (Degrees)

C10	-C1	-C2	-C3	-57.1(2)
C2	-C1	-C10	-C5	53.61(19)
C2	-C1	-C10	-C9	168.98(15)
C2	-C1	-C10	-C16	-70.25(19)
C1	-C2	-C3	-C4	56.0(2)
C2	-C3	-C4	-C5	-51.3(2)
C2	-C3	-C4	-C17	75.2(2)
C2	-C3	-C4	-C18	-168.01(16)
C3	-C4	-C5	-C6	-178.34(15)
C3	-C4	-C5	-C10	50.2(2)
C17	-C4	-C5	-C6	57.0(2)
C17	-C4	-C5	-C10	-74.41(19)
C18	-C4	-C5	-C6	-62.95(19)
C18	-C4	-C5	-C10	165.62(14)
C4	-C5	-C6	-C7	163.53(15)
C10	-C5	-C6	-C7	-62.19(19)
C4	-C5	-C10	-C1	-51.40(19)
C4	-C5	-C10	-C9	-167.23(14)
C4	-C5	-C10	-C16	69.71(19)
C6	-C5	-C10	-C1	175.26(14)
C6	-C5	-C10	-C9	59.44(17)
C6	-C5	-C10	-C16	-63.62(18)
C5	-C6	-C7	-C8	56.1(2)
C6	-C7	-C8	-O19	71.76(18)
C6	-C7	-C8	-C9	-48.37(19)
C6	-C7	-C8	-C15	-170.84(14)
O19	-C8	-C9	-C10	-71.68(17)
O19	-C8	-C9	-C11	60.27(17)

Table 7 - Torsion Angles (Degrees) (continued)

C7	-C8	-C9	-C10	48.45(19)
C7	-C8	-C9	-C11	-179.59(14)
C15	-C8	-C9	-C10	170.26(14)
C15	-C8	-C9	-C11	-57.79(18)
C8	-C9	-C10	-C1	-169.54(14)
C8	-C9	-C10	-C5	-53.58(18)
C8	-C9	-C10	-C16	70.98(18)
C11	-C9	-C10	-C1	59.48(18)
C11	-C9	-C10	-C5	175.44(14)
C11	-C9	-C10	-C16	-60.00(18)
C8	-C9	-C11	-C12	105.86(16)
C10	-C9	-C11	-C12	-121.37(16)
C9	-C11	-C12	-C13	-175.88(14)
C11	-C12	-C13	-O20	-68.03(18)
C11	-C12	-C13	-C14	169.77(14)

Table 8 - Contact Distances(Angstrom)

O19	.O20_a	3.0012(17)	C6	.H13B	2.8100
O19	.C16	3.012(2)	C6	.H17C	2.7400
O19	.O20_b	2.8636(18)	C8	.H16B	3.0100
O19	.C13_b	3.305(2)	C8	.H5	3.0900
O20	.O19_d	2.8636(18)	C11	.H15A	2.6600
O20	.O19_c	3.0012(17)	C11	.H1A	2.7200
O19	.H11B	2.5100	C11	.H20	2.92(3)
O19	.H16B	2.5200	C11	.H20_b	2.99(3)
O19	.H20_b	2.03(3)	C11	.H16A	2.6500
O19	.H6A	2.8200	C12	.H15A	2.9800
O19	.H13_b	2.7900	C14	.H15C_c	2.7700
O20	.H11A	2.7300	C15	.H12B	2.8600
O20	.H19_c	2.11(3)	C15	.H11B	2.7500
O20	.H7B_c	2.9100	C16	.H2A	2.8300
O20	.H11B_d	2.7500	C16	.H6A	2.7400
O20	.H16A_d	2.7400	C16	.H17B	2.7300
C12	.C15	3.423(2)	C16	.H3A_f	3.1000
C13	.O19_d	3.305(2)	C16	.H11A	2.7300
C15	.C12	3.423(2)	C17	.H2A	2.9500
C16	.C17	3.267(3)	C17	.H6A	2.9600
C16	.O19	3.012(2)	C17	.H16C	2.7800
C17	.C16	3.267(3)	C18	.H6B	2.6600
C1	.H11A	2.6700	H1A	.C11	2.7200
C2	.H14B_e	3.0400	H1A	.H11A	2.1100
C2	.H16C	2.7100	H1A	.H16A	2.5400
C2	.H17B	2.8700	H1B	.H3A	2.5800
C4	.H16C	3.0800	H1B	.H5	2.5100
C6	.H16B	2.7000	H1B	.H9	2.2700

Table 8 - Contact Distances(Angstrom) (continued)

H2A	.C16	2.8300	H7A	.H5	2.4000
H2A	.C17	2.9500	H7A	.H15B	2.4800
H2A	.H16C	2.1600	H7A	.H14C_h	2.4400
H2A	.H17B	2.3400	H7B	.O20_a	2.9100
H2A	.H3A_f	2.5400	H7B	.H15C	2.5100
H2B	.H14B_e	2.4500	H7B	.H19	2.2900
H3A	.H1B	2.5800	H9	.H1B	2.2700
H3A	.H5	2.5500	H9	.H5	2.3000
H3A	.H13C	2.3900	H9	.H12A	2.4500
H3A	.C16_g	3.1000	H9	.H12B	2.4400
H3A	.H2A_g	2.5400	H9	.H15B	2.4000
H3A	.H16C_g	2.5000	H11A	.O20	2.7300
H3B	.H13A	2.4700	H11A	.C1	2.6700
H3B	.H17A	2.5200	H11A	.C16	2.7300
H3B	.H14B_e	2.5100	H11A	.H1A	2.1100
H5	.C8	3.0900	H11A	.H16A	2.1200
H5	.H1B	2.5100	H11A	.H20	2.4900
H5	.H3A	2.5500	H11B	.O19	2.5100
H5	.H7A	2.4000	H11B	.C15	2.7500
H5	.H9	2.3000	H11B	.H13	2.4300
H5	.H13C	2.2800	H11B	.H15A	2.2100
H6A	.O19	2.8200	H11B	.O20_b	2.7500
H6A	.C16	2.7400	H11B	.H20_b	2.2500
H6A	.C17	2.9600	H12A	.H9	2.4500
H6A	.H16B	2.0900	H12A	.H14A	2.5800
H6A	.H17C	2.3800	H12B	.C15	2.8600
H6B	.C18	2.6600	H12B	.H9	2.4400
H6B	.H13B	2.1400	H12B	.H14C	2.5300

Table 8 - Contact Distances(Angstrom) (continued)

H12B	.H15A	2.4500	H15B	.H7A	2.4800
H12B	.H15B	2.5900	H15B	.H9	2.4000
H13	.H11B	2.4300	H15B	.H12B	2.5900
H13	.H13A_i	2.6000	H15B	.H14A_h	2.5900
H13	.O19_d	2.7900	H15C	.C14_a	2.7700
H13	.H16B_d	2.5000	H15C	.H7B	2.5100
H13A	.H3B	2.4700	H15C	.H14A_a	2.1700
H13A	.H17A	2.4300	H15C	.H19	2.3500
H13A	.H13_j	2.6000	H16A	.C11	2.6500
H13B	.C6	2.8100	H16A	.H1A	2.5400
H13B	.H6B	2.1400	H16A	.H11A	2.1200
H13B	.H17C	2.5300	H16A	.O20_b	2.7400
H13B	.H16B_k	2.5300	H16B	.O19	2.5200
H13C	.H3A	2.3900	H16B	.C6	2.7000
H13C	.H5	2.2800	H16B	.C8	3.0100
H14A	.H12A	2.5800	H16B	.H6A	2.0900
H14A	.H15C_c	2.1700	H16B	.H13_b	2.5000
H14A	.H15B_l	2.5900	H16B	.H13B_n	2.5300
H14B	.C2_m	3.0400	H16C	.C2	2.7100
H14B	.H2B_m	2.4500	H16C	.C4	3.0800
H14B	.H3B_m	2.5100	H16C	.C17	2.7800
H14C	.H12B	2.5300	H16C	.H2A	2.1600
H14C	.H7A_l	2.4400	H16C	.H17B	2.0300
H15A	.C11	2.6600	H16C	.H3A_f	2.5000
H15A	.C12	2.9800	H17A	.H3B	2.5200
H15A	.H11B	2.2100	H17A	.H13A	2.4300
H15A	.H12B	2.4500	H17A	.H15A_j	2.5900
H15A	.H17A_i	2.5900	H17B	.C2	2.8700

Table 8 - Contact Distances(Angstrom) (continued)

H17B	.C16	2.7300	H19	.H20_a	2.59(4)
H17B	.H2A	2.3400	H19	.H20_b	2.54(4)
H17B	.H16C	2.0300	H20	.C11	2.92(3)
H17C	.C6	2.7400	H20	.H11A	2.4900
H17C	.H6A	2.3800	H20	.H19_c	2.59(4)
H17C	.H13B	2.5300	H20	.O19_d	2.03(3)
H19	.O20_a	2.11(3)	H20	.C11_d	2.99(3)
H19	.H7B	2.2900	H20	.H11B_d	2.2500
H19	.H15C	2.3500	H20	.H19_d	2.54(4)

Table S9 - Hydrogen Bonds (Angstrom, Deg)

O19 -- H19 .. O20	0.90(2)	2.11(3)	3.0012(17)	172(2)	1_455
O20 -- H20 .. O19	0.86(3)	2.03(3)	2.8636(18)	161(3)	3_566
C11 -- H11B .. O19	0.9900	2.5100	2.948(2)	107.00	.
C16 -- H16B .. O19	0.9800	2.5200	3.012(2)	111.00	.

Translation of Symmetry Code to Equiv.Pos

a =[1455.00] = -1+x,y,z
b =[3466.00] = -1/2+x,3/2-y,1-z
c =[1655.00] = 1+x,y,z
d =[3566.00] = 1/2+x,3/2-y,1-z
e =[2664.00] = 3/2-x,1-y,-1/2+z
f =[4655.00] = 1-x,1/2+y,1/2-z
g =[4645.00] = 1-x,-1/2+y,1/2-z
h =[3456.00] = -1/2+x,1/2-y,1-z
i =[2565.00] = 1/2-x,1-y,1/2+z
j =[2564.00] = 1/2-x,1-y,-1/2+z
k =[4545.00] = -x,-1/2+y,1/2-z
l =[3556.00] = 1/2+x,1/2-y,1-z
m =[2665.00] = 3/2-x,1-y,1/2+z
n =[4555.00] = -x,1/2+y,1/2-z

Appendix III Selected ^{1}H and ^{13}C NMR spectra

Table of Contents

Figure 1.1 ^{1}H NMR spectrum of Compound **2.1** (600 MHz, C_6D_6)

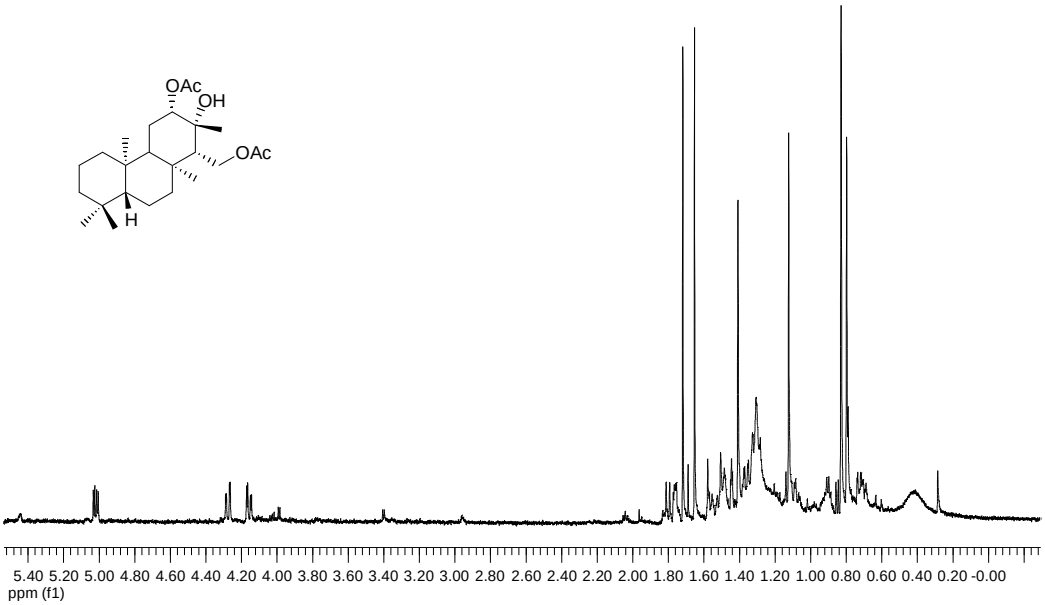

Figure 1.2 ^{13}C NMR spectrum of Compound **2.1** (150 MHz, C_6D_6)

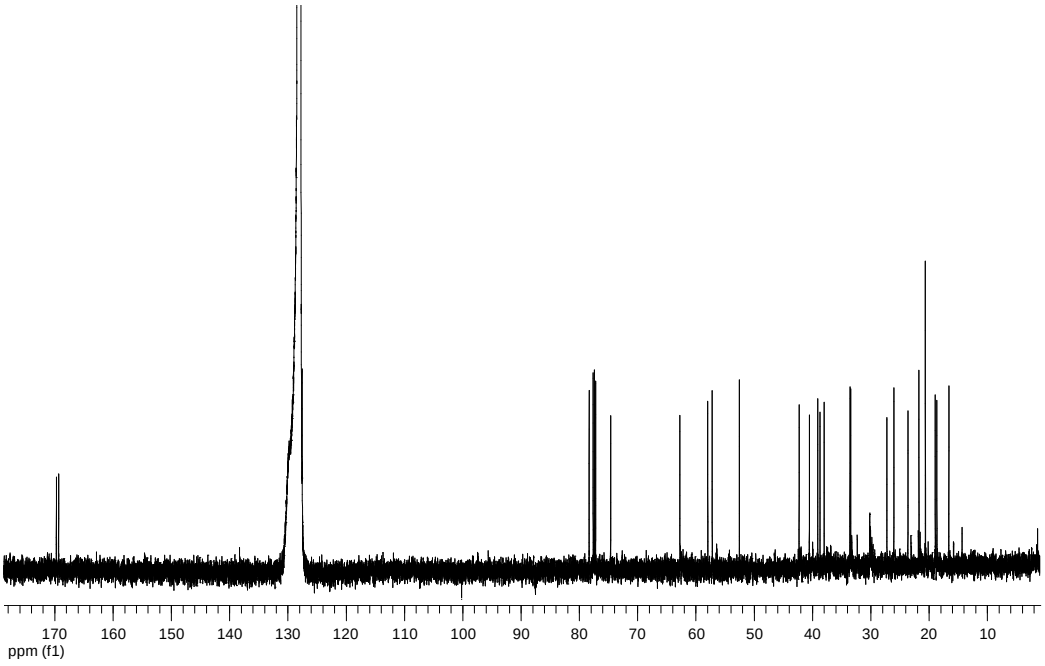

Figure 1.3 ^{1}H NMR spectrum of Compound **3.3** (600 MHz, $CDCl_3$)

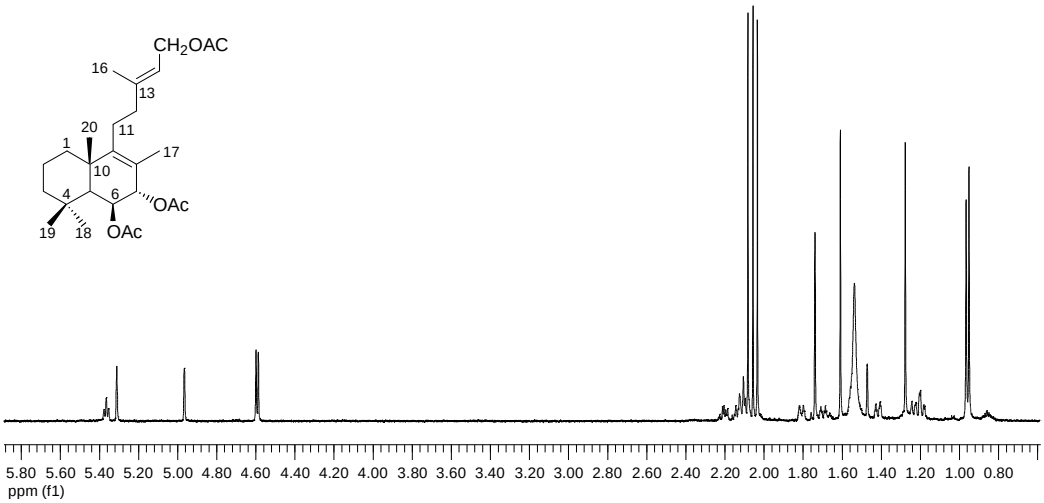

Figure 1.4 ^{13}C NMR spectrum of Compound **3.3** (150 MHz, $CDCl_3$)

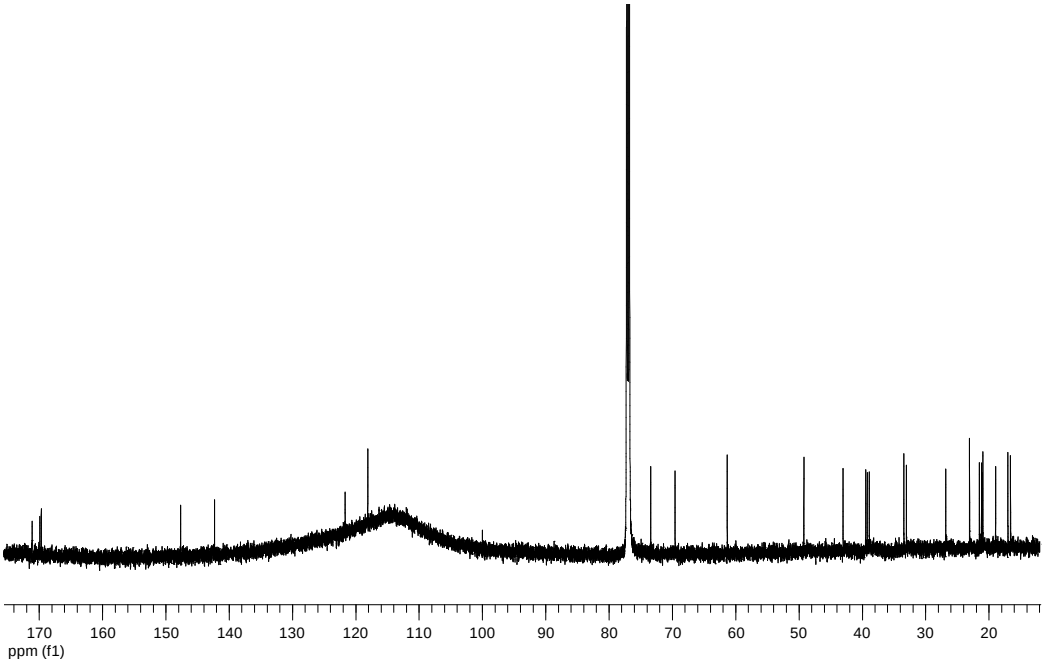

Figure 1.5 ^{1}H NMR spectrum of Compound **3.4** (600 MHz, $CDCl_3$)

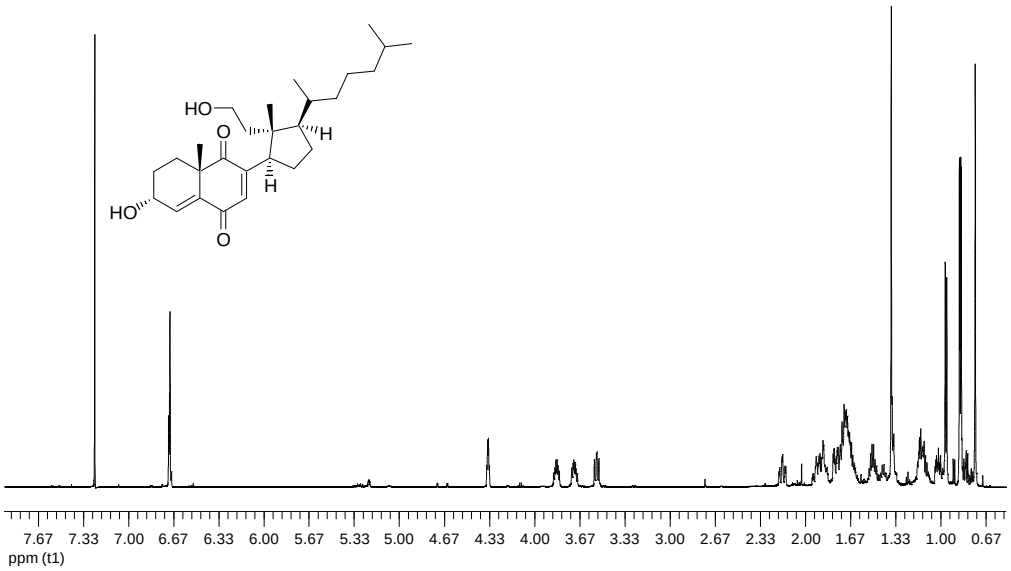

Figure 1.6 ^{13}C NMR spectrum of Compound **3.4** (150 MHz, $CDCl_3$)

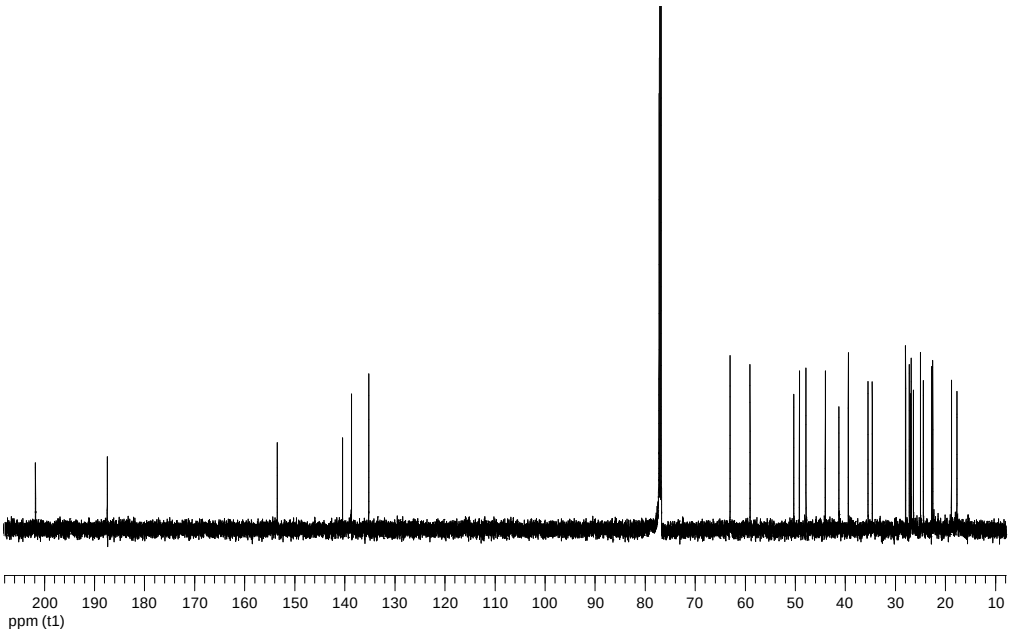

Figure 1.7 ^{1}H NMR spectrum of Compound **3.5** (600 MHz, $CDCl_3$)

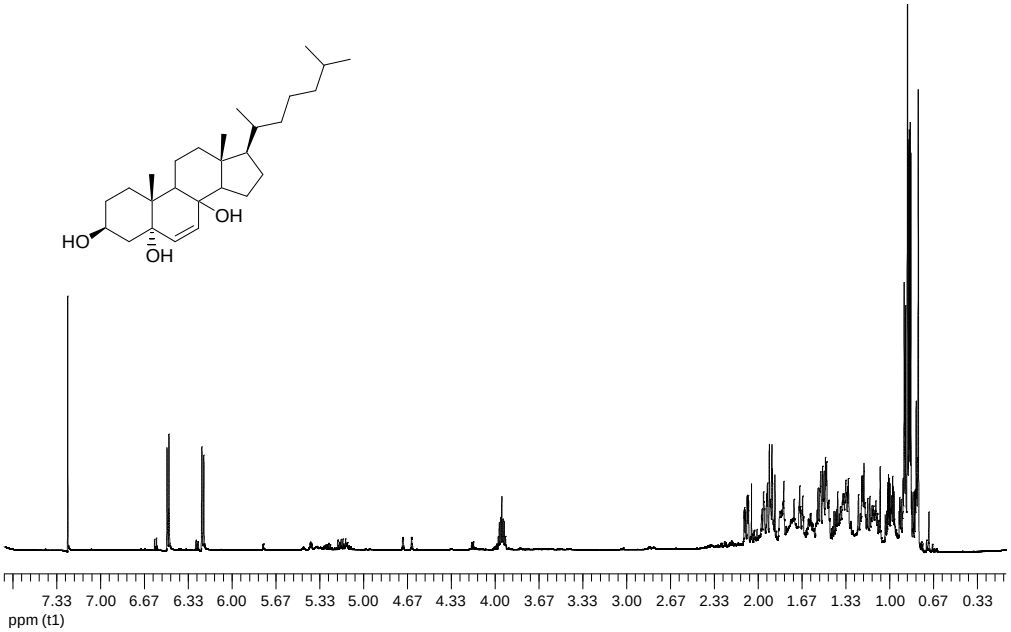

Figure 1.8 ^{13}C NMR spectrum of Compound **3.5** (600 MHz, $CDCl_3$)

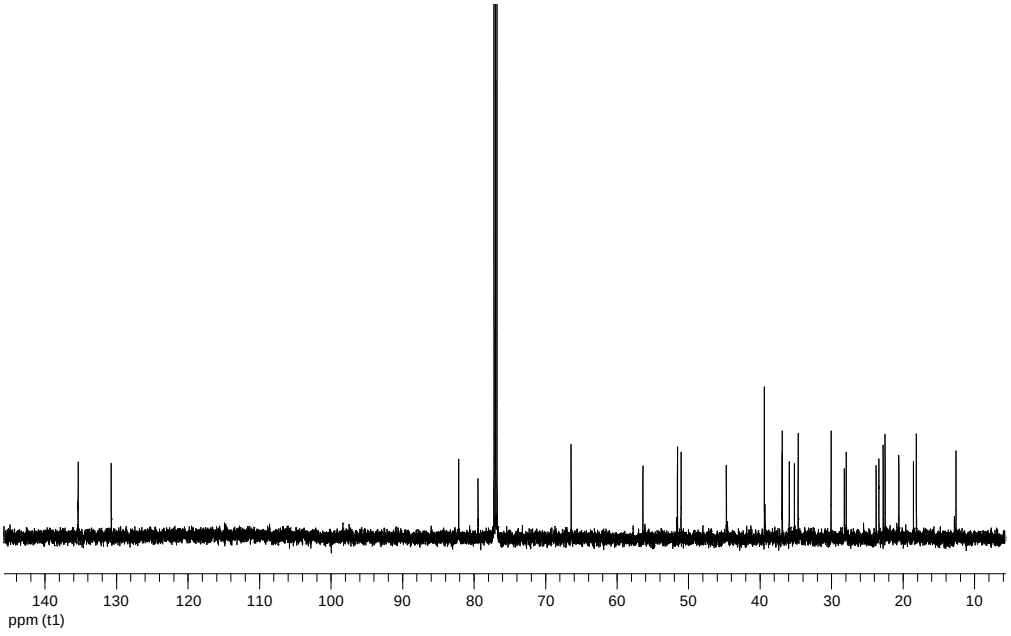

Figure 1.9 ^{1}H NMR spectrum of Compound **4.1** (400 MHz, $CDCl_3$)

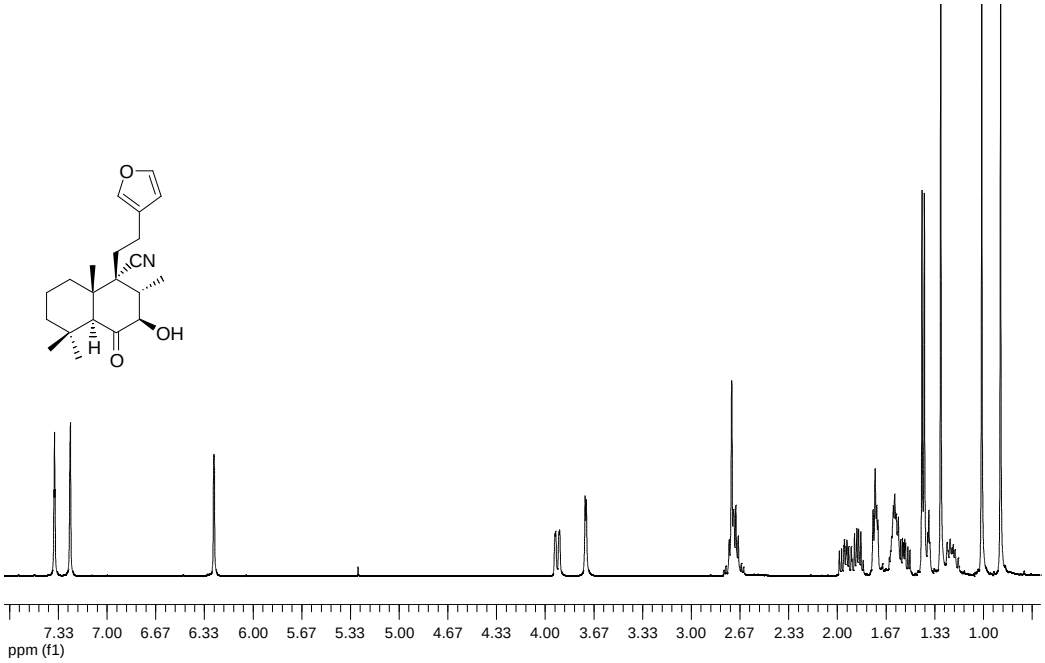

Figure 1.10 ^{13}C NMR spectrum of Compound **4.1** (100 MHz, $CDCl_3$)

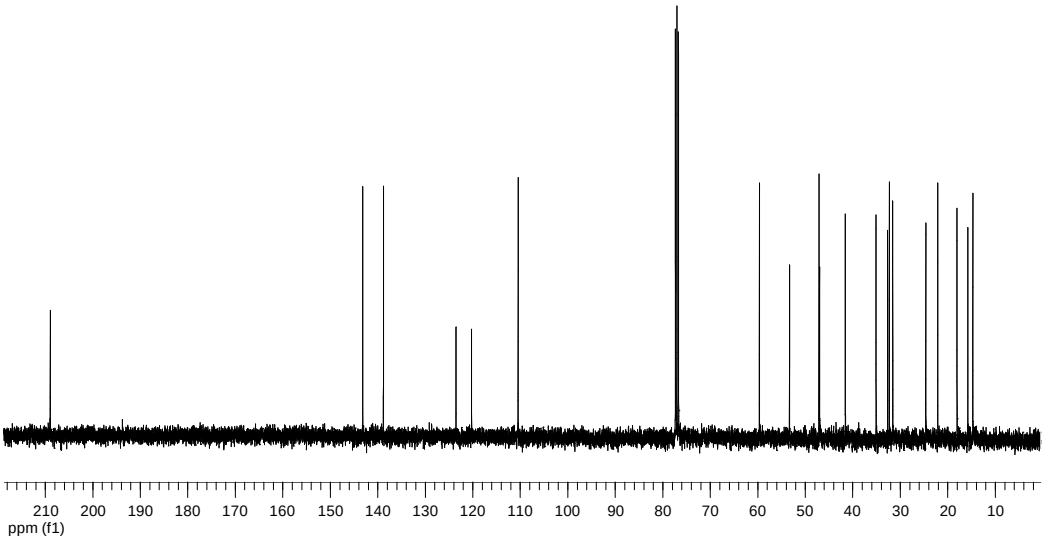

Figure 1.11 ^{1}H NMR spectrum of Compound **4.2** (400 MHz, $CDCl_3$)

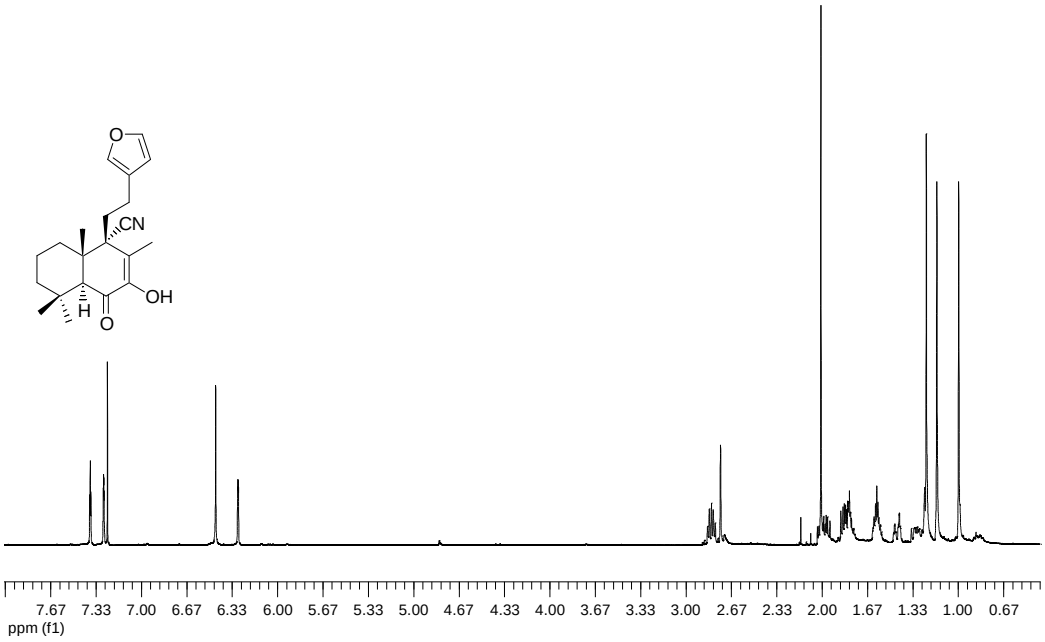

Figure 1.12 ^{13}C NMR spectrum of Compound **4.2** (100 MHz, $CDCl_3$)

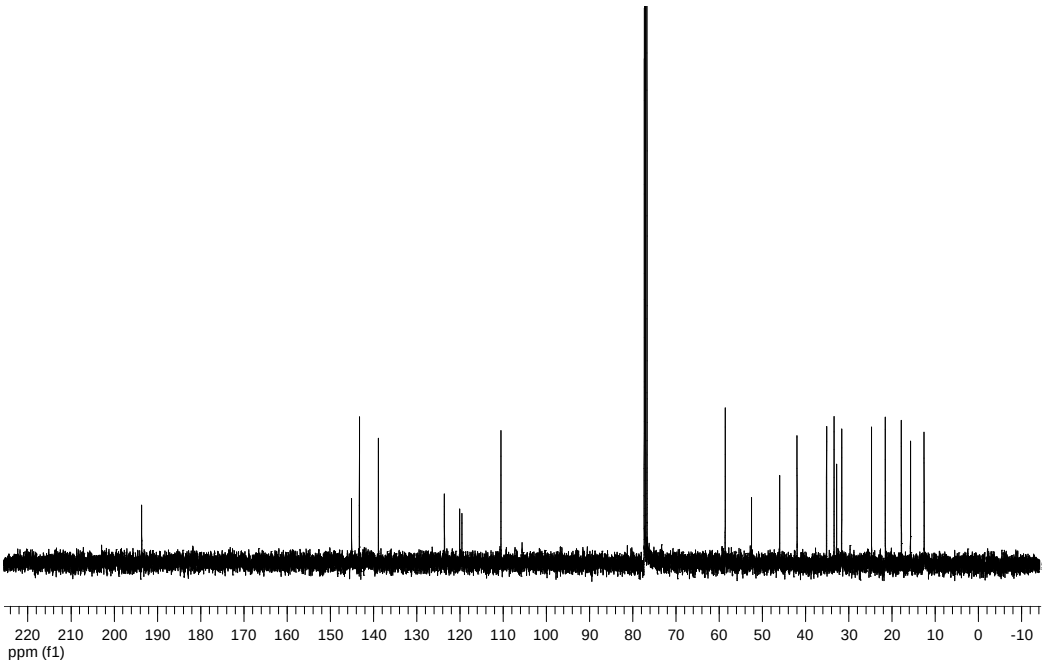

Figure 1.13 ^{1}H NMR spectrum of Compound **4.3** (400 MHz, $CDCl_3$)

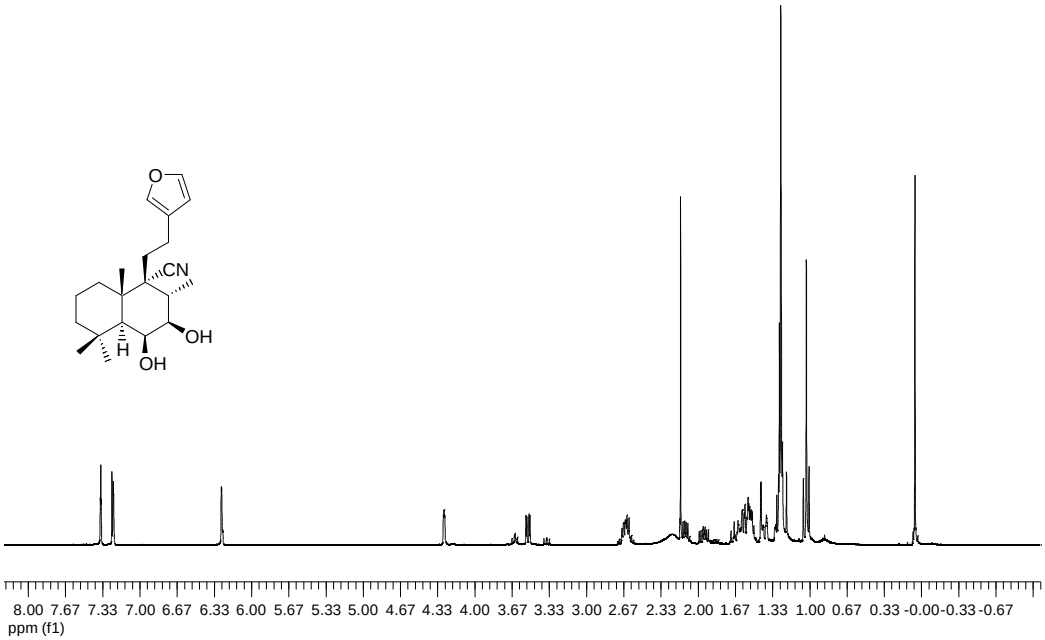

Figure 1.14 ^{13}C NMR spectrum of Compound **4.3** (100 MHz, $CDCl_3$)

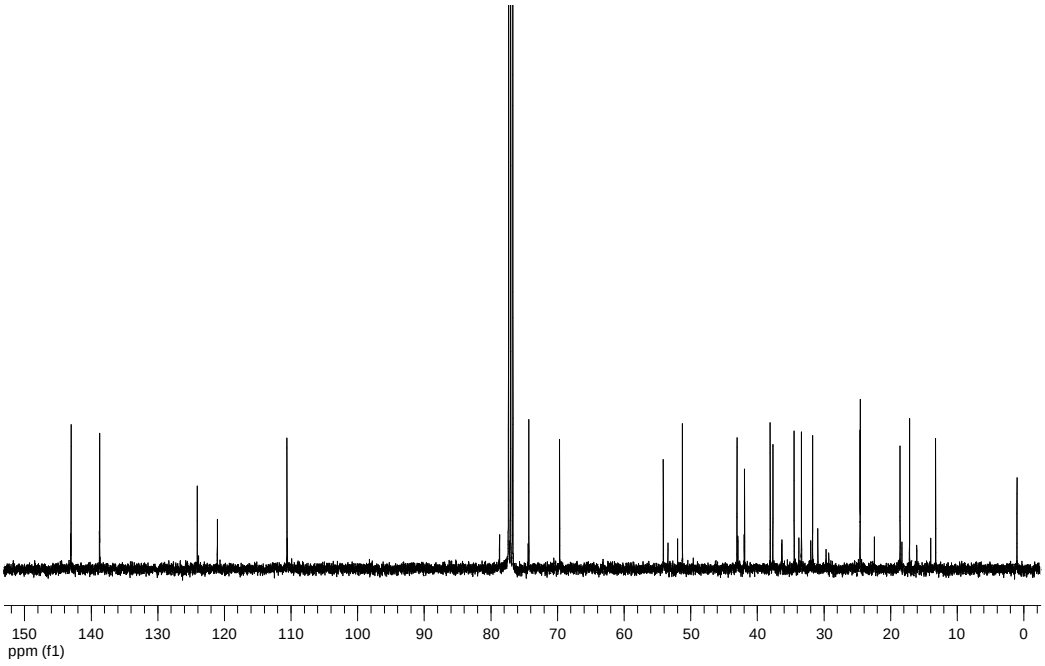

Figure 1.15 ^{1}H NMR spectrum of Compound **5.1** (600 MHz, C_6D_6)

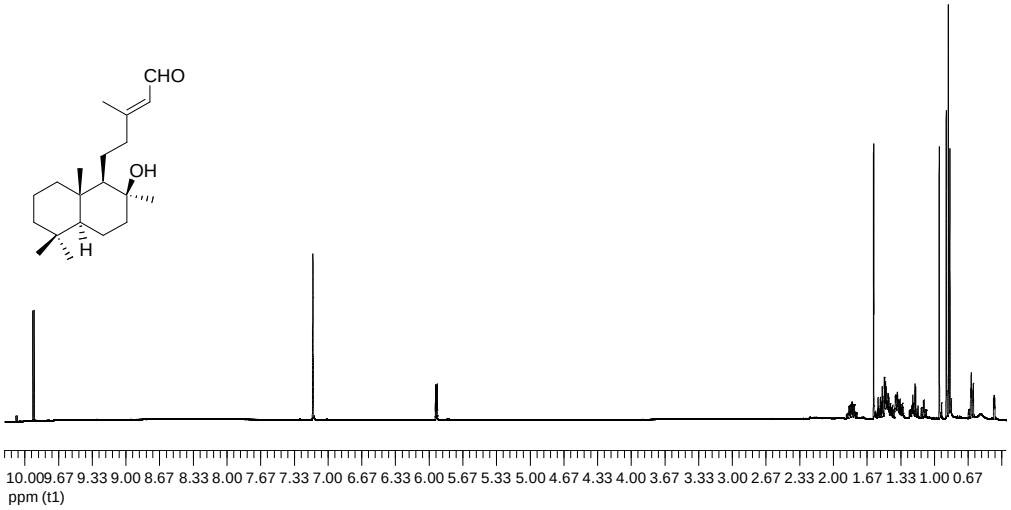

Figure 1.16 ^{13}C NMR of spectrum **5.1** (150 MHz, C_6D_6)

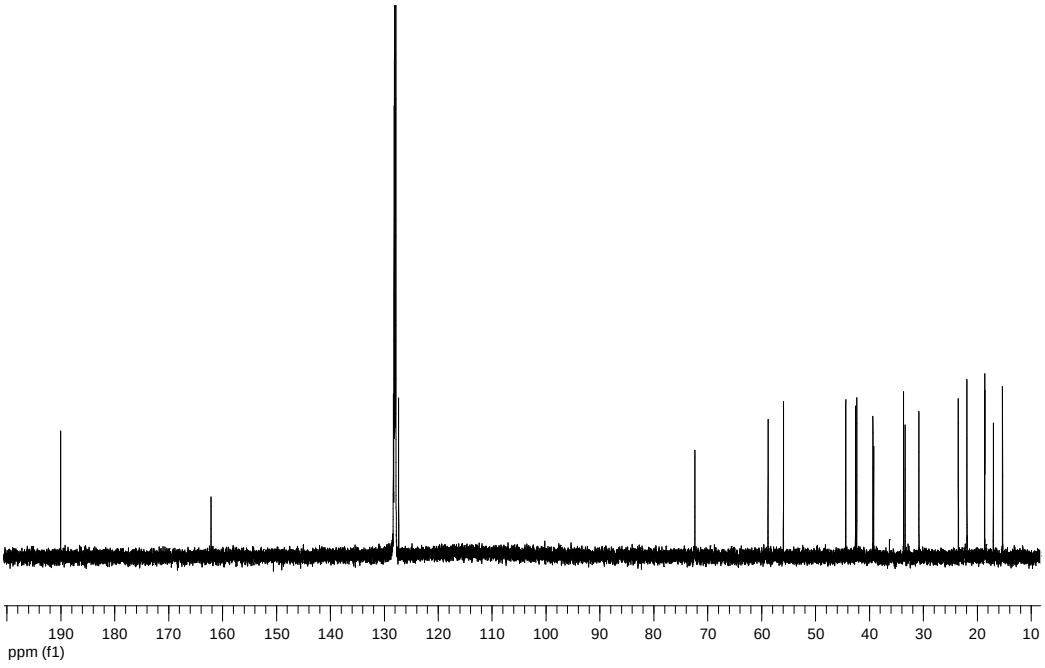

Figure 1.17 ^{1}H NMR spectrum of Compound **5.2** (600 MHz, C_6D_6)

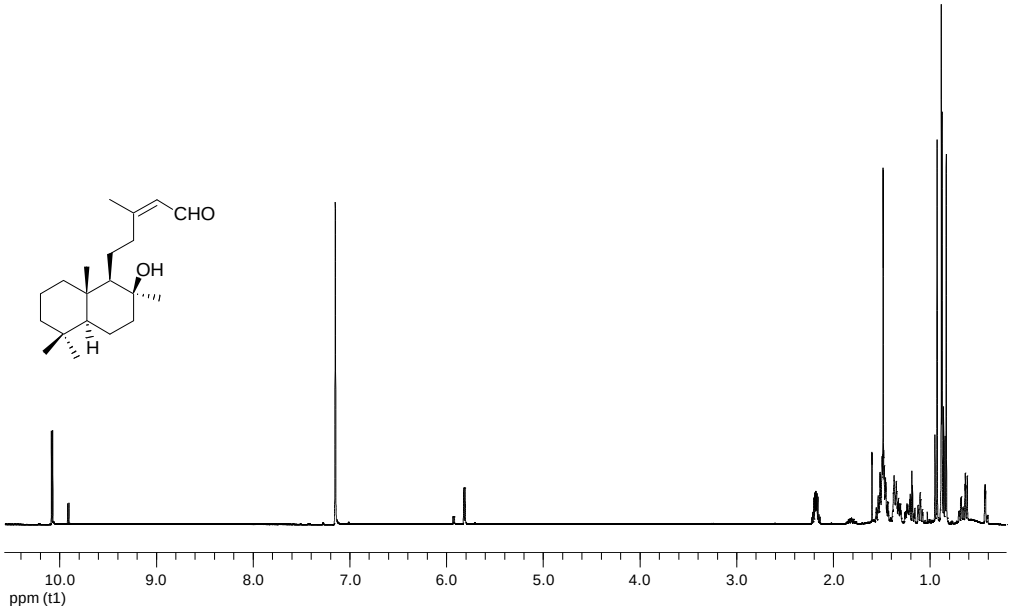

Figure 1.18 ^{13}C NMR spectrum of Compound **5.2** (150 MHz, C_6D_6)

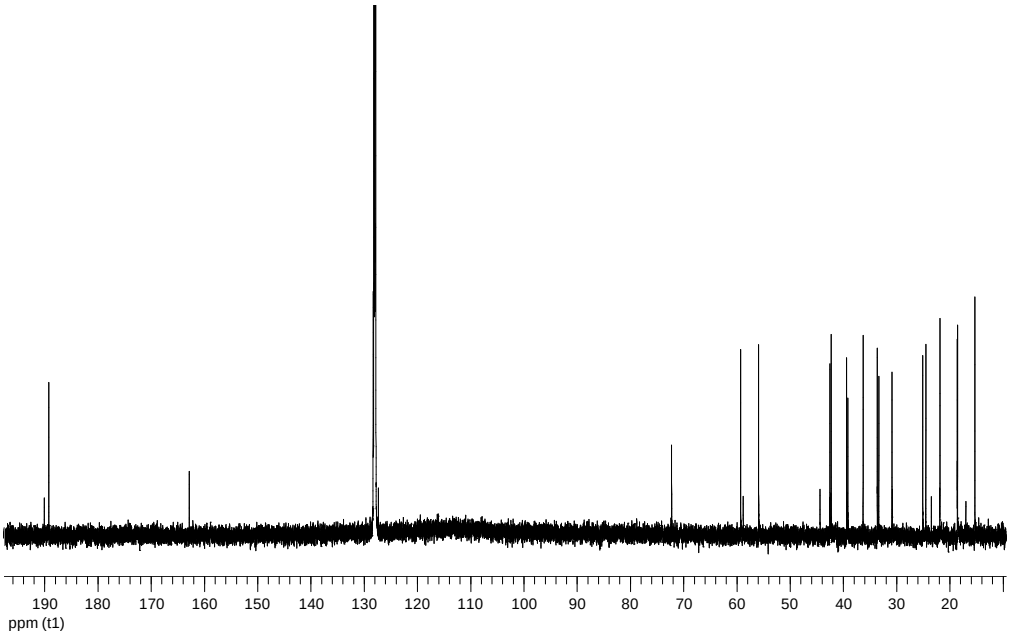

Figure 1.19 ^{1}H NMR spectrum of Compound **5.4** (600 MHz, $CDCl_3$)

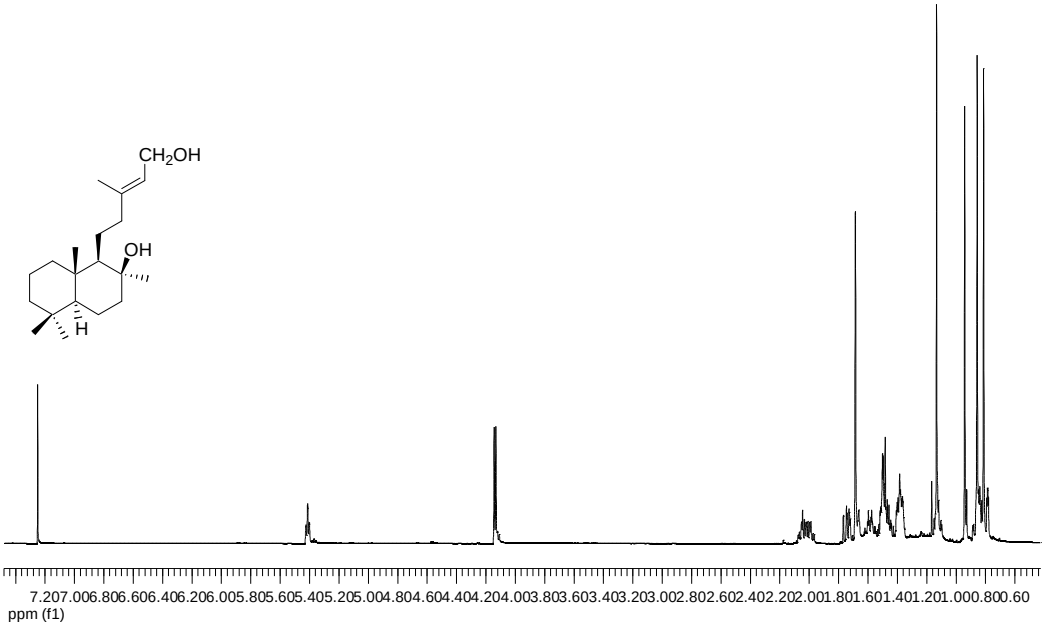

Figure 1.20 ^{13}C NMR spectrum of Compound **5.4** (150 MHz, $CDCl_3$)

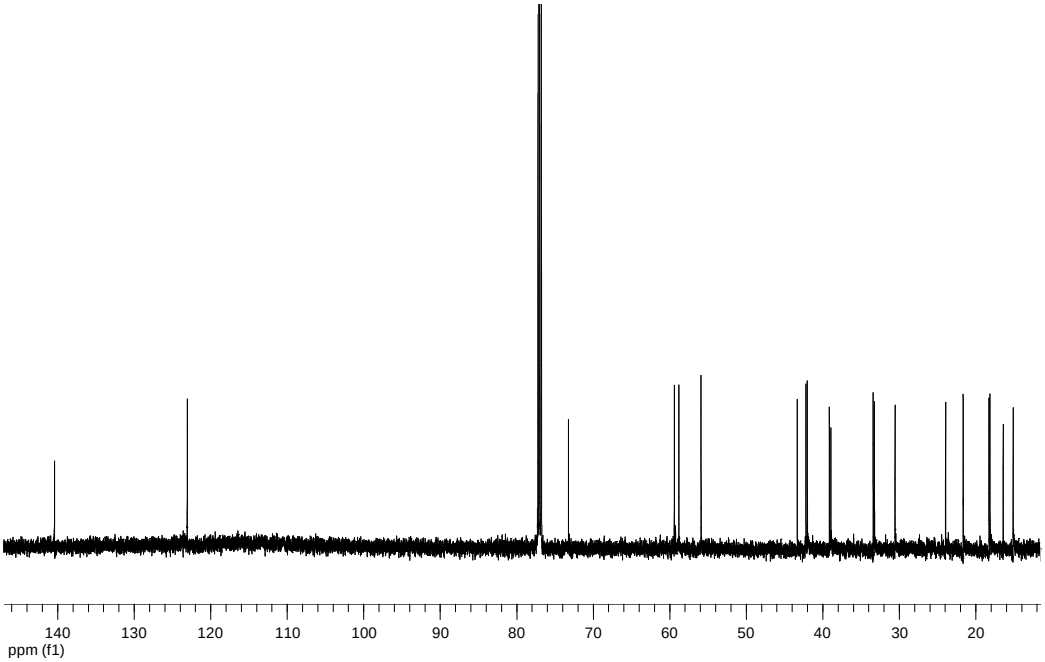

Figure 1.21 ^{1}H NMR spectrum of Compound **5.5** (600 MHz, $CDCl_3$)

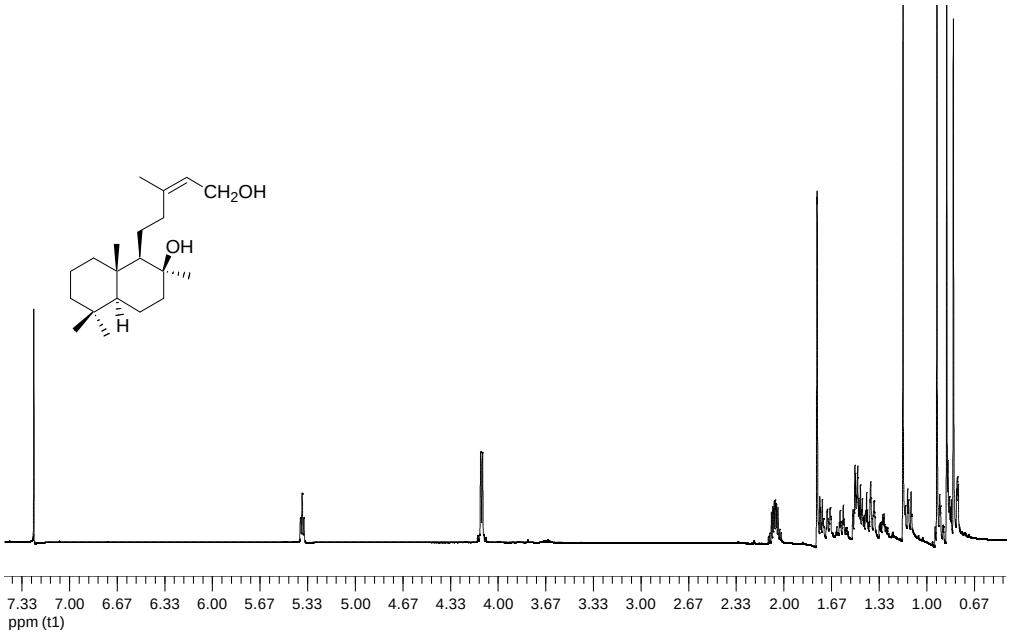

Figure 1.22 ^{13}C NMR spectrum of Compound **5.5** (150 MHz, $CDCl_3$)

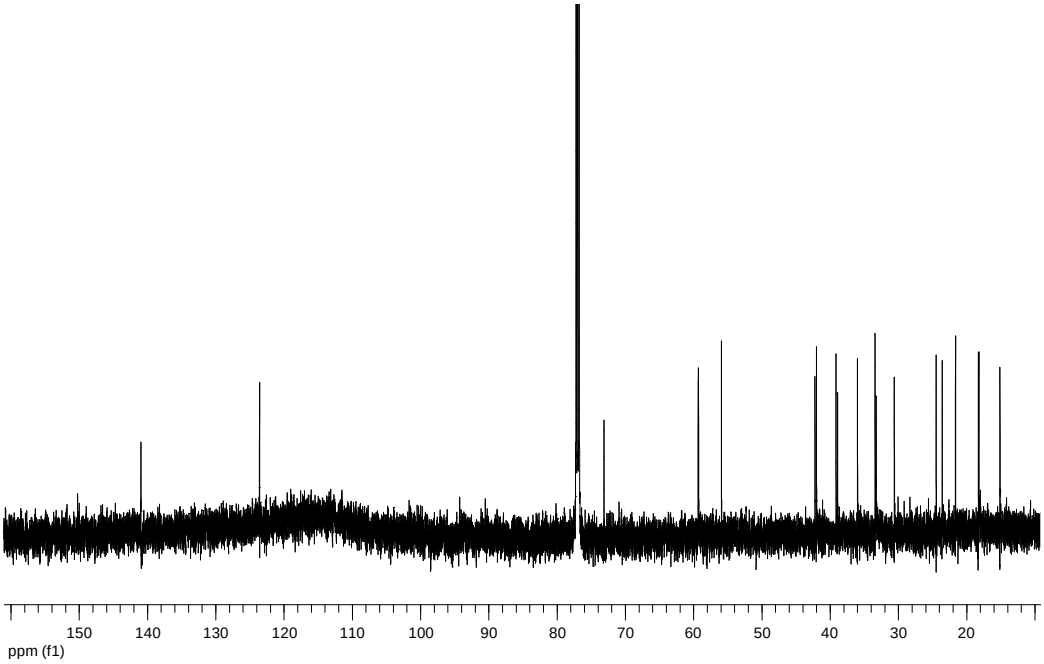

Figure 1.23 ^{1}H NMR spectrum of Compound **5.32** (400 MHz, $CDCl_3$)

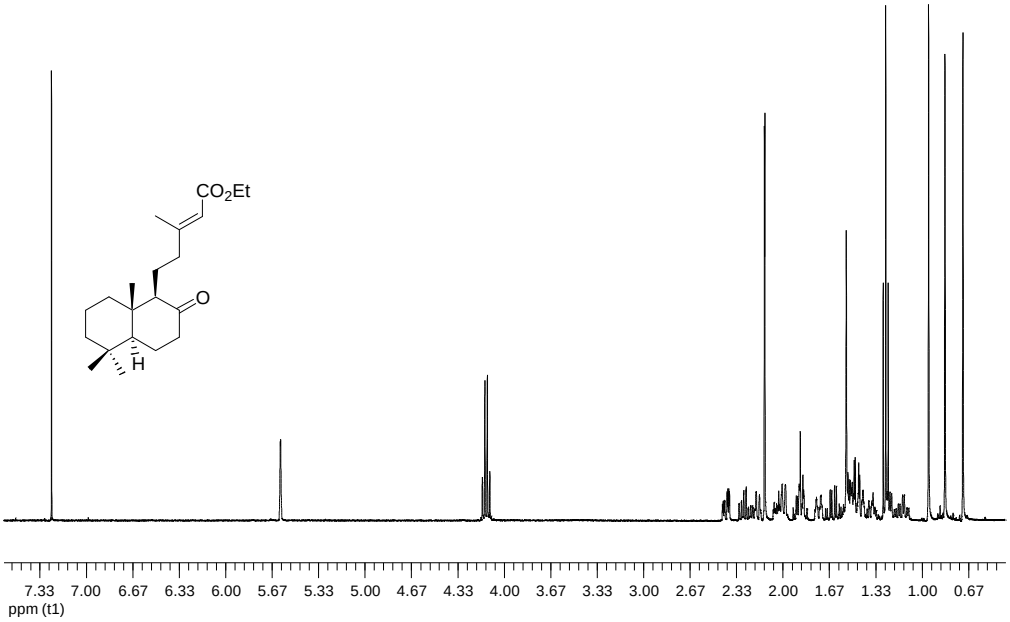

Figure 1.24 ^{13}C NMR spectrum of Compound **5.32** (100 MHz, $CDCl_3$)

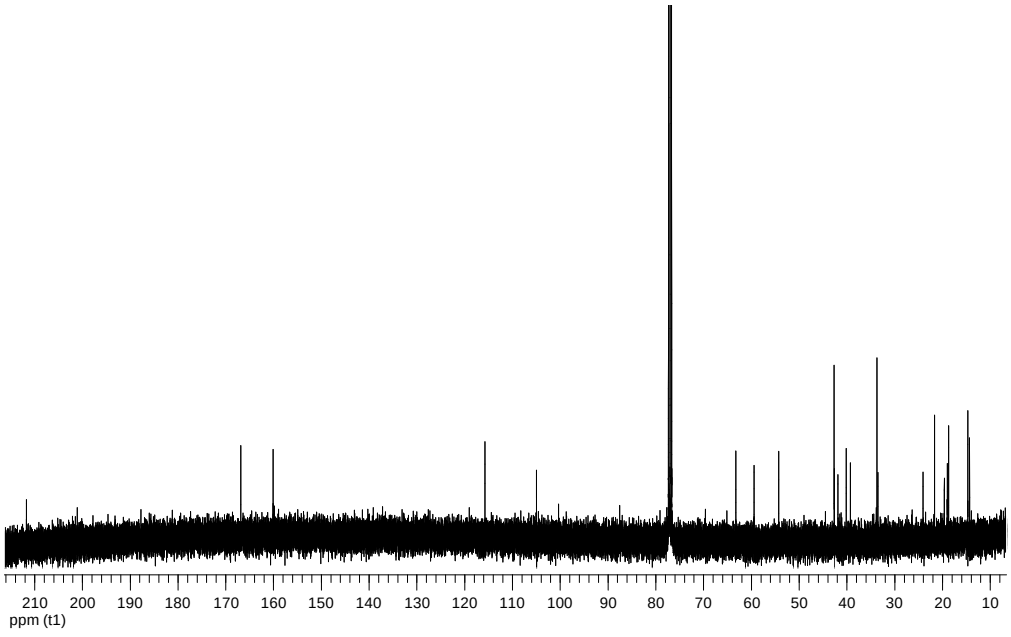

Figure 1.25 ^{1}H NMR spectrum of Compound **5.33** ($CDCl_3$)

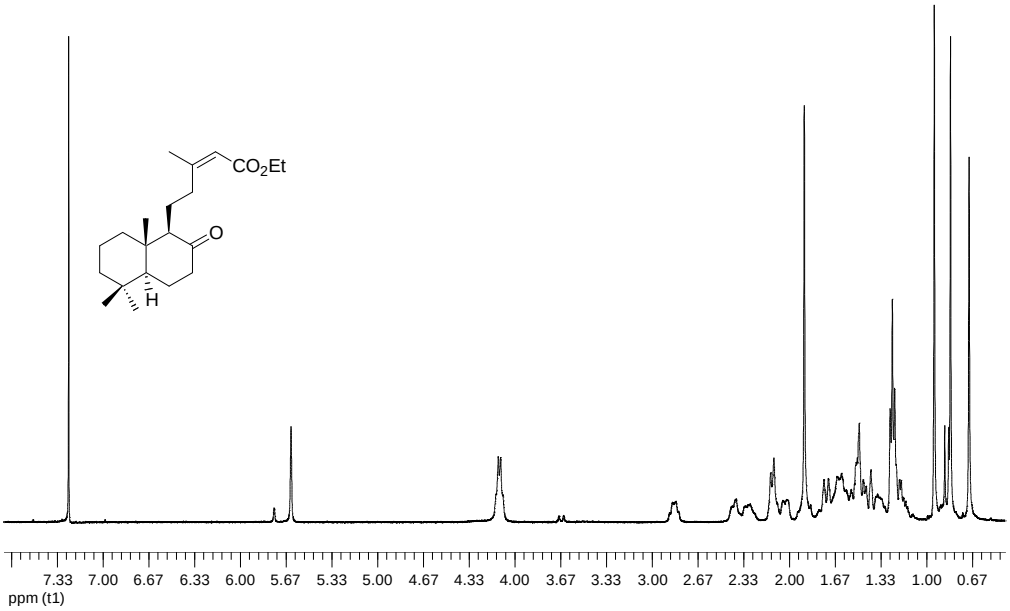

Figure 1.26 ^{13}C NMR spectrum of Compound **5.33** ($CDCl_3$)

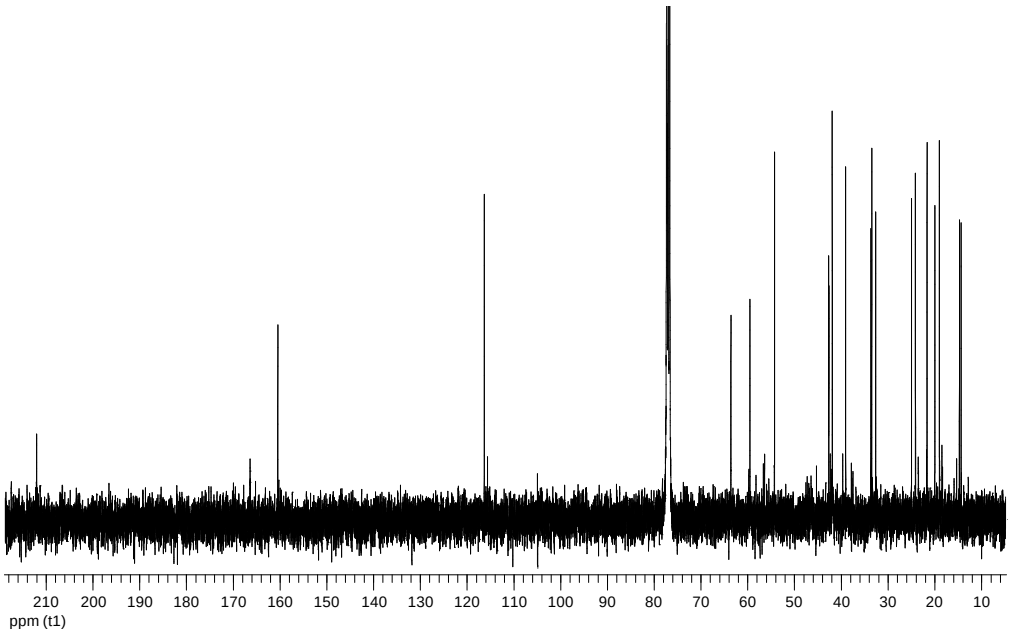

Figure 1.27 ^{1}H NMR spectrum of Compound **5.34** (400 MHz, $CDCl_3$)

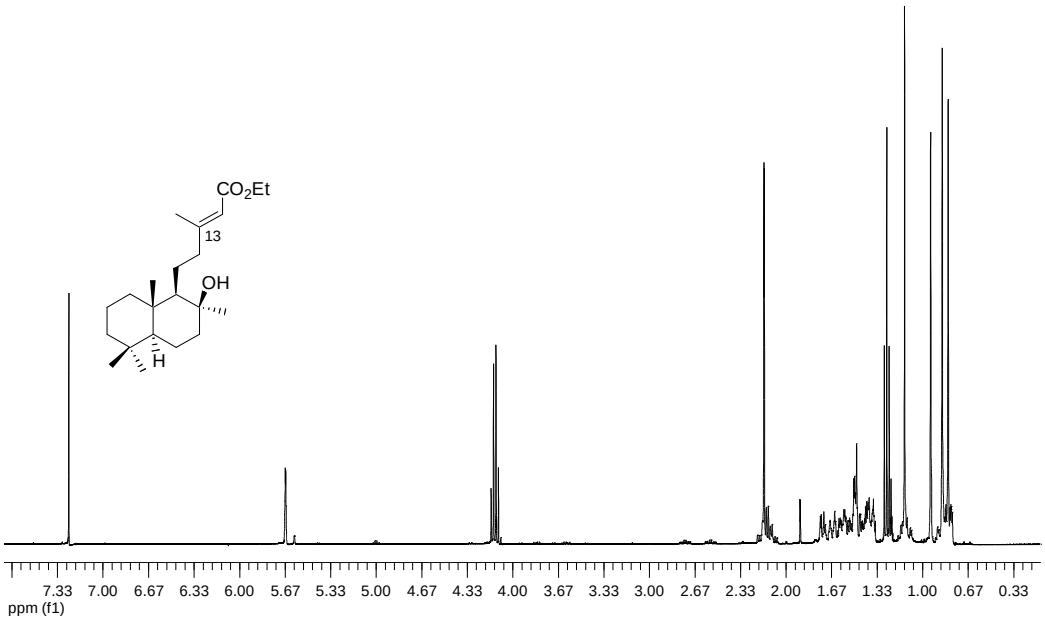

Figure 1.28 ^{13}C NMR spectrum of Compound **5.34** (100 MHz, $CDCl_3$)

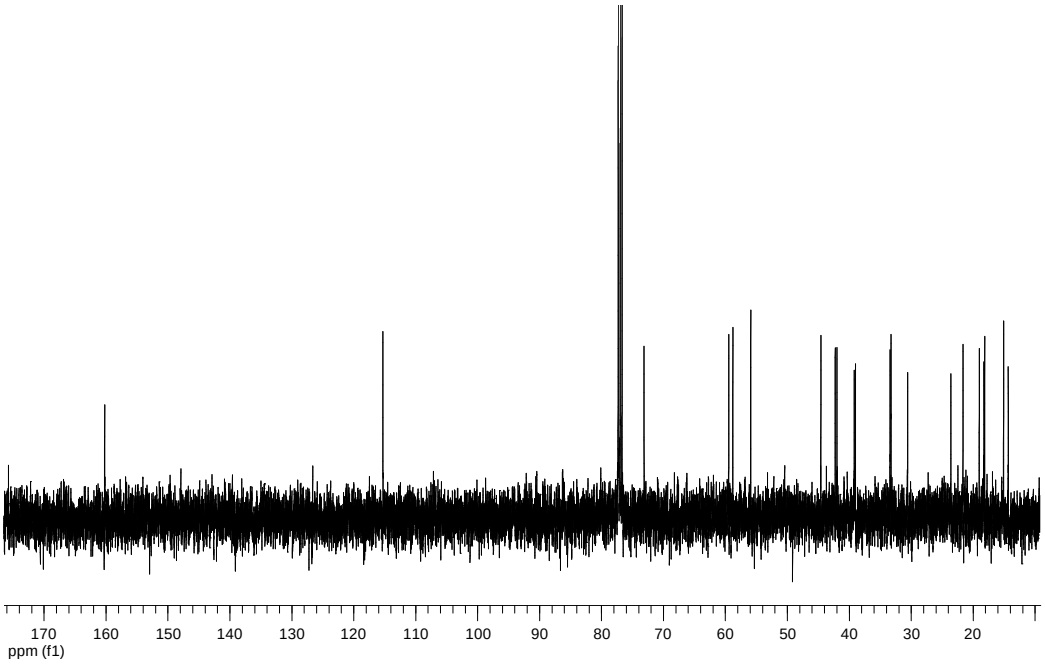

Figure 1.29 ^{1}H NMR spectrum of Compound **5.35** (400 MHz, $CDCl_3$)

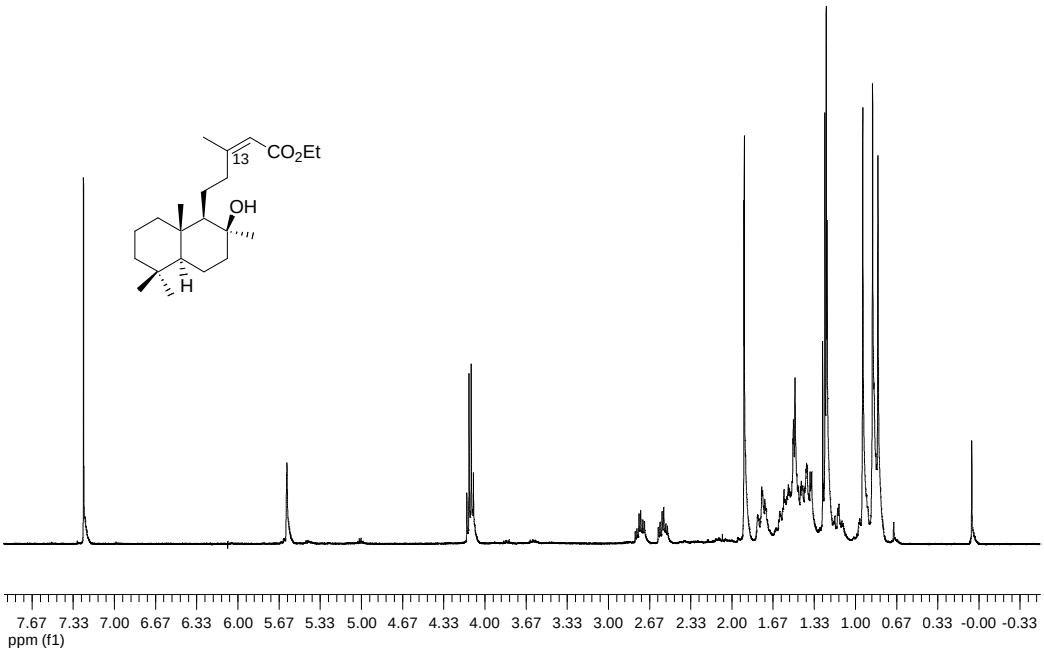

Figure 1.30 ^{13}C NMR spectrum of Compound **5.35** (100 MHz, $CDCl_3$)

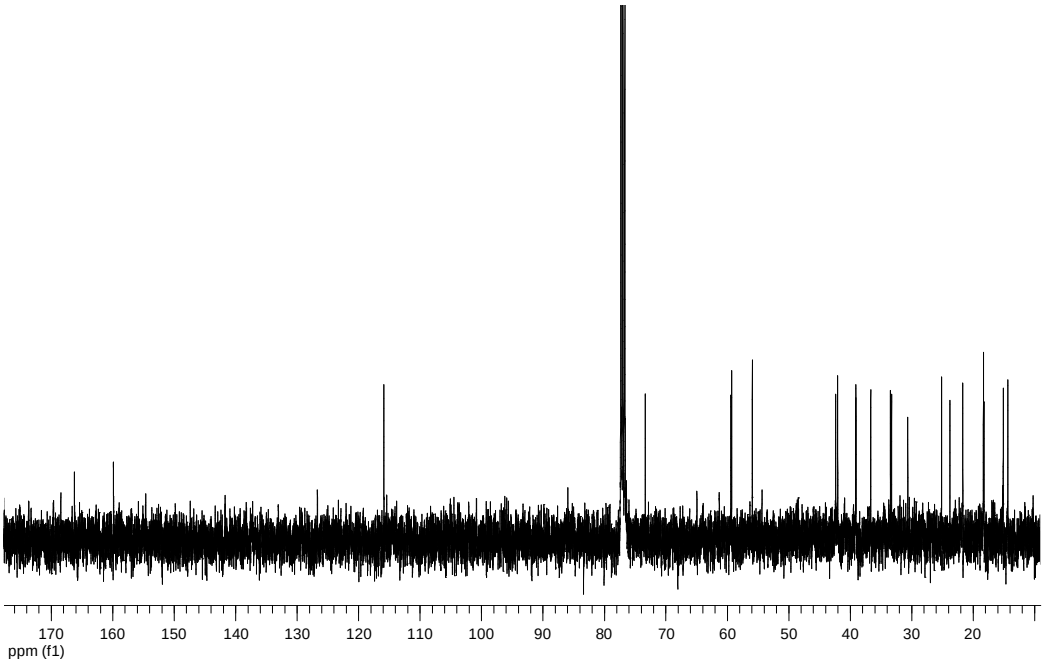

Figure 1.31 ^{1}H NMR spectrum of Compound **5.49** (400 MHz, $CDCl_3$)

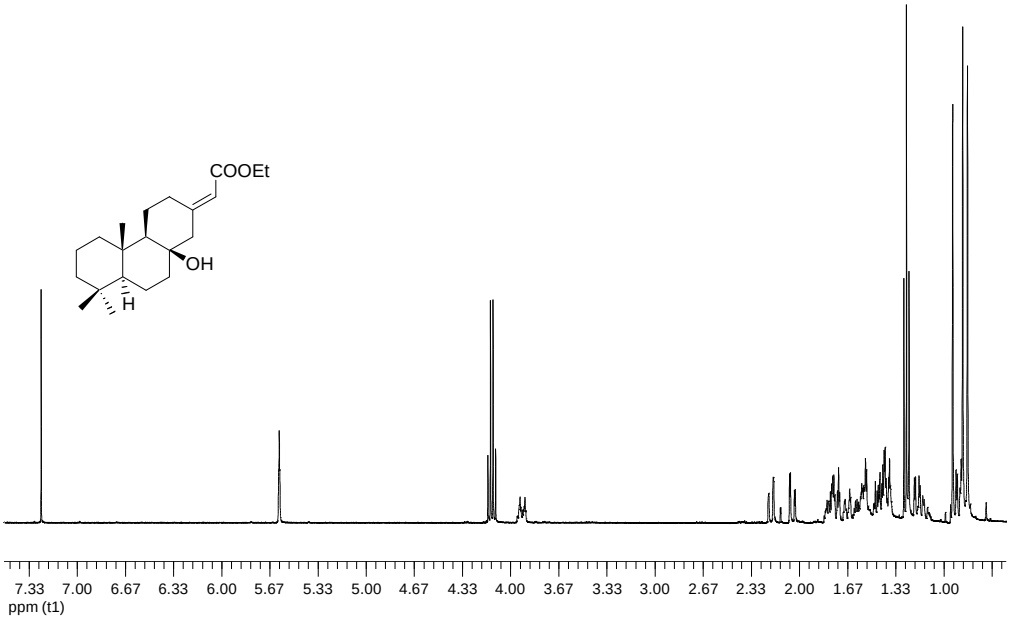

Figure 1.32 ^{13}C NMR spectrum of Compound **5.49** (100 MHz, $CDCl_3$)

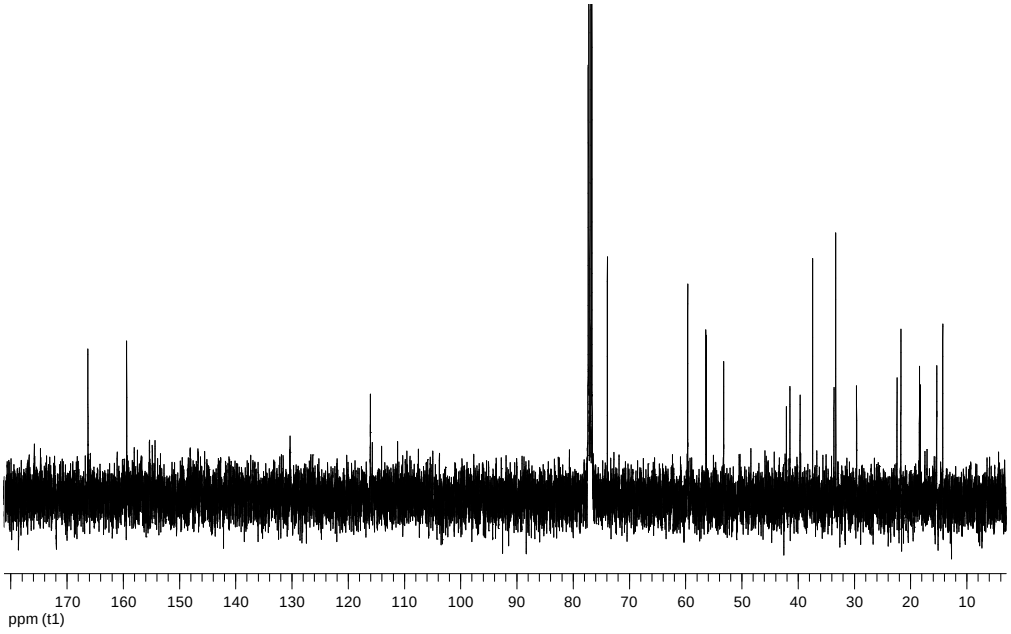

Figure 1.33 ^{1}H NMR spectrum of Compound **5.50** (400 MHz, $CDCl_3$)

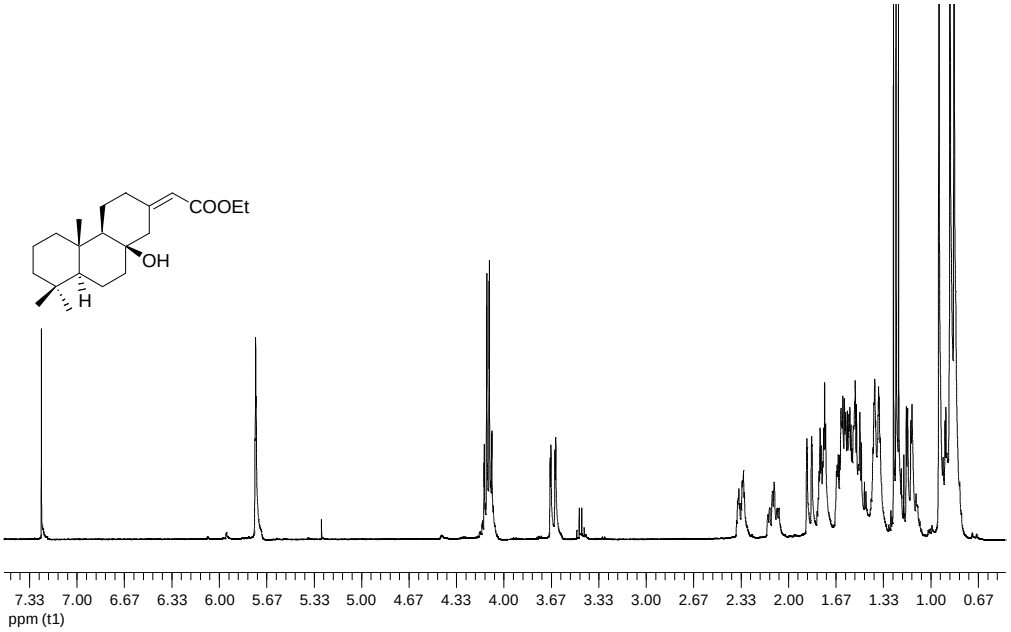

Figure 1.34 ^{13}C NMR spectrum of Compound **5.50** (100 MHz, $CDCl_3$)

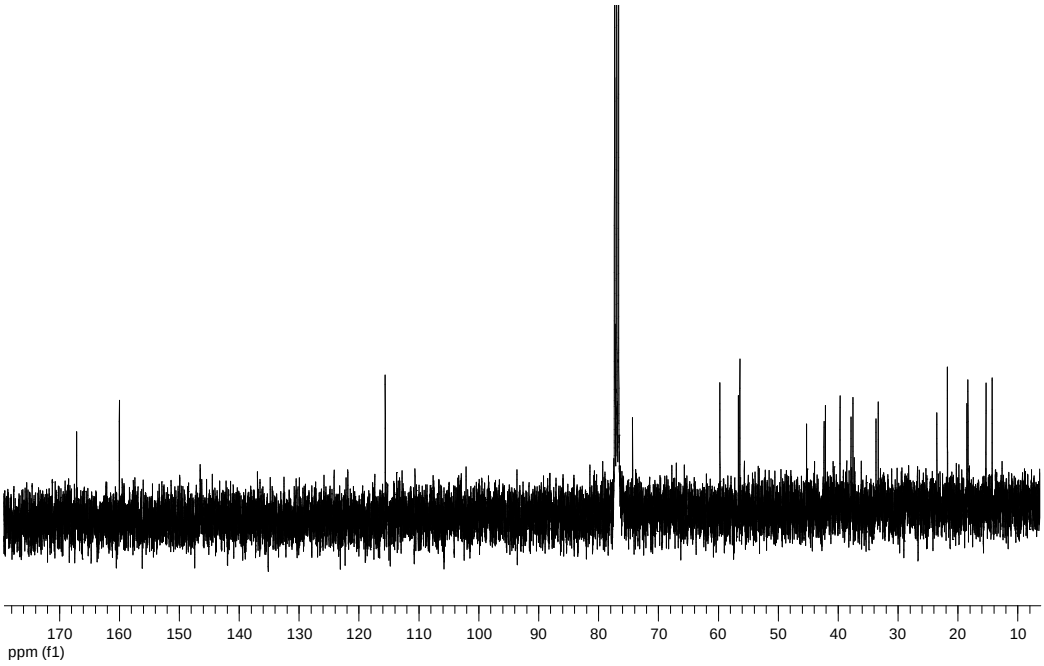

Figure 1.35 ^{1}H NMR spectrum of Compound **6.6** (600 MHz, $CDCl_3$)

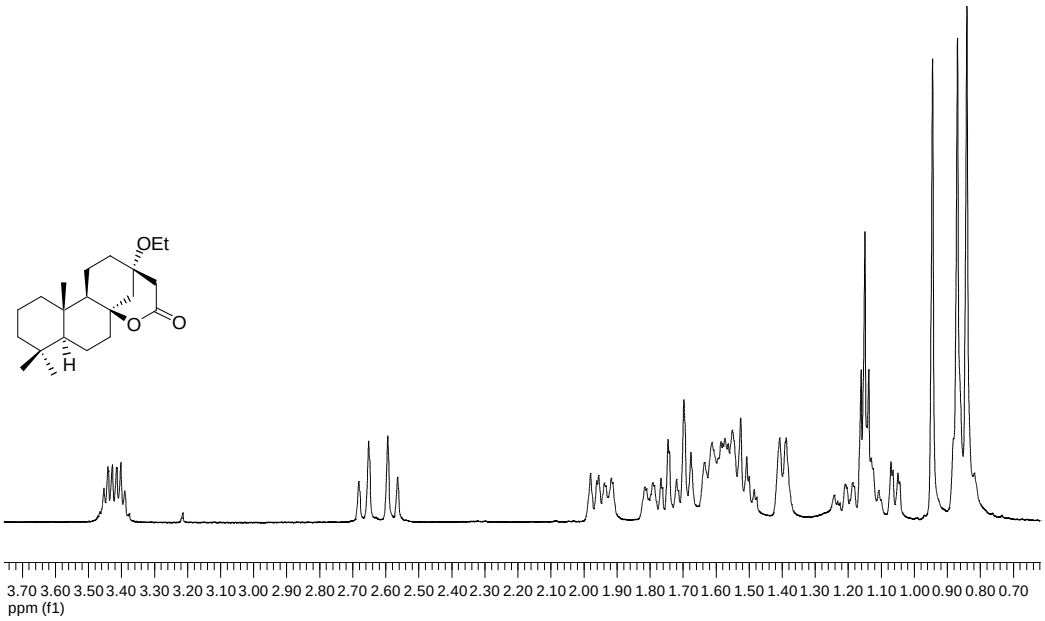

Figure 1.36 ^{13}C NMR spectrum of Compound **6.6** (150 MHz, $CDCl_3$)

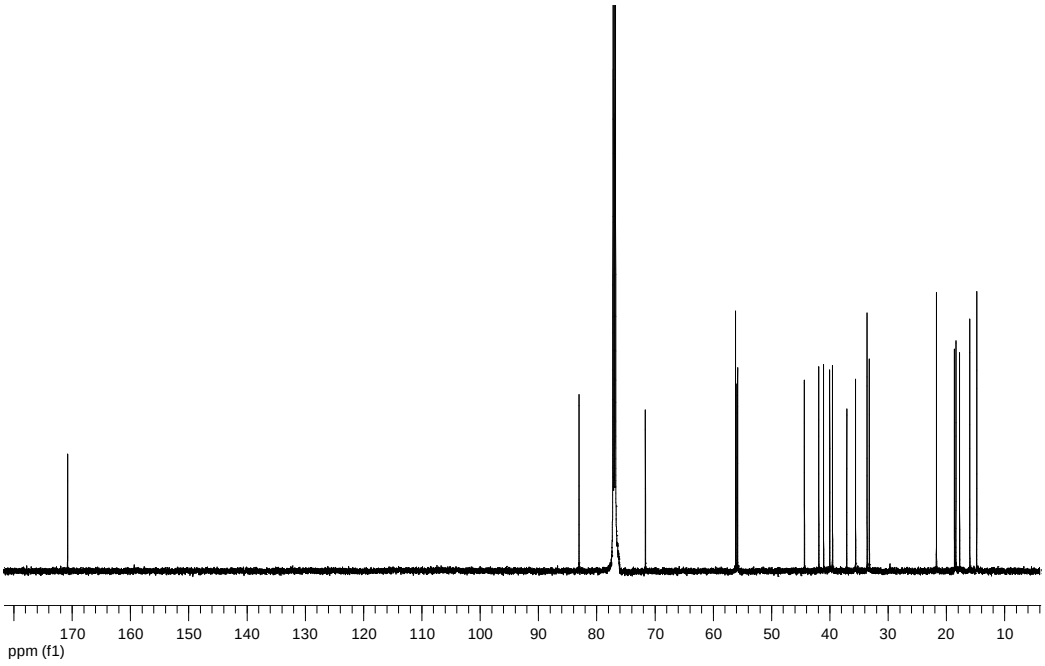

Figure 1.37 ^{1}H NMR spectrum of Compound **6.7** (600 MHz, C_6D_6)

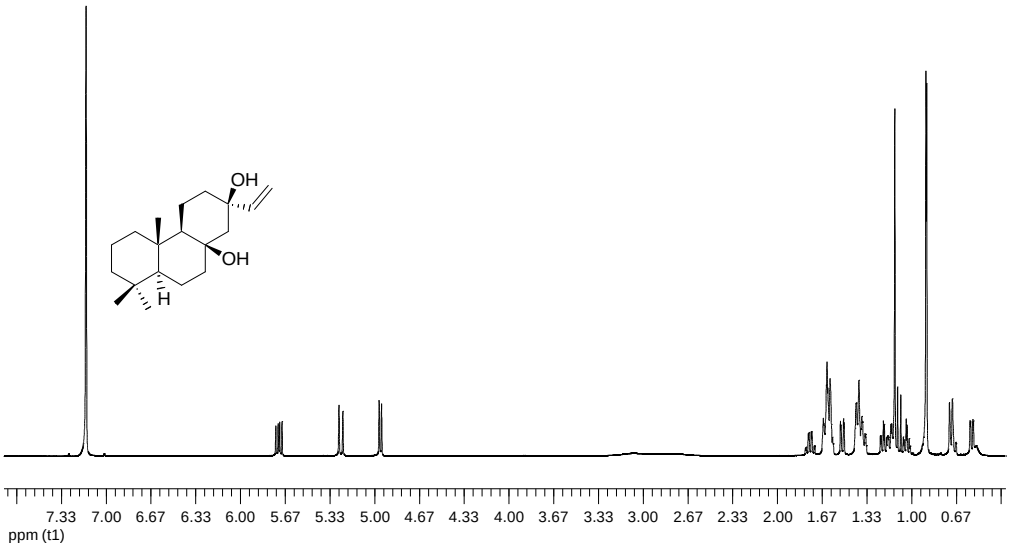

Figure 1.38 ^{13}C NMR spectrum of Compound **6.7** (150 MHz, C_6D_6)

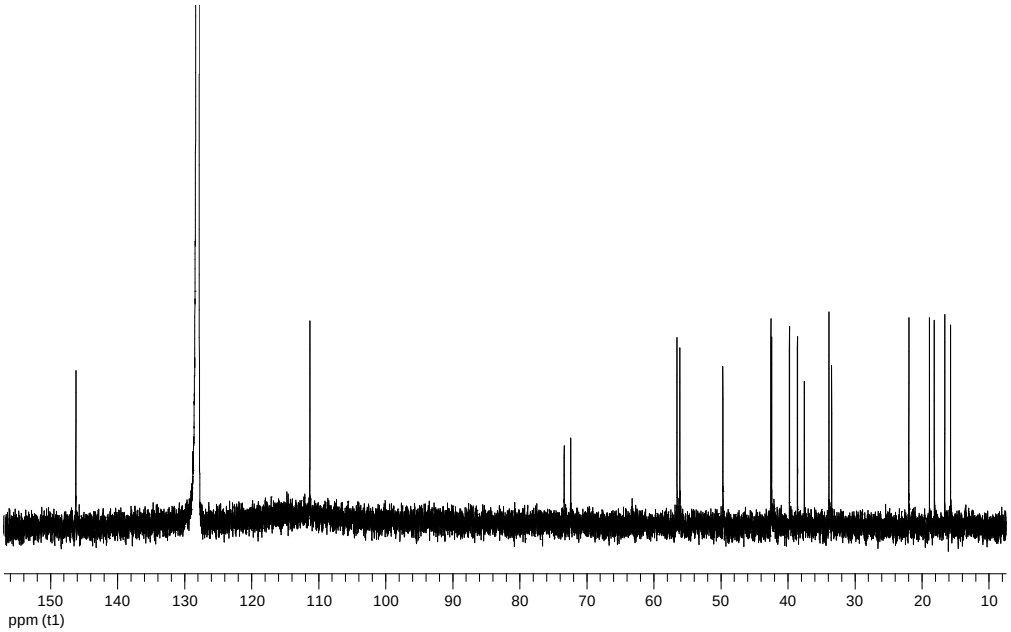

Figure 1.39 ^{1}H NMR spectrum of Compound **6.8** (600 MHz, C_6D_6)

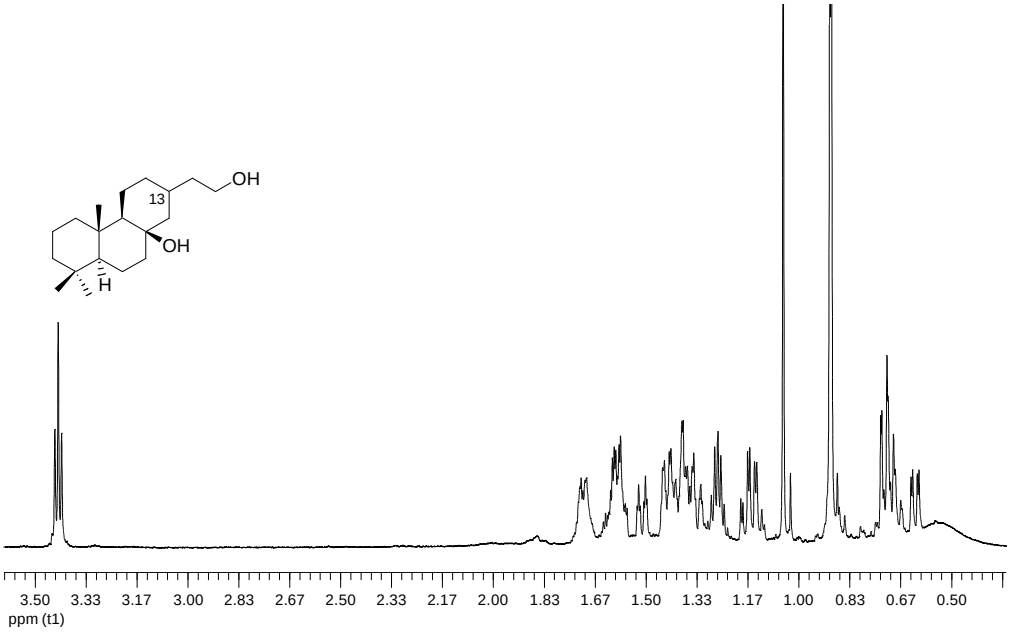

Figure 1.40 ^{13}C NMR spectrum of Compound **6.8** (150 MHz, C_6D_6)

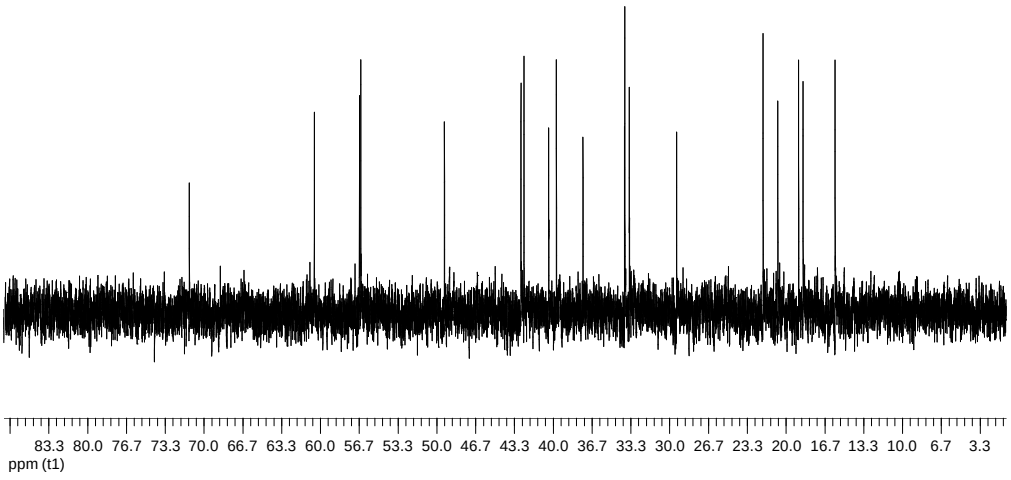

Figure 1.41 ^{1}H NMR spectrum of Compound **6.9** (400 MHz, $CDCl_3$)

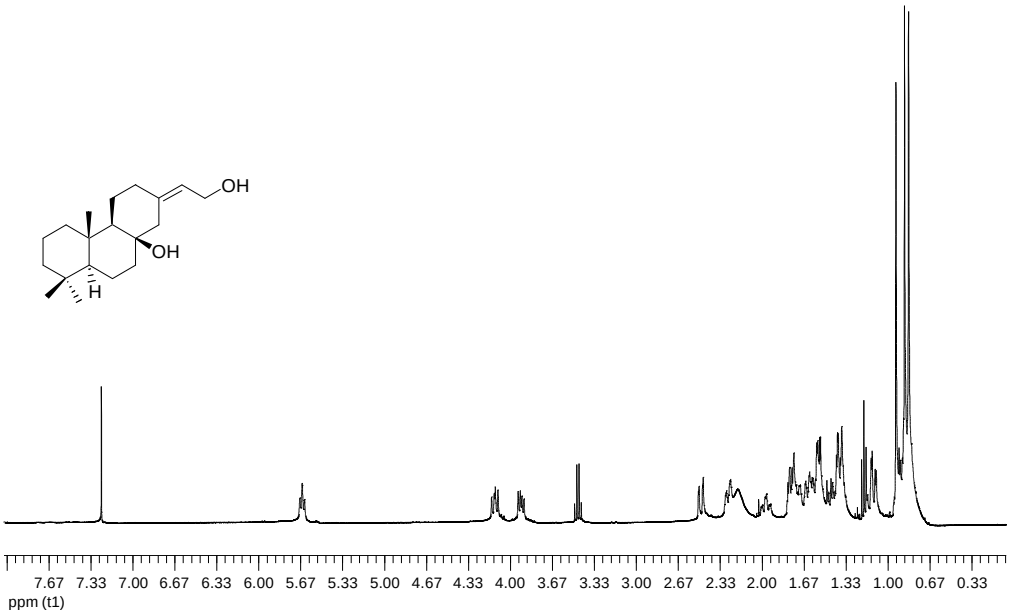

Figure 1.42 ^{13} C NMR spectrum of Compound **6.9** (100 MHz, $CDCl_3$)